COUPLED THERMOMECHANICAL EFFECT ON SWELL PRESSURE AND REACTIVE TRANSPORT THROUGH COMPACTED BENTONITE BUFFER

A thesis submitted

in partial fulfillment of the requirement for the degree of

Doctor of Philosophy

Submitted

By

ROHINI CHHATRAPATI KALE

Department of Civil Engineering

Indian Institute of Technology Guwahati

Guwahati, Assam

India – 781039

March – 2021

Indian Institute of Technology Guwahati

Candidate's Declaration

I hereby declare that the work presented in this thesis is to the best of my knowledge, original, except as acknowledged in the text. This material has not been submitted, either in whole or in part, for degree at any University.

Date: 15-03-2021

Rohini Chhatrapati Kale
Ph.D. Scholar
Registration No. 156104042
Department of Civil Engineering
Indian Institute of Technology Guwahati

Indian Institute of Technology Guwahati

Certificate

This is to certify that the thesis entitled **"Coupled thermomechanical effect on swell pressure and reactive transport through compacted bentonite buffer"** submitted by **Rohini Chhatrapati Kale** (Registration No. 156104042) to the Indian Institute of Technology Guwahati for the degree of Doctor of Philosophy is a record of bonafide research work carried out by him under my supervision and guidance. The thesis work, in my opinion has reached the requisite standard fulfilling the requirement for award of the degree of Doctor of Philosophy. This work has not been submitted earlier for the award of any degree or diploma to the best of my knowledge and belief.

Date: 15-03-2021

(Dr. Ravi K)
Ph.D. Supervisor
Assistant Professor
Department of Civil Engineering
Indian Institute of Technology Guwahati

Acknowledgements

I am indebted to many people who helped me during my research work, and it is my privilege to acknowledge them.

At first, I express my deepest sense of gratitude and reverence to my supervisor Dr. Ravi K, Assistant Professor, Geotechnical Engineering Division, Department of Civil Engineering, who was always available for discussion as a teacher and as a friend. He contributed a great deal to my understanding of the research area through valuable discussions, ideas, useful comments, which were a great source of inspiration. His decent behavior and an affectionate concern for students, as well as his in-depth appreciation of the problem and timely suggestions for its solutions, keeps him on a unique pedestal as an outstanding supervisor.

I express my sincere thanks to the members of my Doctoral Committee, Dr. Anil Kumar Mishra, Dr. Arindam Dey, and Dr. Prasenjit Khanikar, for their valuable suggestions, eternal encouragement, and timely help provided at various stages of the research work. I also thank Prof. Sreedeep S., Dr. Arindam Dey, and Dr. Ankit Garg and Dr. Anil Kumar Mishra for their help during my course work.

I thank the former Head of the Department; Professor Subhasis Dutta, Professor Chandan Mahanta and present Head Professor Sharad Gokhale for providing facilities for conducting the research. I gratefully acknowledge the unstinted help provided by Mr. Samarjyoti Kalita, Mr. Hariram Upadhyay and Ms. Reshima during all phases of my research work. Furthermore, I would like to thank the office staff of the Department of Civil Engineering for their support in administrative works.

I wish to put on record my gratitude to the Editors and Reviewers of all my manuscript published in the respective Journals and Conference proceedings for their valuable comments on upgrading my research study.

I would like to thank my senior Dr. Yagom Gapak, Dr. Janarul Shaikh, Dr. Harinarayan, Mr. Chandrabhanu G, Dr. Shivshankar, Dr. Chiranjib Sarma, Dr. Rana Acharya, Dr. Pradeep K Dammala, and my colleagues for giving their precious time related to my research work.

I would like to thank my colleagues Mr. Anant Aishwarya Dubey, Mr. Siddharth Garia, Mr. Rojimul Hussain, Mr. Deepak Patwa, Ms. Shreya Katre, and Ms. Dhritileka Deka, Ms. Rutuja Kate for giving their precious help related to my research work. I also thank my juniors Mr. Biswajit Panda, Mr. Rituraj Devrani, Mr. Kishore Ghosh, Mr. Annesh Borthakur, Mr. Arnab Pal, Mr. Alok, Mr. Sudhanshu Rathod, and Mr. Kapil Bhanwariwal for helping me during my experimental work.

One other special friend, i.e., my husband, I must mention is Dr. Mayur Shirish Jain for his constant encouragement, communication, love, and respect throughout my stay and during my research work.

At last, I would also like to thank my Grandfather Late B. S. Bhende, who believed, supported, motivated me for the research field, also my parents Mr. C. N. Kale, Mrs. S. C. Kale, and sister, Ms. Ashwini Kale, and my in-laws for their love and support during the study.

Above all, I owe it all to almighty God for granting me the wisdom, health, and strength to undertake this research task and enabling me to its completion.

Rohini Chhatrapati Kale

ABSTRACT

Increasing demand for power generation and in response to avail low-carbon energy source, especially in the countries reliant on coal, oil, or gas, it is essential to develop nuclear-based power plants. Globally almost in all continents, nuclear power is used, and such nuclear power plants produce small quantities of potentially highly hazardous, radioactive wastes. Nuclear power is supplied in various parts of the world, but the management of radioactive waste is of concern. Many countries have developed apt lower-level waste management techniques such as disposal in special facilities. But higher-level wastes require more attention as it may cause several environmental as well as health hazards.

Deep geological disposal has been considered as one of the best ways to handle higher-level nuclear wastes. Compacted bentonite or sand bentonite blocks are used as a buffer material in the deep geological repository (DGR) for the safe disposal of high-level nuclear waste (HLW) due to its favorable physicochemical and hydro-mechanical properties. Buffer surrounding the waste canister experiences variations in the temperature for a long duration of time. Such thermal effects are induced when a high-temperature waste canister comes in contact with buffer and due to seasonal temperature change resulting from a heat source by geothermal gradient in the ground. The long-term performance depends upon the stability of expansive minerals present in the bentonite along with the percentage clay content, exchangeable cations available with it, its swelling capacity, permeability, pH, surface area, etc.

The temperature from the waste canister can initially go as high as 250°C and probably reduce to ambient temperature upon the decay of the waste material. This long duration temperature variation induces a thermal history on the bentonite buffer, affecting its index, physicochemical and hydro-mechanical properties. Besides the above-mentioned characteristics, bentonite also provides sufficient swelling pressure and low hydraulic conductivity to the barrier system giving long-term stability. The high-temperature waste canister and the geothermal gradient in DGR impose a long-term thermal history and may alter the swelling pressure of the compacted bentonite. Hyperalkaline pore fluid can be generated when the fluids from the host rock infiltrate through the cement/concrete layer, which is constructed as a bulkhead or in the vaults or to support the access of galleries between a buffer and the host rock. The swelling

behavior of the bentonite under such hyper alkaline environment as well as the effect of thermal history is essential to study for the stable performance of the buffer during its long-term operations. The unbalanced conditions generated inside the deep geological repository can force steel canister to corrode. Such chemically unstable corrosion may produce harmful leachates that may alter the properties of bentonite, affecting its overall performance. The montmorillonite mineral of the bentonite might be altered into other minerals by these combined interactions of corrosion products and thermal history, altering its swelling capacity. Even the temperature variation, probably because of continuous heat emitting canister (initially-150°C to 250°C) and geothermal gradient, affect its performance, there would be bentonite iron interface reactions due to the corrosion of steel canister, which might cause reactive transport through the compacted bentonite buffer. The generated fluids (leachate produced due to canister corrosion or a hyper alkaline solution from the other side) may cause reactions due to the presence of exchangeable cations inside the bentonite and cause reactive transport, which could ultimately affect the purpose of bentonite as a buffer material.

The bentonite buffer is expected to exhibit stable performance in the presence of such unstable thermal and chemical fluxes. The main focus of this study was divided into four phases. Initially, the thermal treatment was given to powdered bentonite samples and tasted for its index and physicochemical properties. In the second phase, a thermal history was given to compacted bentonite specimens and tested for the swell pressure developed when saturated by distilled water and hyperalkaline cement water, respectively. In the third phase, compacted bentonite specimens were given a thermal history with the addition of corrosion products and saturated by distilled water and hyperalkaline cement water tested for their swell pressure. In the last phase, the compacted bentonite specimens were checked against the reactive transport through it by creating a combination of a thermal and chemical gradient.

It was observed that thermal history has a significant influence on the index and physicochemical properties of powdered bentonite. The swell pressures of both the bentonite decreased with an increase in the historic temperature. The swell pressure reduced by 15% and 7% for B_1 and B_2, respectively, at 200°C. The final swell pressure value of samples saturated with cement water was found to be approximately 22% and 48% less than that of samples saturated with distilled water for B_1 and B_2, respectively, at 200°C. The time of saturation in the case of cement for all the combinations of densities and thermal history was approximately 1.5 times more than in the case of

distilled water. The final swell pressure value of samples containing corrosion products and saturated with distilled water was found to be approximately 15% less than that of samples without corrosion products. At the same time, it was approximately 22% in the case of hyperalkaline cement water (At 2.0 Mg/m^3). The decrease was more significant, with an increase in the historic temperature. The degree of saturation has been reduced by 18% at 200°C than the Sr in the case of distilled water, but for bentonite B_1 the degree of saturation is greater than B_2. In the overall study bentonite B_1 resisted better than B_2 to such an unstable environment possibly due to better index and physicochemical characterization of both the bentonites particularly, specific surface area, cation exchange capacity, liquid limit, etc.

Keywords: HLW's; geological deposits; bentonite; swell pressure; hyperalkaline environment; corrosion; reactive transport.

CONTENTS

LIST OF FIGURES

LIST OF TABLES

NOTATIONS

AAS	Atomic Absorption Spectrophotometer
CEC	Cation Exchange Capacity
CP	Corrosion Product
CW	Cement Water
CWTH	Cement Water and Thermal History
DGR	Deep Geological Repository
DW	Distilled Water
EBS	Engineered Barrier System
EC	Electrical Conductivity
EDX	Energy Dispersive X-Ray
ESP	Exchangeable Sodium Percentage
FESEM	Field Emission Scanning Electron Microscope
g	Gram
L	Litre
min	Minute
Mg/m^3	Mega grams per meter cubed
MDD	Maximum Dry Density
OMC	Optimum Moisture Content
TH	Thermal History
WCP	Without Corrosion Product
XRD	X-Ray Diffraction
XRF	X-Ray Fluorescence
2θ	Angle between diffracted X-ray with incident X-Ray beam

Chapter 1

INTRODUCTION

1.1 OVERVIEW

Nuclear power plants contribute nearly 14% of the total power generation of 31 countries. Most of the nuclear power generation occurs in Europe, North America, East and South Asia. Countries such as the United States and France are the largest nuclear power producers amongst other countries. A paradigm shift towards low carbon energy sources has been witnessed in recent years due to the increasing demand for power generation and to improve the security of supply by diversification, especially in countries dependent on imported coal, oil, or gas (Chapman and Hooper, 2012). Countries like China, India, Russia, and South Korea have come into the limelight due to the construction of new nuclear reactors. India, which is intensely dependent on coal, a high carbon energy source for power generation, is also shifting towards nuclear power program for a pollution-free environment. Along with the existing 22 operational reactors having a capacity of 6780 MW, the developing country will construct seven new reactors with a capacity of 5300 MWe (IAEA, 2018). Like any other industry, nuclear power plants are liable to produce wastes; these wastes are radioactive. However, the quantity of waste generated is remarkably low compared with fossil fuels such as coal, oil, or gas. More precisely, producing 1 GW of power for a year generates approximately 25 tonnes of used nuclear fuel and a few hundred cubic meters of other wastes. On the other hand, a coal-based power plant of the same size produces 6.5 million tonnes of carbon dioxide, about 300,000 tonnes of ash (that includes heavy metals such as uranium). Without air scrubbers, over 5000 tonnes of harmful gases from burning coal (Chapman and Hooper, 2012). But nuclear wastes are a high potential hazard to the environment as well as to human health and, therefore, require proper handling, management, and disposal.

Nuclear waste is broadly classified as low-level, moderate-level, and high-level based on the concentration of radionuclides or radioactivity. The use of radioactive materials for power generation, analysis, and medical imaging produces 84% of low-level waste, 14% of intermediate-level waste, and 2% of high-level radioactive waste (HLW) (Ramana et al., 2001). By taking the custody of the sites under institutional control till the total radioactive threat has decayed to levels below radiological concern, a low

radiation level and has been disposed of in special facilities on or in the trenches, vaults, etc. The low-level waste contains about 0.1% of the total radioactivity, whereas intermediate-level waste has 1% of the radioactivity. Though the volume percentage of high-level radioactive waste is very low, it contributes to 99% of the radioactivity (Ramana et al., 2001), and thus high-level nuclear wastes lead to a more complex story. High-level wastes requires special handling and considerations, such as thick biological shielding and engineered cooling systems because of the radio decay heat load heat (>2kW/m^3). It may take hundreds of thousands of years to decay to become harmless and therefore an idea about the use of the underground environment for disposal developed by some researchers to protect the environment and public. Researchers are also claiming that deep geological repositories are the safe methods for the final disposal of HLW's and are technically proven. A schematic representation of the deep geological repository for the safe disposal of HLW is presented in Fig 1.1.

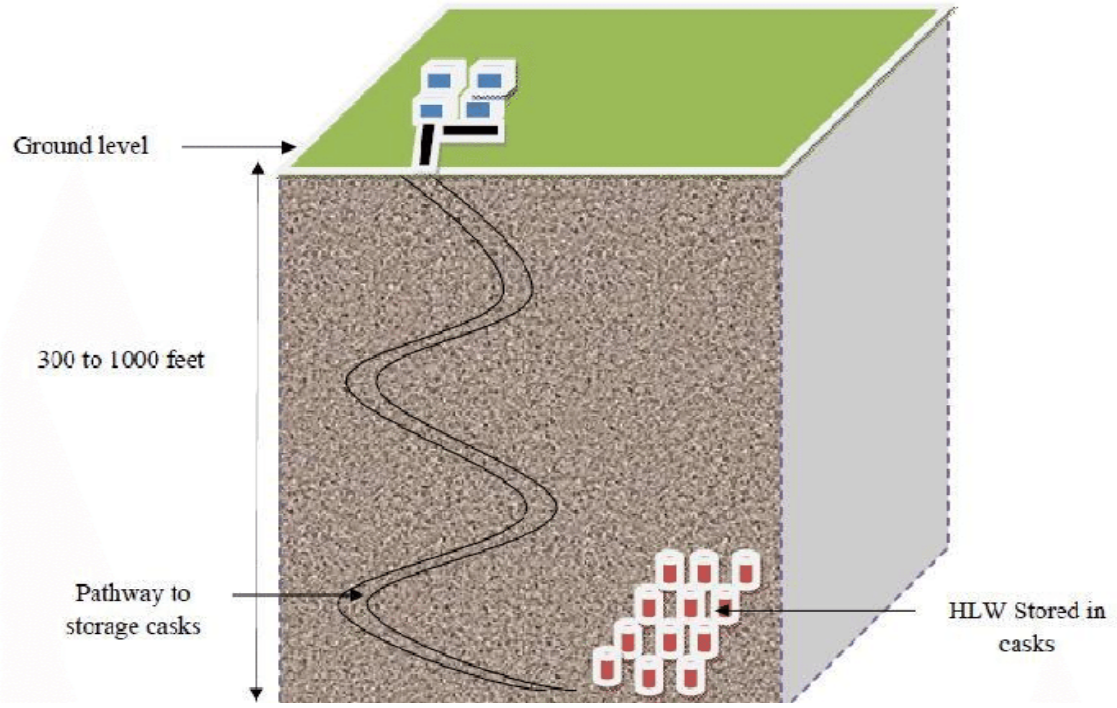

Fig 1.1 A schematic representation of the deep geological repository for the safe disposal of HLW (Khelurkar et al., 2015)

The purpose of the deep geological repository is to store the waste in such a manner that it does not damage the environment or human health, until the waste deacys to safe levels of the radioactivity. It consists of a barrier system with a natural barrier of host rock and its surroundings and the engineered barrier of a waste canister and a sealing

material, which is called a buffer (Delage et al., 2010). Compacted bentonite or bentonite-sand mixtures are placed around the canister as a buffer material due to its favorable physicochemical and hydromechanical properties (Rao and Ravi, 2013). The function of the buffer is to prevent the groundwater from percolating towards the canister and preventing the migration of radionuclides towards the biosphere (OECD, 2003; Pusch, 2002).

The bentonite is selected as a buffer material due to its favourable characteristics when are:

1) Swelling is the most important property due to which it possesses the self-sealing ability to seal gaps between the surrounding host rock and buffer.

2) Due to swelling, it forms a compact structure of low hydraulic conductivity to ensure that reactive transport between the host rock and waste canister.

3) It has high thermal conductivity to ensure fast heat discharge from HLW.

4) It has a high cation exchange capacity and sorption capacity to hold any radioactive impurity released from the waste canister.

5) It is highly inorganic clay; hence it supports low chemical activity for the survival and growth of microorganisms.

Bentonite possesses all these unique characteristics swelling due to the presence of a mineral called montmorillonite. The unit layer of montmorillonite comprises one octahedral aluminum sheet sandwiched between the two tetrahedral silica sheets. These layers are rigid and weakly connected by van der Waals forces. As a consequence, cleavage or adsorption of polar fluids will separate successive layers quickly, resulting in high swelling after wetting. Extensive isomorphic silicon and aluminum replacement with additional cations (magnesium, iron, nickel, zinc, etc.) leads to a net negative charge on the surface of the clay. Montmorillonite has a high cation swapping potential due to a large number of available cations present (Mitchell 1993). The surface area of the montmorillonite is large, and its diameter is typically less than 1 or 2 microns. The hydration of interlamellar cations contributes to the swelling of clay particles, which then fills the gaps, thereby preventing groundwater movement in these preferred routes and ensuring that the waste canister is properly screened inside the deep geological

repository. The structure of montmorillonite is presented in Fig.1.2.

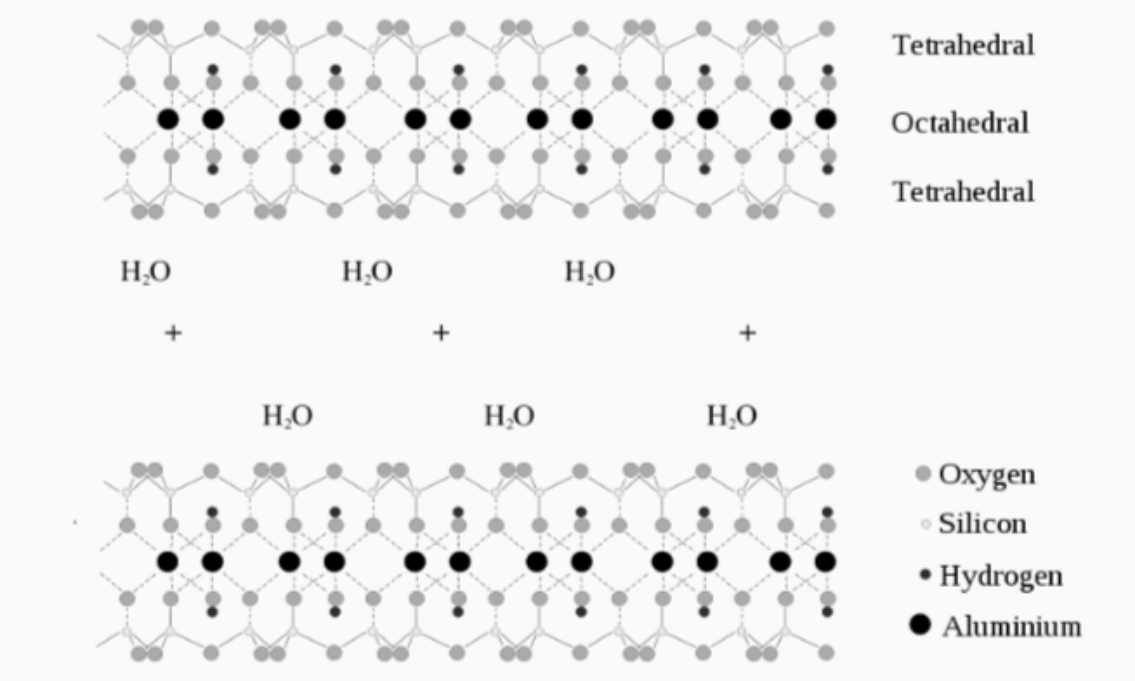

Fig 1.2 Structure of montmorillonite
(http://aneyefortexas.wordpress.com/2012/03/22/colors-of-bentonite)

1.2 BACKGROUND OF THE PROBLEM

The bentonite buffer experiences thermal flux inside the repository because one side of bentonite receives heat from the host rock that is generated from changes due to geothermal gradient (25°C-55°C) (Chapman, 2012), and the other part becomes hot because of the waste canister (150°C-250°C) (Estabragh et al., 2016). The spent nuclear fuel is, used fuel from a reactor that is no longer able to create electricity because its fission process has slowed but still generates thermal energy and is highly radioactive. The buffer is expected to be stable at such dynamic thermal fluxes. The behavior of the buffer at the room as well as at elevated temperature has been reported in a series of literature by various researchers (Lee et al., 2016; Zheng et al., 2015; Ye et al., 2012 a; Ye et al., 2012 b; Xiaodong et al., 2011; Ye et al., 2009;). Lingnau et al. (1996) presented the first results on the performance of saturated buffer at elevated temperatures up to 100°C and reported some changes in the stress-strain behavior of the buffer at high temperatures up to 100°C. It is clear from the reported literature that the micromechanics of the clayey soils are different at room temperature and elevated temperature (Villar et al., 2005; Bayram et al., 2010). Similar studies are reported by Wang et al. (1990),

Jefferson et al. (1998), Ye et al. (2014) presenting the effect of high temperatures ranging from 20°C to 800°C on index physicochemical and hydromechanical properties of clayey soils. A recently reported study given by Estabragh et al. (2016) reported the effect of thermal history on geotechnical properties of bentonite at higher temperatures up to 250°C for various durations and found that the buffer surrounding waste canister is exposed to a temperature variation during an extended period that makes a barrier to change its index, physicochemical and engineering properties. The swell pressure of bentonite decreased with an increase in historic temperatures. Lloret and Villar (2004) observed that the reduction in swelling strain due to an increase in temperature decreased by increasing vertical load.

A layer of cement or a concrete bulkhead (Pusch et al., 2003) is a part of the multi-barrier system that may be used either as a massive embedding (Dauzeres et al., 2010) or in the vaults as a backfill (Vasconcelos et al., 2018) or as mechanical support to a repository and backfilling of cavities (Watson et al., 2013; SKB, 2011) or to support the access galleries and in the final sealing of the access routes (Bao et al., 2016). The presence of cement or the concrete layer comes in contact with the moisture that percolates from the host rock and creates the alkaline environment (pH>12) inside the repository. The continuous degradation of cement produces highly alkaline fluids and may try to diffuse through the compacted bentonite buffer and alter the properties such as swell pressures, permeability, and may control the reactive transport mechanism through the compacted bentonite (Jenni et al., 2017; Torres et al., 2013; Zhu et al., 2013). The high-level nuclear wastes are filled in steel canister or copper canister and then placed inside the deep geological repository (Kaufold et al., 2015; Kaufold et al., 2020). The steel used in the manufacturing of canister is carbon steel because of its better durability. One of the other advantages of selecting carbon steel that it is a non-alloy of steel that has easy welding and its expected working life is thousands of years (Patel et al., 2012). Under the unstable conditions inside the repository, the corrosion of a canister starts producing the leachate, which affects the overall performance of the thermally loaded buffer, especially its swelling characteristics and may create a pathway for the reactive transport (Samper et al., 2008; Marsh and Taylor, 1998).

The heat from the waste canister and comparative lower temperature at the host rock side is the cause of the thermal gradient. The safety of a repository needs to understand the alterations resulting from heating, hydration, and chemical changes. The study of transport through the compacted bentonite by the combined effect of thermal and

chemical gradient is essential to understand, for its long-term sustainability as a buffer material. Also, the anaerobic corrosion of steel could also interact with bentonite in this case, along with the hyperalkaline cement solution from the other end and under the influence of the thermal gradient. However, the long-term success of compacted bentonite as the buffer material relies on the smectite resilience against thermal and technological adjustments, from which all the significant changes inside the repository may be maintained. Hence, the investigation of the alteration of physicochemical and mechanical properties of bentonite through reactive transport by anaerobic corrosion of steel canister (Savage et al., 2010) from one side along with the infiltration of hyperalkaline solution (Ravi and Rao, 2017) from another side under the influence of thermal gradient needed to be studied (Lantenois et al., 2005). Consequently, it is essential to understand the long-term effect of thermal and chemical gradient on its behavior. The main focus of the present work is to understand the coupled thermomechnical behavior of two bentonites from India to serve as a suitable buffer material for the deep geological repository.

1.3 NEED OF THE STUDY

It is safe to assume that, like stress history, the soil has a thermal history. Bentonite is an expansive soil that has high plasticity, low permeability, and high swelling potential. These properties make it suitable to use as a buffer and sealing material for DGR. Due to the low permeability of compacted bentonite, reactive transport from the disposal of waste or groundwater is minimized. The temperature of disposed waste may change with time, and such temperature variations can change the behavior of bentonite (Fig 1.3). Hence, the effect of thermal history on the behavior of bentonite as a buffer is essential to know in the DGR context. At the same time, it is also necessary to know the stability and long-term performance of the buffer against dynamic groundwater conditions. Recent studies have proposed that the interaction of hyperalkaline water and corrosive solutions, with the dissolved and exchangeable cations of bentonite buffer, may trigger reactive transport through the pores of the bentonite, which may influence the performance of the buffer in various means.

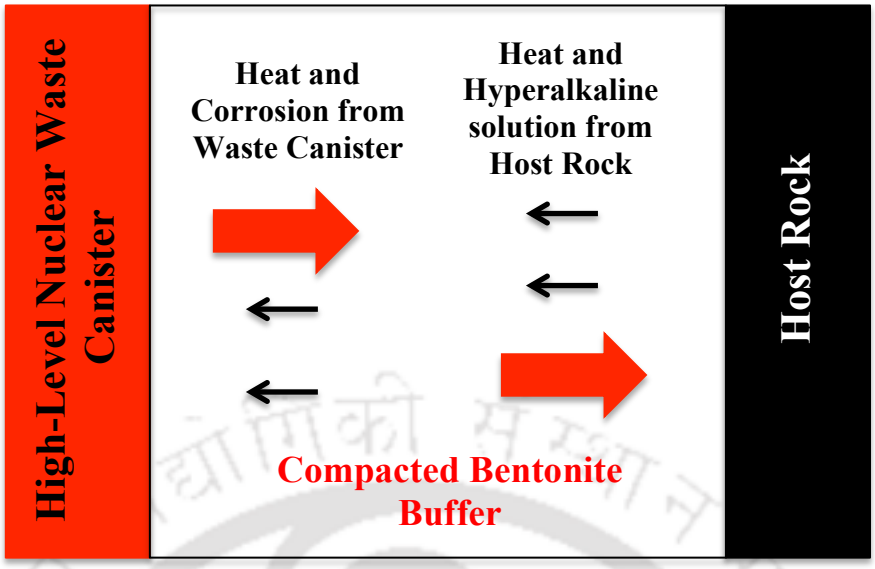

Fig 1.3 Schematic representation of the source of heat, hyperalkaline and corrosive fluids

Understanding of the migration processes in bentonite is necessary as a part of the safety assessments. Hence, the area of reactive transport through bentonite buffer needs to be explored, as mentioned earlier, and the buffer is used for its low permeability so as to reduce the reactive transport through it. If the induced thermal history affects its index, physicochemical and hydromechanical properties, it may accelerate the reactive transport through it; hence it is necessary to know the effect of thermal history and thermal gradient on reactive transport through bentonite.

1.4 THESIS ORGANIZATION

The thesis is organized as follows:

- Chapter 1 is about problem statement associated with the disposal of high-level nuclear waste, introduction to engineering barrier system, buffer material, functions of buffer material, the influence of temperature, hyperalkalinity and corrosive environment on the buffer, the objectives and need of the study; and the scope of the thesis.
- Chapter 2 gives a detailed literature review on the effect of high temperature, thermal history, hyperalkaline solutions, corrosive solution, thermal gradient, and chemical gradient on the behavior of bentonite.

- Chapter 3 contains the experimental study on the effect of thermal history on the index and physicochemical behavior of bentonite.
- Chapter 4 deals with the influence of thermal history on powdered bentonite.
- Chapter 5 gives results and discussion regarding the swell pressure of compacted bentonite added with corrosion products and saturated with distilled water and hyperalkaline cement solution under the influence of thermal history.
- Chapter 6 is about results and discussion regarding the influence of thermal history on the swell pressure of bentonite added with corrosion products and saturated with distilled water and hyperalkaline cement solution.
- Chapter 7 deals with the experimental study on the effect of thermal gradient and chemical gradient on the reactive transport through compacted bentonite buffer.
- Chapter 8 lists the conclusion and the recommendations from this study.

Chapter 2

LITERATURE REVIEW

2.1 INTRODUCTION

This chapter presents a review of published literature on nuclear waste handling and management, the importance of deep geological repository, introduction to problems associated with the bentonite buffer in the deep geological repository because of elevated temperature, hyperalkaline seepage, and canister corrosion. The possible reasons for the increases in temperature inside the repository, the effects of elevated temperature on the performance of the buffer, the possible range of increased temperature, the source of hyperalkaline fluid and its effect, and the canister corrosion on the performance of bentonite reported in the literature are discussed. After the review of the existing state of the art knowledge in this field, a problem statement is presented, and the objectives and the scope of the work are presented.

2.2 NUCLEAR WASTE HANDLING AND MANAGEMENT

Nuclear wastes are quite different than any other wastes that exist on the earth. These are generated during various activities of the nuclear fuel cycle. Various activities including mining, nuclear power plants, processing industry, defense, medicine, and scientific research, produce byproducts that include nuclear wastes (Tang et al., 2008; Romero et al., 2005). It can be present in any form, solid, liquid, or gas, and have variable radioactivity levels. Thus proper handling and management are very much needed. In general, nuclear wastes are broadly classified as low-level, intermediate or moderate level, and high-level wastes. Low-level nuclear wastes have low radioactivity or less active radionuclides, and high-level nuclear wastes are characterized by high radioactivity (Delage et al., 2000). Low-level wastes are generated in large volumes that include materials from highly radioactive parts of nuclear reactors (such as cooling water pipes and radiation suits) and waste from medical procedures. On the other hand, HLW containing most (~99%) of the radioactivity in the entire fuel cycle is produced during reprocessing of spent fuel (Abuel et al., 2005; Villar and Lloret, 2004).

The preparation for the management of HLW takes into account the need for its efficient biosphere isolation and constant surveillance over a duration of many generations (Yilmaz, 1999; Wang et al., 1990, 1998; Towhata et al., 1993). To accomplish this long-term goal, waste separation structures consisting of several barriers

are used to avoid the flow of radionuclides back into the human environment. This includes handling and disposing of the HLW generated during nuclear power generation (Villar and Lloret (2010, 2004); Lloret and Villar, 2007; Tan et al., 2004; Gu et al., 2001; Cho et al., 2000). The waste contains uranium, plutonium, and other highly radioactive materials produced during fission operations. Those high-level radioactive isotopes emit high amounts of radiation and have extremely longer half-lives (about 100,000 years), which result in long periods until the waste reaches a safe level of radioactivity.

In the Indian context, the treatment of high-level waste includes three stages:

1. Dispose of in vitrified borosilicate container with high-level liquid waste.
2. Engineered temporary storage over a period of time and eligible for final disposal of waste for passive refrigeration & control.
3. Full storage disposal in a deep geological repository of the waste.

Bhabha Atomic Research Centre, India, has been developing HLW vitrification technology over the years. The hazardous waste disposal strategies have greatly changed over the last 20 years. The construction and disposal activities of modern storage plants have to follow more rigorous environmental and pollution control standards than those planned at the start of the nuclear era. Radioactive waste disposal is a complicated problem, not only due to its existence but also because of the tight regulatory framework for its management. In the treatment of all forms of hazardous waste, India has gained self-reliance. However, the development of technology to minimize the waste and its safe disposal is still ongoing. This latter advancement has given new emphasis to the use of the underground environment as a disposal site for waste.

2.3 CONCEPT OF DEEP GEOLOGICAL REPOSITORIES

2.3.1 Deep Geological Repository

Disposal of high-level radioactive wastes (HLW) in deep underground geological formation is one of the methods, which has received worldwide attention that involves confinement or isolation of these wastes from the biosphere in the repositories (Fig. 2.1). Geological disposal does a very good, passive job of protecting humans and the natural environment, with the degree of protection matching perfectly with the diminishing hazard of the radioactive wastes (Neil et al. 2012). An engineered barrier system (EBS) approach is followed in the design of a deep geological repository (DGR) for the disposal of these wastes (Kim et al., 2011; Delage et al., 2010; Gibb 1999; Bucher et al. 1989). The overall safety against migration of radionuclide is achieved by proper

selection of suitable engineered barriers, backfill materials, and the characteristics of the geo-environment of the repository site.

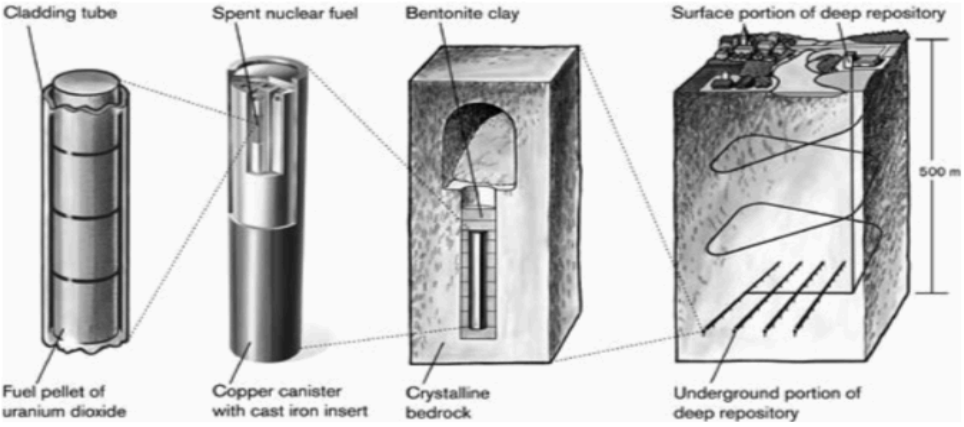

Fig. 2.1 Schematic Representation of Deep geological repository (SKB, 2006)

The design of a deep geological repository (DGR) includes the construction of the successive barrier system (EBS) around the waste canister and the natural barrier, which isolates the harmful radioactive waste material from the surroundings (Rao and Ravi, 2013; 2014). The EBS consists of the waste-containing canister and the sealing materials such as buffer, which seals and isolates the waste-containing canister in the host rock and backfill. It is designed to control the emission of the radionuclides to the environment and thereby protects the biosphere from any kind of detrimental effects of radiation. In this context, the buffer or the sealing material in EBS (Fig. 2.2) has to limit the reactive transport through it by performing two important functions 1) limiting advective transport of groundwater from the natural barrier (host rock) to the waste containing canister and 2) retaining the radionuclides over a long period of time untill the harmful radiation has decayed (Pusch and Yong 2006; OECD 2003; Pusch 2002; Pusch 1992). The multi-barrier waste management principle tackles the shielding of waste and waste-related protection against radionuclides release, i.e., via isolation and retention:

Isolation: prevents wastes from direct contact with humans and with the atmosphere in a healthy manner. This includes the selection of the site for the repository in the remote and secures areas and natural conditions for dumping (Garcia et al., 2006; Garcia, 2007 Guven, 1990; Yong et al., 1986).

Retention: involves retarding the radionuclide within the multi-barrier network until normal mechanisms of radioactive decay have greatly decreased the possible risk for

certain radionuclides and will offer full isolation before they degrade in the immediate region of the waste kit at negligible amounts of radioactivity (van Geet et al., 2009; Chegbeleh et al., 2008).

Even if geological disposal's main separation and containment roles have been effectively accomplished, but one needs to remember for about one million years of the future impacts that those residual radionuclides had on humans and the climate.

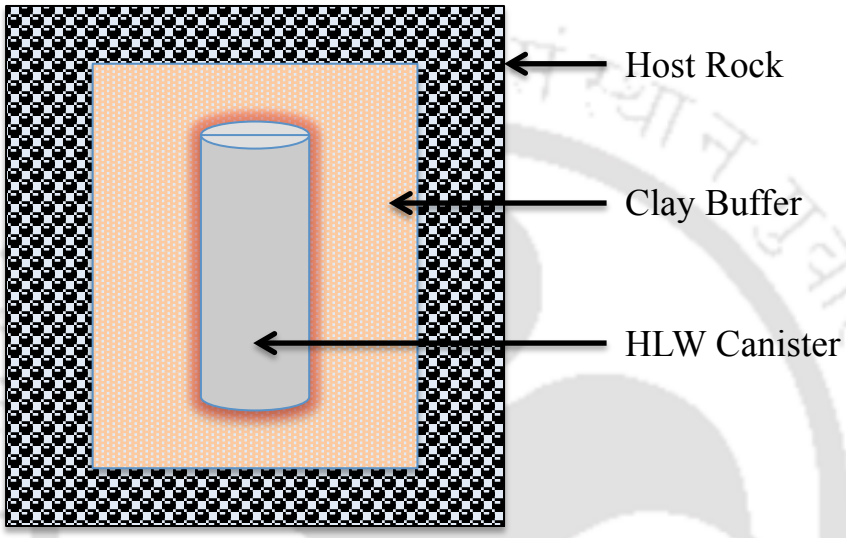

Fig. 2.2 Schematic Representation of EBS

2.3.2 Various concepts of deep geological repository

2.3.2.1 Sweden and Finland

The initial idea involved the disposal in the basement of a 10/90-bentonite/sand mixture of vitrified high-level wastes in titanium tanks as a barrier at a depth of about 500 m. In 1978 an analysis was carried out to explore direct disposal of spent fuel, converted the titanium container into copper, and replaced the bentonite/sand mixture with pure bentonite. Natural Wyoming Na-bentonite was used as the reference material at this early stage. The buffer was mounted as insulated blocks with compacted bentonite powder to fill any voids in the structure. The concept is now called "KBS-3" (SKB, 2011). The disposal of high-level nuclear waste in Finland was based on the fact that the nuclear wastes should be treated and disposed of in the deep geological repository, and the nuclear waste should not be imported from any other country. Posiva suggested the disposal site to Olkiluoto in Eurajoki and the final disposal process to KBS-3.

2.3.2.2 Canada

The Canadian and Ontario Governement (1978) formed the nuclear waste disposal program, and according to the concept, the spent fuel should be disposed of 500-1000m deep in the granite rock. The fuel should be filled in a specially designed corrosion resistant canister. The long-term disposal plan of Canada is called "Adaptive Phased Management and is administrated by the Nuclear Waste Management Organization (NWMO).

2.3.2.3 Spain

The high-level nuclear waste disposal system in Spain is managed by ENRESA (Empresa Nacional de Residuos Radiactivos). It is specifically based on the three activities, i.e., Identification of suitable sites, conceptual design, and performance assessment. The activity is attached to the research and development sector. The wastes are disposed of deep down in the host rock based on clay, granite, and salt.

2.3.2.4 Switzerland

The controlled disposal of all hazardous waste shall be carried out by NAGRA in Switzerland. The project 'Entsorgungsnachweis' showed the viability of waste disposal for high-level waste (NAGRA 2002). In 2008, NAGRA, led by the Federal Energy Office, screened Switzerland's geological underground for appropriate geological conditions, probable host-rock alternatives, and position regions under the Sectoral strategy for deep-geological repository plants. Following a rigorous analysis process, the Swiss Government in 2011 approved the entire six geological place regions suggested by NAGRA. NAGRA's Opalinus Clay repository design envisages a series of parallel tunnels (up to 800 m) containing bentonite-filled canisters of HLW at a depth of 600 900 m, with the area surrounding the canisters. These canisters are made of thick (12-14 centimeter) carbon steel (carbon steel is a steel in the range of 0.12-2.0-percent, and includes a major interstitial alloy part. Carbon steel is also used in regard to steel, which is not made of stainless steel. A reference saturated density of~1.9 mg/m3 is in the bentonite buffer. The formation of Opalinus Clay is usually more than 100 m thick and is surrounded by containers rich in clay. The surface is attached to the repository through the shaft and/or ramp and is partly filled back with sand/bentonite waste repositories.

2.3.2.5 France

Nuclear waste management is done by ANDRA (National Agency for the Management of Radioactive Waste) in France and planned to complete the project by 2025. They also have an underground research laboratory (500 m) with Callovo-

Oxfordian Clay formation at Bure, France. It has also focused on the transportation zone up to 30 km2 within the underground facilities. Since 2015 it is modifying the repository according to future requirements. The simplification of operational methods contributed to the design of uniform packages, which group together 1-4 main packages into a container weighing 6-25 tonnes and measuring between 1,2-3 m in a parallel piped concrete. The concrete liner is designed to provide mechanical stability (ANDRA, 2005). However, these facilities are designed using a steel overpack, and it doesn't use bentonite as a sealant.

2.4 BENTONITE BUFFER

So to accomplish the above-mentioned purpose, the waste canisters are sealed with a layer of buffer material. Blocks of compacted bentonite/bentonite-sand mixture are considered as suitable buffer material for sealing high-level nuclear fuel waste as a part of EBS owing to its highly favorable physical, thermo-hydro-mechanical properties (Garcia 2007; Garcia et al. 2006; Lloret et al. 2003; Komine and Ogata 1996; Pusch 1992; Guven 1990; Yong et al. 1986). The exceptionally high swelling ability of bentonite upon wetting is one property as it helps the clay to maintain tight contact between the waste canister and surrounding rock and seal any gaps, cracks, or fissures which might be present (Pusch 1992). It has low hydraulic conductivity, high swelling, and good self-sealing capacities (Yong et al. 1986). It also possesses colloid filtration, plasticity, high retardation to radionuclides and stability in relevant geological environments, low hydraulic permeability, swelling potential, ability to self-heal cracks in contact with water, and their sorption potential, a large specific surface area, high ion-exchange capacity.

Rao et al. 2008; Rao et al. 2007(a); Rao et al. 2005; Rao and Ravi (2015, 2014, 2013) reported Barmer bentonite from Rajasthan, India is suitable to use as a buffer material in DGR in the Indian context. Table 2.1 compares the physicochemical and index properties of Barmer 1 bentonite with bentonite-buffers reported in the literature.

Table 2.1 Physico-chemical and index properties of bentonites reported in the literature (Rao and Ravi, 2013)

Bentonite	Country	Specific Gravity	Liquid Limit (%)	Plasticity Index (%)	Clay (%)	Smectite (%)	CEC (mequiv./100 g)	Total Surface Area (m2/g)	ESP (%)
Barmer 1 (Rao and Ravi, 2013,2014,2015,2017)	India	2.69	409	367	86	68	80	450	65
Kunigel VI (Komine, 2004)	Japan	2.79	474	447	65	48	73	525	55
Kyungju (Cho et al., 1999)	Korea	2.74	245	198	40	70	58	348	-
GMZ (Zhijian, 2006; Zhang et al., 2009, 2012)	China	2.70	228	196	74	75	77	570	56.09
FoCa clay (Van Geet et al., 2009; Cuii et al., 2011)	Belgium	2.68	112	62	-	80	71	426	5.07
MX-80 (Pusch, 1980, 2001; Mata 2003; Herbert et al. 2008; Espina and Villar 2010; Wang et al., 2012)	Sweden	2.71-2.76	400-520	330-478	84-85	65-92	65-85	562	82.11
FEBEX (Villar and Lloret, 2008)	Spain	2.70	104	48	70	92	119	725	22.69
Avonseal (JNC, 2000)	Canada	2.80	257	208	60	79	82	615	56.71

Over the past few years, there has been a detailed analysis of bentonite (smectite-rich) clays swelling process. Partially saturated bentonite swells due to a reduction in the capillary potential that induces the dissolution of contractile skin of pore-fluid upon entrance of the water-free to the voids (Means, 1959; Schofield, 1946). "Swell pressure" was described by Bolt (1956) as the difference between the osmotic pressure between two particles and the osmotic pressure by the pore fluid. The matric component is the pressure produced when the free water has the same chemical concentration of the pore-fluid and is caused by the capillary phenomenon in unsaturated soils. Based on the soil material, the curvature of the water menisci regulates the matric suction of the unsaturated soil. Osmotic suction is due to variations in pore water and open water distribution of soluble salts. Two mechanisms of swelling of bentonite are (1), by hydration of the exchangeable cations known as crystalline swelling, indicate swelling by DDL repulsion of two neighboring clay particles (Birgersson, and Karnland (2009); Tripathy et al. (2004), and Yong (1999)). In the initial stages of wetting, crystalline swelling causes considerable volume change; water in successive monolayers enters montmorillonite unit layers which lead to unit layers separation until 19:20 A^0. More water penetration contributes to the diffused double layer repulsion. The swelling

comportment of the bentonite has been studied primarily in the laboratory by two means: 1) using free swelling oedometer set up and 2) Using constant volume oedometer set up (Rao and Thyagaraj, 2007a; Rao and Shivananda, 2005; Rao et al., 2004; Delage et al., 1998; Komine and Ogata, 1994).

Several factors impact the swelling of bentonite:

1. The swelling properties of bentonite are clay affected by the dry density, particularly in the case of unsaturated bentonite. With the increase in dry density, the swelling capacity increased (Villar and Lloret, 2008; Komine and Ogata, 1994; Chen, 1988; Sridharan et al., 1986; Yevnin and Zaslavsky, 1970; Seed and Chan, 1959; Holtz, 1948).
2. Pore fluid concentration chemical plays a vital role, controlling its swelling ability. It affects the swelling by two means: 1) change in cation hydration; however, it depends upon the dominant cation present in the clay mineral. 2) Changes in the width of the diffused double layer. The higher the cation concentration in the pore fluid, the lesser the thickness of the diffused double layer (Kaufhold and Dohrman, 2009; Castellanos et al., 2008; Mata et al., 2005; Herbert et al., 2004; Cho et al., 2002; Kim, 2000).
3. The initial moisture content of the sample has an influence on the swelling characteristics. With the increase in initial moisture content, the swelling capacity decreases (Wang et al., 2012; Thakur and Singh, 2005; Rao et al., 2004; Lee et al., 1999; Komine and Ogata, 1994; Chen, 1988; Sridharan et al., 1986; Nayak and Christensen, 1971; Komornik and David, 1969; Holtz and Gibbs, 1956). Borgesson (1985) reported a linear increase in swell pressure with an increase in the initial moisture content of compacted Na-bentonites.
4. The pore structure of the bentonite after compaction can be described in two parts, one is the microstructure, and the other is the macrostructure. The microstructure is related to the interlamellar space of the clay structure, and the macropores are related to interparticle space. So after the compaction of bentonite, how the micro and macropore structure it forms plays a vital role in controlling its swelling ability (Alonso et al., 1999; Gens and Alonso, 1992).

2.5 EFFECT OF TEMPERATURE ON THE PERFORMANCE OF BENTONITE BUFFER

Youssef et al. (1961) studied for the first time the influence of temperature on physical parameters such as the Atterberg limits and soil's compaction properties. They indicated that increasing temperature would result in reduced liquid Limit and plastic limit. Laguros (1969) performed a variety of related experiments on kaolinite, illite, and montmorillonite and found that increasing temperature led to lower liquid levels and plastic levels. The effect of heating on the features of soil plasticity also depends on the mineral type of clay (Wang et al. 1990). The plastic limit shift is not necessarily equivalent to the liquid and plasticity index. Soils containing kaolinite have lower temperature tolerance than those containing montmorillonite, which are the main minerals in the clay. Therefore, when compacted soils were heated to a certain degree, the plasticity of soil and clay minerals could change. Howver, the study conducted by Towhata et al. (1993) concluded that after repeated kaolinite experiments, the temperature did not substantially impact the Atterberg limit (with temperatures varying from 20 to 400°C). Elevated temperature influences index, physicochemical, and the hydromechanical properties of the compacted bentonite buffer (Yilmaz, 1999, Villar and Lloret, 2004). Ye et al. (2012a); Ye et al. (2012b); Ye et al. (2009); Romero et al. (2003); Cho et al. (2000); Volckaert et al. (1993) reported the change in the initial suction, swelling pressure, water retention capacity and volumetric change of soil samples due to variation in temperature. The range of temperature selected in this study is decided based on the design temperature of nuclear waste repositories of different countries reported in the literature (Table 2.2).

2.5.1 Effect of temperature on Index Properties of Bentonite

The percentage of clay content and percentage montmorillonite content of different expansive clays that are reported by various researchers is tabulated in Table 2.3. Fig. 2.3 presents the effect of elevated temperature on the liquid Limit of bentonite. It is clear from the graph that the liquid Limit of bentonite decreases with an increase in temperature. Results reported by Yilmaz (1999) and Wang et al. (1990) were after 24 hrs of heating on bentonites, and Tan et al. (2004); Majed et al. (2001); Jefferson et al. (1998) reported results on montmorillonite rich soils 24 hrs of heating. However, the results reported by Estabragh et al. (2016) are considered after 7 - 30 days of heating of bentonite (for comparison).

Table 2.2 Maximum temperature of repository reported by different countries (Karnland, 1997; Wang et al., 1990, 2008; Delage et al. 2010; Posiva 2006; Cho et al., 2012)

SN	Country	Maximum designed temperature (°C)
1	China	90
2	France	90
3	Sweden	95
4	Korea	98
5	Belgium	100
6	Canada	100
7	Finland	100
8	Switzerland	160
9	Germany	200

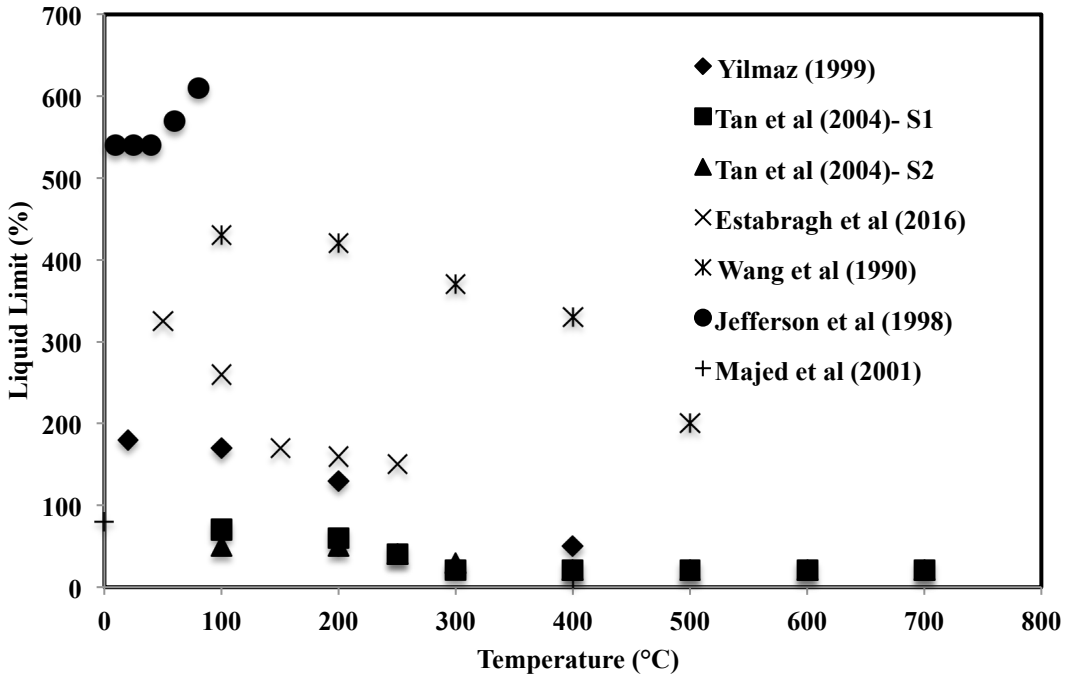

Fig. 2.3 Variation of liquid Limit with the temperature of different montmorillonite rich clays reported in the literature.

Table 2.3 The percentage of clay content and percentage montmorillonite content of different expansive clays that are reported by various researchers

Sr No	Author	Name of Bentonite	Clay Content (%)	Montmoril-lonite content (%)
1	Yilmaz (1999)	Bentonite	75	-
2	Wang et al. (1990)	Western Bentonite	85	-
3	Jefferson et al. (1998)	Wyoming Bentonite	90	-
4	Majed et al (2001)	Clay with major mineral montmorillonite	78	-
5	Tan et al (2004) - 1	Clay with major mineral montmorillonite	51	-
6	Tan et al (2004) - 2	Clay with major mineral montmorillonite	54	-
7	Villar and Lloret (2004)	FEBEX	70	90
8	Choi et al. (2007)	Bentonite	-	75
9	Wang et al. (2008)	Western Bentonite	-	74
10	Sharif et al. (2010)-K	Kunigel	75	64
11	Sharif et al. (2010)-S	Superclay	87	85
12	Villar et al. (2010)	FEBEX	-	93
13	Yilmaz (2011)	bentonite	75	-
14	Ye et al. (2014)	GMZ01 Na-bentonite	-	75.4
15	Estabragh et al (2016)	Bentonite of type Na-Montmorillonite	-	-
16	Abdelazim et al (2016)	Bentonite	-	-
17	Bag and Rabbani (2017)	Bikaner bentonite	71	-

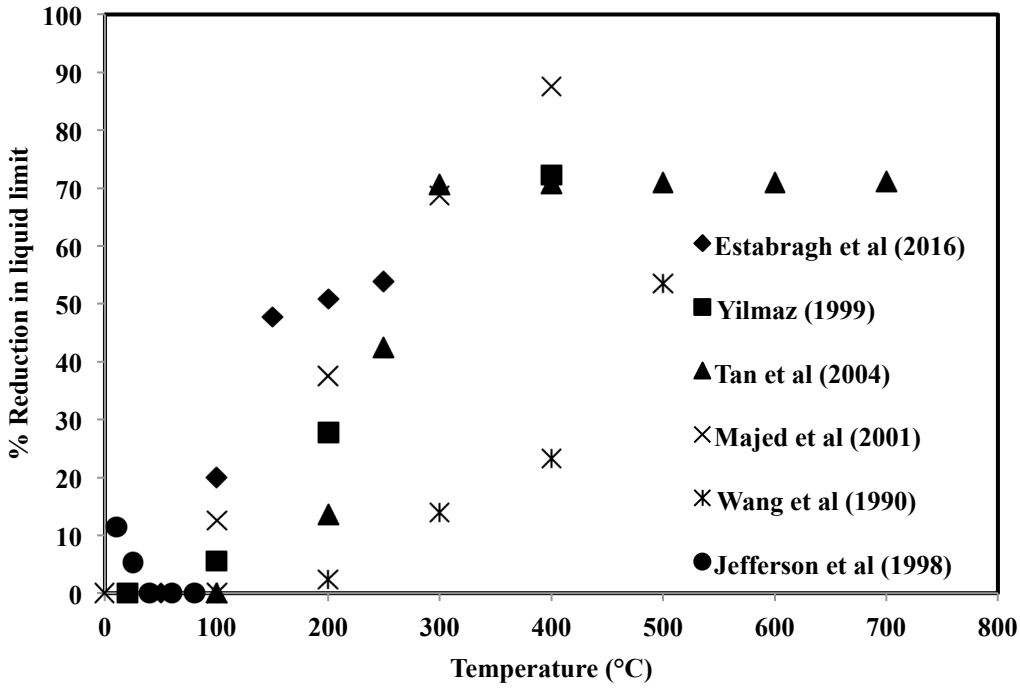

Fig. 2.4 Variation of percentage reduction in liquid Limit with the temperature of different montmorillonite rich clays reported in the literature (Estabragh et al., 2016; Tan et al., 2004; Majed et al., 2001; Jefferson et al., 1998; Yilmaz, 1999; Wang et al., 1990).

Fig. 2.4 presents the variation of percentage reduction of the liquid Limit with temperature. The results reported by Estabragh et al. (2016) showed that at a temperature of 250°C for 30 days, the value of liquid Limit was changed to 155 % from 349.70 %, which showed a reduction of about 50 %. Wang et al. (1990) observed that the liquid Limit of western bentonite was reduced by 13.9% with an increase in temperature from 100°C to 300°C. The reported clay content of western bentonite is 85%. Comparatively, Yilmaz (1999) observed that the liquid Limit of Na-bentonite reduced by 27.8%, with an increase in the temperature from 20°C to 200°C. This bentonite has a clay content of 75%. It is evident from the data presented in Table 2.3 and Fig. 2.4 that the clay having lesser clay content showed a more percentage reduction in the liquid Limit.

Table 2.4 shows the effect of temperature on the plasticity index of bentonite. As the liquid Limit decreased with an increase in the temperature, and the plasticity index is the difference between the liquid limit and plastic limit, the plasticity index showed a decreasing trend.

Table 2.4 Variation of plasticity index with a temperature of different bentonite reported in the literature.

Sr No	Temperature	Plasticity Index	
		Yilmaz (2011)	Estabragh et al. (2016)
1	20	120	---
2	25	---	295
3	50	---	275
4	100	110	220
5	150	---	130
6	200	70	120
7	250	---	110
8	400	0	---

The effect of high temperatures on the Free Swell Index (FSI) of bentonite is presented in Fig. 2.5. The Free Swell Index is the increase in volume of a soil, without any external constraints, on submergence in water. The results reported for the effect of temperature on the swelling index of clay differs according to different studies. Choi et al. (2007) and Estabragh et al. (2016) found that the potential of swelling reduced with an increase in the time and for a specific time, and the final swelling reduced with an increase in the temperature. However, the swelling increased initially and then decreased beyond 400°C in the case of Wang et al. (2008), whereas the percentage swelling increased with an increase in temperature in the study of Ahmed et al. (2016).

When clays come in contact with high temperatures, the absorbed water layer starts reducing (Lingnau et al., 1996). It happens in two stages (1) the removal of the absorbed layer when the temperature ranges from 100°C - 110°C. (2) the loss of adsorbed water and depletion of chemically bound OH group when the temperature ranges from 500°C to 1000°C (Chandrasekhran et al., 1969). Moreover, according to the theory of the diffused double layer, the thickness of the diffused double layer depends on the dielectric constant of the pore solution, cation valence, and the concentration of the electrolyte. If the dielectric constant decreases, the thickness of the diffused double layer decreases (Mitchell, 1993).

Fig. 2.6 shows the variation of elevated temperature on the specific gravity of smectite soil reported by Tan et al. (2004). With the increase in temperature, the specific gravity of both smectite soils is found to be reducing. The reduction is gradual up to 400°C, after which the decrease is slow at 500°C and 600°C, and at 700°C and 800°C, it becomes almost constant. The probable reason for the reduction in the specific gravity is

due to the loss of adsorbed water of bentonite clay particles. The density of individual clay particles might have reduced, which led to a decrease in specific gravity.

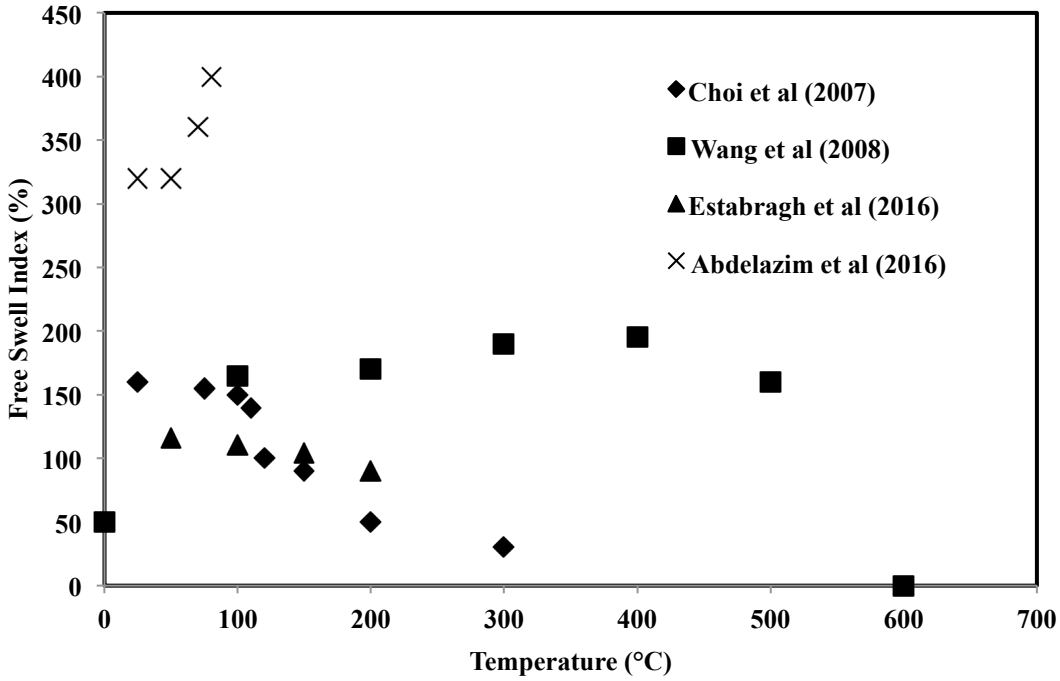

Fig. 2.5 Variation of the free swell index with a temperature of different bentonites reported in the literature

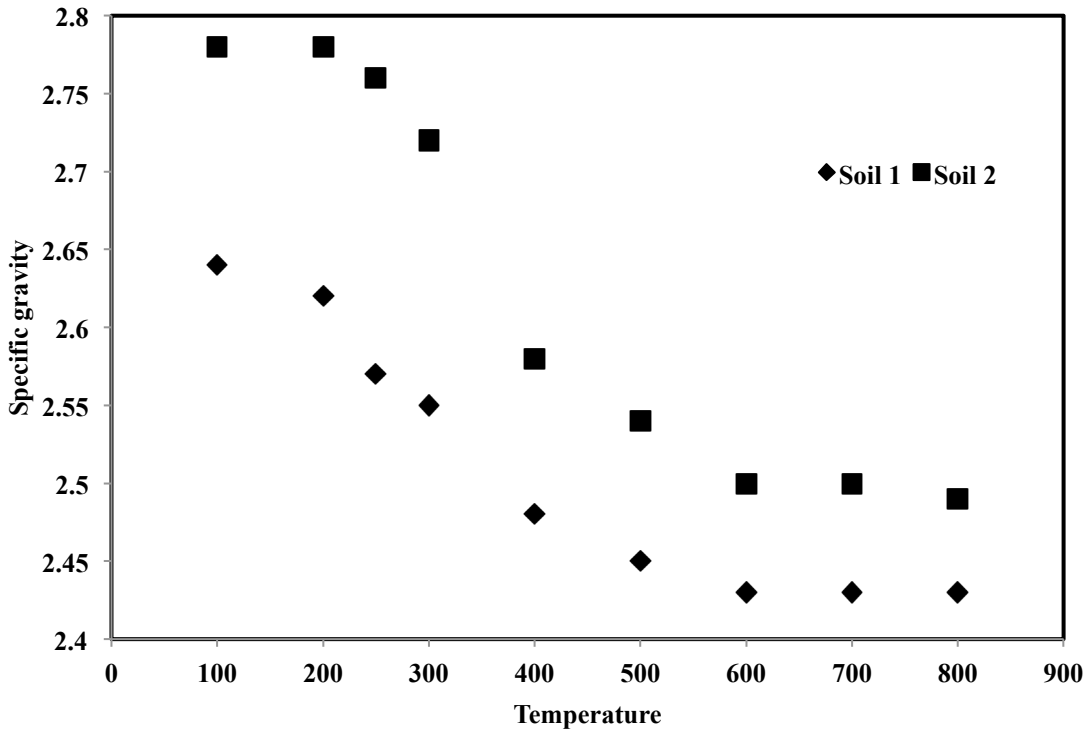

Fig. 2.6 Variation of specific gravity with the temperature of different montmorillonite-rich clays reported in the literature by Tan et al. (2004).

Yilmaz (2011) reported the effect of high temperatures on properties such as clay content, silt content, cohesion, an angle of internal friction, the activity of clay, and these are presented in Fig. 2.7 & 2.8. According to reported results, the activity, cohesion, and the clay content of bentonite decrease with an increase in temperature; however, the silt content and angle of internal friction increase with an increase in temperature. If the pore water contains salts, it may form precipitation in the pores when the water is evaporated at high temperatures. It blocks the particle-to-particle contacts reducing the cohesion between the particles (Zhang et al., 2004).

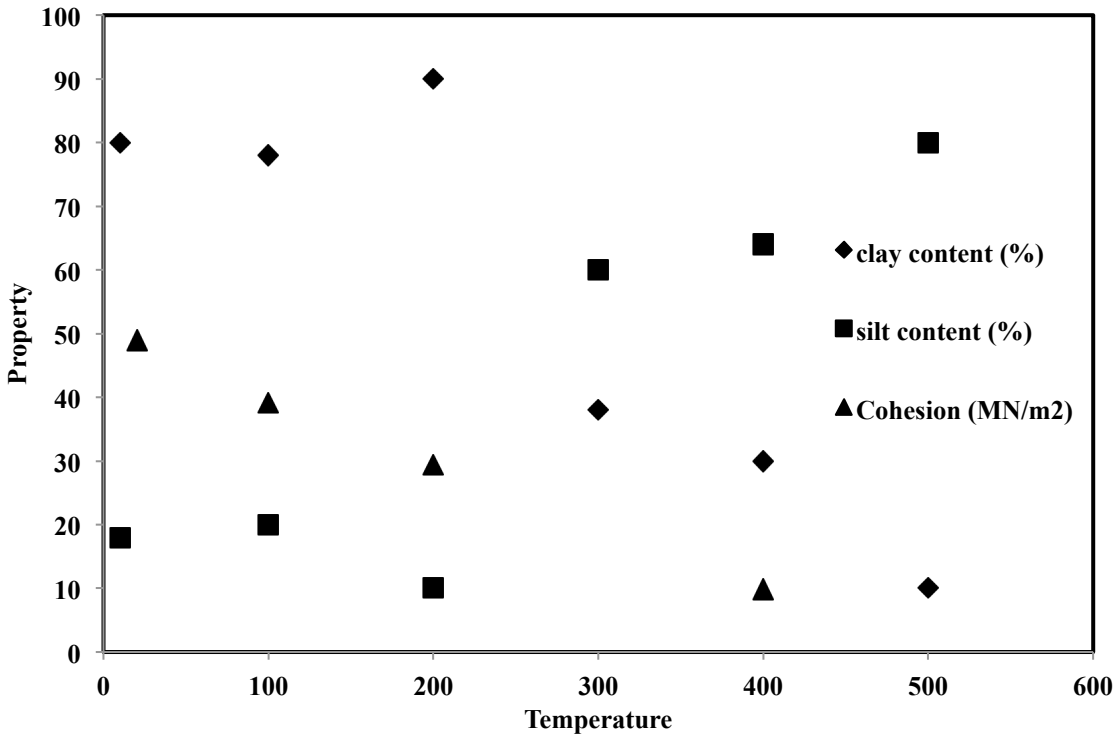

Fig. 2.7 Variation of cohesion, silt content, clay content of bentonite with the temperature reported in the literature by Yilmaz (2011).

The effect of temperature on optimum moisture content and maximum dry density has been reported by Estabragh et al. (2016); Tan et al. (2004); Majed et al. (2001) stated that with an increase in temperature, the optimum moisture content decreased whereas the maximum dry density increased which can clearly be seen from Fig. 2.9 & 2.10. The optimum moisture content was less affected at a temperature up to 100°C. From 100°C to 400°C, there was a drastic decrease in the optimum moisture content. Again after 500 °C, the decrease was very slight, and in the case of Tan et al. (2004), it was constant after

500 °C. Tan et al. (2004) – S1 observed that the optimum moisture content of montmorillonite-rich clayey soil was reduced by 52.8% with an increase in temperature from 100°C to 400°C. The reported clay content of the clay is 51%.

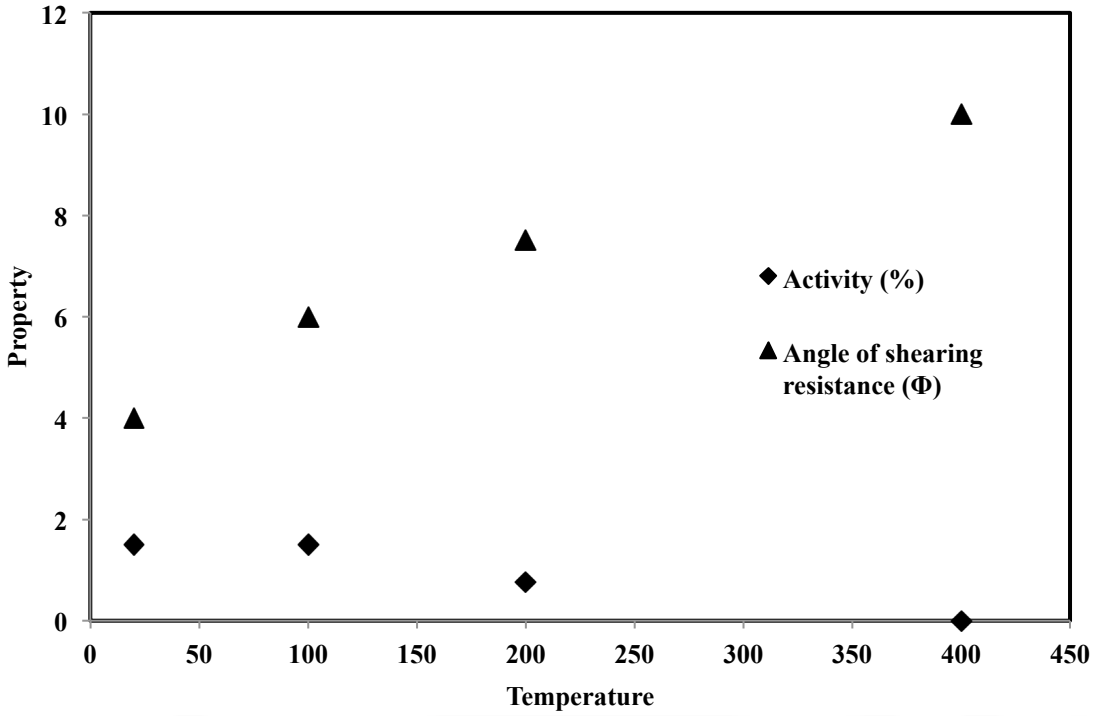

Fig. 2.8 Variation of activity and angle of internal friction of bentonite with the temperature reported in the literature by Yilmaz (2011).

Comparatively, Majed et al. (2001) observed that the optimum moisture content of bentonite was reduced by 68.8%, with an increase in the temperature from 100°C to 400°C. This bentonite has a clay content of 78%. It is evident from the data presented in Table 2.3 and Fig. 2.9 that the clay that had more percentage of clay content showed a lesser percentage reduction in optimum moisture content. As the temperature increased, the rearrangement of clay particles occurred. The more it subjected to the temperature for a longer duration, the more the soil structure got disturbed. Hence the moisture carrying capacity of the clay was reduced. However, the maximum dry density showed an increasing trend in all the reported studies. Tan et al. (2004) – S1 observed that the maximum dry density of montmorillonite-rich clayey soil increased by 14.9% with an increase in temperature from 100°C to 250°C. The reported clay content of the soil type was 51%. Comparatively, Majed et al. (2001) observed that the optimum moisture content of bentonite increased by 10.4% with an increase in the temperature from 100°C

to 200°C, with the clay content of 78%. It is evident from the data presented in Table 2.3 and Fig. 2.10 that the clay having more clay content showed a lesser percentage increase in the maximum dry density.

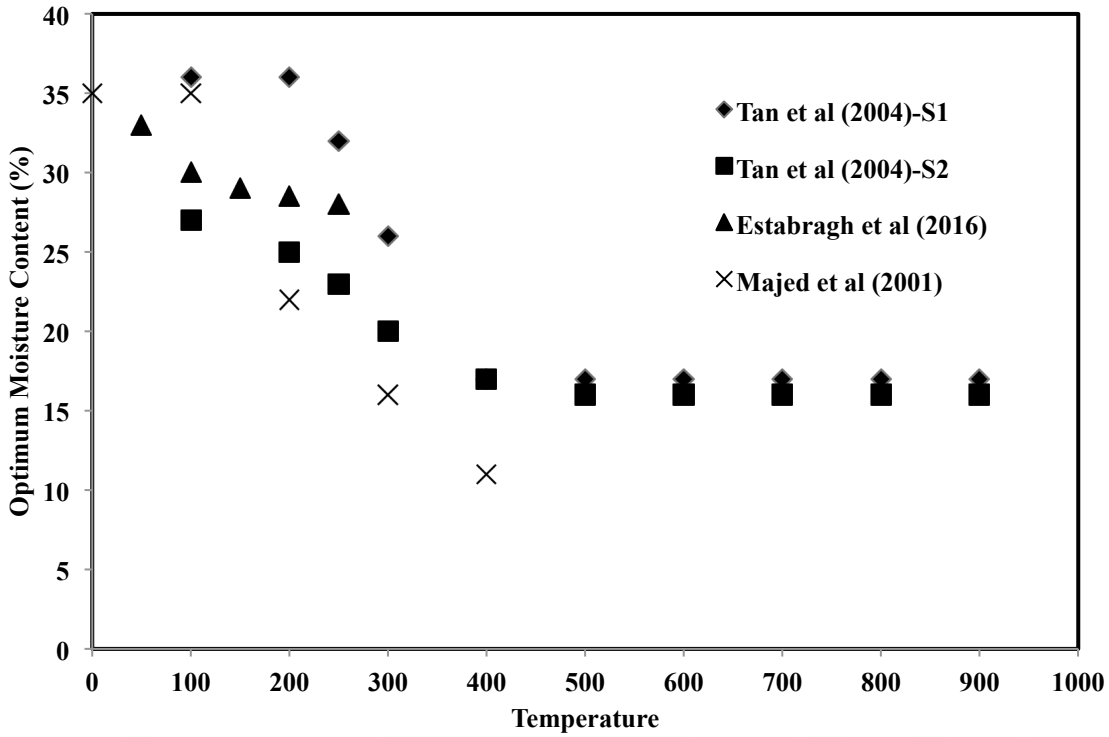

Fig. 2.9 Variation of optimum moisture content with a temperature of different montmorillonite rich clays reported in the literature.

In the deep geological repository, depending upon the major radioactive element in the waste, the temperature of the canister will be high for long durations, and it will reduce gradually. All past studies in the literature were reported on the heating treatment of 24 hrs except Estabragh et al., (2016). The study reported the influence of thermal history on the index and physicochemical properties of bentonite. The selected temperature range was 50°C to 250°C for various time intervals. It was observed that the liquid Limit, Plastic Limit, free swell index, optimum moisture content, the specific surface area of the bentonite decreased with an increase in the temperature as well as time, whereas the maximum dry density increased. They also commented on the influence of thermal history on the swell pressure of compacted bentonite that it decreased with an increase in temperature.

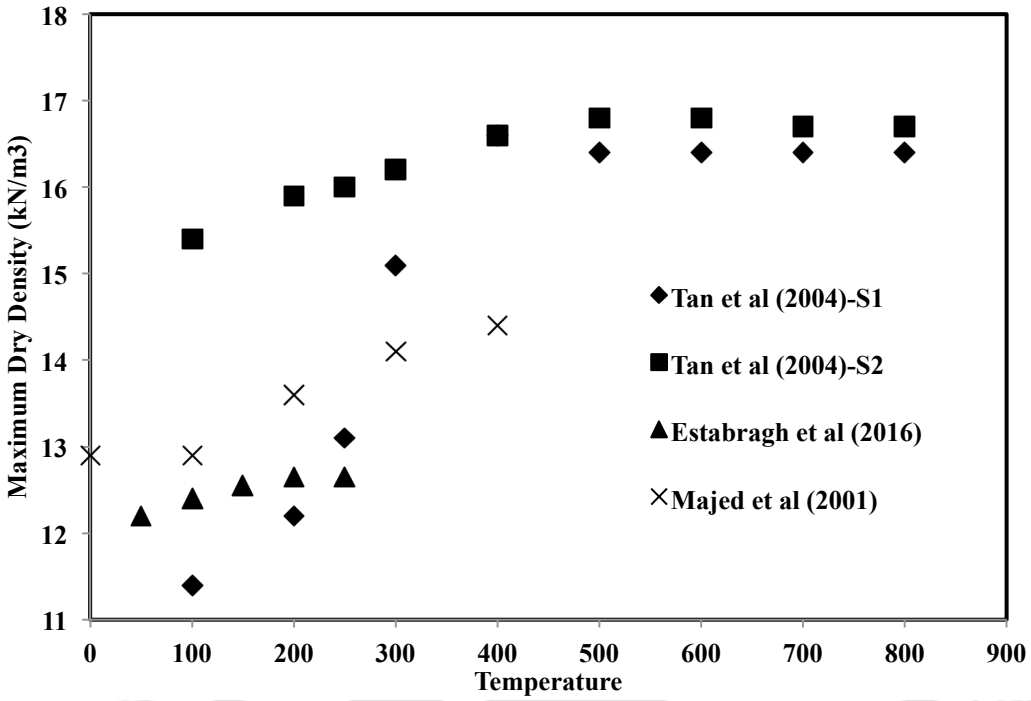

Fig. 2.10 Variation of maximum dry density with the temperature of different montmorillonite rich clays reported in the literature.

2.5.2 Effect of temperature on physicochemical properties of bentonite

Table 2.5 presents the variation of cation exchange capacity (CEC) and exchangeable sodium composition with temperature, and Table 2.6 presents the variation of pH and electrical conductivity with temperature reported by different researchers. It was observed that the cation exchange capacity of bentonite reduced with an increase in temperature. Results reported by Estabragh et al. (2016) showed a decrease in Na+ concentration with an increase in temperature. However, pH and electrical conductivity of bentonite were also showed a decreasing trend with an increase in temperature. According to Sawhney and Israel (1969), the effective negative charge on the silicate sheet of the adjacent layer of a smectite mineral reduced when it was subjected to increasing temperature, and thus prevented the entry of the cation into the adjoining layer. Hence the cation exchange capacity of the bentonite reduced with an increase in the temperature.

Table 2.5 Variation of cation exchange capacity and exchangeable sodium composition with a temperature of different bentonite reported in the literature.

Sr No	Temperature	Gu et al. (2001) CEC (mg/g)	Estabragh et al. (2016) Na+ (meq/L)
1	10	54	---
2	50	---	30.5
3	100	---	29.5
4	150	55	26.5
5	200	---	23.5
6	250	---	21
7	350	56	---
8	400	45	---
9	500	15	---
10	700	5	---
11	900	0	---

Table 2.6 Variation of pH and electrical conductivity with a temperature of different bentonite reported by various researchers.

Sr No	Temperature	Estabragh et al. (2016)	
		pH	EC(dS/m)
1	50	7.57	6.54
2	100	7.56	6.52
3	150	7.54	6.51
4	200	6.55	5.56
5	250	6.54	4.5

2.5.3 Effect of temperature on hydromechanical properties of bentonite

Fig. 2.11 shows the effect of temperature on the swell pressure of expansive clays. All reported results were taken at a density of 1.58 - 1.6 gm/cc. The swell pressures of different expansive clays and bentonites are the function of temperature. It was observed by some of the researchers (Estabragh et al., 2016; Ye et al., 2014; Cho et al., 2010; Villar and Lloret, (2010, 2004); Lloret and Villar, 2007; Majed et al., 2001) that the swelling capacity of expansive clays especially bentonites decreased with an increase in the temperature, however, the exact opposite trend was reported by some other researchers (Bag and Rabbani, 2017; Shirazi et al., 2010). Expansive soils possessed the swelling capacity due to high montmorillonite content. At high temperatures, the

montmorillonite might get converted into illite, which was called illitization (Wersin et al., 2006; Wang, 1990). These results proved with the help of microstructural investigations such as X-ray diffraction and FESEM. Similar results were also reported by Lingnau et al. (1996) that the reduction in the swell pressure occurred when the temperature increased, but up to 100 °C, the bentonite did not lose its self-healing capacity.

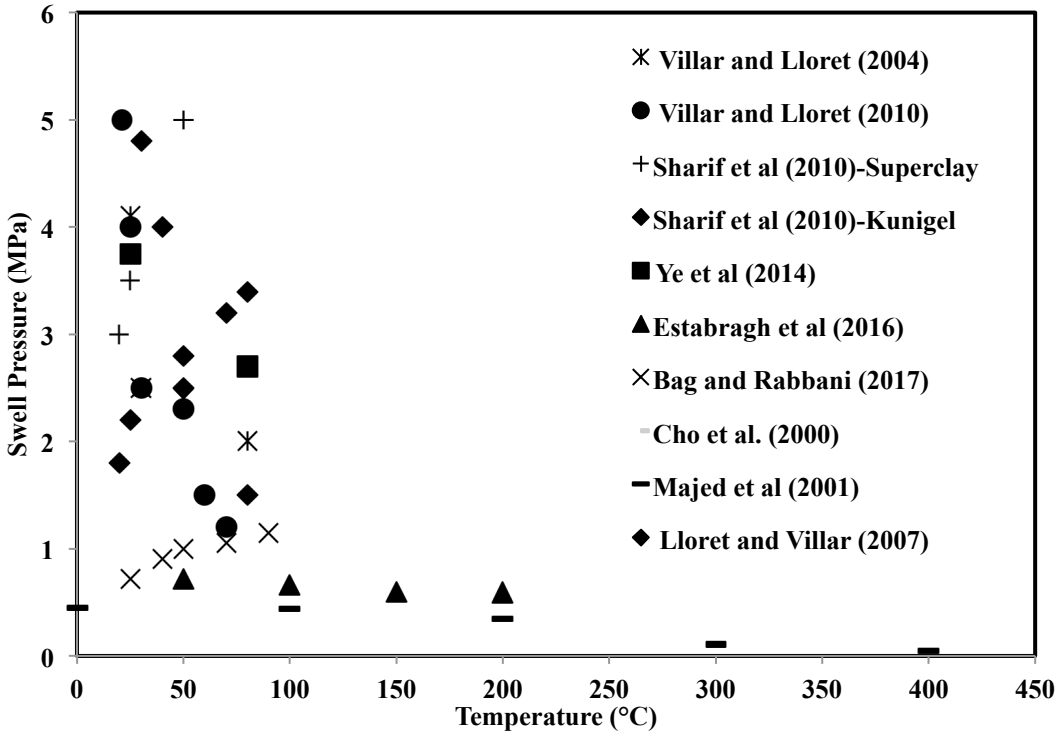

Fig. 2.11 Variation of swell pressure with the temperature of different bentonites reported in the literature.

Fig. 2.12 represents the effect of temperature on the hydraulic conductivity of bentonite. It was observed that the hydraulic conductivity showed an increasing trend with an increase in temperature (Ye et al., 2014; Lloret and Villar, 2007; Villar and Lloret, 2004; Cho et al., 2000; Cho et al., 1999). With the increase in temperature, the viscosity of the pore fluid increased, triggering the smooth flow of the fluid through pores. As mentioned earlier, the swelling potential and cation exchange capacity reduced when the temperature increased. Due to loss of swelling potential and cation exchange capacity, it created an easy path for pore fluid to flow. Hence the permeability of compacted bentonite was found increasing when samples were subjected to elevated temperatures (Ye et al., 2012a; Ye et al., 2009; Abuel, 2006).

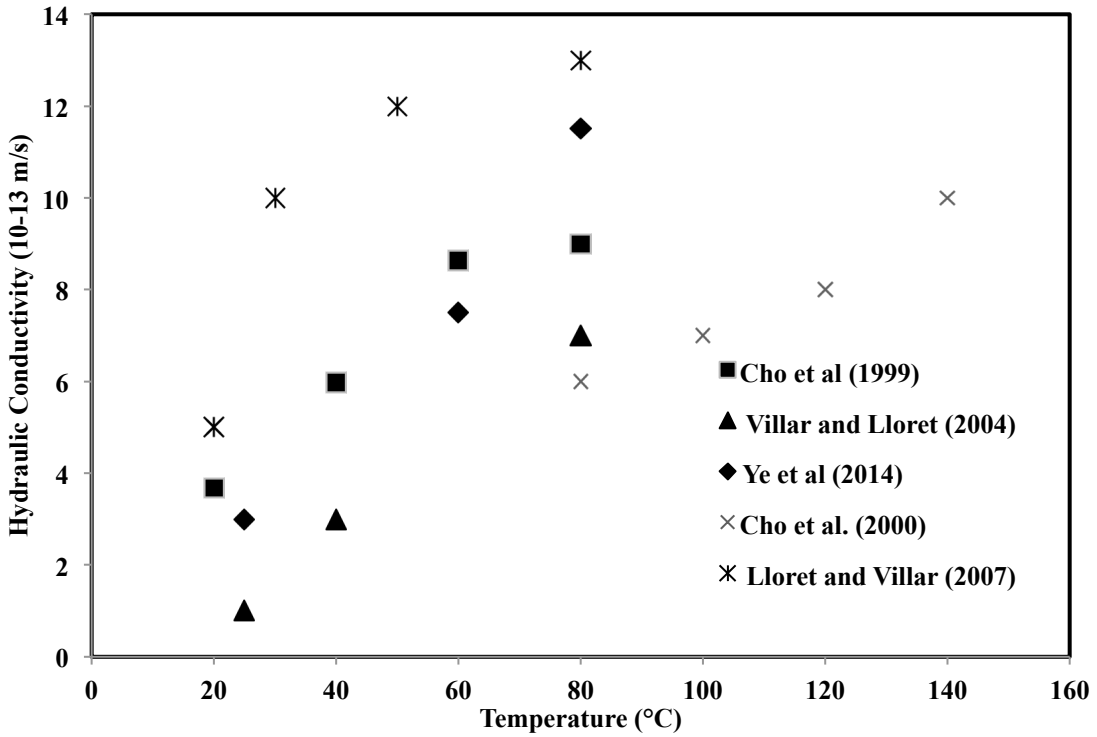

Fig. 2.12 Variation of hydraulic conductivity with the temperature of different bentonites reported in the literature.

A recent study reported by Estabragh et al. (2016) on the influence of thermal history on the swell pressure of compacted bentonite revealed that the swell pressure of compacted bentonite decreased with an increase in the temperature. These changes were attributed to the variations in density of compaction and the high temperature at which the samples were subjected. It was reported by Wersin et al. (2007) that the smectite might be slowly transformed to illite upon heating, and the illitization process reduced swelling capacity and plasticity of the bentonite material. This process can be schematically described by the reaction:

Na − smectite + K+ + Al3+ → illite + Si4+

Various researchers have tried to correlate different factors for the conversion of smectite to illite. According to Huang et al. (1993), the smectite may be converted into illite in the presence of high temperature, the time at which the smectite is exposed to high temperature and the K^+ ion concentration in the porewater chemistry whereas the type of interlayer cation, swell pressures (Eberl et al., 1978). The study reported by Meunier et al. (1998) suggested that the illitization reaction depends mainly on the time-temperature history.

2.5.4 Thermal History

The hot canister surrounded by the buffer experiences a continuous heating effect until the radioactivity of the active element reaches more than its half-life decay. It takes thousands of years to end the activity of the radioactive element, and thus, the experience of heating continues. This temperature reduces with time, and hence this change in temperature induces a thermal history on the compacted bentonite. Very few studies reported the importance of thermal history and its influence on the expansive clays (Estabragh et al., 2016).

2.6 SWELLING OF BENTONITE

According to Komine and Ogata (1996), the swelling mechanism of compacted bentonite is due to the moisture adsorption of interlayers of montmorillonite that forces it to swell. It has the ability to swell under constant volume conditions. When the volume is restricted, the bentonite tries to swell as much as it can without letting the overall volume to increase. Therefore the pressure caused by this process is known as swelling pressure. The swelling can occur either in uniform directions or in random orientations depending upon certain conditions such as compaction density, temperature, saturated solution, pore chemistry, etc. The swelling occurs due to the surface tension that is present inside the soil sample being unsaturated in nature, the ion concentration of saturating fluid and the ions present in the soil, due to the presence of weak Van der Waals forces between the montmorillonite sheets, and when it comes in contact with the saturating fluid, the repulsion between montmorillonite sheets occurs swelling and due to the exchangeable cations which get attracted towards the negatively charged clay surface, expanding the diffused double layer volume (Mitchell and Soga, 1993).

The swelling behavior of bentonite buffer is extensively studied during the past few years, and lots of models and theories are developed to understand the swelling mechanism of the bentonite buffer in DGR conditions (Rao and Ravi, 2013; Lee et al., 2012; Tripathy et al., 2004). Previously reported studies experienced an elevated temperature due to the high-temperature waste canister and the inside conditions in DGR (Estabragh et al., 2016). The expected range of temperature of waste canister was reported as 80-200°C in past studies. Laboratory swelling pressure tests have been carried out on bentonite by many researchers. The experimental results showed that the swelling properties could be influenced by many factors, such as temperature, initial dry density, chemical composition of pore water, Montmorillonite/void ratio (M/e) ratio, etc.

(Zhu et al., 2015; Rao and Ravi, 2015; Siddiqua et al., 2011; Baille et al., 2010; Schanz and Tripathy, 2009; Castellanos et al., 2008; Tripathy et al., 2004; Musso et al., 2003; ENRESA, 2000; Karnland, 1997; Dixon et al., 1996; Komine and Ogata, 1996; Di Maio, 1996).

Temperature variations can induce various changes in the soil-water system and affect its engineering behavior (Estabragh et al., 2016; Abuel et al., 2005; Villar and Lloret, 2004; Tan et al., 2004; Delage et al., 2000; Towhata et al., 1993). Lingnau et al. (1996) presented the first publication of results on the performance of saturated buffer at elevated temperatures up to 100°C and reported some changes in the stress-strain behavior of the buffer at high temperatures up to 100°C. It had been observed that heating of soils could cause porewater pressure development and altered the swell pressure values of soils. Results reported by Lambe and Whitman (1969) and Wang et al. (1990) showed that heating reduced the swelling index of an expansive soil, which may convert an expansive soil to non-expansive soil, and the process is called illitization. The montmorillonite rich soil can be converted into the water-resistant material when heated up to 360°C (Gupta and Dutta, 1967). Beles and Stanculescu (1954) observed the reduction in swelling when a loess soil is heated up to 800°C. Wohlbier and Henning (1969) performed a swell test on Zettlitz kaolin and concluded that it did not swell when soaked in water at 400°C. A drop in swelling pressure was observed in the soil with smectite as its major clay mineral when heated up to 400°C (Abu-Zreig et al., 2001). Lloret and Villar (2004) observed that the reduction in swelling strain due to increase in temperature decreased by increasing vertical load. When the high-level radioactive waste canisters are disposed of in the deep geological repository, the initial temperature of the canister is very high (up to 200°C), and it reduces to 80-50°C (Estabragh et al., 2016) by the time depending upon the decaying life of the dominating element in the radioactive waste (Gibb, 1999). High-level wastes may take hundreds of thousands of years to decay and to reduce the high temperature to become harmless (Ramana et al., 2001). Therefore the impact of continuous high temperature inside the repository creates a thermal history on the compacted bentonite buffer, which alters its physicochemical and hydromechanical properties (Estabragh et al., 2016).

2.7 EFFECT OF HYPERALKALINITY ON BENTONITE

A layer of cement or a concrete bulkhead (Ceuvas et al., 2006; Pusch et al., 2003) is a part of the multi-barrier system that may be used either as a massive embedding (Bao et al., 2016; Dauzeres et al., 2010) or in the vaults as a backfill (Vasconcelos et al., 2018) or as mechanical support to a repository and backfilling of cavities (Watson et al., 2013; SKB, 2011) or to support the access galleries and in the final sealing of the access routes (Bao et al., 2016). The presence of cement in the concrete layer comes in contact with the moisture that percolates from the host rock and creates an alkaline environment (pH>12) inside the repository. The continuous degradation of cement produces highly alkaline fluids and may try to diffuse through the compacted bentonite buffer and alter the properties such as swell pressures, permeability, and may control the reactive transport mechanism through the compacted bentonite (Jenni et al., 2017; Torres et al., 2013; Zhu et al., 2013). The alkaline pore fluids may enhance the chances of solubility of radioactive elements (Hummel and Schneider, 2005).

The hyperalkaline fluids arising from the cement will react with the bentonite buffer altering its original properties (Zhu et al., 2013; Nakayama et al., 2004; Andersson et al., 1989). Various studies were reported in the past on the effect of alkaline solutions on the swell pressure of compacted bentonite (Komine et al., 2009; Lloret and Villar, 2007). The interaction of hyperalkalinity with expansive clay was experimentally studied by Pusch et al. (2003). Series of experiments were run to see the effect of cement water on the behavior of compacted bentonite. It was noted that the interaction of saturated cement water showed a slight drop in hydraulic conductivity and a small variation in the dissolution of minerals. To investigate the interaction of ordinary Portland cement with Opalinus clay, Jenni et al. (2018) performed series of experiments and reported that the porosity at the cement clay interface changed, and the pores were clogged by reactive transport of diffusive solute fluxes and various reaction kinetics. Cuisinier et al. (2008) studied the influence of the hyperalkaline environment on the properties of bentonite buffer material. Saturated cement water was passed through samples for a time span of 3, 6, and 12 months and microstructural observations were performed before and after the circulation of the cement water. It was observed that the circulation of cement water increased the macropore void ratio 1.5 times for the MX-80 bentonite. Not only the experimental series was performed, but also a modeling of cement clay interaction was also reported in previous studies by some of the researchers.

Watson et al. (2013) reported a reactive transport model of a large-scale, in situ, long-term cement/clay system. It was reported that the ion exchange played an important role, and the dissolution of portlandite, calcite, and ettringite in the concrete and the precipitation of calcite on the concrete clay interface and dissolution of clay minerals was observed. Savage et al. (2002) modeled the reaction transport between the bentonite and cement pore fluids by using PRECIP. Minerals were allowed to dissolve and precipitate with the help of the reaction mechanism. Analyses were carried out with the combinations of various cement pore fluids compositions, rates of growth of minerals, dissolutions of minerals such as montmorillonite, the solubility of minerals, etc. It was studied that the transport of pore liquids through the compacted bentonite was the main reason for the alterations that was occurred. Along with the experimental studies, some of the researchers had modeled the reactive transport through the compacted particular bentonites (Navarro et al., 2017; Ye et al., 2016; Savage et al., 2002). Various studies were reported in the past to understand the swelling mechanism of bentonite under the influence of highly alkaline solutions (Ye et al., 2014a; Karnland et al., 2007). He et al. (2019) observed the reduction of swell pressure when the compacted bentonite comes in contact with the highly alkaline fluids. The reduction in swell pressure of GMZ bentonite when reacted with a highly alkaline cement solution was reported by Sun et al. (2018), and it is essentially due to the montmorillonite dissolution and the precipitation of secondary minerals. Furthermore, concrete degradation generates a diffusive alkaline plume, which can affect the swelling and transport properties of the bentonite, as well as the properties of the adjacent host rock and groundwater. Many studies have been performed in order to study the influence of alkaline media on bentonite (Fernández et al., 2014).

Results from Ye et al. (2016) showed that the alteration of bentonite was expected to be significant for reaction with KOH solutions at 80°C, during which some cementitious material was produced, leading to kaolinitization. Generally, the hyperalkaline solution (pH > 12) mainly consists of hydration cations (Na^+, K^+, etc.) and OH^- anions, which can reduce the swelling capacity of compacted bentonite to a great extent (Chen et al., 2016; Karnland et al., 2007). According to Bauer and Velde (1999) and Bauer and Berger (1998), the smectite reacts to form an illite/smectite mixed layer in potassium alkaline medium (KOH_4 M) up to 80°C. But the formation of mixed-layer phases is an intermediate step in a series of processes of dissolution-precipitation. Such interactions can alter the mineralogical composition and, in particular, the swelling properties and

hydraulic conductivity of bentonite, and thus the long-term performance of the engineered barrier system (Herbert et al., 2008). Kaufhold and Dohrmann (2010) reported that their reversible K^+ fixation could induce the loss of swelling capacity when contacting KCl solutions for bentonite for five months at 60°C. At the same time, K^+ might be put into smectite for lower temperatures (Karnland and Birgersson, 2006). While working on the effects of pH or salt solutions on swelling properties of compacted bentonite has proliferated (Ye et al., 2014a), there is little effort to examine the exchange of ions and mineral dissolution by salt / alkaline solutions and their impact on bentonite's swelling properties, particularly for salt / alkaline solutions containing K^+ ions.

In the meantime, the swelling activity also led to the hydration cation ion exchanges from the solution accompanied by hydration with water molecules. In addition, the swelling properties were influenced by the repulsive forces between different particles and the osmotic pressure in the micro-pores due to variations in saline solution concentrations (Musso et al., 2003). Subsequently, certain non-swelling minerals grew, and then the potential for swelling decreased. The dry density of compacted bentonite, its montmorillonite content, solution concentration, and temperature might influence this process (Wersin et al., 2007; Nakayama et al., 2004). The swelling pressure of compacted bentonite decreased with increasing NaOH concentration, associated with high ionic strength and dissolving montmorillonite and silicate minerals, was found by Chen et al., 2016; Ye et al., 2014b; Fernández et al., 2013; Castellanos et al., 2008; Karnland et al., 2007; Bauer and Velde, 1999). The results indicate that montmorillonite was no longer stable at intense alkaline solutions (pH > 12); hydroxy anions compete strongly against other anions, and their reactivity causes the destruction and degradation of many silicate minerals to break off and disintegrate (Siddiqua et al. 2014; Taubald et al. 2000). The alkaline pore fluids may enhance the chances of solubility of radioactive elements (Gaucher and Blanc, 2006). As the swell pressure of compacted bentonite varies when it comes in contact with the hyper alkaline solutions as well as when there is an increase in the temperature, it is essential to study the combined effect of temperature and hyperalkaline solutions on the swell pressure of bentonite. As the compacted bentonite undergoes temperature variation due to the high-temperature of the waste canister, it is subjected to thermal history. Therefore it is essential to know the effect of hyperalkaline solutions under the influence of thermal history on the compacted bentonite.

2.8 EFFECT OF IRON CORROSION ON BENTONITE

The buffer surrounding the waste canister continuously experiences high temperatures due to active radionuclides. This temperature reduces over the period of time, depending upon the half-life of the radioactive element. When the canister is installed in a deep geological repository, the temperature of the canister is too high (150°C -200°C, Villar et al., 2016). This temperature reduces over a long period of time, i.e., after 100's to 1000's years, which creates a thermal history on the compacted bentonite. The influence of thermal history was explained in past studies by many researchers (Estabragh et al., 2016). It was clear from the past studies that the induced thermal history is responsible for the alteration in physicochemical and hydromechanical properties of compacted bentonite, affecting its overall performance. The high-level nuclear wastes are filled in a steel canister and then placed inside the deep geological repository. The steel used in the manufacturing of canister is carbon steel because of its better durability. Some of the other advantages of selecting carbon steel that it is a non-alloy of steel and has a predictable corrosion process; its welding is easy, and its expected working life is thousands of years (Patel et al., 2012). Hence, initially, due to the high temperature (>100°C), there would be the absence of moisture near the surface of the canister and in the part of compacted bentonite, which would be near to canister surface. As the temperature goes on, reducing with time, the presence of moisture will start corroding the canister surface, and the compacted bentonite will be induced with the thermal history. Under such unstable conditions, the corrosion of the canister starts producing the leachate, which affects the overall performance of the thermally loaded buffer and may create a pathway for the reactive transport (Samper et al., 2008; Marsh and Taylor, 1998).

The corrosion of canister occurs in anaerobic conditions inside the repository (Feron et al., 2008). It not only affects the durability and long-term performance of the storage media but also the properties of bentonite by affecting its pore water chemistry, therefore, affecting its physicochemical properties.

The corrosion of the canister includes the following series of reactions:

The oxidation iron (Fe) under anaerobic conditions involves

$$Fe \Rightarrow Fe_2+ + 2e- \qquad (1)$$

Followed by the above reaction next reaction is

$$Fe + 2H_2O \Rightarrow Fe(OH)_2 + H_2 \qquad (2)$$

Where the H_2O represents the oxidizing agent for the canister the formation of ferrous hydroxide, i.e., $Fe(OH)_2$. Since the ferrous hydroxide is unstable, the further reaction is -

$$3Fe(OH)_2 \Rightarrow Fe_3O_4 + 2H_2O + H_2 \qquad (3)$$

Where Fe_3O_4 is magnetite. According to past studies, other minerals such as siderite, green rust, maghemite, akaganeite, lepidocrocite were also reported as secondary minerals (Hill, 2016).

The formation of magnetite, hematite, and SiO_2 was produced when low alloy steel corrosion came in contact with the Boom clay at 90°C (Debruyn et al., 1991), whereas the formation of siderite and green rust was observed and reported by Legrand et al. (2000) at 90°C. Lantenios et al. (2005) observed the interaction of Fe^{3+} with compacted bentonite under pH>8 at 80°C. It was reported that the destabilization of smectite minerals occurred when the smectite contains Fe^{3+} in the octahedral sheets. The swell pressure of compacted bentonite under such a corrosive environment under the influence of thermal history is still unclear.

2.9 REACTIVE TRANSPORT THROUGH COMPACTED BENTONITE

The bentonite barrier can be surrounded by a layer of cement/concrete as structural support for access galleries, which is the source of alkaline fluid (Bao et al., 2016). In the first few hours, dissolved elements and water transfer to bentonite from the fresh cement paste. Later the deterioration of the concrete lining of galleries after thousands of years creates an alkaline solution (pH>12) that will diffuse through the compacted bentonite buffer (Deneele et al., 2010; Savage et al., 2007). For significant changes to the smectite component, pH=12.6 seems to be the threshold value (Torres et al., 2013). Montmorillonite, the principal component of the bentonite buffer, is expected to alter under such extremely alkaline conditions created by cementitious products inside the deep geological repository. Various experiments have shown that strongly alkaline pore fluid affects the swelling properties of bentonite. However, the improved permeability and cation concentration was also reported (Cuisinier et al., 2008; Karland et al., 2007). The dissolution process of smectite under alkaline conditions was observed through mass dissolution experiments by (Sato et al., 2002; Vigil et al., 2001; Bauer and Velde, 1999). Suzuki et al. (2008) observed that smectite in the bentonite might be dissolved and facilitated harm to low hydraulic conductivities under hyperalkaline environment, but the information on improvements in bentonite mineralogy and porosity, hydraulic conductivity, or mechanical properties were minimal. Where the majority of studies had

been carried out as batch experiments with a high solution / solid ratio between bentonite and cement pore water, this work concentrates on the reactive transport of hyperalkaline solutions through the compacted bentonite.

These extremely toxic and constant heat-emitting wastes are contained in a metal canister. The choice of material for the canister depends on the country, i.e., copper, carbon steel, or stainless steel (Gate et al. 2009). However, carbon steel, i.e., non-alloy of steel, is preferred due to its defined corrosion process. For several past studies, both experimental and model reactions to the waste canister corrosion and the bentonite interface canister were documented (De Combarieu et al., 2011; Lantenois et al., 2005). The mineral instability could be explained by clay-iron interaction in all reported works. Some of the studies especially showed the formation of iron-rich smectite and the development of non-swelling mineral substances in anaerobic conditions had been recorded at high temperatures (150°C) (De Combarieu et al. 2011; Habert et al. 2006). Bildstein et al. (2006) documented the implications of porosity and reactive transport within the buffer. The reduction in swelling capacity and total external surface area and the increase in pore volume was reported by Neaman et al. (2003). The enhancement of the pH due to the presence of metallic iron was also one of the reasons for the alterations. Hence, the anaerobic corrosion of steel could also interact with bentonite in this case along with the hyperalkaline cement solution from the other end and under the influence of thermal gradient. However, the long-term success of compacted bentonite as the buffer material relies on the smectite resilience against thermal and technological adjustments, from which all the significant changes inside the repository may be maintained. Hence, the aim of this study was to investigate the alteration of physicochemical and mechanical properties of bentonite through reactive transport by anaerobic corrosion of steel canister from one side along with the infiltration of hyperalkaline solution from another side under the influence of thermal gradient.

2.10 STATEMENT OF PURPOSE

According to Zheng et al. (2015), soils change their index and engineering properties when the clay soils are exposed to a high temperature. In addition to the index and physicochemical properties, high temperatures influence the hydromechanical characteristics (Karland, 1997). Abuel et al. (2005) and Towhata et al. (1993) reported a temperature effect on permeability that increased with temperature. Cho et al. (2000) reported a decrease in swell pressure of bentonite with a rise in temperature.

Nevertheless, the temperature influence on buffer properties could depend on the soil's type of clay mineral (Wang et al. 1990). Few studies are also available on the impact of thermal history on Bentonite buffer. A recent study by Estabragh et al. (2016) shows the effect of temperature over a prolonged period, which influenced its index and physicochemical characteristics. The hot canister surrounded by the buffer experiences a continuous heating effect until the radioactivity of the active element reaches more than its half-life decay. It takes thousands of years to end the activity of the radioactive element, and thus, the experience of heating continues. This temperature reduces with time, and hence this change in temperature induces a thermal history on the compacted bentonite. As the engineering behavior of the bentonite is different at room temperature and at the elevated temperature, but the buffer is expected to perform exceptionally well for the safety against radioactive and reactive transport through it. While significant resources and effort are being devoted to studying the effect of temperature on the properties of clayey and expansive soils in the past, the effect of thermal history with a duration of heating on the behavior of bentonite buffer is still unclear, and the knowledge is essential for the safe disposal of HLW.

The swelling capacity of the Bentonite buffer was extensively studied in the past few years, and several models and hypotheses have been developed in order to explain the DGR construction process of the buffer (Rao and Ravi 2013; Lee et al., 2012; Tripathy et al., 2004). The high-temperature waste canister and the conditions in DGR (Estabragh et al., 2016) allow it to reach a high temperature. In recent studies, 80-200°C were reported as the expected temperature range in waste canisters. The findings of the experiment showed that several factors such as temperature, initial dry density, the chemical composition of pore water, the ratio of Montmorillonite M/e, etc., have affected the swelling properties (Rao and Ravi, 2015; Siddiqua et al., 2011; Schanz and Tripathy, 2009; Musso et al., 2003; Karnland, 1996). When high-level waste canisters are disposed of in the deep-geological repository, the initial temperature of the canister is very high (up to 200°C) and by the time dependant on the half life of the dominant radioactive waste product, it decreases to 80-50°C (Estabragh et al., 2016). Bentonite buffers modify their original properties when reacting to the hyperalkaline fluids arising from cement (Zhu et al., 2013; Ramírez et al., 2002). Pusch et al. (2003) have experimentally investigated the interaction of hyperalkalinity with expansive clay. There was a minor drop in hydraulic conductivity and a small variation in the breakdown of minerals due to the reaction with the hyperalkaline cement water. It was confirmed that the ion exchange

played a significant role and that portlandite, calcite, and ettringite had been dissolved in the concrete, and calcite precipitation on the concrete clay interface and the clay minerals dissolution was observed. The main reason for the alterations was the conveyance of pore fluids through the compacted bentonite. In accordance with experimental studies, some investigators modeled reactive transport-compacted bentonites (Navarro et al., 2017; Savage et al., 2002). Different studies have previously been reported on the swelling pressures of compressed bentonite with the influence of alkaline solutions (Komine et al., 2009; Lloret and Villar, 2007), stating that the swell pressure decreased when the compacted bentonite came in contact with the hyperalkaline solutions. Once low alloy steel corrosion exceeded 90°C Boom Tone (Debruyn et al., 1991), magnetite, hematite, and SiO_2 are formed when Legrand et al. (2000) detected and confirmed siderite formation and green rust formation at 90°C. The $Fe3^+$ interaction with compacted bentonite has been observed by Lantenio et al. (2005) at 80°C under pH>8. It is stated that Smectite minerals have been destabilized when $Fe3^+$ is present in the octahedral layer. In such a corrosive condition, the swell strength of compacted bentonite is also uncertain under the impact of thermal experience.

The safety of the geological repository of high-level radioactive waste relies on a multi-barrier system, and bentonite buffer as part of the engineered barrier system plays a critical role. The swelling capability of bentonite is one of the features that bentonite buffer can perform its role. Bentonite buffer is expected to receive the heat from the waste canister and hydrated from host rocks. Understanding the change of swelling capability as a result of heating, hydration, and chemical changes are important for evaluating the safety of a repository. As the concrete liner is likely to be used as tunnel support in host rock like argillite, the change of swelling capability of bentonite when reacting to alkaline water coming from concrete is definitely worthwhile to investigate. Also, the influence of iron corrosion on the performance of bentonite under thermal history needs to be known. Though the influence of high temperature on swell pressure of bentonite had been studied in the past, the influence of thermal history on swell pressure of bentonite was still not clear.

The diffusion of cement water was found to increase the macroporous void ratio of bentonite to 1.5 times in MX-80 (Cuisinier et al., 2008). Several researchers have already documented in previous studies not only the experimental sequence but also a simulation of cement clay interaction as well as canister surface corrosion interaction with bentonite. A broad-scale, in situ long-term cement/clay network reactive transport

model, was published in Watson et al. (2013). Savage et al., 2003, by using PRECIP, modeled the transportation of reaction between bentonite and cement pores. With the aid of the reaction mechanism, minerals may dissolve and precipitate. Analyzes were made with the combination of different compositions of cement-pore fluids, mineral growth rates, mineral dissolution, such as montmorillonite, mineral solubility, etc. Lu et al., 2011 modeled the reactive transport of canister corrosion through compacted bentonite using ENRESA (2005). Inside the repository, the compacted bentonite layer between the hot canister and the host rock experiences the thermal gradient due to the high temperature by the canister and comparatively lower temperature by the host rock. At the same time, it also experiences the chemical gradient by hyperalkaline cement water through the host rock side and canister corrosion leachate from the other side. The study of transport through the compacted bentonite by the combined effect of thermal and chemical gradient was essential to understand, considering its long-term sustainability as a buffer material. So the study was started keeping in mind the above literature gaps. The findings of this study would provide a database useful for choosing the engineered barrier material for the deep geological repository.

2.11 OBJECTIVES

With the broad objective to study the coupled thermomechanical effect on the performance of compacted Barmer bentonite, the following sub-objectives were defined:

1. To study the effect of thermal history on the index and physicochemical properties of Barmer bentonite. The index, physicochemical properties of bentonite was studied by inducing a thermal history on the powdered bentonite samples.
2. To study the influence of thermal history and hyperalkaline solution on the swell pressure of compacted bentonite. The compacted bentonite specimens were subjected to thermal history then saturated with hyperalkaline cement water and compared with the results of specimens saturated with distilled water.
3. To study the influence of corrosion leachate on the swell pressure compacted bentonite subjected to thermal history. The addition of corrosion product was done followed by the compaction of bentonite specimen, subjected to thermal history, saturated by hyperalkaline cement water, and compared with the results

of specimens saturated with distilled water.

4. To investigate the reactive transport through compacted bentonite buffer under the influence of the thermal gradient. The fabricated lab-scale set up was used for the study. The compacted bentonite specimens were heated from one end at various temperatures and saturated by hyperalkaline cement water and distilled water from the other end.

2.12 SCOPE OF THE THESIS

The scope of the thesis is confined to the study of the thermal history heating and the ingress of hyperalkaline solution on the physicochemical and engineering properties of bentonite collection from the Barmer district of Rajasthan, India. Two different bentonites were collected and named B_1 and B_2. Both are distinguished on the basis of the cation exchange capacity. The major portion of work was on the effect of different temperatures with the length of heating on the behavior of Barmer bentonite. The purpose was also to compare the data for two bentonites with different index and physicochemical properties that are used in this work. Bentonite soil, in general, has a very high swell pressure index and is a very important property for designing the nuclear waste barrier system. Hence, the thermal history on compacted bentonite mixed with various chemicals (such as hyperalkaline and corrosion solution) was performed at varying heating temperatures, and the impact of these reactive solutions is on compacted bentonite is identified. The scope of the thesis also includes the design and fabrication of continuous heating assembly to evaluate the effect of thermal and chemical gradient on the bentonite buffer. Also, preparation of the compacted bentonite samples with different chemical (metallic iron and cement water); observation/monitoring of the index properties, physicochemical, and hydromechanical properties during the thermal history and continuous heating process and handling and analysis of the data.

Chapter 3

MATERIALS AND METHODS

Different experimental approaches were used to accomplish the stipulated objectives. The research work was carried out in different phases using various experimental setups and materials. The detailed methodology is given in this chapter.

3.1 MATERIALS

3.1.1 Bentonites

In order to accomplish the objectives, the study was proposed to carry out in different phases. Two bentonites (B_1 and B_2) from the Barmer district of Rajasthan State, India, are used in the studies (Fig. 3.1). The bentonite sample was passed through an IS (Indian Standards) 0.425-mm sieve prior to use in laboratory studies. Index, Physicochemical, and Hydromechanical properties of Barmer-1 bentonite and Barmer- 2 bentonites are reported in this study.

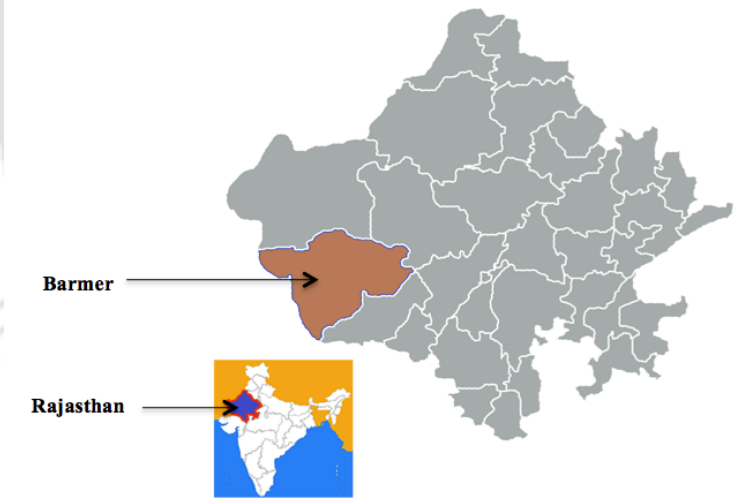

Fig. 3.1 Location of Barmer, Rajasthan, India

3.1.2 Cement

The ordinary Portland cement of grade 53 was used in this study. The fineness of cement was determined by IS 4031 (Part 1): 1996, and the value came out to be 3%, i.e., less than 10% of the material coarser than 90% sieve (Satisfies the criteria according to IS 4031 (Part 1): 1996).

3.1.3 Metallic Iron Powder

The metallic iron (Fe) powder with maximum particle size of 4 μm was used for this study.

3.2 METHODS

Phase I - Influence of thermal loading on index and physico-chemical properties of barmer bentonite

3.2.1 Determination of index and physicochemical properties

Determination of properties such as Moisture content, quantitative determination of grain size distribution, compaction characteristics, specific gravity, free swell index test, Atterberg's limit was done as per Indian Standards (IS) procedures, i.e., IS 2720 (Part 2, 1973), IS 2720 (Part 4, 1985), IS 2720 (Part 8, 1983), IS 2720 (Part 3, 1980), IS 2720 (Part 40, 1970), IS 2720 (Part 5, 1985) respectively and cation exchange capacity of bentonites was determined by the method given by Chapman (1965). The Flame photometer (Company: Thermofisher, Model no: MSA0A0104) was used to calculate the Na+, Ca+, K+ concentration, and the Atomic Absorption Spectrometer (AAS) (Company: Thermofisher, Model no: iCE 3500) was used to calculate the Mg+ concentration. The total surface area of bentonite specimen (passing IS 425 μ sieve) was determined by the Ethylene Glycol Monoethyl Ether (EGME) adsorption method (Cerato and Lutenegger, 2002). Soil samples were mixed with distilled water in the ratio 1:20 and stirred well. After keeping the suspension for one h (Appx.), the pH was measured by pH probe (Supplier: labtronics, Model no: LT 50).

3.2.2 Inducing thermal history to powdered bentonite

To study the influence of temperature on the properties of the powdered bentonite, the powdered bentonites were subjected to various temperatures and time spans, i.e., 60°C, 110°C, 150°C, and 200°C for a time duration of 3, 7, 15, 21, 28 days. The samples were taken out of the oven at the desired time span and cooled in a desiccator before used for experimentation.

Phase II - Influence of thermal loading on swell pressures of compacted bentonite

3.2.3 Swell pressure

The constant volume method given by Komine (2004) is used to determine the swell pressure of the bentonite. Air-dried specimens of both bentonites (water content = 13% (B1) and 12% (B2)) are compacted into oedometer ring (diameter = 6.1 cm; height = 2 cm) to a thickness of 8 mm (Fig. 3.2). The bentonite specimens are compacted into dry densities of 1.5 Mg/m3, 1.75 Mg/m3, and 2 Mg/m3 by keeping the volume of the specimen constant and changing the bulk mass of the specimen. The oedometer rings are mounted on swell pressure assembly consisting of a 10 kN load cell (capacity = 10 kN; sensitivity = 0.01 kN) and LVDT (maximum displacement = 20 mm; sensitivity = 0.01 mm). The wetting fluid is allowed to permeate from the bottom of the oedometer ring from a suitable height to provide the necessary head for sufficient infiltration (Fig. 3.2). As the wetting fluid permeates through the specimen, the load cell measures the pressure-induced due to the swelling of the bentonite, and the LVDT measures any induced changes in the volume. The experiment was continued until the load measured by the load cell displayed a constant value for more than 72 hours, at which the setup was dismantled. Constant reading verified the complete saturation of the specimens.

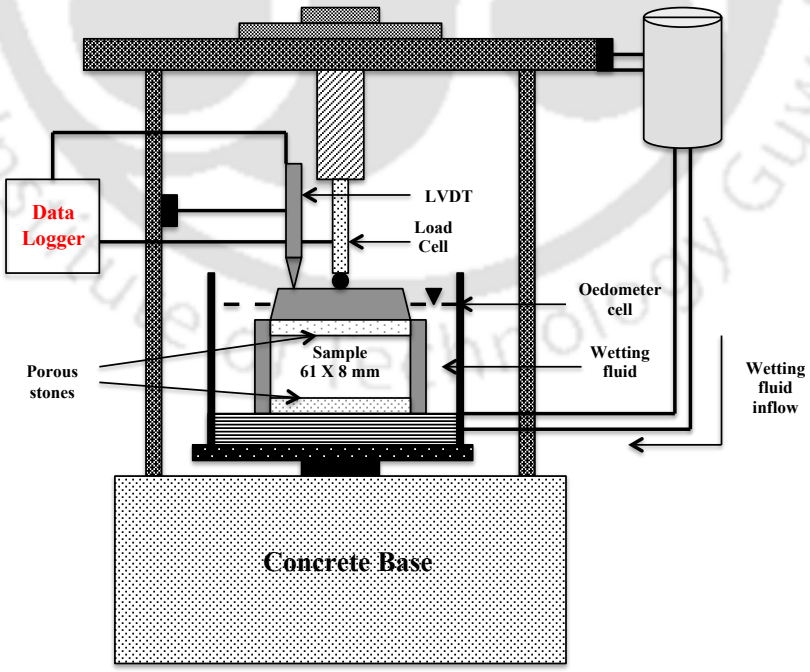

Fig. 3.2 Schematic representation of swell pressure apparatus

3.2.4 Cation Exchange Capacity

The cation exchange capacity of bentonites was determined by the method given by Chapman (1965). The Flame photometer (Company: Thermofisher, Model no: MSA0A0104) was used to calculate the concentration of Na+, Ca+, K+, and the Atomic Adsorption Spectrometer (AAS) (Company: Thermofisher, Model no: iCE 3500) were used to calculate the concentration of Mg+.

3.2.5 Inducing thermal history to compacted bentonites

To study the effect of thermal history on the swell pressure of bentonite, the compacted bentonite specimens of each density were exposed to temperatures 110°C and 200°C for about 3 hours, and results are compared with the non-heated specimen.

Phase III - Swell pressure of compacted bentonite saturated with hyperalkaline cement water at different thermal histories

3.2.6 Preparation of cement water

The ordinary Portland cement powder was mixed with distilled water in a ratio equal to 1:1 (Pusch et al. 2003). The powder was thoroughly mixed and allowed to settle so that the supernatant water could be separated and filtered. The pH value of the cement solution used in this study is 12.5, i.e., hyperalkaline solution. The chemical composition of the cement solution is listed in Table 3.1.

3.2.7 Preparation of specimen

Bentonite samples were compacted at three densities (1.5 Mg/m3, 1.75 Mg/m3, and 2 Mg/m3). The thermal history was induced to compacted samples, as mentioned in section 3.3.5, and Swell pressure was determined using the methodology mentioned in section 3.2.3.

Table 3.1 Chemical composition of cement water (mg/L)

Si	Al	Mg	Na	Ca	K	Fe	Cl	SO_4	Cu	F	NO_3	pH
218.337	44.64	0.1625	1320.453	658.285	921.225	0.2365	3.3234	1910.34	2.5318	1.4293	0.7035	12.5

Phase IV - Effect of iron corrosion on swell pressure of compacted bentonite subjected to thermal history

3.2.8 Preparation of specimen

The bentonite powder and metallic iron powder were mixed in the ratio 1:0.1 and compacted at targeted densities, i.e., 1.5 Mg/m3, 1.75 Mg/m3, and 2.0 Mg/m3. The samples were then subjected to impose thermal history at 110°C and 200°C for about 3 hours. Swell pressure was determined using the methodology mentioned in section 3.2.3.

Phase V - Effect of iron corrosion on swell pressure of compacted bentonite subjected to thermal loading in a nuclear waste repository

3.2.9 Preparation of specimen

Bentonite samples were statically compacted to dry densities 1.5 Mg/m3, 1.75 Mg/m3, and 2 Mg/m3 in stainless steel mould of 35 mm diameter and 70 mm height. The sample height was kept as 50 mm. The schematic representation of the experimental setup is presented in Fig. 3.3. The gap of 10 mm each was left from both sides so that metallic iron powder could be accommodated in the lower 10 mm gap, and a porous stone could be placed in the upper 10 mm gap (Fig. 3.3(a)). The side of the mould, which had metallic iron powder, was kept in touch with the heating plate, and the other side had an inlet through which the distilled water was passed through the sample. Both the upper and lower cover of the mould was tightly threaded so as to prevent the volumetric swelling of the specimens upon wetting. The experimental setup used in this work is illustrated in Fig. 3.3(b). To introduce the thermal gradient, the heating plate was heated at 60°C, 110°C, 150°C, and 200°C for 28 days each. After 28 days, the specimens were extracted from the mould and were cut into three equal parts vertically and two parts (outer = 10 mm and inner = 25 mm) concentrically (Fig. 3.3 (c) and 3.3 (d)). The degree of saturation of each specimen was observed after extracting it from the experimental setup. The nomenclature for the parts of a sample was given as per Table 3.2.

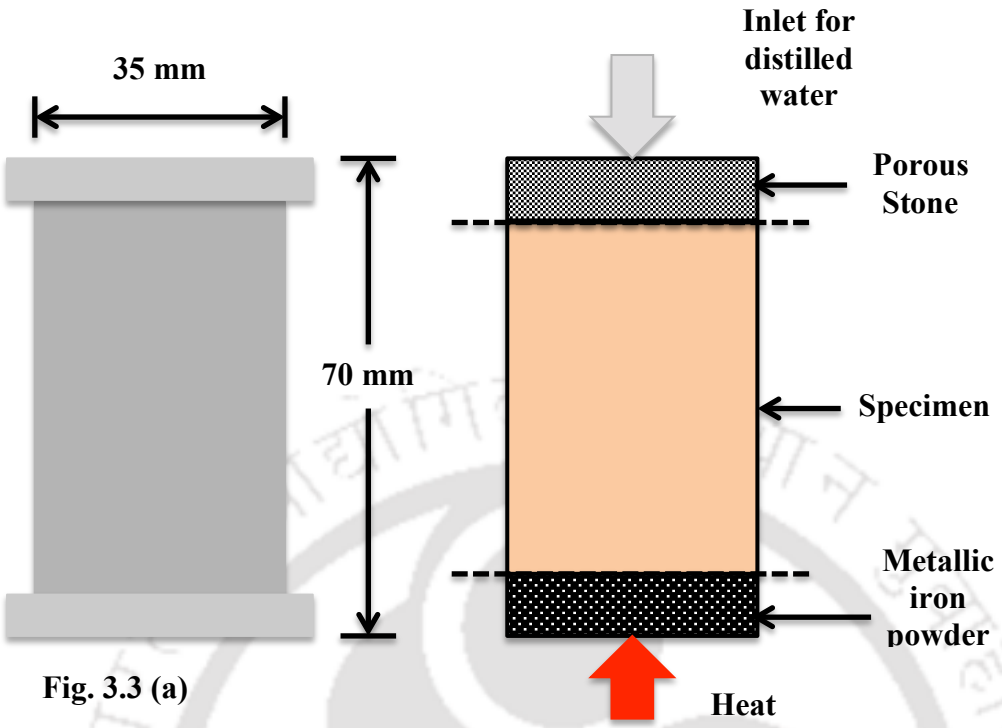

Fig. 3.3 (a)

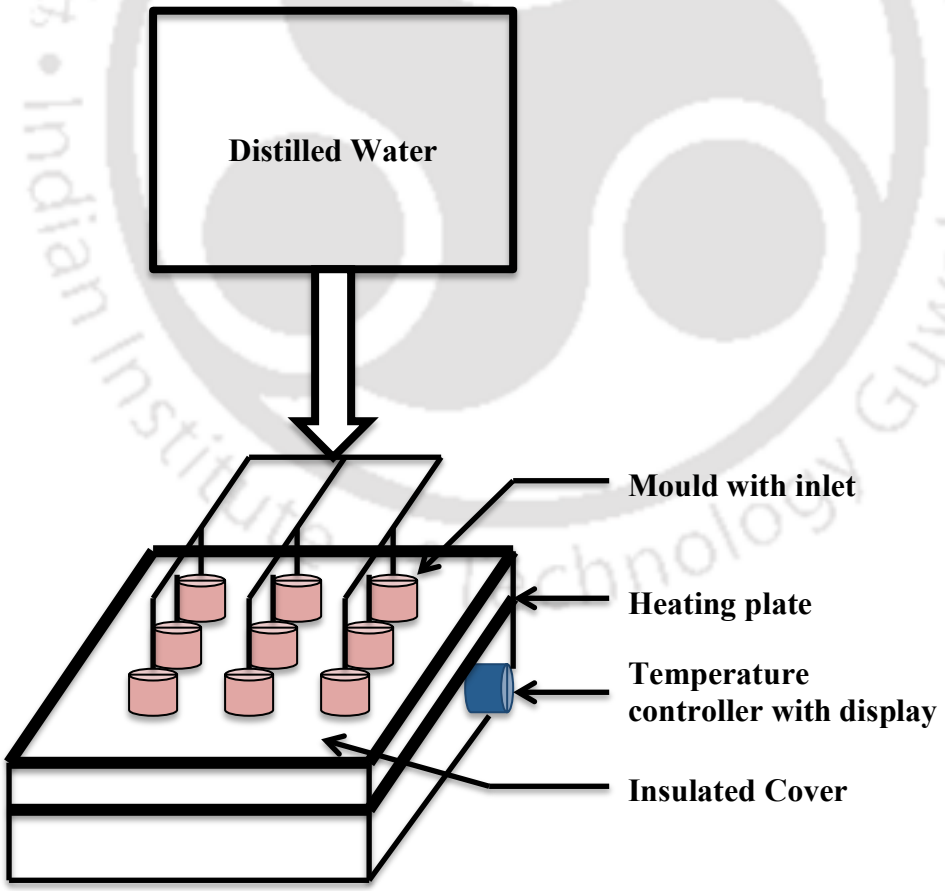

Fig. 3.3 (b)

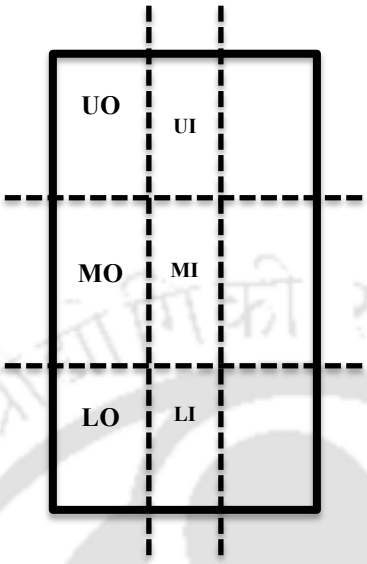

Fig. 3.3 (c)

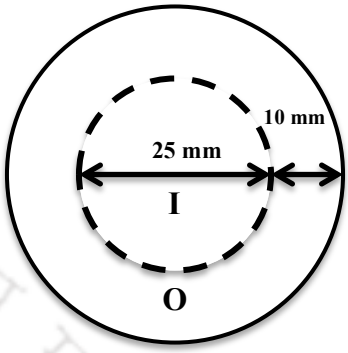

Fig. 3.3 (d)

Fig. 3.3 (a) The specimen mould and the description of a inner assembly

Fig. 3.3 (b) Lab scale set up to create thermal gradient

Fig. 3.3 (c) Nomenclature of parts of sample (vertically)

Fig. 3.3 (d) Nomenclature of parts of sample (diametrically)

Table 3.2 Abbreviations used for the sample analyses

Sr no	Part	Abbreviations
1.	Upper outer	**UO**
2.	Upper inner	**UI**
3.	Middle outer	**MO**
4.	Middle inner	**MI**
5.	Lower outer	**LO**
6.	Lower inner	**LI**

Phase VI - Effect of iron corrosion on swell pressure of compacted bentonite subjected to thermal loading in a nuclear waste repository

To satisfy the aim of this experiment, the same experimental set up and procedure that is mentioned in section 3.2.9. The only change is the wetting fluid i.e. hyperalkaline cement water that is mentioned in section 3.2.6.

3.2.10 Microstructural investigation

The microstructural investigation of the specimens after a thermal analysis was performed by observing the mineralogical alterations of both bentonites after 28 days were determined by the X-Ray Diffraction (Company: Rigaku, Model No: TTRAX III (5 kW)). The input for 2θ (Angle between diffracted X-ray with incident X-Ray beam) was ranging from 5-50° with a scanning speed of 2° 2θ/min and step size at 0.03°. The minerals present were analyzed using the expert high score. The structural changes and mineralogical formations were detected with the help of a field emission scanning electron microscope (FESEM). The chemical composition of both the bentonites is given by a non-destructive analytical technique called XRF (X-Ray Fluorescence) spectrometry. It is expressed in the percentage weight of major elemental oxides, and the analyses were performed in Gauhati University SAIF, Guwahati, Assam, India.

3.3 INSTRUMENTS USED

Following Table 3.3 shows the various instruments used for performing the analyses during this research work.

Table 3.3 Different standard instruments used in experimentation

Parameters	**Instrument**	**Company (Make/Model)**
Thermal history/moisture content	Hot air oven	Satwik scale industries
Cations (Na, Ca, K)	M controller based flame photometer with compressor	Systronics
Cations (Mg)	Atomic Absorption Spectroscopy	Thermo fisher Scientific
pH	pH system 361	Systronics
Electrical conductivity	Conductivity meter (vsi- 04 deluxe)	VSI electronics pvt. Ltd.
Swell Pressure	Swell Pressure Apparatus	Locally assembled

3.4 CHARACTERISATION OF BENTONITES

3.4.1 Physicochemical and index properties of bentonites

The physicochemical and index properties of Barmer 1 (B_1) and Barmer 2 (B_2) bentonites are presented in Table 3.4. It is understood from the data that Barmer 1 (B_1) bentonite has a higher liquid limit, plasticity index, cation exchange capacity, specific surface area, and the free swell index in comparison to Barmer 2 (B_2) bentonite.

Table 3.4 Initial characterizations of bentonite powders

Properties	Barmer 1	Barmer 2
Specific Gravity	2.79	2.77
Clay content (%)	89	76
Liquid Limit (%)	447.28	248.92
Plastic Limit (%)	49.23	40.90
Plasticity Index (%)	398.05	208.02
Specific Surface Area (m^2/gm)	507.74	273.9
Maximum Dry Density (Mg/m^3)	1.42	1.18
Optimum moisture content (%)	35	33
Cation Exchange Capacity (meq/100 gm)	94.58	64.07
Free swell index (%)	833.33	693.33
pH	8.29	8.47
Sand Sized Fraction (4.75–0.075 mm)	1.63	3.70

3.4.2 Textural and mineralogical properties of bentonites

The quantitative analysis of the chemical composition of both the bentonites given by XRF spectrometry is expressed in the percentage weight of major elemental oxides in Table 3.5. The scanning electron microscope (SEM) images of Barmer 1 (B_1) and Barmer 2 (B_2) bentonites are presented in Fig. 3.4(a) and 3.4(b). The SEM images reveal that the crystals of montmorillonite were present in the samples that are represented by lamellar and globular microcrystalline aggregate structure. The X-ray diffraction patterns of bentonites are presented in Fig. 3.5(a) and 3.5(b).

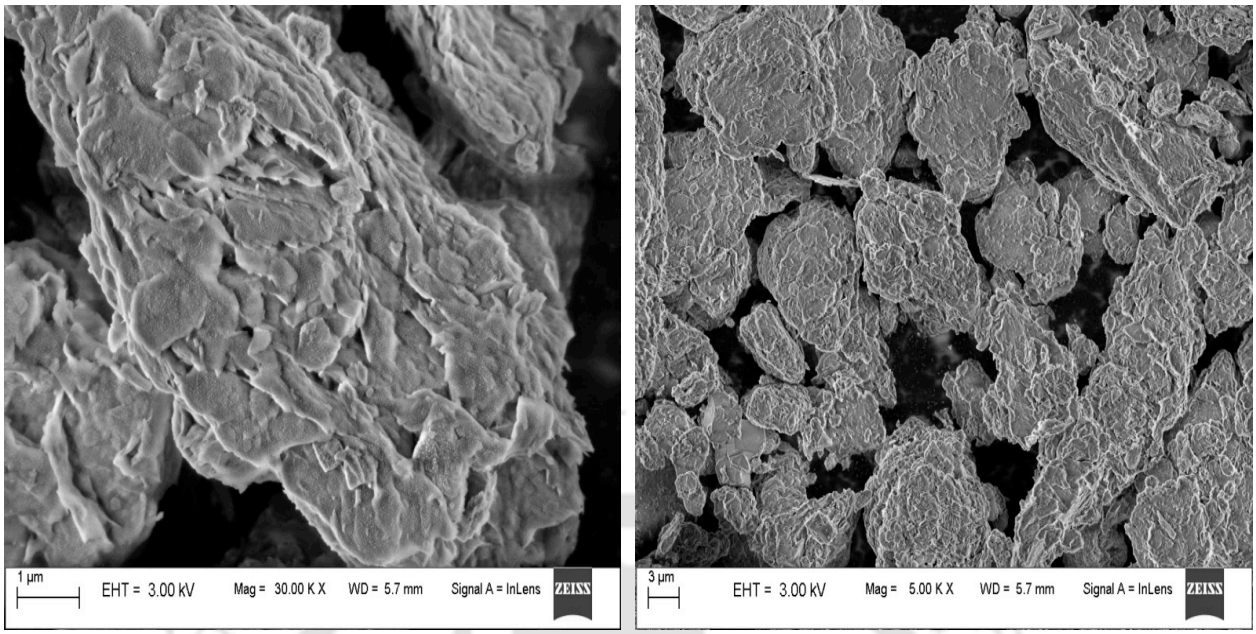

(a) **(b)**

Fig. 3.4 FESEM image of B_1

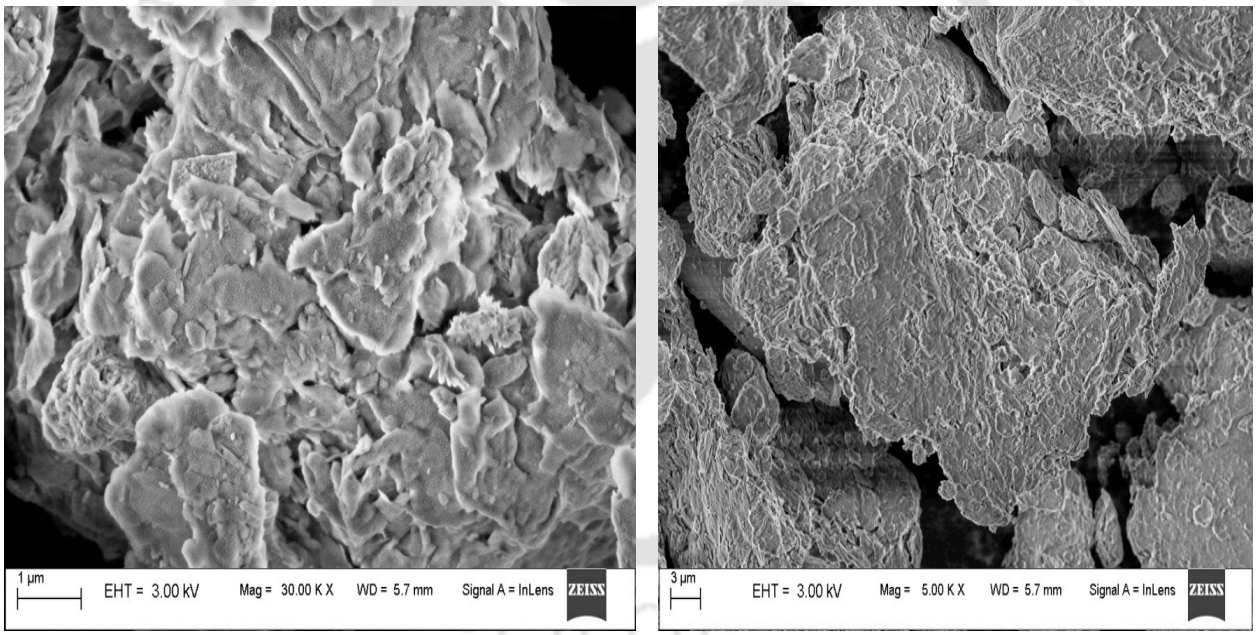

(a) **(b)**

Fig. 3.5 FESEM image of B_2

Table 3.5 Elemental composition of bentonites (B_1 and B_2) by X-Ray fluorescence spectrometry.

S.N.	Sample	SiO_2	Al_2O_3	Fe_2O_3 (T)	MnO	MgO	CaO	Na_2O	K_2O	TiO_2	P_2O_5
1	B_1	49.70	19.23	17.58	0.347	0.58	0.91	4.08	1.60	2.63	0.19
2	B_2	50.27	20.40	16.99	0.214	0.64	1.83	2.57	1.50	2.55	0.18

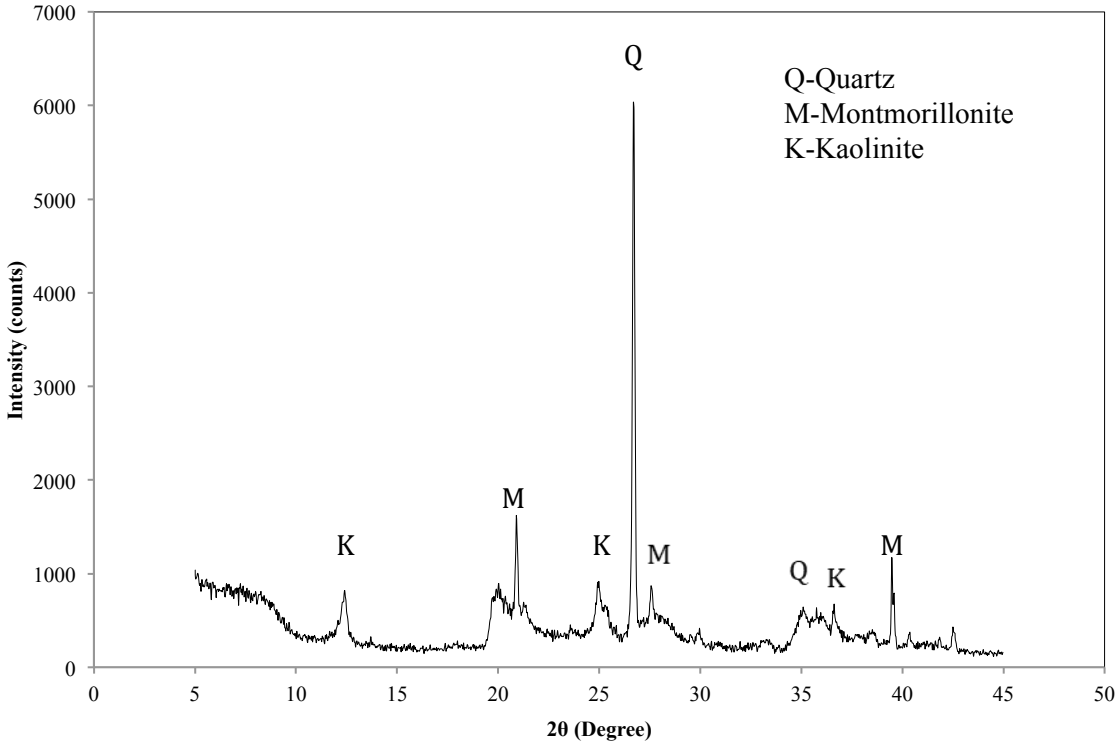

Fig. 3.6 X-ray diffraction pattern of B_1

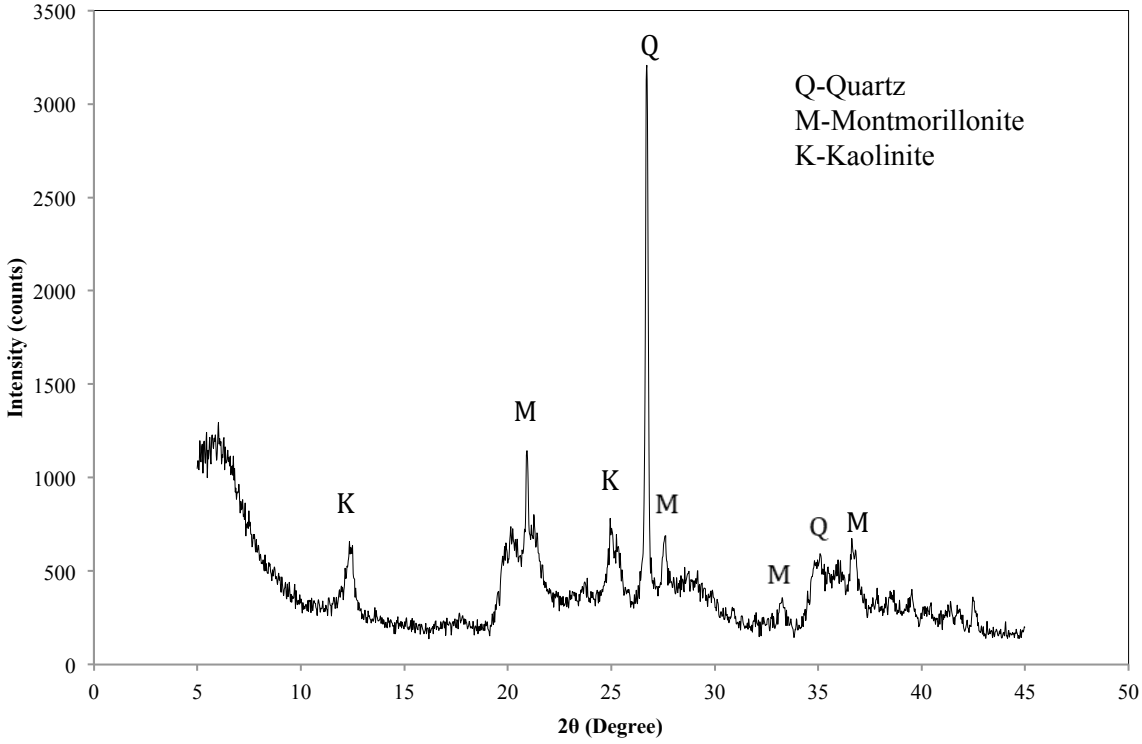

Fig. 3.7 X-ray diffraction pattern of B_2

Chapter 4

INFLUENCE OF THERMAL HISTORY ON PHYSICOCHEMICAL PROPERTIES OF POWDERED BENTONITE

4.1 INTRODUCTION

The hot canister surrounded by the buffer experiences a continuous heating effect because of the radioactivity of the element. It takes thousands of years to reduce the activity of the radioactive element, and thus, the experience of heating continues. This temperature reduces with time, and hence this change in temperature induces a thermal history on the compacted bentonite. Very few studies reported the importance of thermal history and its influence on the expansive clays (Estabragh et al., 2016).

From the past reported studies in literature, it could be collected that the elevated temperature conditions could change properties of bentonite such as Atterberg limits, soil plasticity (Laguros, 1969; Youssef et al., 1961). Acoording the past reported studies, the elevated temperature influenced index, physicochemical, and the hydromechanical properties of the compacted bentonite buffer (Ye et al., 2012a; Ye et al., 2012b; Ye et al., 2009; Villar and Lloret, 2004; Romero et al., 2003; Cho et al., 2000; Yilmaz, 1999), and Volckaert et al. (1993); reported the change in the initial suction, swelling pressure, water retention capacity, and volumetric change of soil samples due to variation in temperature, it was decided to continue to study the influence of thermal history on the performance of bentonite as no data is available on the influence of thermal history on bentonite.

In this chapter, the influence of thermal history on the physicochemical and index properties of powder bentonite is presented. The powdered bentonite samples were subjected to a thermal history at 60°C, 110°C, 150°C, and 200°C for a time duration of 3, 7, 15, 21, 28 days. The index and physicochemical properties, along with microstructural observations (X-ray diffraction and FESEM), were examined after these time spans and are reported. The variations in the properties are compared with the specimens, which were not subjected to thermal history.

4.2 RESULTS AND DISCUSSION

4.2.1 Effect of temperature on Specific Gravity of bentonites

Fig. 4.1(a) and 4.1(b) present the variation of the specific gravity for B_1 and B_2 bentonites, heated at 60°C, 110°C, 150°C and 200°C for 7, 14, 21 and 28 days. The specific gravity of B_1 bentonite reduced from 2.791 to 2.771 after treating at 60°C for 28 days. Comparatively, the specific gravity decreased from 2.788 to 2.768 after treating at 200°C for the same period. A similar pattern was observed in the variation of specific gravity of B_2 bentonite when heated for different time spans. The change in specific gravity due to the increase in temperature was almost the same at 60°C and 110°C for both soils. Further, at 150°C and 200°C, a slight decrease was observed with the increase in temperature and duration of heating as well for both bentonites. The decrease in specific gravity due to an increase in temperature may be attributed to the loss of inter-lamellar water of bentonite, and thereby a possible reduction may have occurred in the mass of solid particles. Comparatively, the density of the individual clay particles might have reduced, resulting from a lower value of specific gravity. The specific gravity of soil is required for the calculation of properties such as void ratio, the degree of saturation, etc., and the hydro-mechanical properties of soil, i.e., suction, and depend upon the extent of saturation.

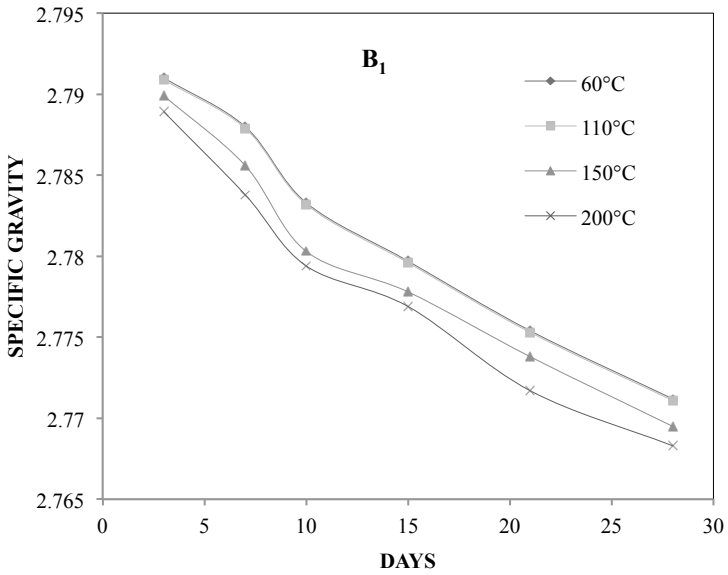

Fig. 4.1 Variation of specific gravity of B_1 heated at different temperature for different days

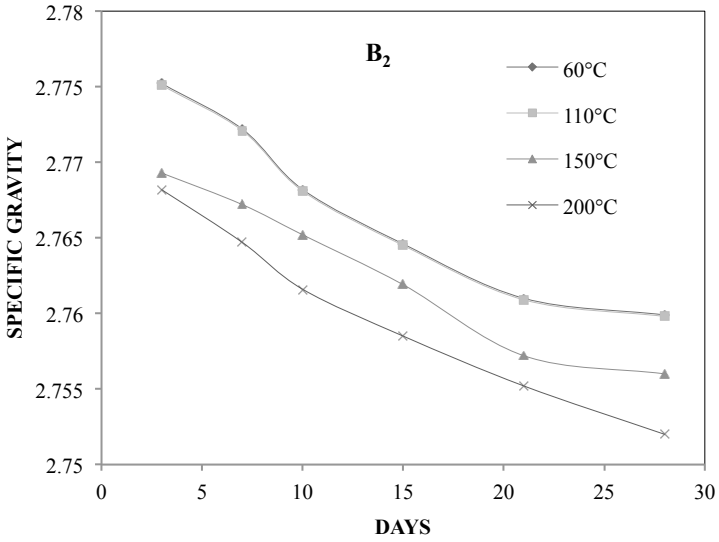

Fig. 4.2 Variation of specific gravity of B_2 heated at different temperature for different days

4.2.2 Effect of temperature on Plasticity characteristics of bentonites

Fig. 4.2(a), 4.2(b), 4.3(a), 4.3(b), 4.4(a), 4.4(b), present the variation of the liquid limit, plastic limit, and plasticity index respectively, heated at 60°C, 110°C, 150°C and 200°C for 7, 14, 21 and 28 days. The liquid limit of B_1 bentonite reduced from 446% to 299% after treating at 60°C for 28 days. Comparatively, the liquid limit reduced from 446% to 253% after treating at 200°C for the same period. A similar pattern was observed in the variation of the liquid limit of B2 bentonite with heating for different days. The plasticity index of B1 bentonite reduced from 246% to 132% after treating at 60°C for 28 days and 246% to 90% after treating at 200°C for the same time span. Comparatively, the plasticity index reduced from 397% to 207% after processing at 200°C for the same period.

A similar trend was observed in the variation of the plasticity index of B_2 bentonite with heating for different days. It is interesting to note that the considerable changes in liquid limit and plasticity index were not observed for the initial five days, but after five days significant decrease was found up to 28 days for both the bentonites. The effect of temperature was not significant from 60°C to 110°C, but after 110°C, it was observed to be meaningful. However, a slight decrease was observed in the plastic limit of both bentonites. The plastic limit reduced from 48.5% to 46.9% and 40.8% to 39.8% after treating at 60°C for 28 days; comparatively, the plastic limit reduced from 48.2% to

46.5% and 40.2% to 38.3% after treating at 200°C for the same period for B1 and B2 bentonite respectively.

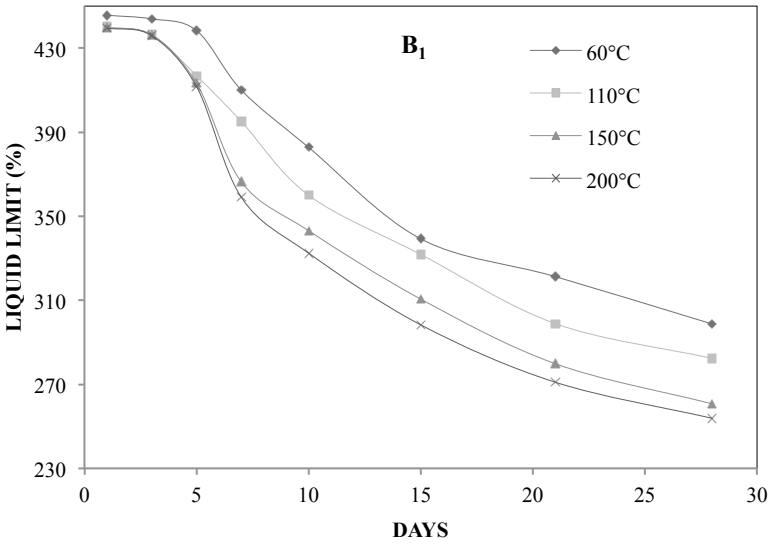

Fig. 4.3 Variation of liquid limit of B_1 heated at different temperature for different days

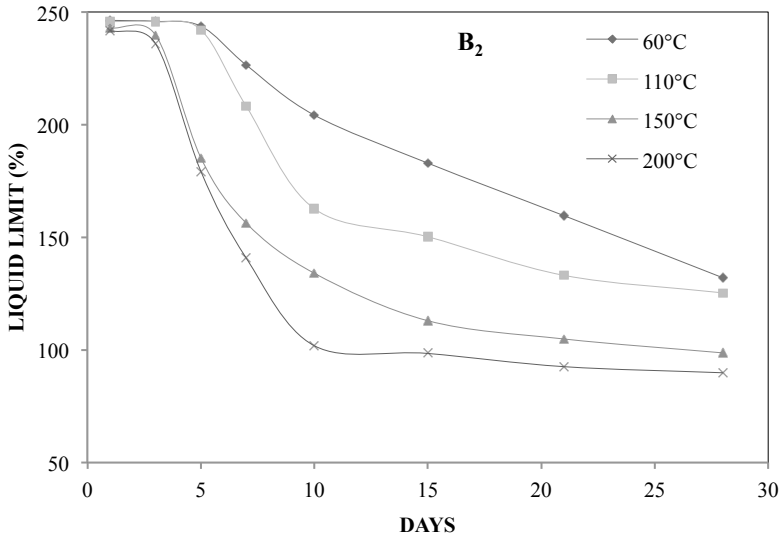

Fig. 4.4 Variation of liquid limit of B_2 heated at different temperature for different days

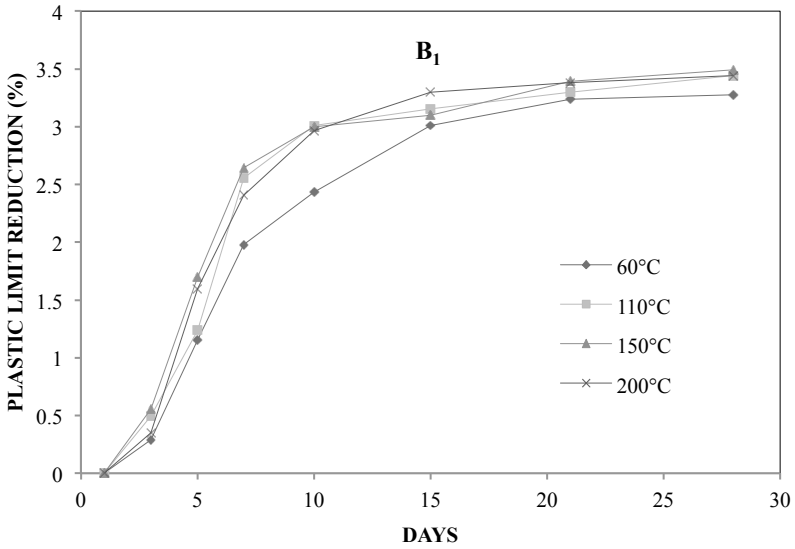

Fig. 4.5 Reduction in plastic limit of B_1 heated at different temperature for different days

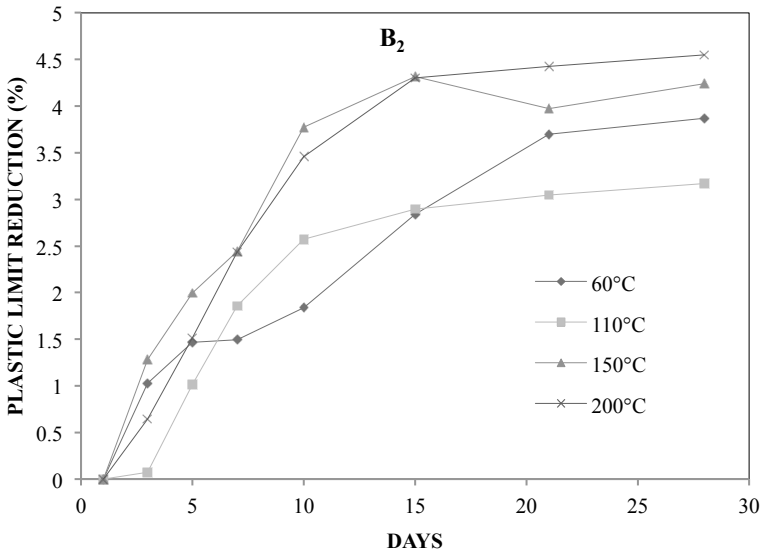

Fig. 4.6 Reduction in plastic limit of B_2 heated at different temperature fordifferent days

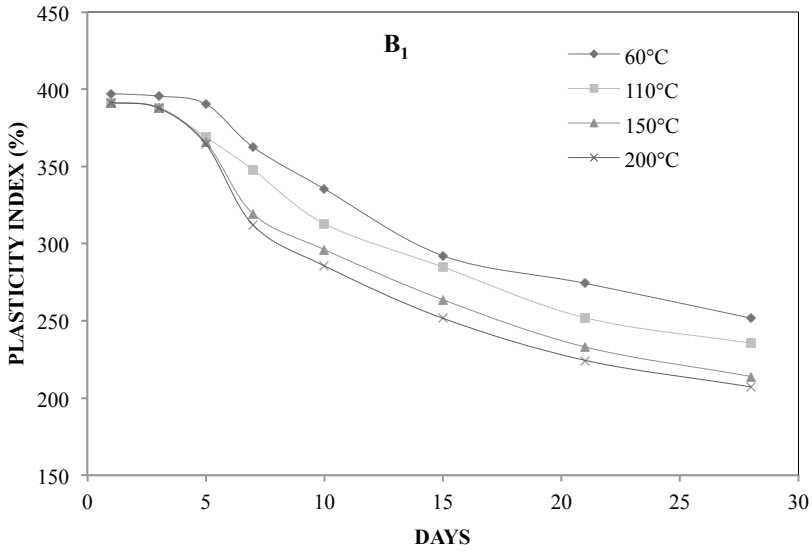

Fig. 4.7 Variation of plasticity index of B_1 heated at different temperature for different days

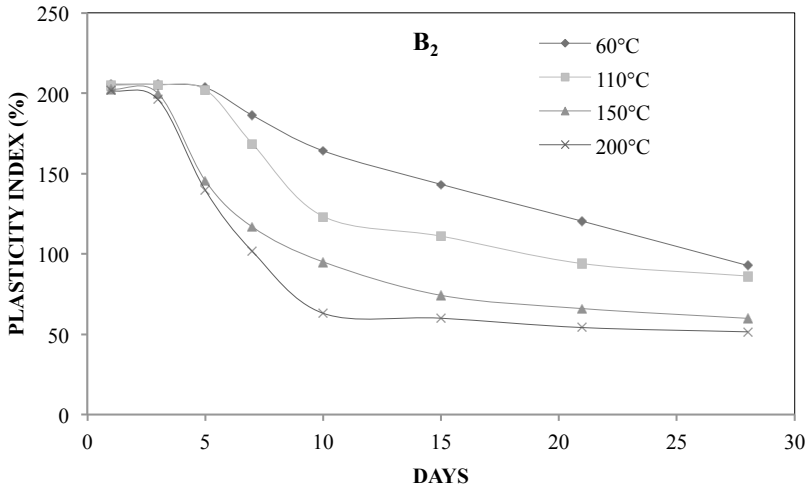

Fig. 4.8 Variation of plasticity index of B_2 heated at different temperature for different days

When clays come in contact with high temperatures, they start losing water (Lingnau et al., 1996). It happens in two phases (1) the removal of physical water when the temperature ranges from 100°C -110°C. (2) the smectite dehydroxylation that occurs when the temperature ranges from 500°C to 800°C - 1000°C (Wang et al., 2008; Chandrasekhran et al., 1969). The plasticity of the clay minerals alters due to the loss of interlamellar water, as it tends to the change in macro and microporosity of the clay

mineral. Another possible reason for the decrease in plasticity at thermal history is the evaporation of pore water and the accumulation of impurities in the pores. The precipitated impurities may clog the pores and act as a binder material between two soil particles, decreasing its plasticity (White, 2006). Moreover, according to the theory of diffused double layer, if the dielectric constant of the pore solution decreases, the thickness of the diffused double layer decreases (Mitchell, 1993). At high temperatures, the dielectric constant of pore solutions decreases, due to which a decreasing trend may be observed in liquid limits of both bentonites with an increase in temperature.

4.2.3 Effect of temperature on Specific Surface Area of bentonites

Fig. 4.5(a) and 4.5(b) presents the variation of the specific surface area for B_1 and B_2 bentonite, heated at 60°C, 110°C, 150°C, and 200°C for 7, 14, 21, and 28 days. The specific surface area of B1 bentonite decreased from 508 m2/g to 448 m2/g and 396 m2/g for 60°C to 200°C respectively, at the end of 28 days. Comparatively, the specific surface area of B2 bentonite decreased from 274 m2/g to 171 m2/g and 160 m2/g for 60°C to 200°C respectively at the end of 28 days—the empirical relationship given by Dolinar and Stanislav (2013).

$$LL_e = 31.90\ p + 0.81\ A_{se} \qquad (1)$$

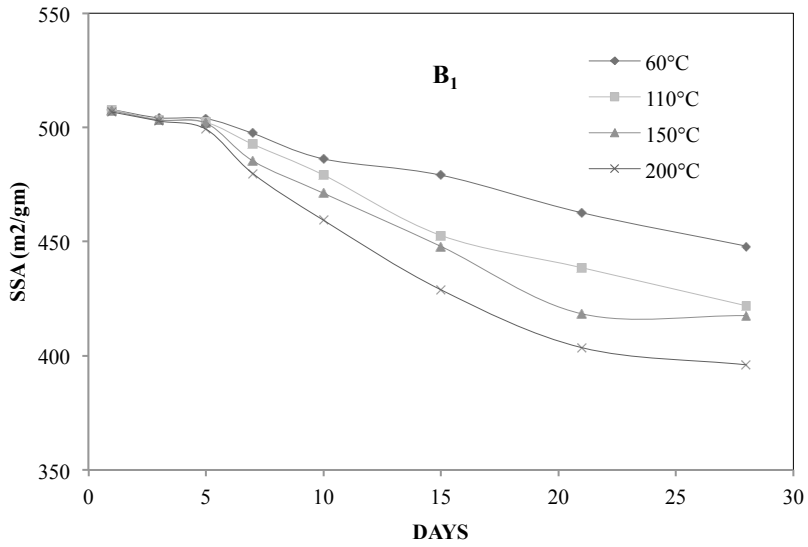

Fig. 4.9 Variation of specific surface area of B_1 heated at different temperature for different days

Where,

Ase is the external specific surface area of the soil, and p is the content (%) of clay minerals in the soil. The above equation expresses that the liquid limit depends on the clay content and the specific surface area of soil. For expansive soils, the amount of pore water and adsorbed water on the external surface of clay depend on Ase and p, whereas the interlayer water content depends on the type and the quality of clay minerals, exchangeable cations, and salinity of solute present in the pores. According to Dolinar and Stanislav (2013), the physical properties of fine soils depend only on the pore solution because the adsorbed water is tightly tied to the external and internal surfaces of clay and can be removed only at high temperatures. The change in the specific surface area, led to the change in the liquid limit of the soil.

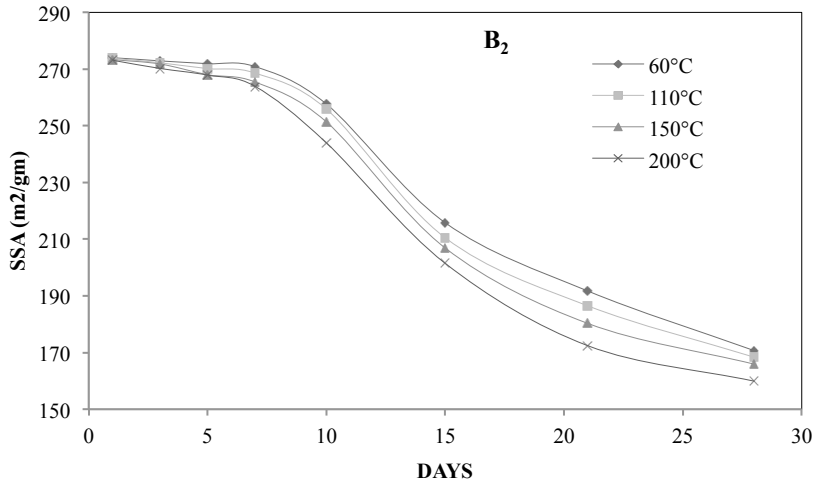

Fig. 4.10 Variation of specific surface area of B_2 heated at different temperature for different days

4.2.4 Effect of temperature on the Free Swell Index of bentonites

Fig. 4.6(a) and 4.6(b) illustrates the variation of the free swell index of bentonites with temperature. The free swell index of B_1 bentonite reduced from 833% to 773% after treating at 60°C for 28 days. Comparatively, the free swell index decreased to 740 % after treating at 200°C for the same period. A similar pattern was observed in the variation of the free swell index of B_2 bentonite with heating for different days. The free

swell index of B_2 bentonite reduced from 693% to 656% after treating at 60°C for 28 days. Comparatively, the free swell index decreased to 626% after treating at 200°C for the same period.

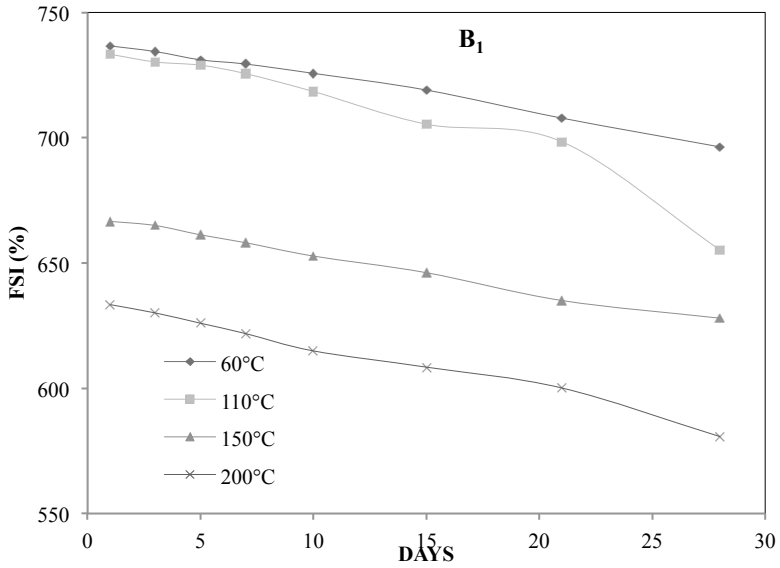

Fig. 4.11 Variation of free swell index of B_1 heated at different temperature for different days

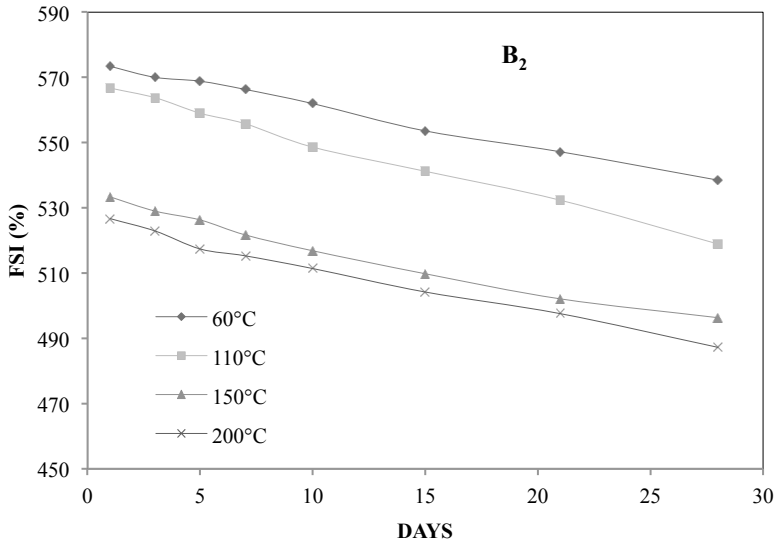

Fig. 4.12 Variation of free swell index of B_2 heated at different temperature for different days

The process of formation of sediments, their nature, and the resulting equilibrium sediment volume is controlled by the interparticle attractive and repulsive forces as well as clay mineralogy and the micro and macrostructure. Forces due to self-weight,

electrical forces of attraction, and electrical forces of repulsion are three primary forces that exist in the settling systems. When soil particles settle under gravity, the underlying layers of soils get compacted because of settling layers (Sridharan, 2014, 1991). The initial water content and the change in clay mineralogy of the clay due to an increase in the temperature play a vital role in affecting the settling process. In the case of montmorillonite soil, the limiting water content decreases with the decrease in soil plasticity (Sridharan and Prakash, 1999). Due to the loss of interlamellar water and loss of plasticity, the free swelling of expansive soils reduces at the higher temperatures.

4.2.5 Effect of temperature on sodium ion (Na+) concentration of bentonites

Fig. 4.7(a) and 4.7(b) illustrates the variation of the exchangeable sodium percentage of bentonites with temperature. The initially calculated sodium ion concentration was reported as 51 meq/100g and 35 meq/100g for B_1 and B_2, respectively. It then reduced to 45 meq/100g and 24 meq/100g when heated at 60°C for 28 days. Similarly, it decreased to 40 meq/100g and 22 meq/100g when heated at 60°C for 28 days for B_1 and B_2, respectively. Smectite is composed of individual layers, which are not identical in chemical composition (Brown et al., 1987; Schanz et al., 2018), layer charge, and other structural characteristics.

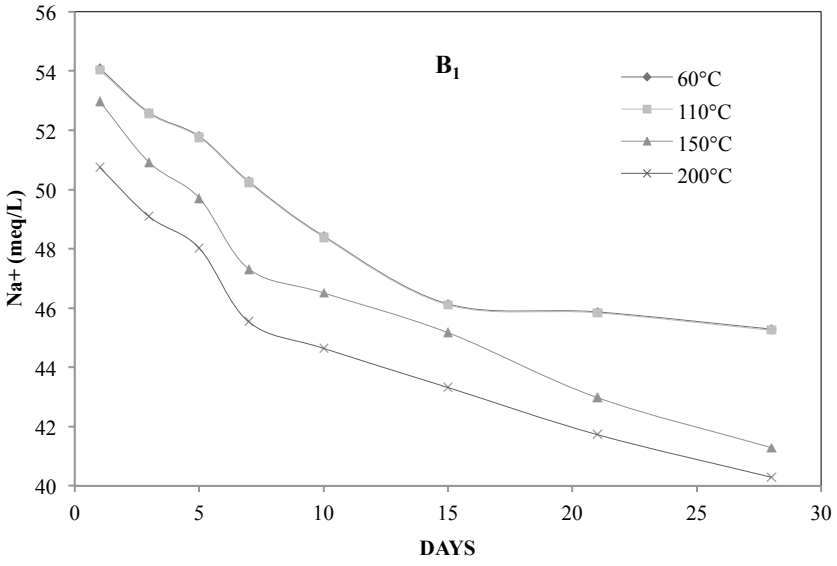

Fig. 4.13 Variation of sodium ion concentration (Na+) of B_1 heated at different temperature for different days

They also have heterogeneous layer-charge distributions (Lagaly, 1982). Grim and Kulbicki (1957) have shown that the high-temperature phases developed on heating montmorillonite are significantly influenced by the nature of the exchanged cation composition. Sawhney and Israel (1969) observed that, with an increase in the temperature, the effective negative charge on the silicate sheet of the adjacent layer will be reduced, and thus prevents the entry of the cation into this adjoining layer. The cation adsorbed on the clay surface influences its behavior. Sodium ions have a single positive charge, indicating the weak clay particle binding ability. Due to an increase in temperature, the inadequate bonding of the clay particles is broken by these sodium cations. The discussion can be supported by the Boltzmann equation (equation 2).

$$ni = ni0 \exp \frac{Ei0 - Ei}{kT} \qquad (2)$$

Where,

E is the potential energy, T is the temperature in Kelvin, k is the Boltzmann constant, and "0" represents the state that is at a significant distance from the surface. The results reported by Gu et al. (2001) are in agreement with the fact that the concentration of exchangeable cations such as Na^+ is decreased with increasing the temperature.

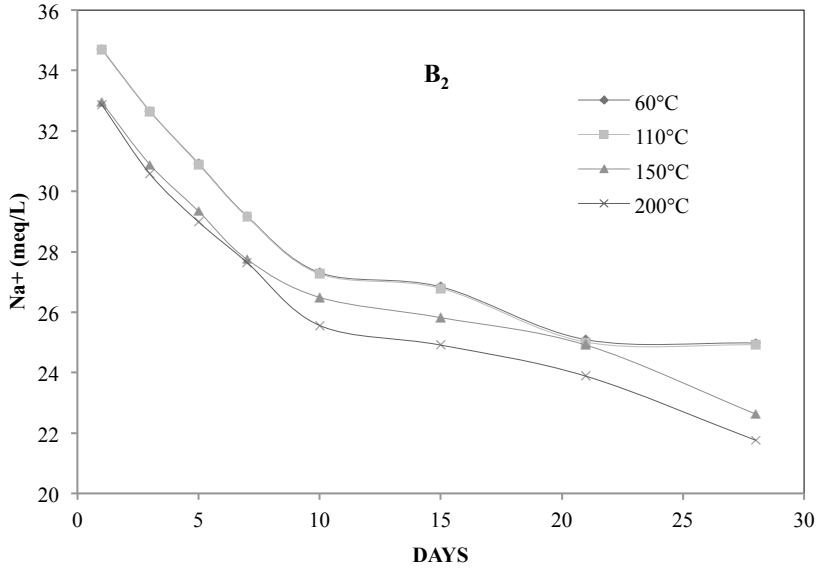

Fig. 4.14 Variation of sodium ion concentration (Na+) of B_2 heated at different temperature for different days

4.2.6 Effect of temperature on pH of bentonites

According to Lechatelier's Principle, if the temperature of the water is increased, more hydrogen ions will be formed. As the temperature of bentonite rises to 150°C and 200°C, the observable [H+] from interlamellar water of bentonite also increases.

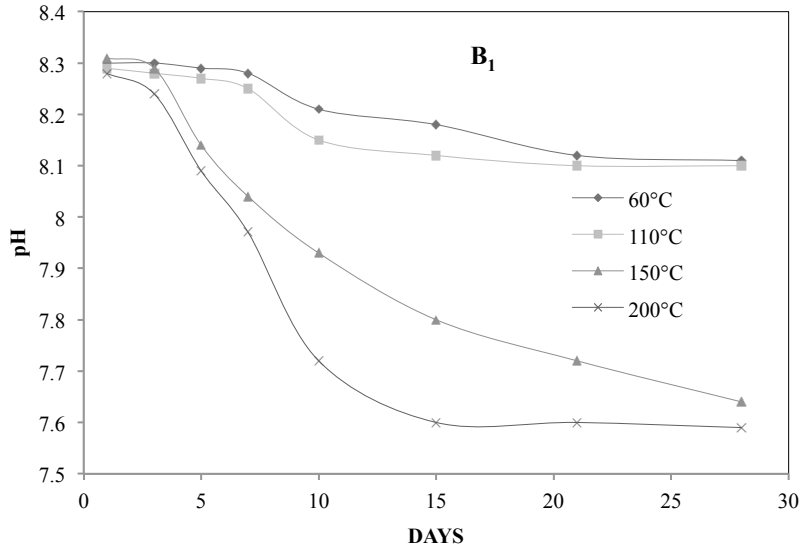

Fig. 4.15 Variation of pH of B_1 heated at different temperature for different days

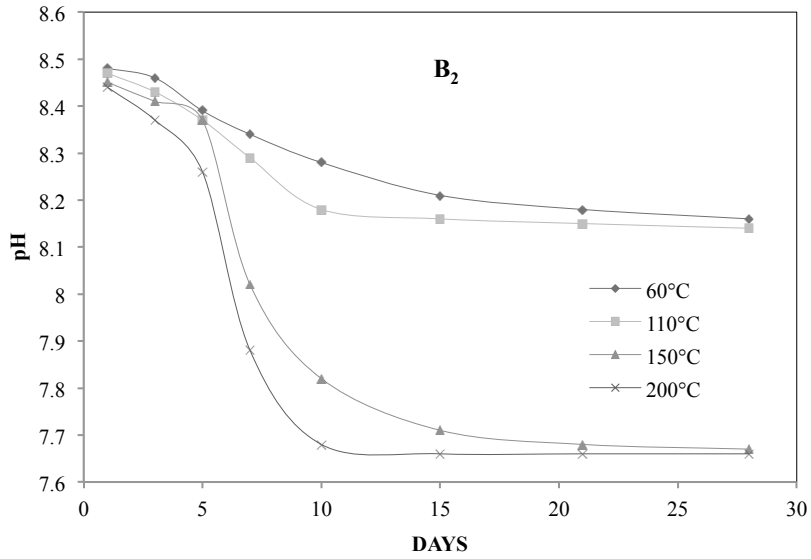

Fig. 4.16 Variation of pH of B_2 heated at different temperature for different days

This fact might occur due to a decreased tendency of forming Hydrogen bonds. Hence, the reduction in the pH (equation 3) was observed more after 110°C. For B_1, the

pH reduced from 8.29 to 7.59 after treating at 200°C, and it reduced to 7.66 from 8.44 after treating at 200°C in the case of B_2 (Fig. 4.8(a) and 4.8(b)).

$$pH = - \log 10 [H+] \qquad (3)$$

4.2.7 Effect of temperature on compaction characteristics of bentonites

Fig. 4.9(a) and 4.9(b) and Fig. 4.10(a) and 4.10(b) depict the compaction characteristics of both bentonites. It was observed that the optimum moisture content (OMC) of both bentonites decreased, and the maximum dry density (MDD) of both bentonites increased when the temperature was increased along with the time span. The initial OMC of B_1 and B_2 is 35% and 33%, respectively. It reduced to 28% and 26% when heated at 200°C for 28 days. The impact of an increase in temperature was found on OMC because the growth in temperature causes the rearrangement of soil structure.

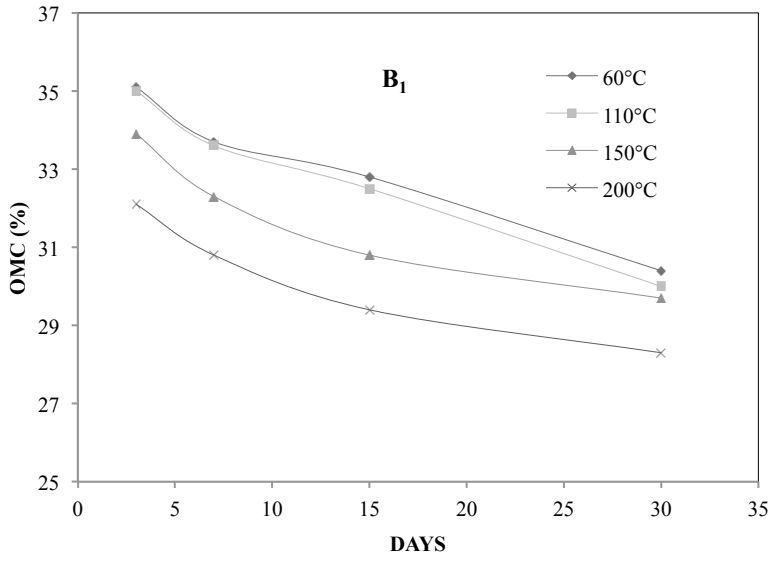

Fig. 4.17 Variation of optimum moisture content of B_1 heated at different temperature for different days

More it subjects to the temperature for a longer duration more will the disturbed soil structure. Maximum dry density was observed to be increased with temperature as well as duration. The maximum dry density increased to 14.8 kN/m3 from 14 kN/m3 for B_1, and in the case of B_2, it increased to 12.5 kN/m3 from 11.9 kN/m3.

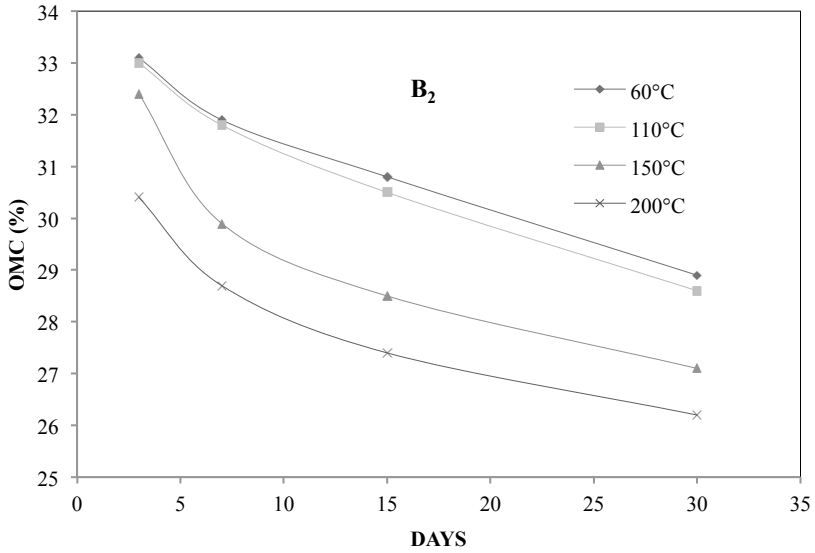

Fig. 4.18 Variation of optimum moisture content of B_2 heated at different temperature for different days

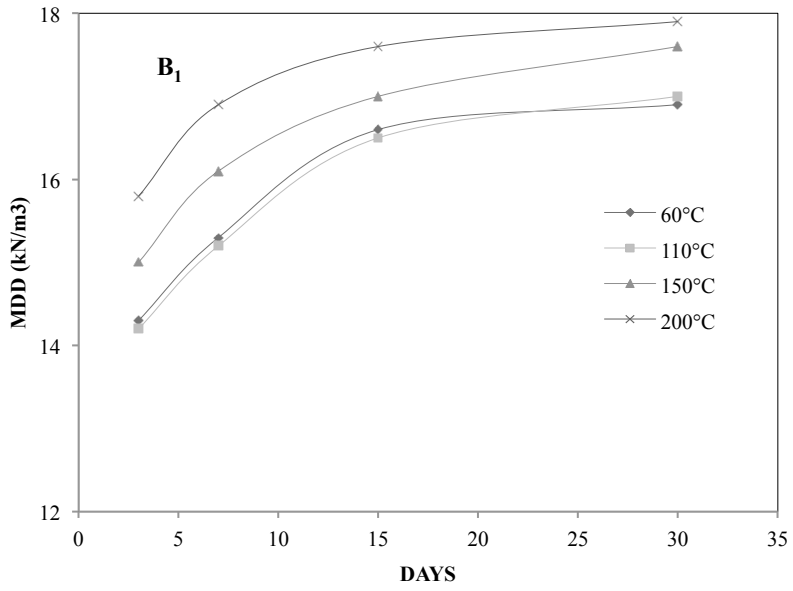

Fig. 4.19 Variation of maximum dry density of B_1 heated at different temperature for different days

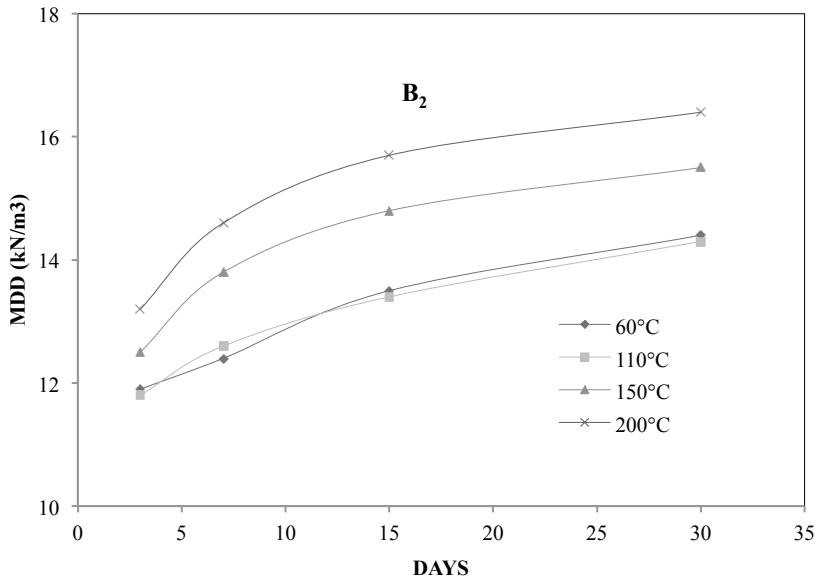

Fig. 4.20 Variation of maximum dry density of B_2 heated at different temperature for different days

The increase in temperature causes the smectite mineral to become unstable and transform to more stable silicate phases, known as illitization (Wang, 1990; Wersin et al., 2007).

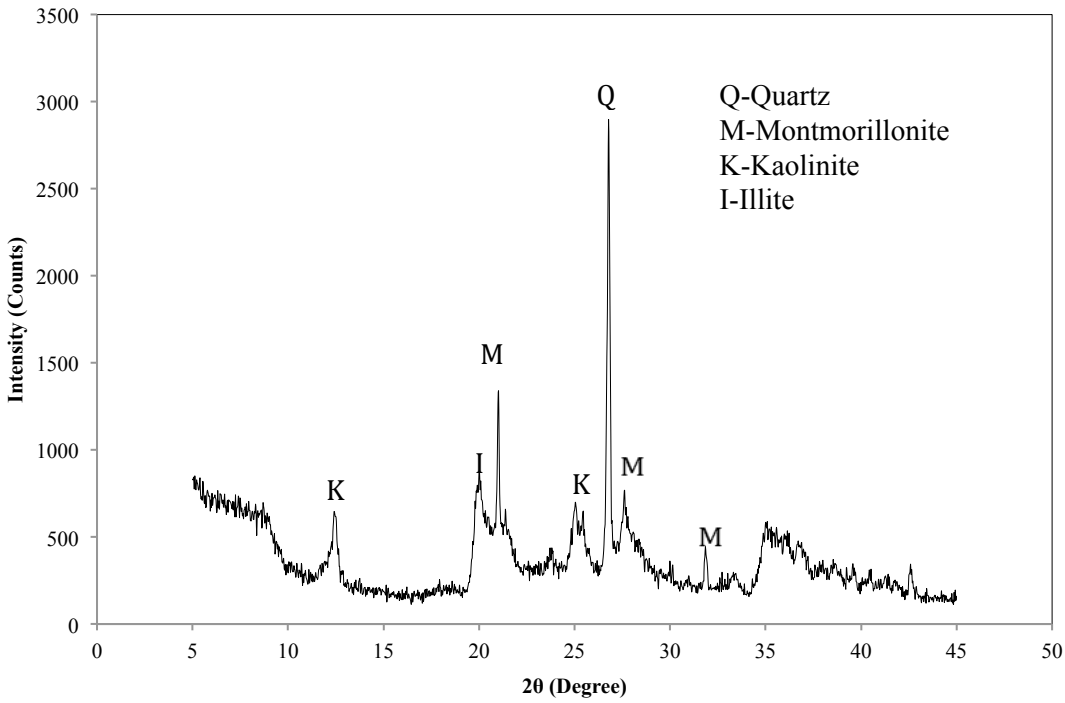

Fig. 4.21 X-ray diffraction pattern of B_1 (200°C for 28 days)

This illitization occurs through smectite-illite formation process that starts before the dehydroxylation of smectite, which also results in decreasing the ability of the bentonite to retain the water.

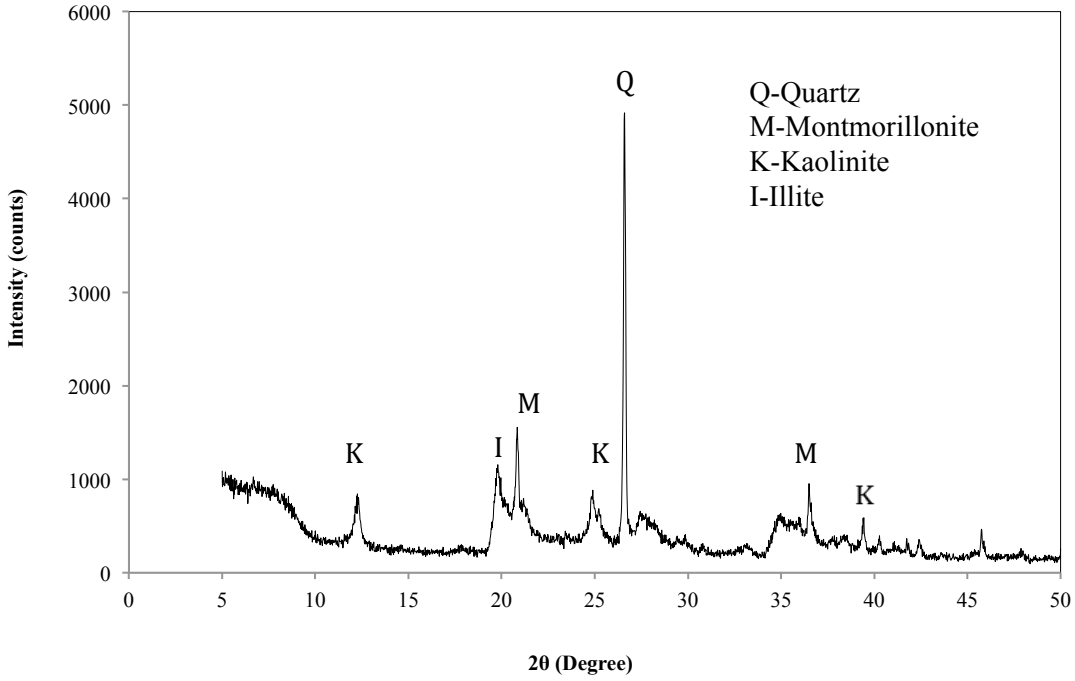

Fig. 4.22 X-ray diffraction pattern of B_1 (200°C for 28 days)

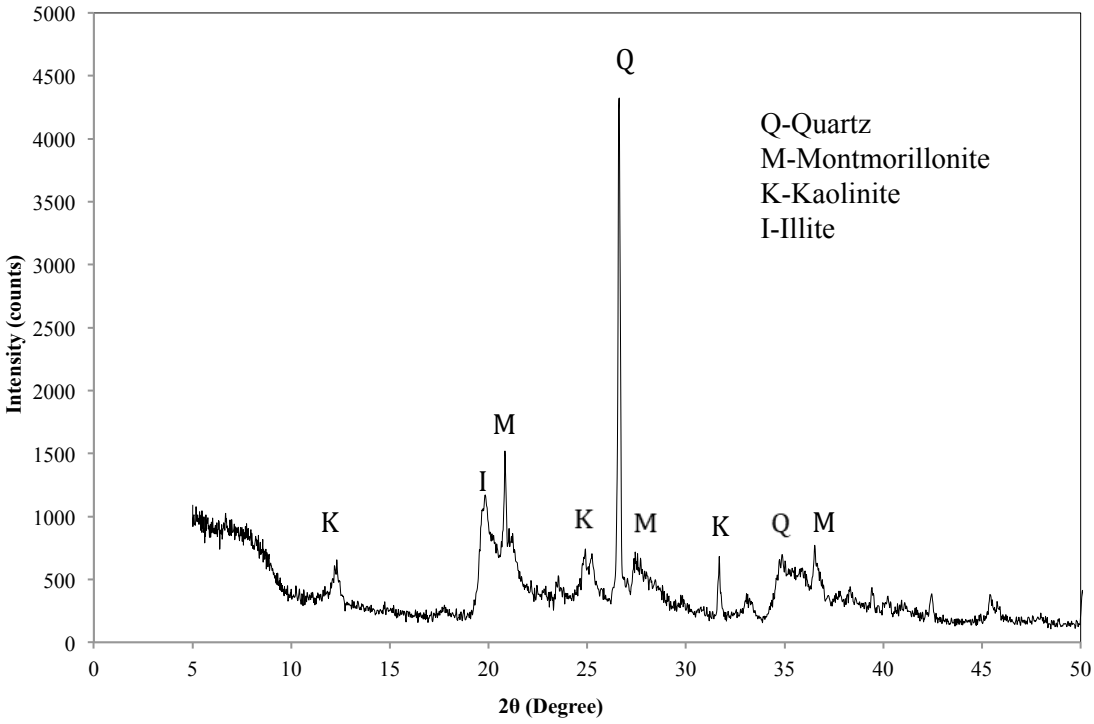

Fig. 4.23 X-ray diffraction pattern of B_1 (150°C for 28 days)

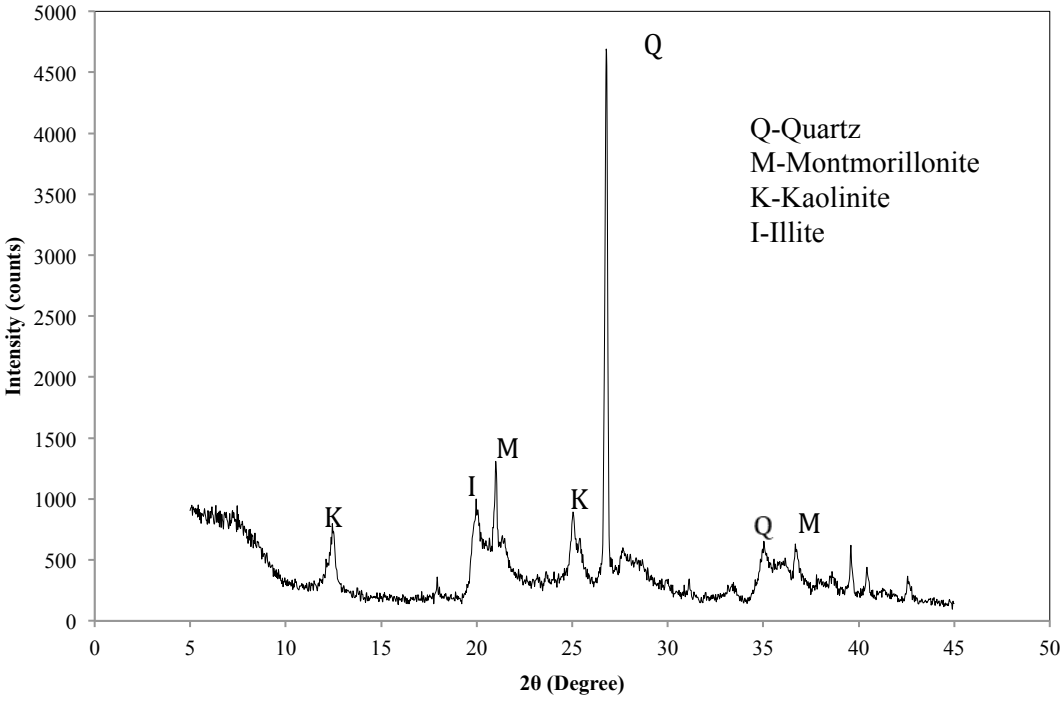

Fig. 4.24 X-ray diffraction pattern of B_1 (150°C for 28 days)

Fig. 4.25 The color variations in bentonite after 14 and 28 days of thermal history.

These results are supported with the help of microstructural investigation by X-ray diffraction. The X-ray diffraction patterns of both bentonites for 28 days heated at 150°C and 200°C for both bentonites are presented in Fig. 4.21 and 4.22 and Fig. 4.23 and 4.24. The results showed that the heating of bentonite for up to 28 days might cause the mineralogical changes. However, the expansive soil is completely converted to non-expansive when it is subjected to temperatures more than 600°C (Yilmaz, 2011). The

physical variations, i.e., color change, were observed in the appearance of bentonite after 14 days and 28 days of thermal loading, which is shown in Fig. 4.25.

4.3 CONCLUSION

The bentonite buffer used in the DGR has to be stable even with the variations in the temperature from the waste canister. Different thermal histories induced on powdered bentonite samples from the Barmer district of Rajasthan, India, showed that the thermal history had a significant influence on the physicochemical properties of the bentonite. The specific gravity, Atterberg's limit, free swell index, particle-sized distribution, and compaction characteristics of these bentonites were altered with the changes in the temperature. Index properties such as Atterberg's limit, specific gravity, free swell index, optimum moisture content decreased with the increase in the temperature and the duration of heating. However, the maximum dry density increased with the increase in temperature and time. The Na+ concentration and pH and exhibited a decreasing trend with an increase in temperature and time. The specific gravity of B1 bentonite was reduced by 0.7%, whereas for B2, it was 0.9% at 200°C for 28 days. The reduction in liquid limit of B1 was 43%, whereas, for B2, it was 63% after 28 days heated at 200°C. Similarly, the percentage reduction in specific surface area was 22% and 41%, as well as a percentage reduction in the free swell index was 11% and 9%, respectively, for B1 and B2. The percentage reduction in OMC was 5% and 7%, and the percentage increase in MDD was 5% and 4.5%, respectively, for B1 and B2. These changes are attributed to the variations in the pore solution chemistry, etc. X-ray diffraction analysis on the bentonite samples subjected to thermal history revealed that the prolonged heating of bentonite might cause mineralogical changes that will have detrimental effects on the engineering behavior of the buffer in DGR conditions.

Chapter 5

SWELL PRESSURE OF COMPACTED BENTONITE SPECIMENS: INFLUENCE OF THERMAL HISTORY AND HYPERALKALINITY

5.1 INTRODUCTION

The compacted bentonite specimens experience swelling once the specimens are in contact with water. This is primarily due to the moisture adsorption in the interlayers of montmorillonite (Komine and Ogata 1996, van Olphen, 1977; Yong, 1999; Birgersson and Karnland, 2009). However, when the volume is restricted, the bentonite tries to swell as much as it can without letting the overall volume to increase, which create a pressure at the interface of the container and the specimen, generally termed as swell pressure (Komine and Ogata, 1994; Komine, 2004; Villar and Lloret, 2008). The swelling can occur either in uniform directions or in random orientations depending upon certain conditions such as compaction density, temperature, saturated solution, pore chemistry, etc. (Castellanos et al., 2008; Mata et al., 2005; Musso et al., 2003; Kim, 2000). The swelling occurs due to the surface tension that is present inside the soil sample being unsaturated in nature, the ion concentration of saturating fluid and the ions present in the soil, due to the presence of weak Van der Waals forces between the montmorillonite sheets, and when it comes in contact with the saturating fluid, the repulsion between montmorillonite sheets occurs swelling and due to the exchangeable cations which get attracted towards the negatively charged clay surface, expanding the diffused double layer volume (Mitchell and Soga, 1993).

The buffer surrounding the waste canister continuously experiences high temperatures due to active radionuclides. This temperature reduces over the period of time, depending upon the half-life of the radioactive element. When the canister is installed in a deep geological repository, the temperature of the canister can be high (150°C -200°C, Villar et al., 2016). This temperature reduces over a long period of time, i.e., after 100's to 1000's years, which creates a thermal history on the compacted bentonite. The influence of thermal history was explained in past studies by many researchers (Estabragh et al., 2016). It was clear from the past studies that the elevated temperature is responsible for the alteration in swelling properties of compacted bentonite, affecting its overall performance. Along with this, the hyperalkaline fluids arising from the cement will react with the bentonite buffer altering its original properties (Zhu et al., 2013; Nakayama et

al., 2004; Ramírez et al., 2002; Andersson et al., 1989). Various studies were reported in the past on the effect of alkaline solutions on the swell pressure of compacted bentonite (Komine et al., 2009; Lloret and Villar, 2007). To investigate the interaction of ordinary Portland cement with Opalinus clay, Jenni et al. (2018) performed series of experiments and reported that the porosity at the cement clay interface changed, and the pores were clogged by reactive transport of diffusive solute fluxes and various reaction kinetics. Watson et al. (2013) reported a reactive transport model of a large-scale, in situ, long-term cement/clay system. It was reported that the ion exchange played an important role, and the dissolution of portlandite, calcite, and ettringite in the concrete and the precipitation of calcite on the concrete clay interface and dissolution of clay minerals was observed.

Chapter 4 had mainly focussed on the influence of thermal history on powdered bentonite. As in the field condition, the bentonite used in the compacted form at the particular density and the compacted mass experiences the thermal history; the role of thermal history on the swell pressure response of compacted bentonite specimens was studied in the phase I of this chapter. The influences of hyperalkaline cement solution on swell pressure of thermally loaded compacted bentonite specimens are discussed in phase II. The focus was on understanding the swell pressure response under combined hyperalkaline and thermal history conditions.

5.2 RESULTS AND DISCUSSIONS

Phase I - Influence of thermal history on swell pressures of compacted bentonite

5.2.1 Time-swelling of compacted bentonites subjected to thermal history

The variation of swell pressure with a time of compacted specimens of B_1 (compaction densities 1.5, 1.75, 2.0 Mg/m^3) without heating (WH) and heated to 110°C and 200°C are presented in Fig. 5.1. The specimens compacted to 1.5 Mg/m^3 and without heating attained the equilibrium swell pressure after 19440 mins of starting the test. Comparatively, the specimens of the same density and heated at 110°C and 200°C attained the equilibrium swell pressure after 15120 and 12960 mins of starting the test, respectively. Similarly, the specimens compacted to 1.75 Mg/m^3 and without heating attained the equilibrium swell pressure after 20880 mins of starting the test. Comparatively, the specimens of the same density and heated at 110°C and 200°C attained the equilibrium swell pressure after 18720 and 16560 mins of starting the test, respectively. Furthermore, the specimens compacted to 2 Mg/m^3 and without heating

attained the equilibrium swell pressure after 22320 mins of starting the test. Comparatively, the specimens of the same density and heated at 110°C and 200°C attained the equilibrium swell pressure after 19440 and 17280 mins of starting the test, respectively.

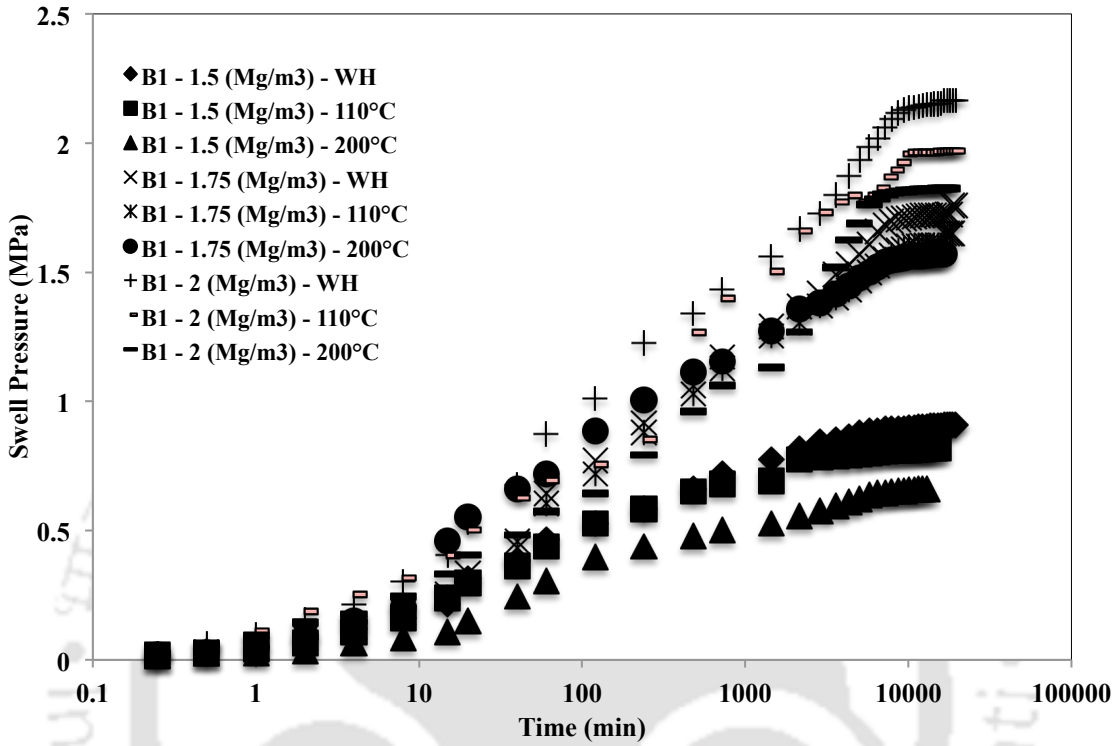

Fig. 5.1 Time swelling curve of B_1 bentonite when heated at different temperatures.

The variation of swell pressure with a time of compacted specimens of B_2 (compaction densities 1.5, 1.75, 2.0 Mg/m^3) without heating (WH) and heated to 110°C and 200°C are presented in Fig. 5.2. The specimens compacted to 1.5 Mg/m^3 and without heating attained the equilibrium swell pressure after 19440 mins of starting the test. Comparatively, the specimens of the same density and heated at 110°C and 200°C attained the equilibrium swell pressure after 16560 and 12960 mins of starting the test, respectively. Similarly, the specimens compacted to 1.75 Mg/m^3 and without heating attained the equilibrium swell pressure after 20880 mins of starting the test. Comparatively, the specimens of the same density and heated at 110°C and 200°C attained the equilibrium swell pressure after 18000 and 15120 mins of starting the test, respectively. Furthermore, the specimens compacted to 2 Mg/m^3 and without heating attained the equilibrium swell pressure after 21600 mins of starting the test. Comparatively, the specimens of the same density and heated at 110°C and 200°C

attained the equilibrium swell pressure after 18720 and 16560 mins of starting the test, respectively.

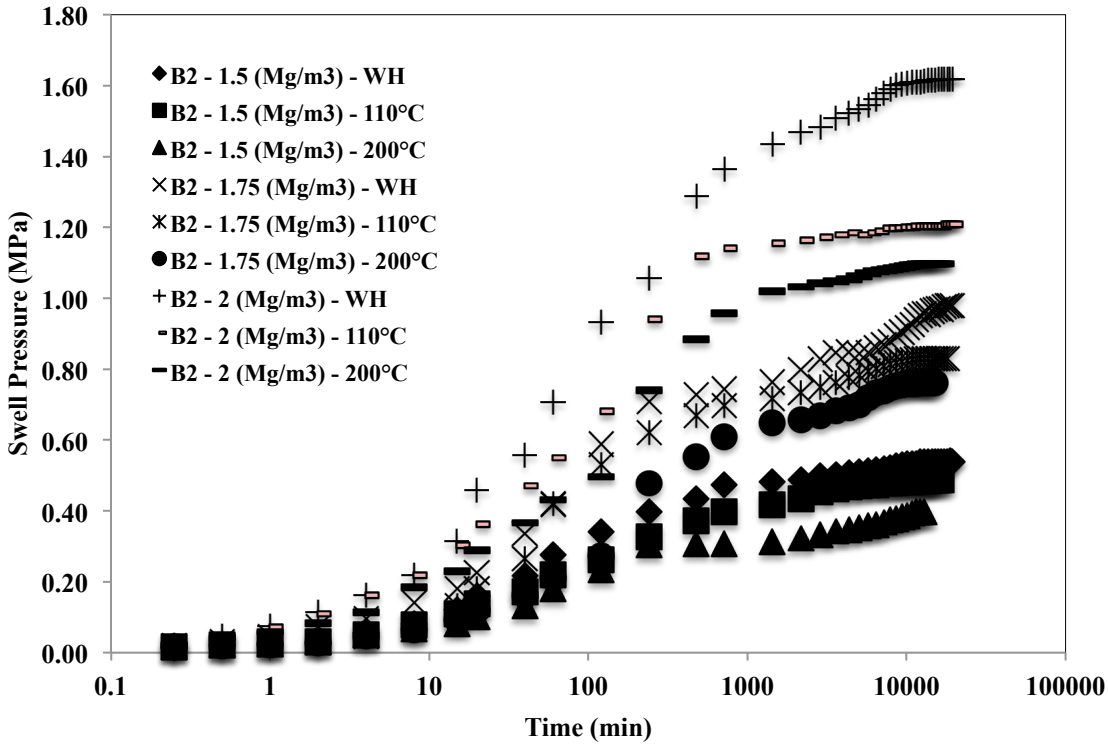

Fig. 5.2 Time swelling curve of B_2 bentonite when heated at different temperatures.

The values of swell pressure of B_1 bentonite at 1 min were observed as 0.035 MPa, 0.042 MPa, and 0.050 MPa for specimens compacted at 1.5 Mg/m^3 without heating, 110°C and 200°C respectively. Similarly, for specimens compacted at 1.75 Mg/m^3, the values were recorded as 0.049 MPa, 0.051 MPa, and 0.052 MPa without heating, 110°C, and 200°C, respectively. Furthermore, for specimens compacted at 2 Mg/m^3, the values were recorded as 0.092 MPa, 0.094 MPa, and 0.0102 MPa for 200°C, 110°C, and without heating, respectively. Similarly, The values of swell pressure of B_2 bentonite at 1 min were observed as 0.023 MPa, 0.025 MPa, and 0.025 MPa for specimens compacted at 1.5 Mg/m^3 at 200°C, 110°C, and without heating, respectively. Similarly, for specimens compacted at 1.75 Mg/m^3, the values were recorded as 0.025 MPa, 0.025 MPa, and 0.031 MPa for 200°C, 110°C, and without heating, respectively. Furthermore, for specimens compacted at 2 Mg/m^3, the values were recorded as 0.068 MPa, 0.072 MPa, and 0.074 MPa for 200°C, 110°C, and without heating, respectively. The values of swell pressure of B_1 bentonite at 120 min were observed as 0.400 MPa, 0.521 MPa, and 0.524 MPa for specimens compacted at 1.5 Mg/m^3 at 200°C, 110°C, and without

heating, respectively. Similarly, for specimens compacted at 1.75 Mg/m^3, the values were recorded as 0.719 MPa, 0.771 MPa, and 0.878 MPa for 200°C, 110°C, and without heating, respectively. Furthermore, for specimens compacted at 2 Mg/m^3, the values were recorded as 0.644 MPa, 0.757 MPa, and 1.012 MPa for 200°C, 110°C, and without heating, respectively. The values of swell pressure of B_2 bentonite at 120 min were observed as 0.23 MPa, 0.26 MPa, and 0.34 MPa for specimens compacted at 1.5 Mg/m^3 at 200°C, 110°C, and without heating, respectively. Similarly, for specimens compacted at 1.75 Mg/m^3, the values were recorded as 0.27 MPa, 0.48 MPa, and 0.59 MPa for 200°C, 110°C, and without heating, respectively. Furthermore, for specimens compacted at 2 Mg/m^3, the values were recorded as 0.50 MPa, 0.68 MPa, and 0.93 MPa for 200°C, 110°C, and without heating, respectively. It was observed that the time taken for the saturation is less in the case of the specimen heated at 200°C than 110°C than without heating the specimen.

Fig. 5.3 Representation of a tiny gap created after heating of compacted bentonite

When the compacted samples were heated at 110°C and 200°C for about 3 hours, a gap was observed between the oedometer ring and the compacted bentonite samples (Fig. 5.3), which was not observed in the case of samples taken without heating. So initially, at 1 min, there is no significant difference in the time swelling curves of both the bentonites at various thermal histories for all the densities for all the samples, whereas after 1 min, the change was observed. As the compacted bentonites come in contact with wetting fluid, it starts swelling, but due to the observed gap at higher temperatures, it takes time to settle inside the ring. Hence the difference is observed in the time swelling curve of both the bentonites at all the densities and higher temperature as compared to the samples taken without heating.

5.2.2 Swell pressure of compacted bentonites subjected to thermal history

The variation of swell pressure with the temperature of compacted bentonites (compaction densities 1.5 Mg/m^3, 1.75 Mg/m^3, 2 Mg/m^3) is presented in Fig. 5.4, and Fig. 5.5. The swell pressure of B_1 bentonite compacted at a targeted density of 1.5 Mg/m^3 reduced from 0.910 MPa to 0.662 from and for 1.75 Mg/m^3 reduced from 1.725 to 1.565 MPa after treating at 200°C for 3 hrs. Comparatively, the swell pressure of B_1 bentonite compacted at a targeted density of 2 Mg/m^3 reduced from 2.166 to 1.822 MPa after treating at 200°C for 3 hrs. A similar pattern is observed in the variation of the swell pressure of B_2 bentonite with heating at the same temperatures for the same duration. The swell pressure of B_2 bentonite compacted at the targeted density of 1.5 Mg/m^3 reduced to 0.389 from 0.557 MPa and for 1.75 Mg/m^3 reduced from 0.979 to 0.761 MPa after treating at 200°C for 3 hrs. Comparatively, the pressure of B_2 bentonite compacted at the targeted density of 2 Mg/m^3 reduced from 1.617 to 1.497 MPa after treating at 200°C for 3 hrs.

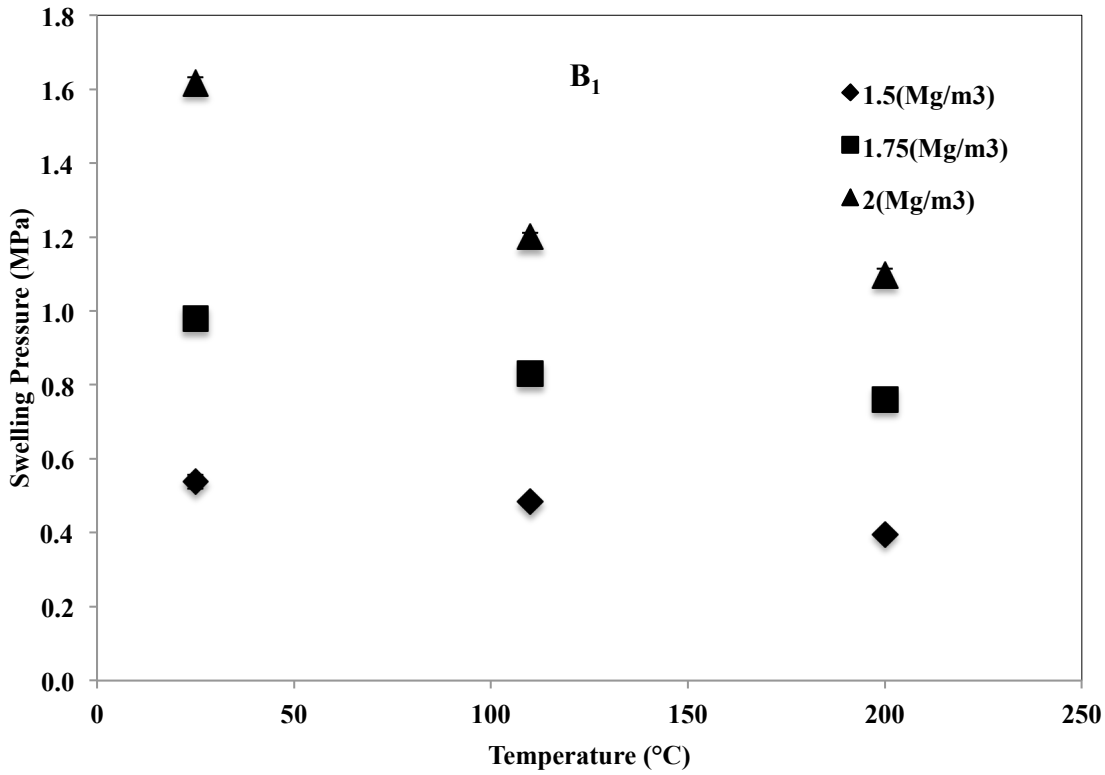

Fig. 5.4 Variation in swell pressures of B_1 with temperature and density

Estabragh (2016) reported that thermal history has an effect on the performance of powdered bentonite, and it is not only temperature-dependent but also time-dependent. The thermal history has influenced the index and physicochemical properties of bentonite such as liquid limit, specific surface area, cation exchange capacity, pH, OMC, MDD, etc. When clays are heated at high temperatures, they start losing water (Lingnau et al., 1996). It can be expressed as, initially (1) the removal of physical water when the temperature ranges from 100°C - 110°C and then (2) the loss of interlamellar water when the temperature ranges above 110°C up to 1000°C (Chandrasekhran et al., 1969). The swelling of the bentonite is usually considered at 1) macro-structural level and 2) microstructural level. The micro-pores consist of clay minerals and available exchangeable cations (Ravi and Rao, 2017). The macro-pores comprise structural pores that depend upon the compaction density.

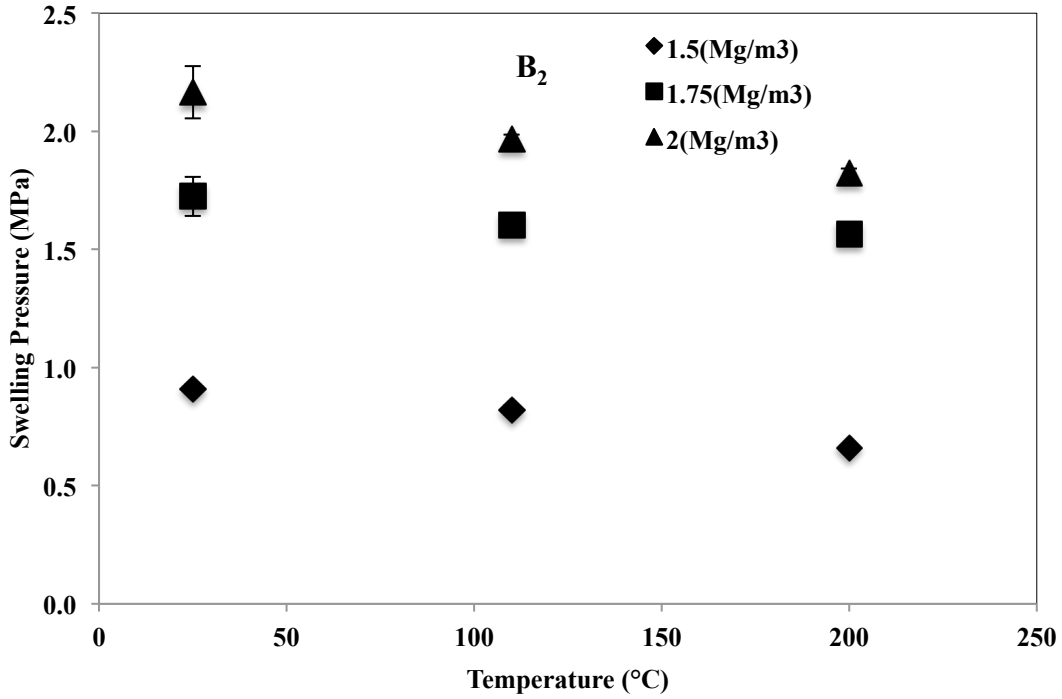

Fig. 5.5 Variation in swell pressures of B_2 with temperature and density

When the compacted bentonites were heated at 200°C for 3 hours, they were showing a difference in moisture content (Table 5.1) when compared with the samples heated at 110°C for 3 hours. As the difference in the moisture content at the same density at constant heating span depicts that there must be a loss of interlamellar moisture from the bentonite when it was heated at 200°C and the moisture moved from macropores to

micropores, in order to balance the moisture content. The microstructural water placed in the interlayer mainly causes swelling of bentonite. As the temperature increases, the microstructural water is triggered to the macrostructure, and it becomes unsaturated, which then further leads to the reduction in the swelling potential with the increase in temperature (Villar et al., 2009). Factors such as density, amount of compaction, and moisture content are recognized as factors affecting swell pressure. An increase in the temperature of bentonite decreases the hydration force due to the reduction in the number of hydrates in the smectite surface within bentonite and increases the osmotic pressure in the molecular system. These led to the reduction in the swelling pressure of compacted bentonite depending on the type of bentonite used, i.e., Na – bentonite or Ca-bentonite (Pusch et al. 1980). Cho et al. (1999) observed that the increase in temperature results in the increased porewater pressure due to the differences in thermal expansion of the pore water and the clay structure.

Table 5.1 Percentage reduction in the moisture content of both the compacted bentonites heated at different temperatures.

Bentonite	Density (g/cc)	WC at 200 after 3 hours	WC at 110 after 3 hours	% Reduction from 110 to 200
B_1	1.5	6.33	7.20	13.78
	1.75	7.04	8.54	21.29
	2	7.53	9.59	27.28
B_2	1.5	7.68	8.74	13.78
	1.75	8.28	9.81	18.54
	2	8.75	10.68	22.12

Phase II - Swell pressure of compacted bentonite saturated with hyperalkaline cement water at different thermal histories

5.3 Effect of thermal history and saturating cement water on swell pressure

5.3.1 Time swelling of compacted bentonites subjected to thermal history

Fig. 5.6 depicts the plot of swell pressure vs. time of bentonite B_1 for the combination of all compaction densities and thermal histories. The time of saturation for the sample compacted at 1.5 Mg/m^3 was noted as 28800 min, 24480 min, and 15120 min without heating, 110°C, and 200°C, respectively. Similarly, the time of saturation for the sample compacted at 1.75 Mg/m^3 was noted as 36720 min, 33840 min, and 27360 min without heating, 110°C, and 200°C, respectively. Furthermore, the time of saturation for the

sample compacted at 2 Mg/m^3 was noted as 43920 min, 39600 min, and 38160 min without heating, 110°C, and 200°C, respectively.

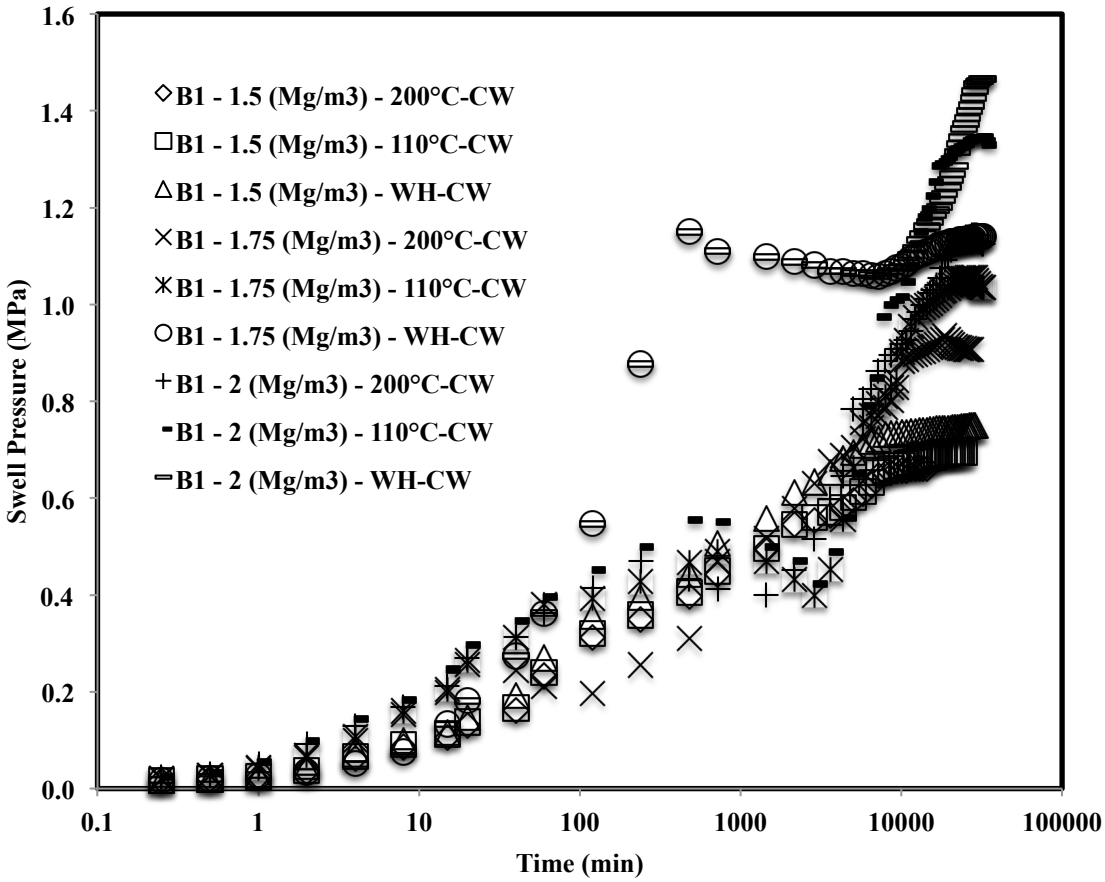

Fig. 5.6 Time swelling curve of B_1 bentonite when heated at different temperatures saturated with cement water.

Similarly, Fig. 5.7 represents the plot of swell pressure vs. time of bentonite B_2 for the combination of all compaction densities and thermal histories. It was observed that the time of saturation for the sample compacted at 1.5 Mg/m^3 was noted as 22320 min, 18720 min, and 15840 min without heating, 110°C, and 200°C, respectively. Similarly, the time of saturation for the sample compacted at 1.75 Mg/m^3 was noted as 24480 min, 20160 min, and 16560 min without heating, 110°C, and 200°C, respectively. Furthermore, the time of saturation for the sample compacted at 2 Mg/m^3 was noted as 31680 min, 24480 min, and 19440 min without heating, 110°C, and 200°C, respectively.

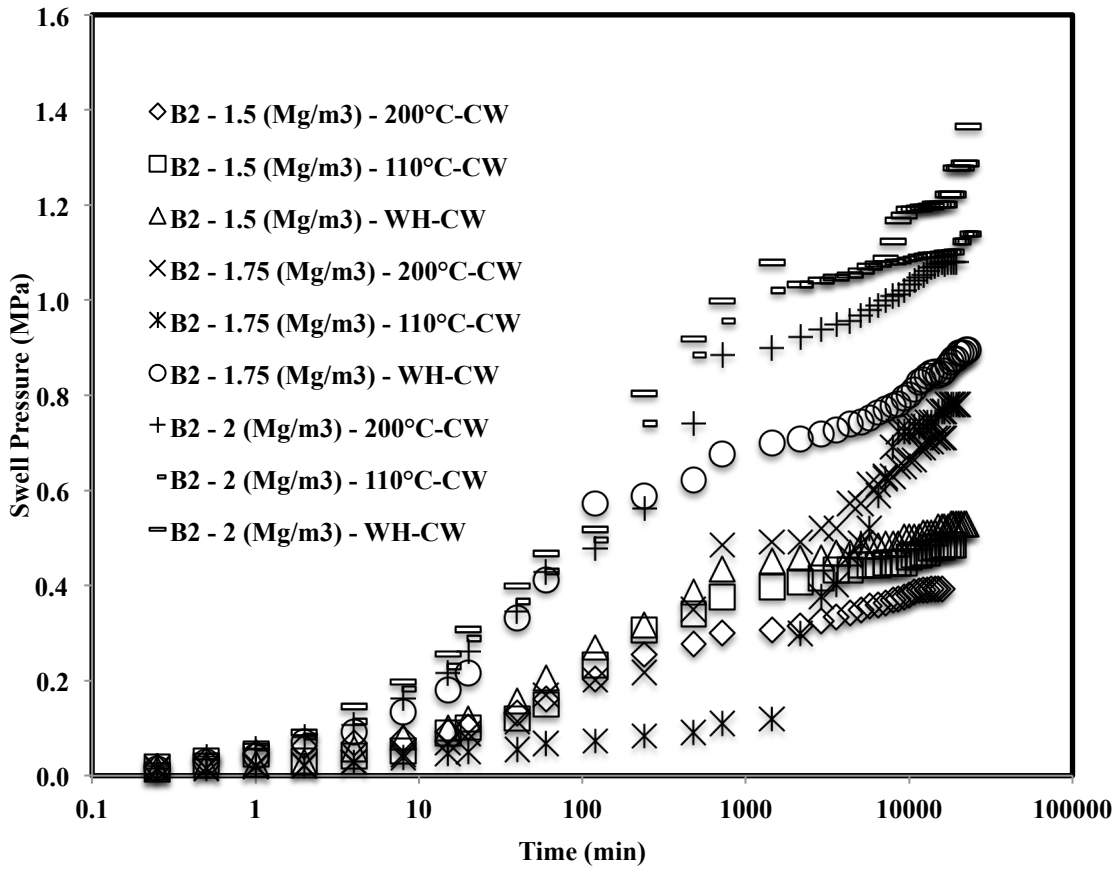

Fig. 5.7 Time swelling curve of B_2 bentonite when heated at different temperatures saturated with cement water.

5.3.2 Swell pressure of compacted bentonites subjected to thermal history

The swell pressure vs. temperature variation of the bentonite B_1 and B_2 saturated with cement water for three different compaction densities 1.5 Mg/m^3, 1.75 Mg/m^3, 2 Mg/m^3 is presented in Table 5.2, and the water contents of the specimens after applying the thermal history are presented in Table 5.3.

Table 5.2 Final swell pressure values of both the bentonites at each temperature for various densities.

Bentonite	Temperature (°C)	Swell pressure (MPa) at dry densities 1.5, 1.75, and 2.0 Mg/m^3		
		1.5 (Mg/m^3)	1.75 (Mg/m^3)	2 (Mg/m^3)
B_1	200	0.661	0.948	1.143
	110	0.694	1.055	1.345
	25	0.75	1.14	1.472
B_2	200	0.392	0.485	0.53
	110	0.71	0.781	0.896
	25	1.08	1.139	1.285

Table 5.3 The water contents of the specimens after subjected to thermal history

Sr no	Bentonite	Density (Mg/m^3)	Water Content at 200°C after 3 hours	Water Content at 110°C after 3 hours
1	B_1	**1.5**	7.02	7.45
		1.75	7.27	8.89
		2	8.12	10.04
2	B_2	**1.5**	8.08	8.96
		1.75	8.56	10.12
		2	8.98	11.04

The reduction in the final swell pressure values was observed with the increase in the temperature for all compacted densities and both the bentonites.

5.4 Comparison of swell pressure of bentonite saturated with cement water and distilled water

5.4.1 Comparison of time swelling of thermally loaded compacted bentonites saturated with distilled and cement water

The variation of swell pressure of compacted bentonites specimens compacted at targeted densities of 1.5 Mg/m^3, 1.75 Mg/m^3, 2 Mg/m^3 due to thermal history and cement solution is shown in Fig. 5.8, 5.9, and 5.10. Fig. 5.8 represents the variation in swell pressure of bentonite B_1 at a density of 1.5 Mg/m^3. It could be seen from the curves the swell pressure of bentonite without heating the compacted sample and saturated with distilled water was 0.909 MPa, whereas the swell pressure when heated at 110°C was 0.821 MPa, and at 200°C, it was observed as 0.662 MPa. Similarly, swell pressure of the same bentonite was observed as 0.750 MPa, whereas the swell pressure when heated at 110°C was 0.694 MPa, and at 200°C, it was observed as 0.661 MPa when saturated with cement solution. A similar trend of results was reported for the higher densities of 1.75 Mg/m^3, 2 Mg/m^3 when saturated with both the solutions (Fig. 5.9 and 5.10). The results reported for bentonite B_2 showed a similar trend as B_1. It is represented in Fig. 5.11, 5.12, and 5.13.

The main observation from these comparisons was the formation of the double peak when both the bentonites were subjected to saturation with cement water, i.e., hyperalkaline solution. The first peak may be observed due to the density at which the sample was compacted and the elastic network that is built up by the bentonite particles at the particular density. Initially, when the bentonite came in contact with the highly

alkaline cement water, the swelling occurred due to crystalline swelling, and the elastic nature of compacted bentonite would still have a strong structural bond due to interlamellar bonding.

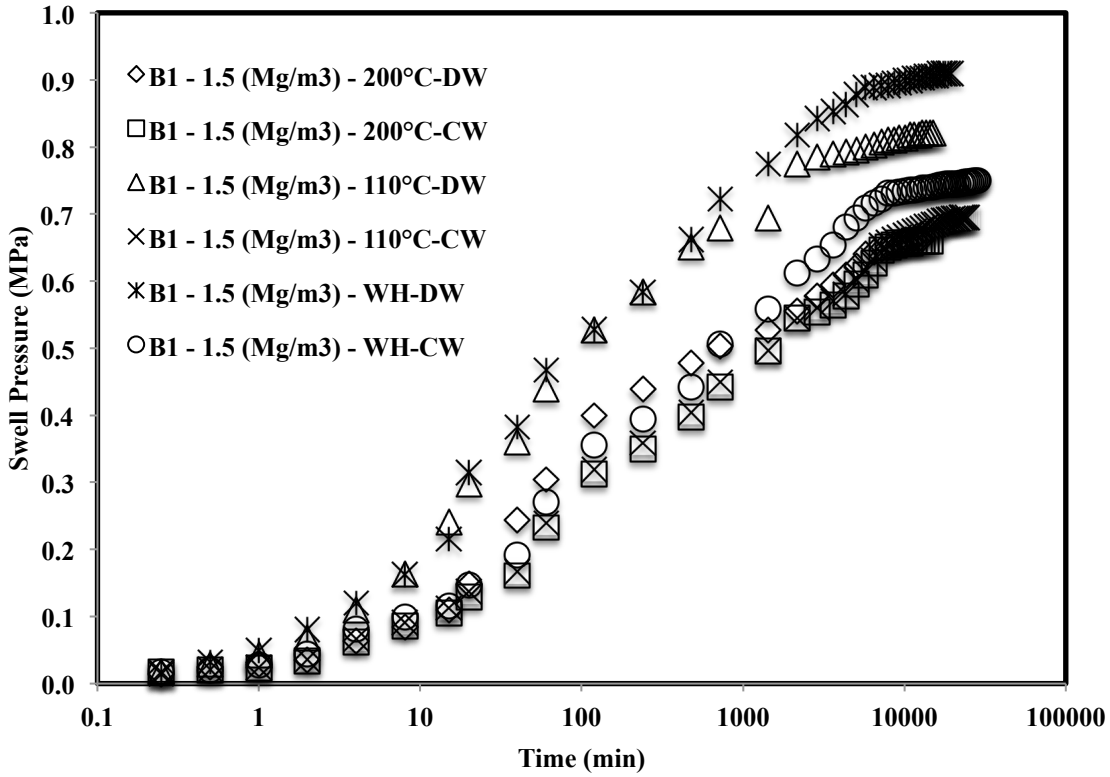

Fig. 5.8 Time swelling curve of B_1 bentonite (1.5 Mg/m^3) when heated at different temperatures saturated with distilled water and cement water.

Hence it started swelling as well as creating pressures on the adjacent clay units. After the first peak, it got a relaxation for the deformation as well as the displacement, and hence for some point of time after the first peak, the swell pressure reduced slightly, or in some cases, it was constant. With the further ingression of hyper alkaline solution, the clay particles tried to form a homogeneous structure by rearranging themselves and therefore creating an unbalanced net charge. In order to balance these unbalanced net charges, the bentonite started swelling and tried to reach to the saturation by moisture intake. Therefore this second phase after rearrangement of particles gave rise to a secondary peak.

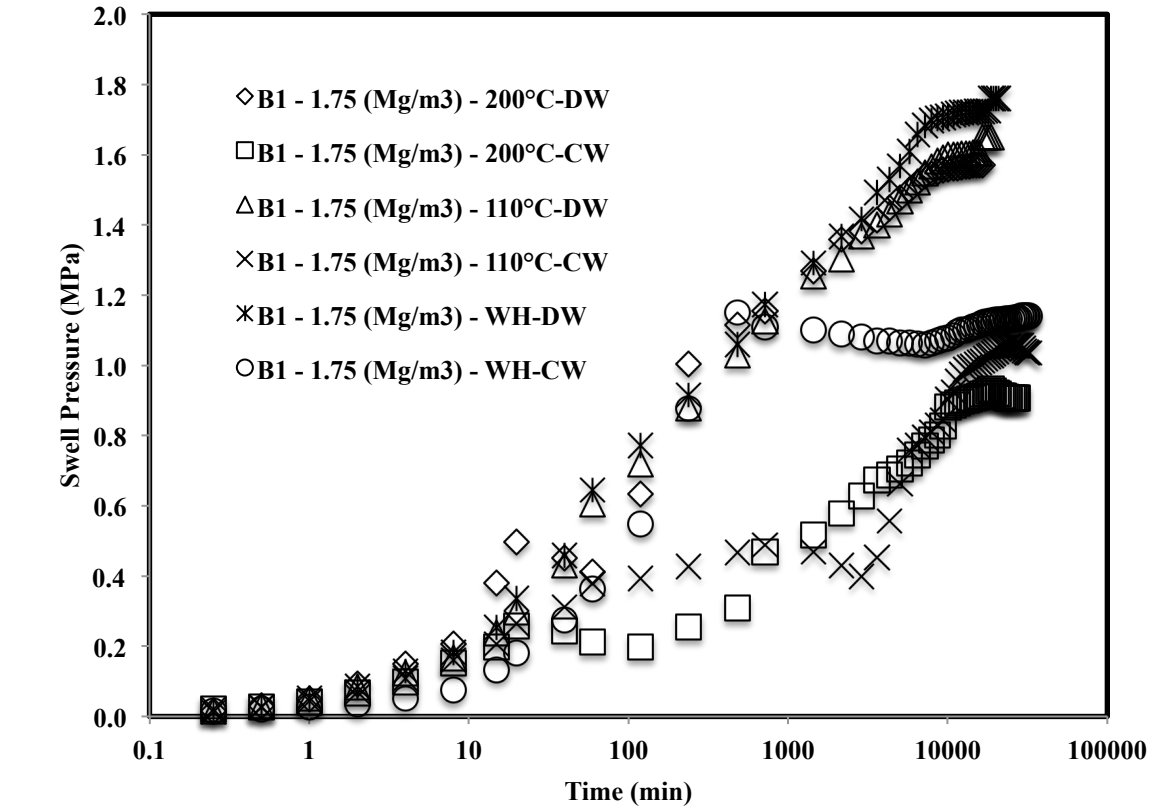

Fig. 5.9 Time swelling curve of B_1 bentonite (1.75 Mg/m^3) when heated at different temperatures saturated with distilled water and cement water.

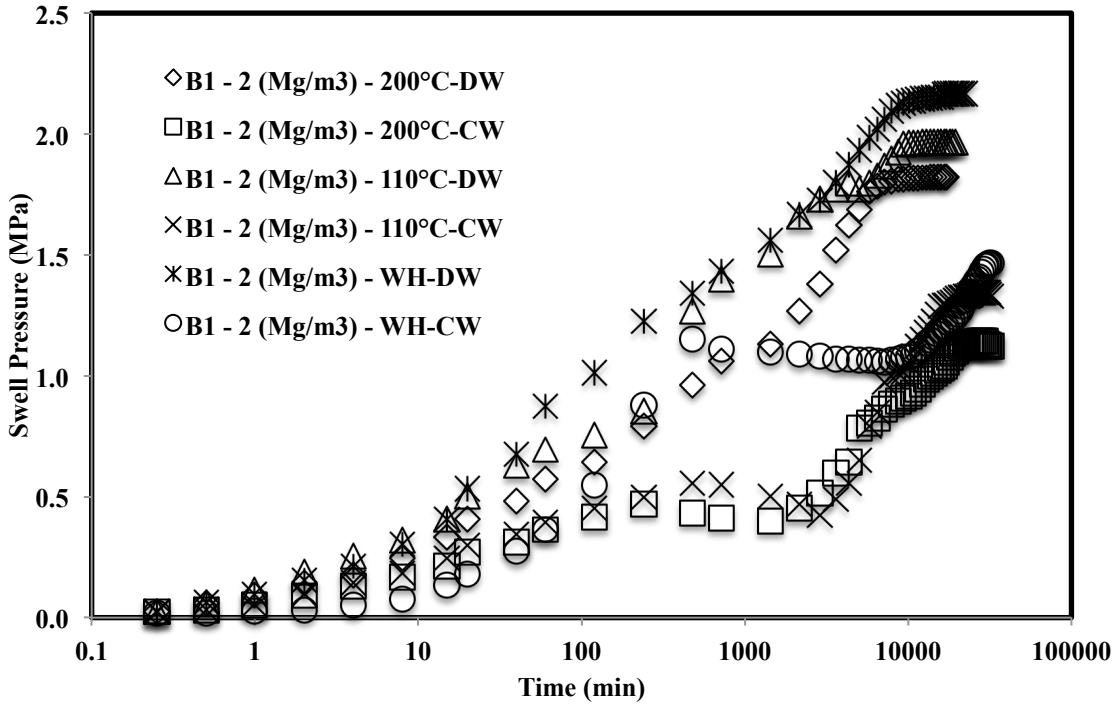

Fig. 5.10 Time swelling curve of B_1 bentonite (2 Mg/m^3) when heated at different temperatures saturated with distilled water and cement water.

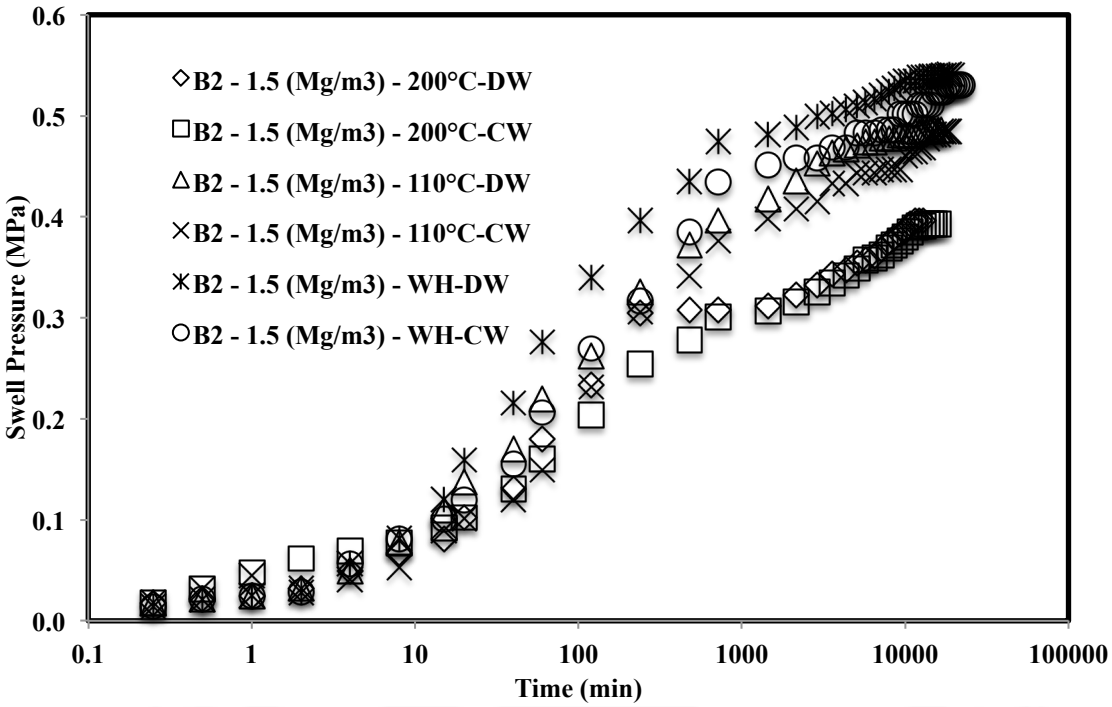

Fig. 5.11 Time swelling curve of B_2 bentonite (1.5 Mg/m^3) when heated at different temperatures saturated with distilled water and cement water.

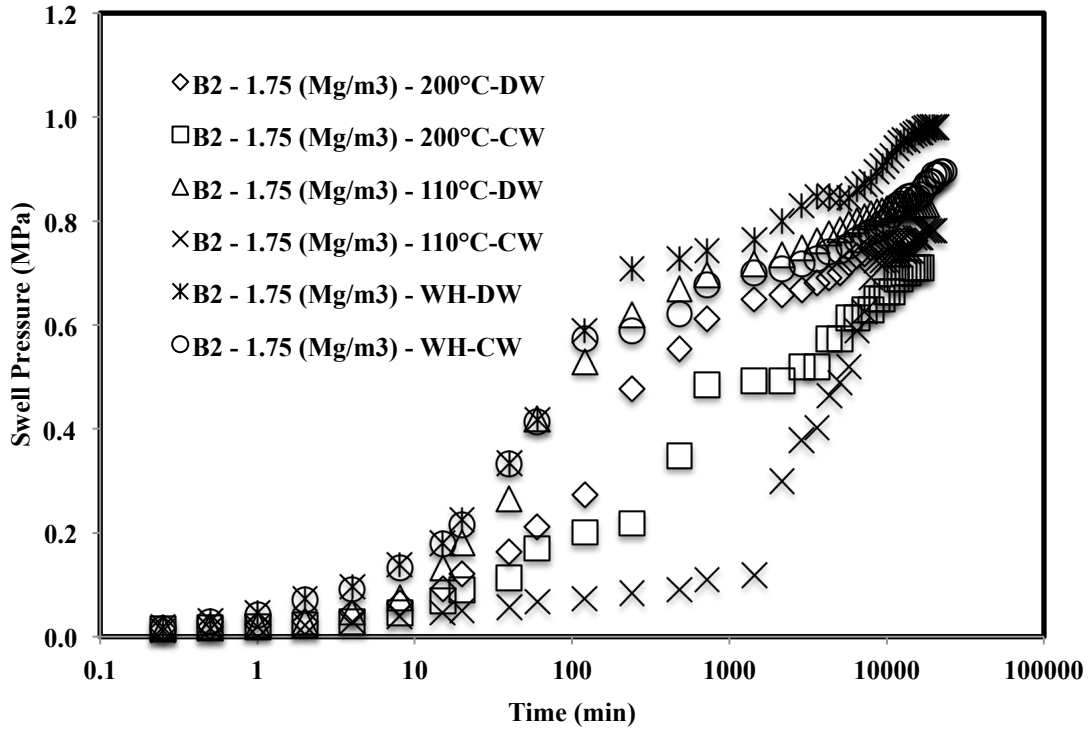

Fig. 5.12 Time swelling curve of B_2 bentonite (1.75 Mg/m^3) when heated at different temperatures saturated with distilled water and cement water.

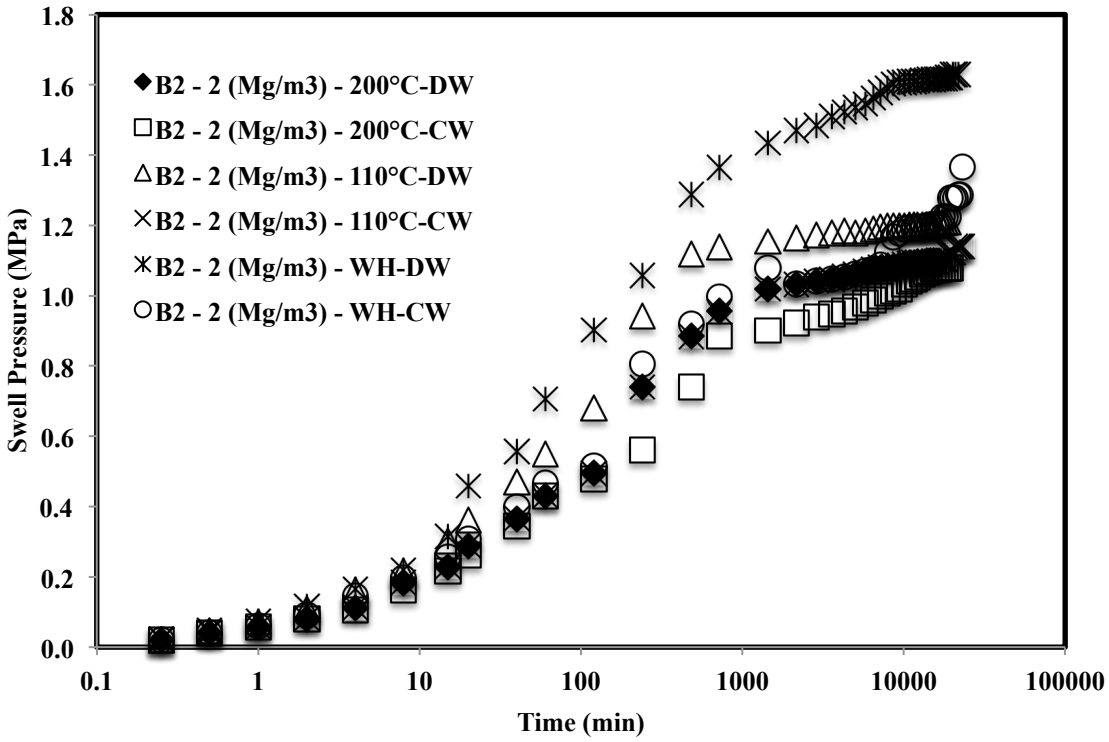

Fig. 5.13 Time swelling curve of B_2 bentonite (2 Mg/m^3) when heated at different temperatures saturated with distilled water and cement water

5.4.2 Comparisons of swell pressure of thermally loaded compacted bentonites saturated by distilled and cement water

Fig. 5.14 and 5.15 represent a comparison of variation in swell pressures of both bentonites with temperature and density saturated with distilled water and cement water, respectively. It was observed that the swell pressure of bentonite compacted at 1.5 Mg/m^3 and saturated with cement water and distilled water was 0.661 MPa and 0.662 MPa, respectively, when heated at 200^{0}C. Whereas it was 0.694 MPa and 0.821 MPa, respectively, when heated at 110^{0}C and 0.750 MPa and 0.909 MPa, respectively, for samples without heating.

However, the swell pressure of bentonite compacted at 1.75 Mg/m^3 and saturated with cement water and distilled water was 0.907 MPa and 1.570 MPa, respectively, when heated at 200°C. Whereas it was 1.035 MPa and 1.650 MPa respectively when heated at 110°C and 1.123 MPa and 1.760 MPa respectively for samples without heating and the swell pressure of bentonite compacted at 2 Mg/m^3 and saturated with cement water and distilled water, was 1.122 MPa and 1.823 MPa respectively when heated at 200^{0}C. Whereas it was reported as 1.320 MPa and 1.969 MPa, respectively when heated at 110°C and 1.448 MPa and 2.166 MPa respectively for samples without heating.

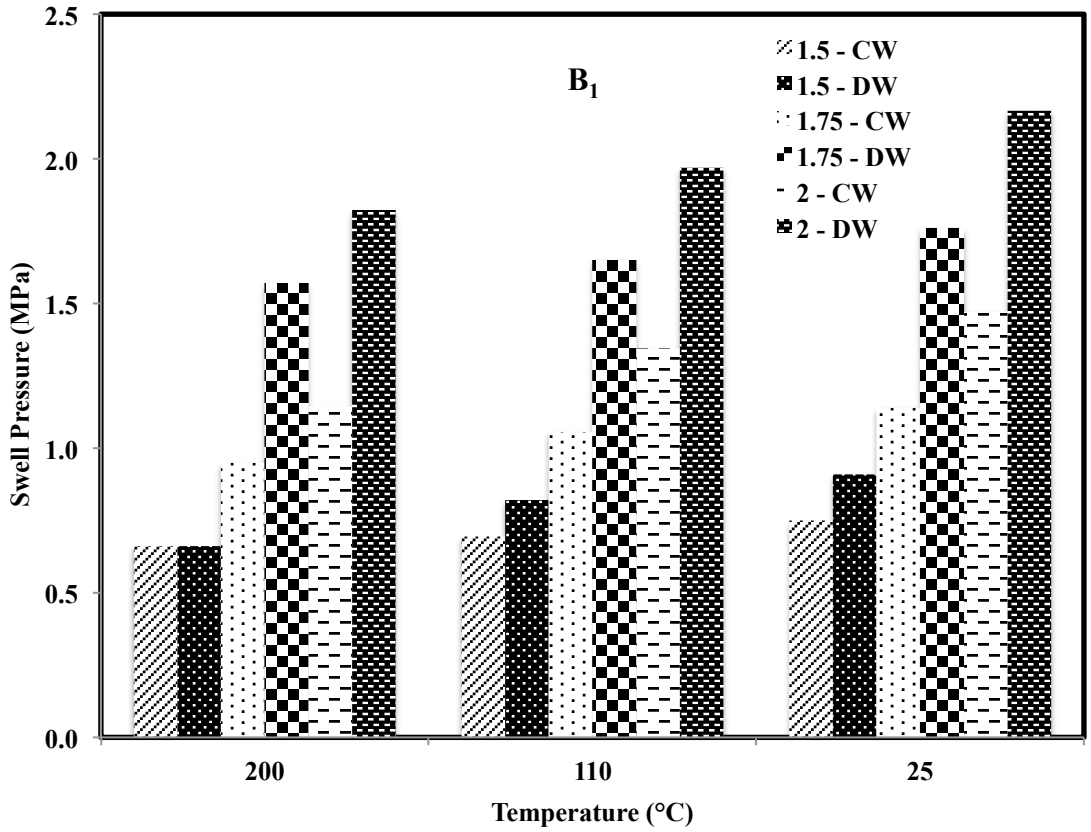

Fig. 5.14 Comparison of variation in swell pressures of B_1 with temperature and density saturated with distilled water and cement water.

A similar trend was noted in the case of bentonite B_2, and it was observed that the swell pressure in the case of bentonite B_1 was recorded to be more than that of B_2 when saturated with both the solutions. Also, the swell pressure in the case of cement water was recorded less than that of distilled water for both the bentonites.

In this particular reaction of hyperalkaline water with the montmorillonite mineral, two important reactions were taking place. 1) The hyperalkaline solution attacked the structure lattice pattern of the montmorillonite mineral. 2) On the further reaction of $Ca(OH)_2$ with water, it formed free Ca^{2+} ions with OH^- ions, and these Ca^{2+} ions might have occupied the space between the interlamellar gaps of bentonite by the exchange of cations.

$$Ca(OH)_2 + H_2O \Longrightarrow Ca^{2+} + 2OH^- \qquad (1)$$

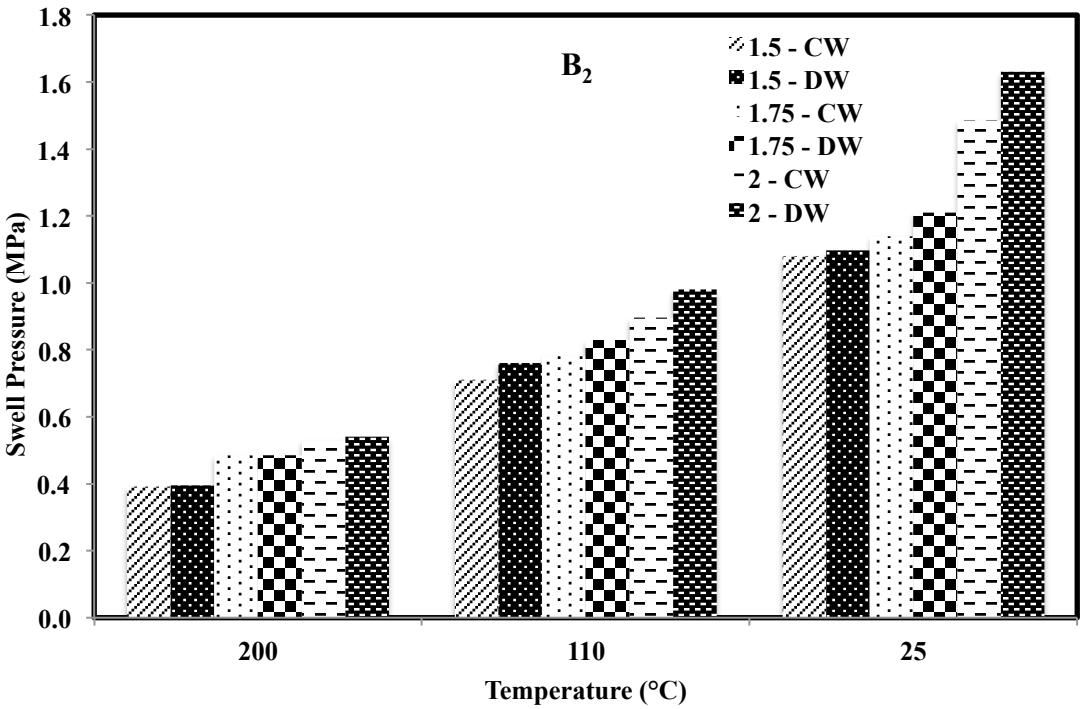

Fig. 5.15 Comparison of variation in swell pressures of B_2 with temperature and density saturated with distilled water and cement water.

These exchanges of cations might have reduced the interlamellar spacing of montmorillonite and therefore reducing the swelling and swell pressure of the bentonite. However, the OH^- ions being an anion migrated far away from the smectite lattice. As there was less possibility of an anion entering in the narrow interlamellar space of the smectite and react with the cation from the specific surface, the probability of breaking down of structure lattice was very low (Pusch, 1982).

5.4.3 Comparison of time of saturation in case of distilled and cement water

There is a comment on the time of saturation of compacted bentonites when saturated with cement water and distilled water (Fig. 5.16 and 5.17). Though the swell pressure of both the bentonites was more in the case of distilled water than cement water, the time taken for the saturation of the samples of all densities with all-temperature variations was more than that of time taken in the case of distilled water. The various samples were observed under a field emission scanning electron microscope, and the presence of some secondary minerals in the pores of bentonites was observed.

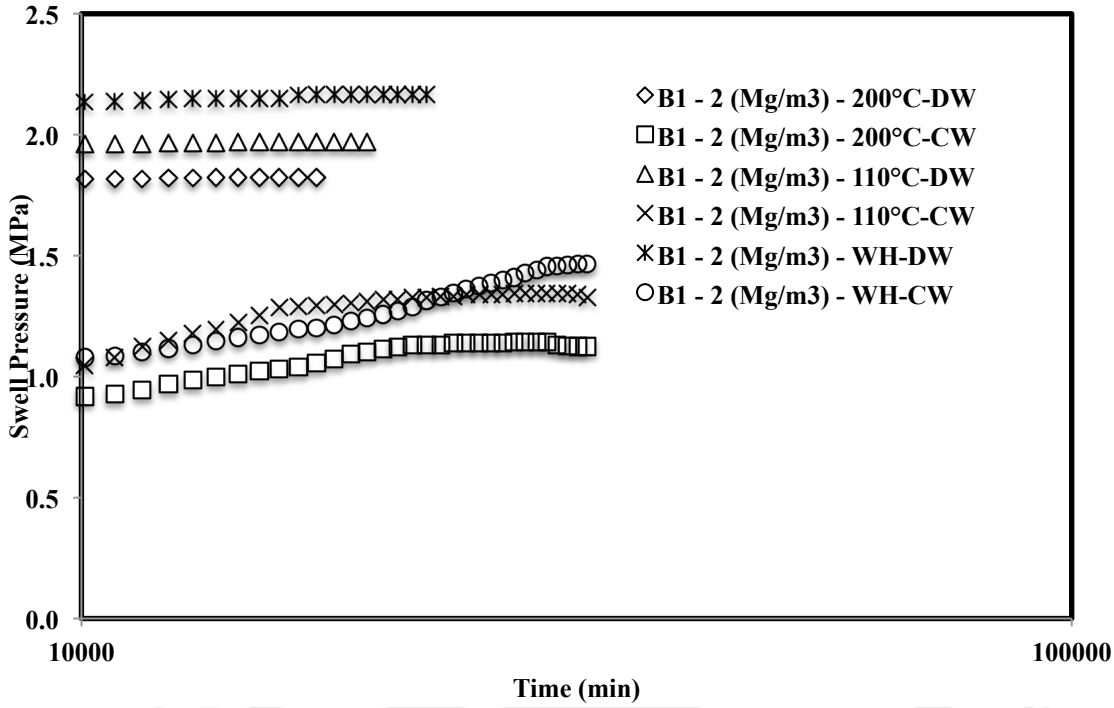

Fig. 5.16 Comparison of variation of time of saturation of compacted bentonite B_1 saturated with distilled water and cement water

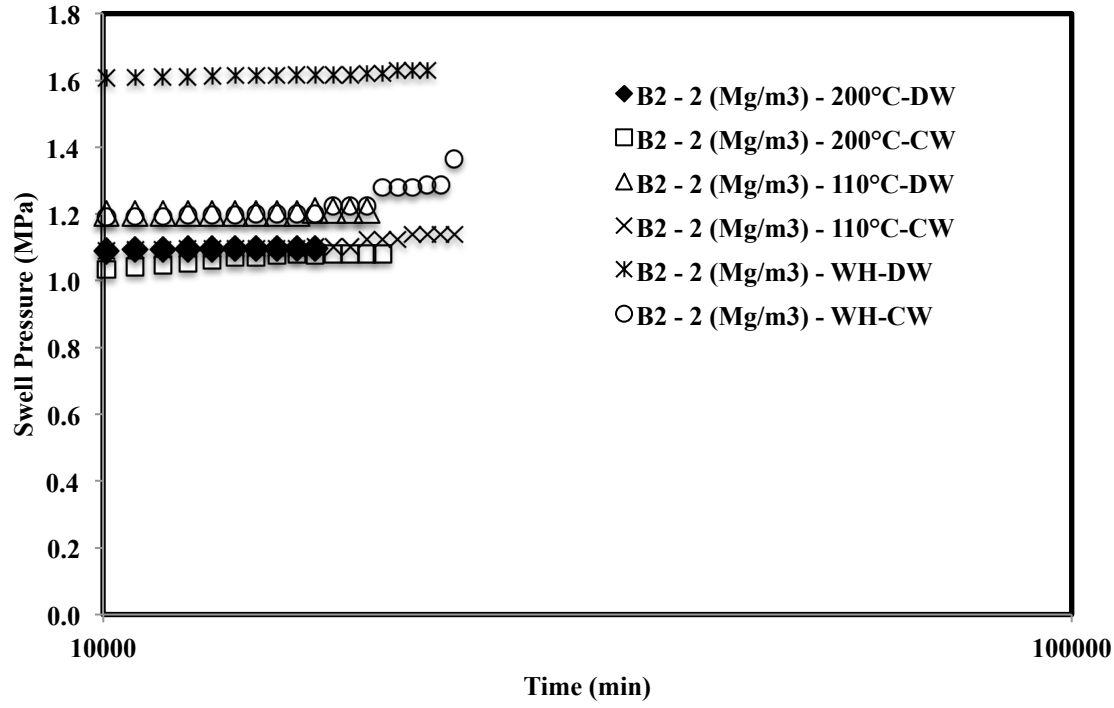

Fig. 5.17 Comparison of variation of time of saturation of compacted bentonite B_2 saturated with distilled water and cement water

Fig. 5.21 is a FESEM image of a bentonite sample compacted at 1.75 Mg/m^3 and saturated with cement water. The details of secondary minerals could be clearly seen from the image. It was observed that the plate-shaped secondary mineral was deposited between the pores of bentonite, and it was probably a non-swelling mineral called portlandite. The portlandite mineral was formed when calcium from cement reacted with water and formed calcium hydroxide ($Ca(OH)_2$).

$$Ca + 2H_2O \rightarrow Ca(OH)_2(aq) + H_2(g)$$

The alkaline nature of the pore water that was present in the concrete was due to the presence of portlandite (pH=12.5). The precipitation of calcite was also observed in FESEM images of some of the bentonite samples (B_2). From Fig. 5.22, the calcite deposition could be clearly observed.

Table 5.4 Comparison of the total time of saturation of samples saturated with distilled water and hyperalkaline cement water.

S.N.	Bentonite	Dry Density (Mg/m^3)	Temperature (°C)	Time (min) for DW	Time (min) for CW
1	B_1	1.5	200	12960	14400
			110	15120	24480
			WH	17280	27360
		1.75	200	16560	28080
			110	18720	33840
			WH	20880	36720
		2	200	17288	38160
			110	19440	39600
			WH	22320	43920
2	B_2	1.5	200	12960	15840
			110	16560	18720
			WH	19440	22320
		1.75	200	15120	16560
			110	18000	20160
			WH	20888	24480
		2	200	16560	19440
			110	18720	24480
			WH	21600	31680

Fig. 5.18 and 5.19 show the EDX pattern of the bentonite saturated with cement water and distilled water, respectively. The percentage of Na was observed to be reduced when saturated with cement water, whereas the percentage of calcium showed a tremendous increase. Along with these changes, the drastic increase in the percentage of Fe was also observed when saturated with cement water. Fig. 5.20 depicts the XRD pattern of both bentonites saturated with cement water and distilled water. The 8 mm sample was cut into two parts for the XRD analyses, the lower part was indicated by 4mm (a), and the upper part was indicated by 4mm (b). It can be observed that the lower part of the sample that came in contact with the cement water first showed a peak of portlandite mineral, whereas it is not observed in the upper part of the sample but not in the case of B_2 and samples saturated with distilled water. The peak of calcite was observed in the case of samples saturated with cement water and not for samples saturated with distilled water.

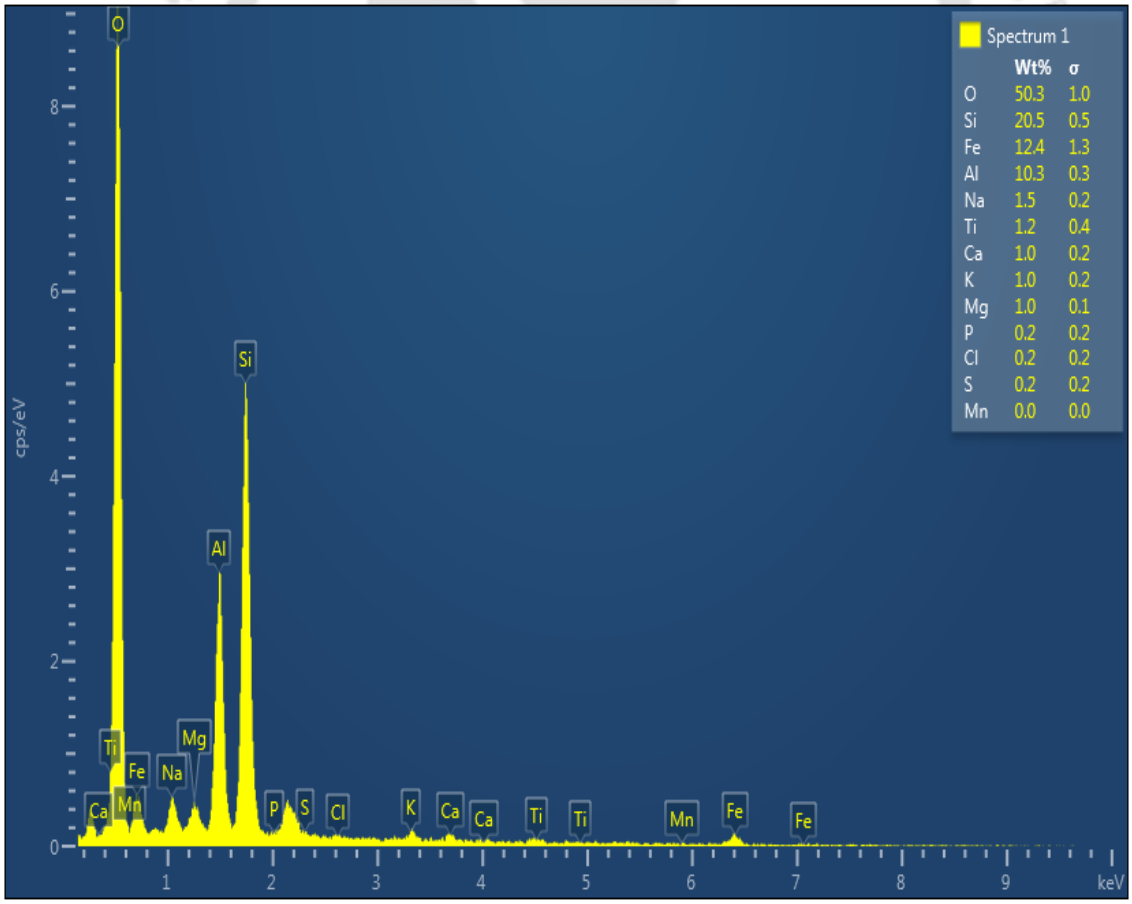

Fig. 5.18 EDX analysis of bentonite saturated with cement water

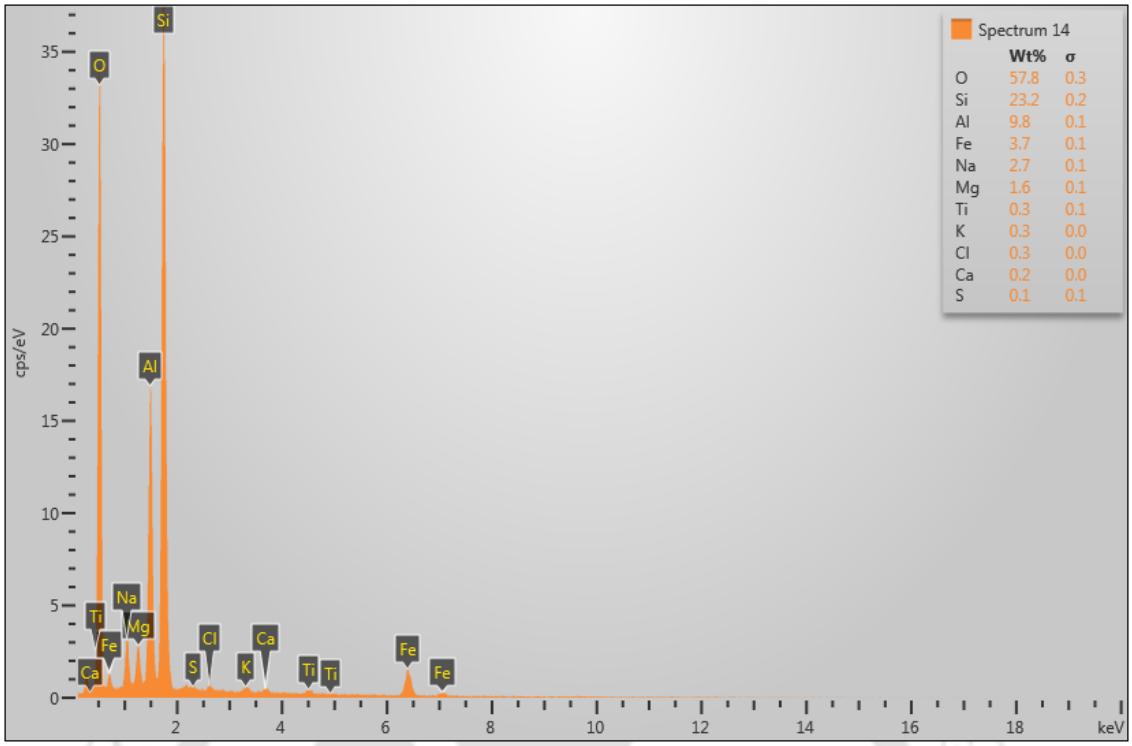

Fig. 5.19 EDX analysis of bentonite saturated with distilled water

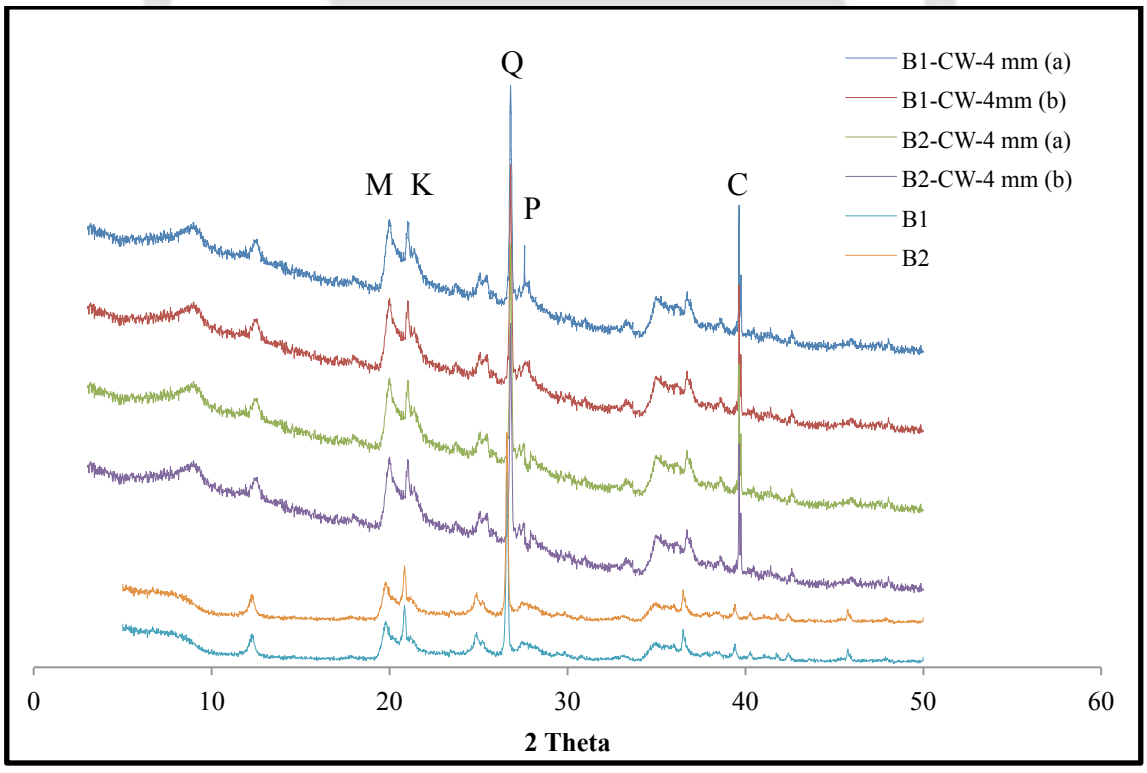

Fig. 5.20– XRD analysis of bentonites. M – montmorillonite, K – kaolinite, Q – quartz, P – portlandite, C – Calcite

It is clear from the discussion in the preceding section that the specimens saturated with distilled water exhibited larger values of swell pressure and achieved full saturation with lesser time compared to the specimens saturated with the cement solutions. A probable reason for this observation is 1) due to the presence of secondary minerals such as portlandite and 2) the precipitation of calcium in the specimen saturated with the cement water. According to (Pusch, 1982) the presence of portlandite might have clogged the pores of the specimens saturated with the cement solution, leading to a reduction in the permeability. Hence the time taken for the solution to reach all the accessible pores is more in these specimen compacted to the specimen saturated with the distilled water. The presence of portlandite is evident in Fig. 5.21.

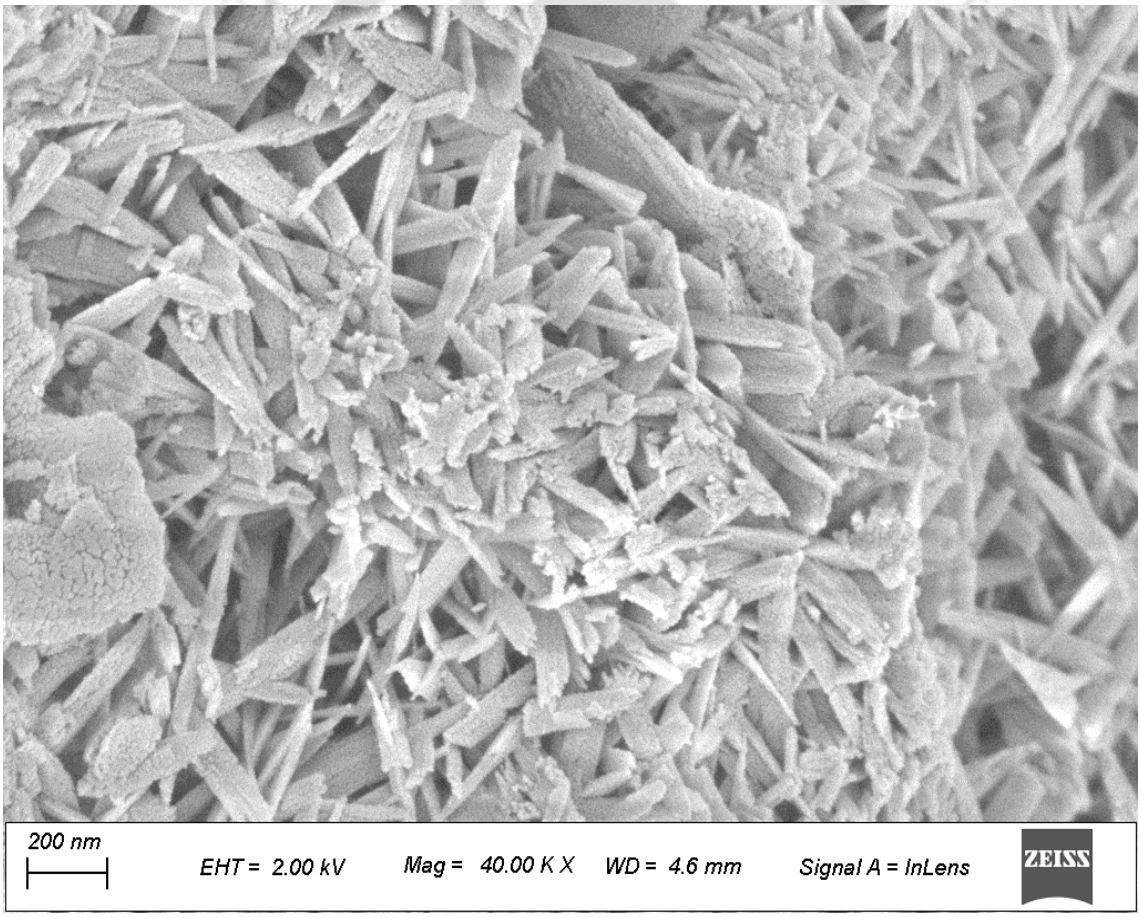

Fig. 5.21 Portlandite plates between the bentonite pores.

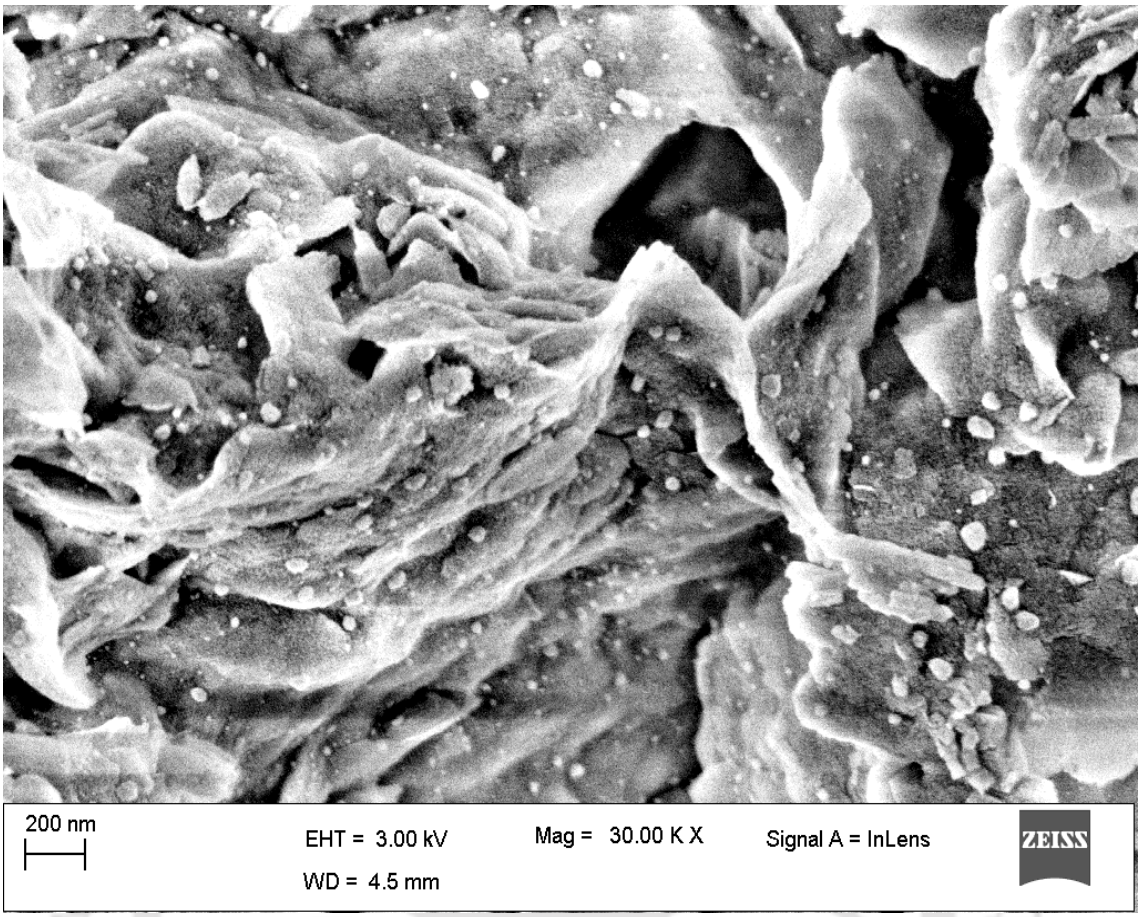

Fig. 5.22 Calcite deposition on the flakes of bentonite

More evidence on the reduction in permeability due to the formation of the secondary mineral can be seen in Fig. 5.22, where the lower part of the specimen exhibited the presence of portlandite while the upper part did not. Moreover, the percentage of Na in the composition is reduced and Ca increased in the specimen saturated with the cement solution (Fig. 5.18 and 5.19). Hence the final swell pressure value is less in these specimen compared to the specimen saturated with the distilled water since the presence of monovalent cations in the porewater will impart more swelling than the divalent cations (Mitchell and Soga, 2005)

5.4.4 Comparison of the initial time of saturation for different temperatures

The initial time of saturation of all samples heated at 200°C, 110°C, and WH were compared, and it was observed that for the first 10 min of swelling of the sample, which was without heating showed, the faster swelling than the sample heated at 110°C than 200°C. When the compacted samples were subjected to various thermal histories for

about 3 hours, the compacted samples shrank, and a tiny space was observed between the oedometer ring and the compacted bentonite samples (Fig. 5.23). This gap was due to the evaporation of the water during the thermal loading, which could be considered as the pre-consolidation of the specimen. According to Alonso et al. (1990, 1999, 2005), Weimin et al. (2014), the cyclic wetting and drying of expansive clays might induce permanent plastic strains in the pore-network of the compacted specimens. Comparatively, the large amount of thermal loading in the specimens of the current study might have experienced this plastic strain in the microstructure that led to the reduction in the final swell pressure values. Hence, there was a difference in the swell pressure observed for the initial 10 min of the test for all specimens, and the lower value of swell pressure was observed during the first 10 min for higher temperatures.

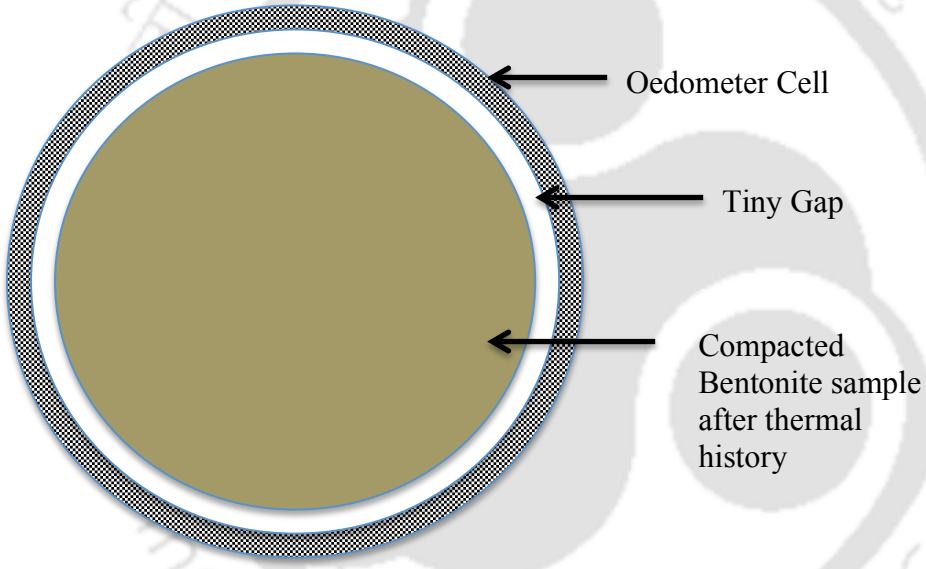

Fig. 5.23 Representation of a tiny gap

5.5 Conclusion

Deep geological disposal of high-level nuclear waste is based on a multi-barrier system concept to isolate the waste from the biosphere. The bentonite buffer used in the DGR has to be stable even with the variations in the temperature from the waste canister as well as due to repository conditions. Various thermal histories induced on the compacted bentonite samples from Barmer district of Rajasthan, India, compacted at different targeted densities, i.e., 1.5 Mg/m^3, 1.75 Mg/m^3, and 2 Mg/m^3, and subjected to heating at 110°C and 200°C for about 3 hours, showed that the thermal histories have a

significant influence on the swell pressures of the compacted bentonites. The swell pressures of both the bentonite decreased with an increase in the temperature. The swell pressure reduced by 15% and 7% for B_1 and B_2, respectively, at 200°C.

The presence of cement/concrete layer creates an alkaline environment (pH>12) inside the deep geological repository by percolating pore fluids through the cement layer towards compacted bentonite buffer. The temperature variations that occurred due to the presence of a hot canister may alter the properties of compacted bentonite buffer. The final swell pressure value of samples saturated with cement water was found to be approximately 22% and 48% less than that of samples saturated with distilled water for B_1 and B_2, respectively, at 200°C. The time of saturation in the case of cement for all the combinations of densities and thermal history was approximately 1.5 times more than in the case of distilled water.

The microstructural observations revealed that the clogging of the pores might have been done due to the presence of portlandite mineral and precipitation of calcite, thus increased the time of saturation. The swell pressure values of bentonite B_2 was less than that of B_1 because of the difference in its initial characterization, especially liquid limit, specific surface area, and cation exchange capacity. The time of saturation taken in case of samples compacted at 2 Mg/m^3 was more than that of samples compacted at lower densities for all thermal histories as well as for both the saturating solutions; therefore, it can be said that the higher density can delay the time of saturation of the compacted bentonite buffer in the deep geological repository. However, the present study is a laboratory-scale experiment, and the data can be used while designing large scale field monitoring. Also, the long-term effect of thermal history on the swell pressure could be modeled with the help of the above experimental data.

Chapter 6

SWELL PRESSURE OF COMPACTED BENTONITE SPECIMENS: COUPLED INFLUENCE OF CANISTER CORROSION, HYPER ALKALINE SOLUTION, AND THERMAL HISTORY

6.1 INTRODUCTION

Bentonite is compacted around waste canisters so as to ensure the sealing of the canister by blocking the entry of harmful radiations. However, the canister may have an initially high temperature (150°C - 200°C), which gradually reduces due to the continuous decay of radioactive waste over a long period of time, depending upon the half-life of the radioactive material. This process creates a thermal history on the surrounded compacted bentonite. The unbalanced conditions generated inside the deep geological repository can force the steel canister to corrode (Lantenios et al. 2005; Debruyn et al. 1991). Such chemically unstable corrosion may produce harmful leachates that may alter the properties of bentonite, affecting its overall performance. Hence, initially, due to the high temperature (>100°C), there would be an absence of moisture near the surface of the canister in the compacted bentonite. As the temperature, reduces with time moisture will flow towards the canister, and the presence of moisture will start corroding the canister surface, and the compacted bentonite will be induced with the thermal history. Under such unstable conditions, the corrosion of the canister starts producing leachate, which affects the engineering properties of the thermally loaded buffer and may create a pathway (Samper et al., 2008; Marsh and Taylor, 1998) for the reactive transport. The montmorillonite mineral of the bentonite might be altered into other minerals by these combined interactions of corrosion products and high temperatures, altering its swelling capacity, which is mainly possessed due to the montmorillonite mineral (Hill, 2016; Legrand et al., 2000). On the other hand, the hyperalkaline fluids infiltrated from the host rock could simultaneously interfere with the compacted bentonite subjected to thermal history and reaction with metallic corrosion.

This chapter presents an investigation of the influence of corrosion products on the swell pressure of compacted bentonite specimens subjected to thermal history. Bentonite specimens (B_1 and B_2) were mixed with metallic iron powder in the ratio (1:0.1) and compacted at dry densities of 1.5 Mg/m^3, 1.75 Mg/m^3, and 2.0 Mg/m^3. These specimens were subjected to thermal loadings at 110°C and 200°C and saturated with distilled water and hyperalkaline cement water. The swell pressure of compacted and thermally

loaded bentonite specimens saturated by both fluids were recorded and compared with the samples without thermal history. Microstructural observations were performed with the help of Field Emission Scanning Electron Microscope (FESEM), X-ray diffraction (XRD), and Energy Dispersive X-ray (EDX). This chapter is divided into two phases. Phase 1 presents the influence of corrosion products on swell pressure of compacted bentonites saturated with distilled water, and Phase 2 presents the influence of corrosion products on swell pressure of compacted bentonites saturated with hyperalkaline cement water and its comparison with distilled water.

6.2 RESULTS AND DISCUSSIONS

Phase I - Effect of iron corrosion on swell pressure of compacted bentonite subjected to thermal history

6.2.1 Time swelling of compacted bentonites subjected to thermal history

Fig. 6.1 depicts the plot of the variation of swell pressure with time for bentonite B_1 for the combination of thermal histories and compaction densities in addition to corrosion products. The time of saturation for the sample compacted at 1.5 Mg/m^3 was noted as 35280 min, 31680 min, and 18000 min for samples without heating, 110°C, and 200°C, respectively. Similarly, the time of saturation for the sample compacted at 1.75 Mg/m^3 was noted as 41760 min, 36720 min, and 33120 min for samples without heating, 110°C, and 200°C, respectively. Furthermore, the time of saturation for the sample compacted at 2 Mg/m^3 was noted as 48960 min, 45360 min, and 44640 min for samples without heating, 110°C, and 200°C, respectively.

Similarly, Fig. 6.2 represents the plot of swell pressure vs. time of bentonite B_2 for the combination of all compaction densities and thermal histories in addition to corrosion products. It was observed that the time of saturation for the sample compacted at 1.5 Mg/m^3 was noted as 29520 min, 25920 min, and 23040 min without heating, 110°C, and 200°C, respectively. Similarly, the time of saturation for the sample compacted at 1.75 Mg/m^3 was noted as 30240 min, 26640 min, and 22320 min without heating, 110°C, and 200°C, respectively. Furthermore, the time of saturation for the sample compacted at 2 Mg/m^3 was noted as 40320 min, 30240 min, and 24840 min without heating, 110°C, and 200°C, respectively.

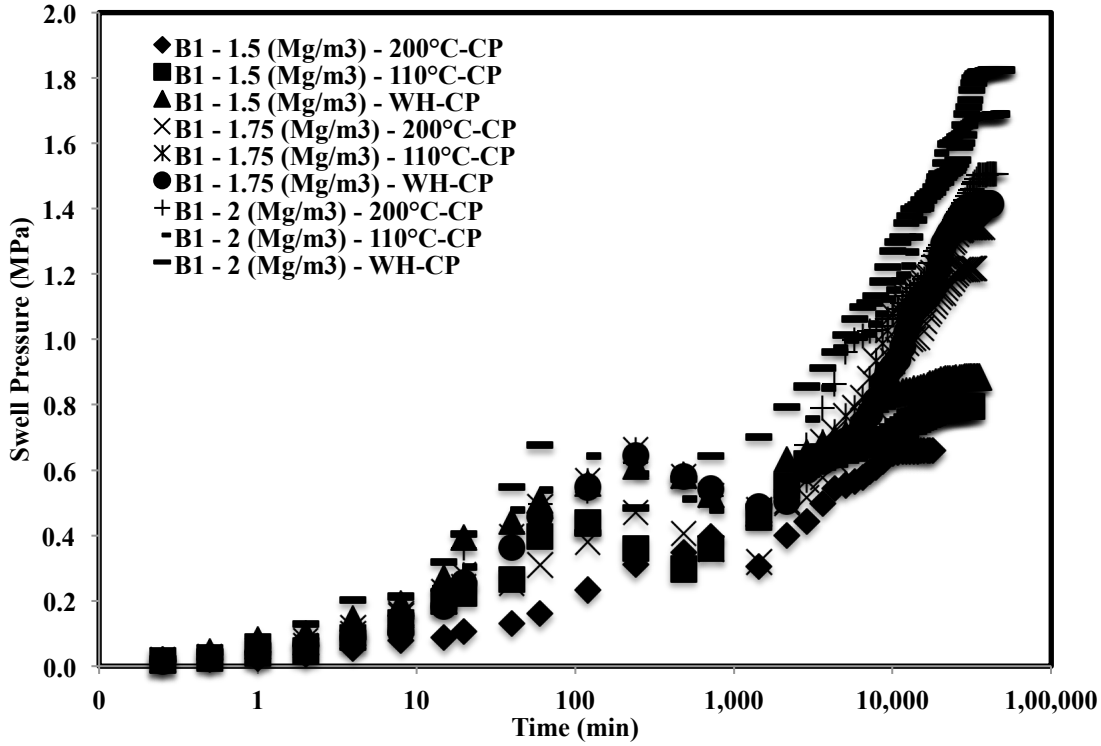

Fig. 6.1 Variation of swell pressure with a time of B_1 bentonite added with corrosion product and heated at different temperatures.

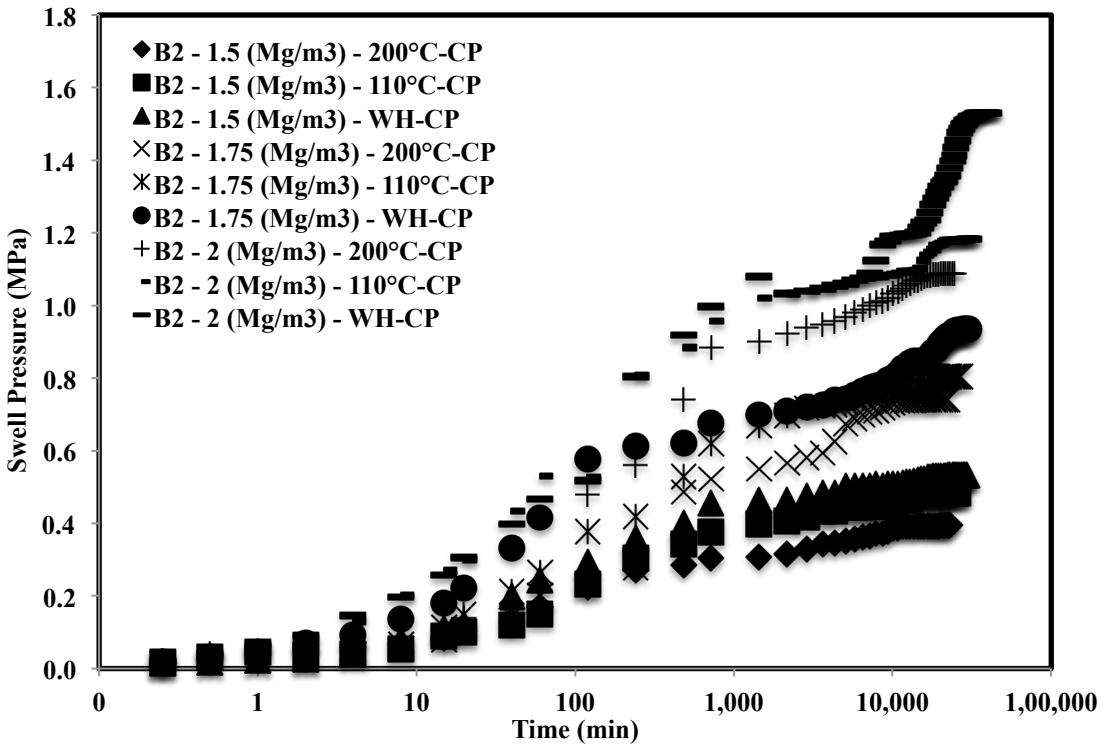

Fig. 6.2 Variation of swell pressure with a time of B_2 bentonite added with corrosion product and heated at different temperatures.

6.2.2 Swell pressure of compacted bentonites subjected to thermal history

The variation of swell pressure with a temperature of the bentonite B_1 and B_2 in addition to corrosion product and compacted at three different compaction densities 1.5 Mg/m^3, 1.75 Mg/m^3, 2 Mg/m^3 is presented in Fig. 6.3 and Fig. 6.4, respectively. The data points B_1-1.5-CP presents the swell pressure of the specimens of bentonite B_1 compacted at 1.5 Mg/m^3 in the presence of the corrosion products. Similarly, data points B_1-1.75-CP present the swell pressure of the specimens of bentonite B_1 compacted at 1.75 Mg/m^3 in the presence of the corrosion products, and data points B_1-2-CP presents the swell pressure of the specimens of bentonite B_1 compacted at 2 Mg/m^3 in the presence of the corrosion products.

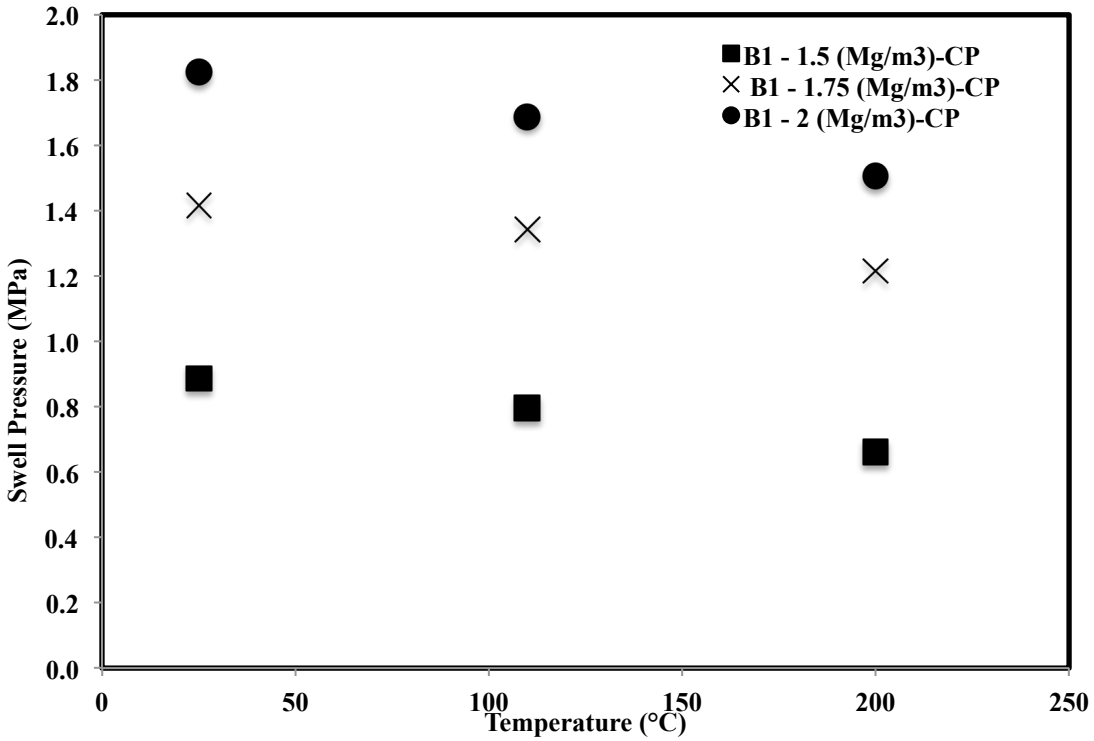

Fig. 6.3 Variation in swell pressures of bentonite B_1 with temperature added with corrosion product (CP) at various densities

The reduction in the final swell pressure values was observed with the increase in the temperature for all compacted densities and both the bentonites. In the case of B_1 bentonite, the final swell pressure reduced from 0.886 to 0.662 MPa, 1.145 to 1.216 MPa, and from 1.825 to 1.507 MPa for the compaction densities 1.5 Mg/m^3, 1.75 Mg/m^3, and 2 Mg/m^3 when added with corrosion product. Similarly, in the case of B_2 bentonite, the final swell pressure reduced from 0.396 from 0.534 MPa, 0.934 to 0.741

MPa, and from 1.531 to 1.008 MPa for the compaction densities 1.5 Mg/m^3, 1.75 Mg/m^3, and 2 Mg/m^3 when added with corrosion product. The reduction in swell pressure values for B_1 bentonite compacted at 2 Mg/m^3 was 17%, whereas it is 34% in the case of B_2.

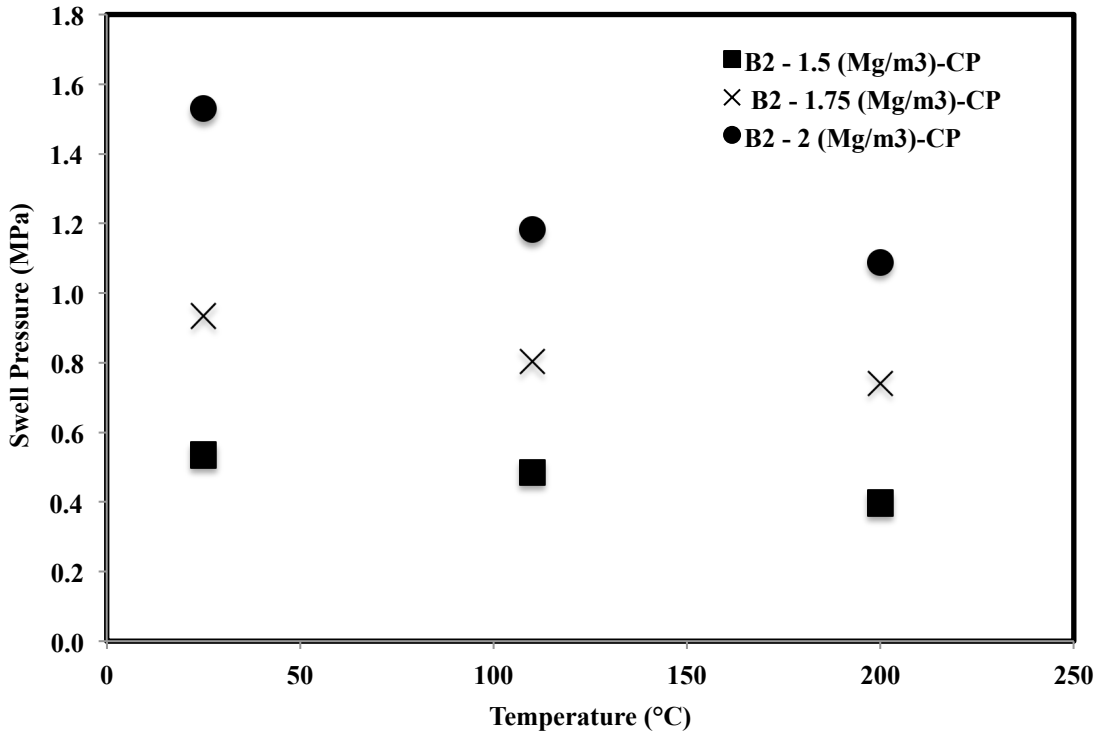

Fig. 6.4 Variation in swell pressures of bentonite B_2 with temperature added with corrosion product (CP) at various densities

6.2.3 Comparison of time swelling of compacted bentonites with and without the addition of corrosion product when subjected to thermal history

The variation of swell pressure of compacted bentonites specimens compacted at targeted densities of 1.5 Mg/m^3, 1.75 Mg/m^3, 2 Mg/m^3 due to thermal history and corrosion product is shown in Fig. 6.5, 6.6, and 6.7. Fig. 6.5 represents the variation in swell pressure of bentonite B_1 in addition to corrosion product at a density of 1.5 Mg/m^3 at three different temperatures and its comparison with the specimens without corrosion products. Similarly, Fig. 6.6 represents the variation in swell pressure of bentonite B_1 in addition with corrosion product at a density of 1.75 Mg/m^3 at three different temperatures and its comparison with the specimens without corrosion products, and Fig. 6.7 represents the variation in swell pressure of bentonite B_1 in addition with corrosion

product at a density of 2 Mg/m^3 at three different temperatures and its comparison with the specimens without corrosion products.

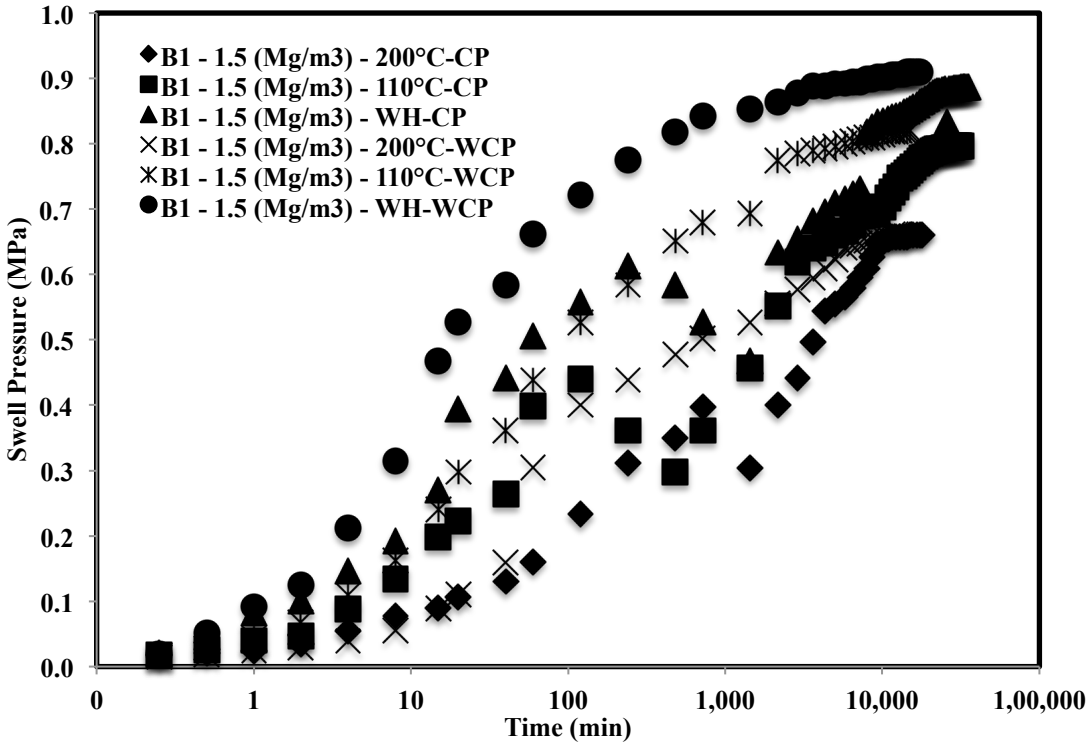

Fig. 6.5 Time swelling curve of B_1 bentonite (1.5 Mg/m^3) when heated at different temperatures saturated with distilled water without the addition of corrosion product and when added with corrosion product.

It could be seen from the curves that the swell pressure of bentonite added with corrosion product and saturated with distilled water without heating was 0.909 MPa, whereas the swell pressure when heated at 110°C was 0.821 MPa, and at 200°C, it was observed as 0.662 MPa. Similarly, swell pressure of the same bentonite was observed as 0.886 MPa, whereas the swell pressure when heated at 110°C was 0.796 MPa, and at 200°C, it was observed as 0.662 MPa when saturated with cement solution. A similar trend of results was reported for the higher densities of 1.75 Mg/m^3, 2 Mg/m^3 when saturated with both the solutions (Fig. 6.6 and 6.7). The results reported for bentonite B_2 showed a similar trend as B_1. It is represented in Fig. 6.8, 6.9, and 6.10. Fig. 6.8 represents the variation in swell pressure of bentonite B_2 in addition to corrosion product at a density of 1.5 Mg/m^3 at three different temperatures and its comparison with the specimens without corrosion products.

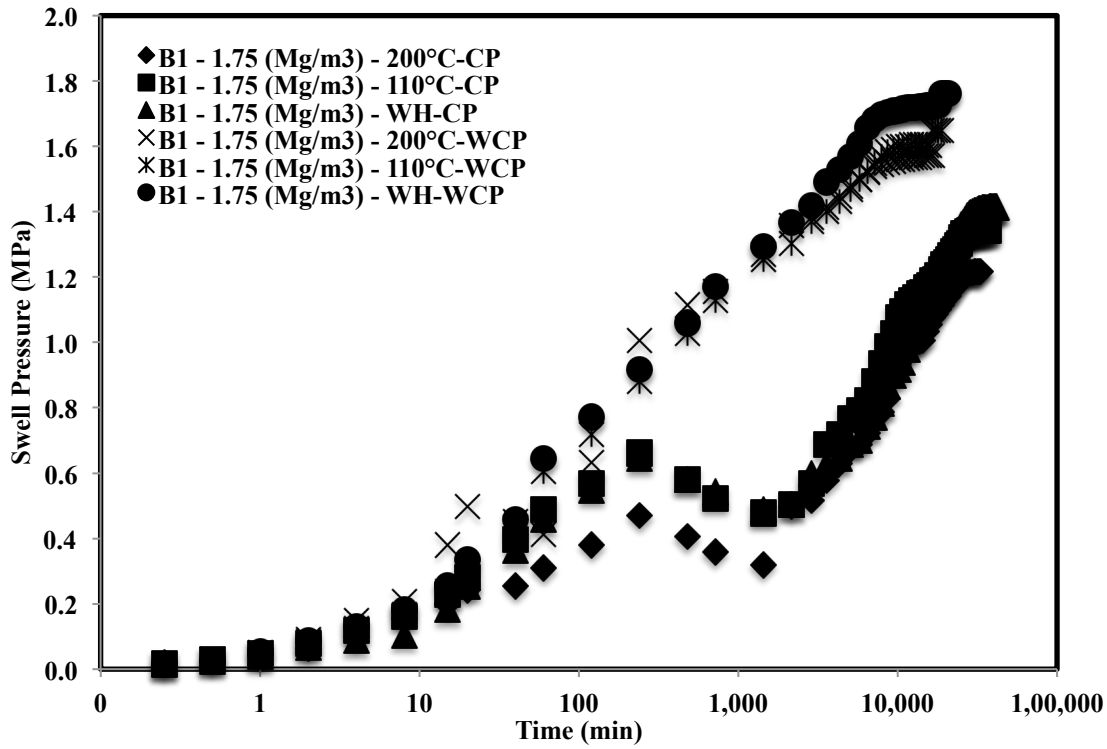

Fig. 6.6 Time swelling curve of B_1 bentonite (1.75 Mg/m^3) when heated at different temperatures saturated with distilled water without the addition of corrosion product and when added with corrosion product.

Similarly, Fig. 6.9 represents the variation in swell pressure of bentonite B_2 in addition to corrosion product at a density of 1.75 Mg/m^3 at three different temperatures and its comparison with the specimens without corrosion products. Fig. 6.10 represents the variation in swell pressure of bentonite B_2 in addition to corrosion product at a density of 2 Mg/m^3 at three different temperatures and its comparison with the specimens without corrosion products.

From these comparison curves, it was observed that there is a formation of the double peak in all the specimens, which had the presence of corrosion products and not in the specimens without the corrosion products. It may happen because; when the metallic iron came in contact with the moisture, it started forming corrosion leachate. The corrosion causes the pH value of bentonite to increase (Lantenios et al., 2005). The mechanism behind the increase in the pH may be considered as the exchange of Fe^{2+} ions with the cations of lesser valances that are present inside the bentonite. Due to the increased pH (>8), the inside environment became alkaline, and therefore a double peak was observed in the samples in which metallic iron was present (Lantenios et al., 2005).

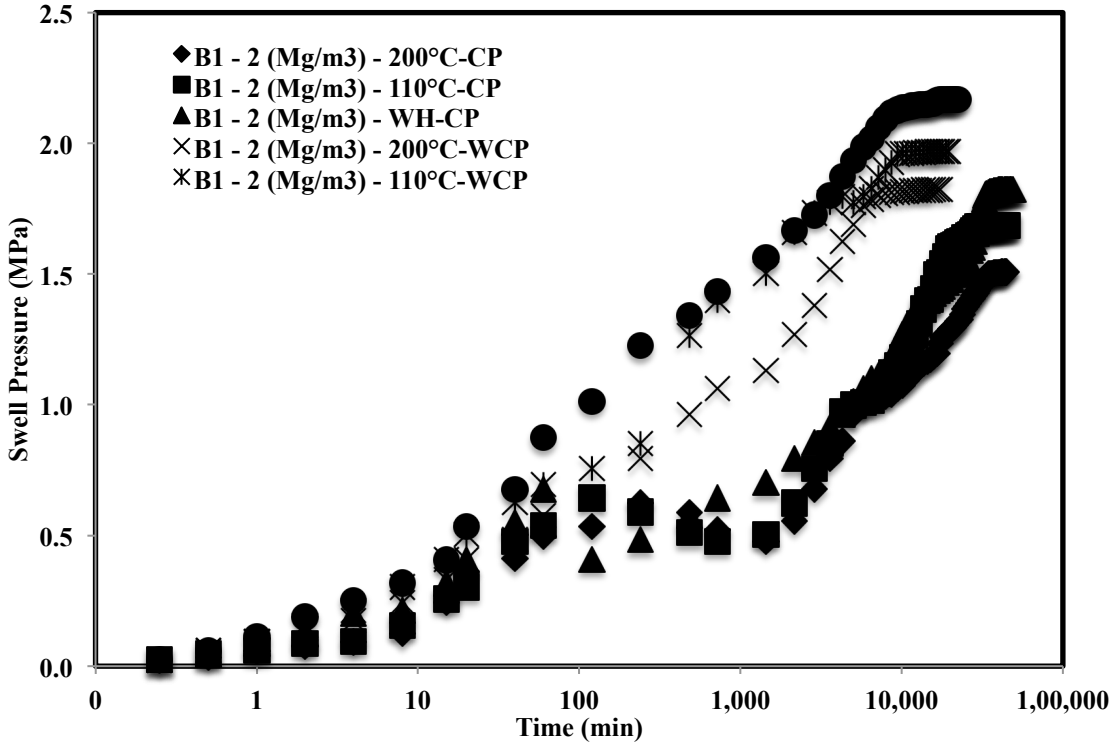

Fig. 6.7 Time swelling curve of B_1 bentonite (2 Mg/m^3) when heated at different temperatures saturated with distilled water without the addition of corrosion product and when added with corrosion product.

Initially, the swell pressure increased due to the compaction density of the bentonite samples. It attained the first peak till it could, due to its elastic nature, and at some point in time, it started decreasing, maybe due to the presence of metallic iron present in the samples. After attaining the first peak, the internal rearrangement of the particles started because of the elastic nature. With the further contact of moisture with the samples containing metallic iron, the bentonite particles started to balance the unbalanced net charge, which it got during the rearrangement of particles. Hence the swell pressure increased to form a double peak. The possible reason behind the lesser values of swell pressure in the presence of corrosion products may be the dissolution of montmorillonite by the formation and precipitation of secondary minerals such as magnetite, siderite, etc. The presence of these minerals is identified in the X-ray diffraction patterns presented in the following section. Therefore the swell pressure values are lesser in the presence of corrosion products. Moreover, the increase in temperature might also have accelerated the smectite dissolution rate.

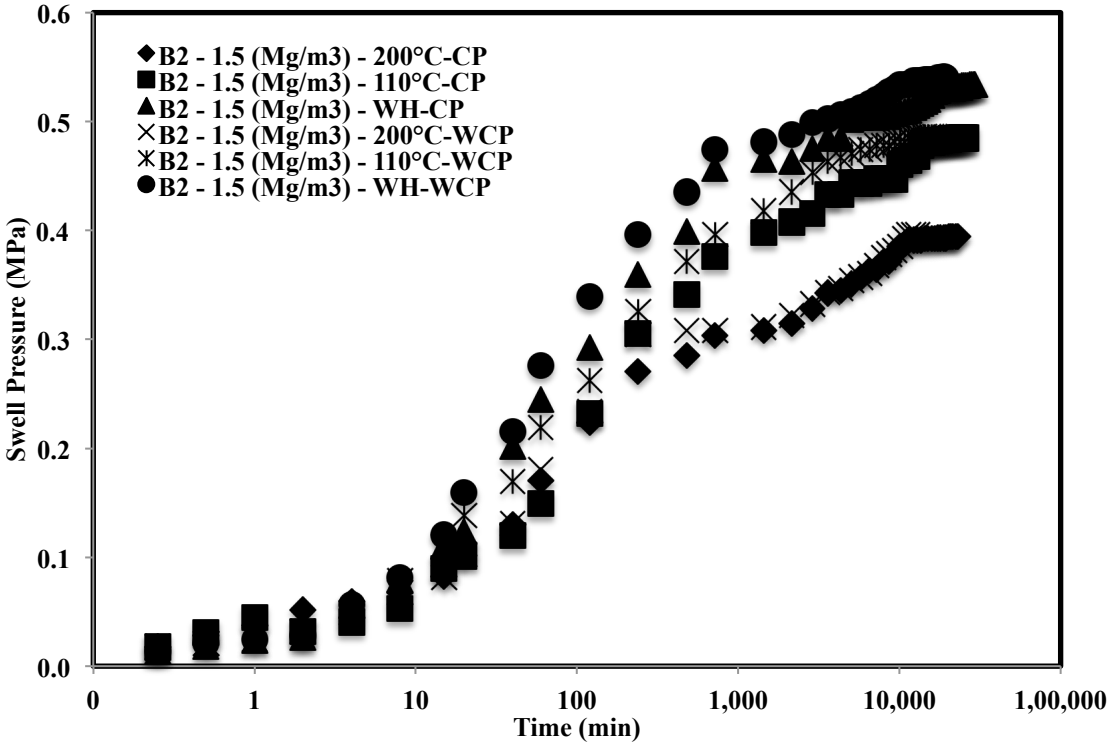

Fig. 6.8 Time swelling curve of B_2 bentonite (1.5 Mg/m^3) when heated at different temperatures saturated with distilled water without the addition of corrosion product and when added with corrosion product.

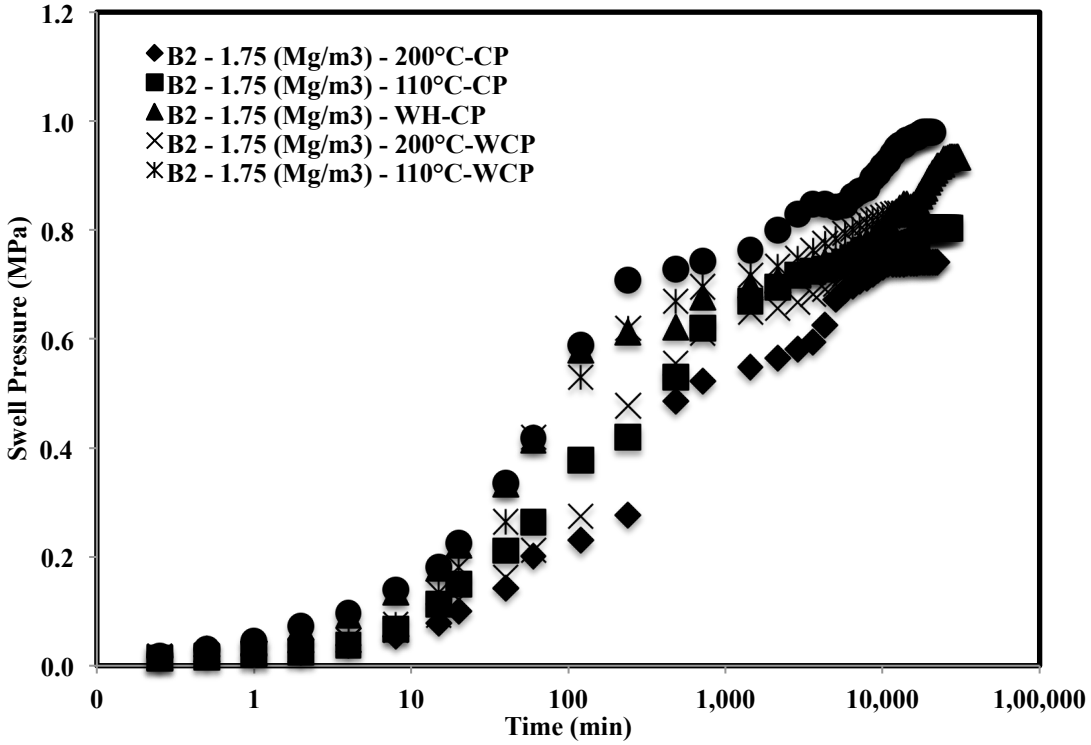

Fig. 6.9 Time swelling curve of B_2 bentonite (1.75 Mg/m^3) when heated at different temperatures saturated with distilled water without the addition of corrosion product and when added with corrosion product.

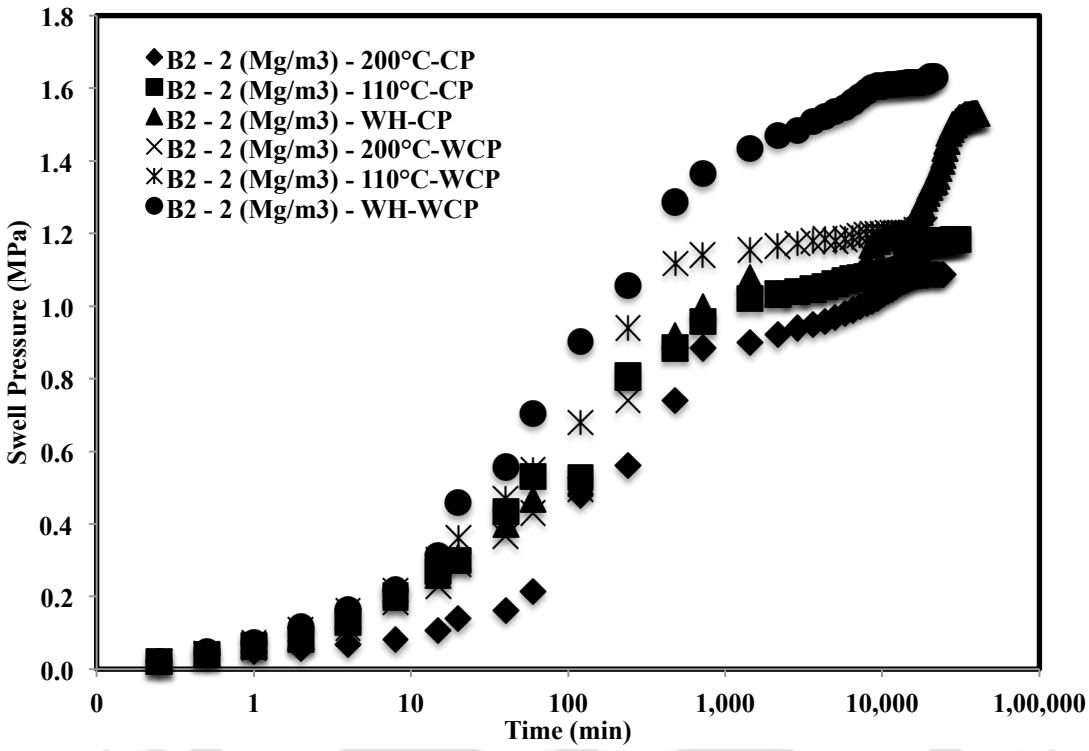

Fig. 6.10 Time swelling curve of B_2 bentonite (2 Mg/m^3) when heated at different temperatures saturated with distilled water without the addition of corrosion product and when added with corrosion product.

6.2.4 Comparison of swell pressure of compacted bentonites with and without the addition of corrosion product when subjected to thermal history

Fig. 6.11 represents the variation of swell pressure of compacted bentonite B_1 with and without corrosion product respectively, compacted at different densities of 1.5 Mg/m^3, 1.75 Mg/m^3, and 2 Mg/m^3 and subjected to thermal history. It was observed that the swell pressure of bentonite (B_1) compacted at 1.5 Mg/m^3 with and without corrosion product was 0.661 MPa and 0.662 MPa, respectively, when heated at 200°C. Whereas it was 0.796 MPa and 0.821 MPa, respectively, when heated at 110°C and 0.886 MPa and 0.909 MPa, respectively, for samples without heating. However, the swell pressure of bentonite B_1 compacted at 1.75 Mg/m^3, with and without corrosion product, respectively, was 1.216 MPa and 1.570 MPa, respectively, when heated at 200°C. Whereas it was 1.343 MPa and 1.650 MPa respectively when heated at 110°C and 1.415 MPa and 1.760 MPa respectively for samples without heating and the swell pressure of bentonite compacted at 2 Mg/m^3 with and without corrosion product, was 1.507 MPa and 1.823 MPa respectively when heated at 200^0C.

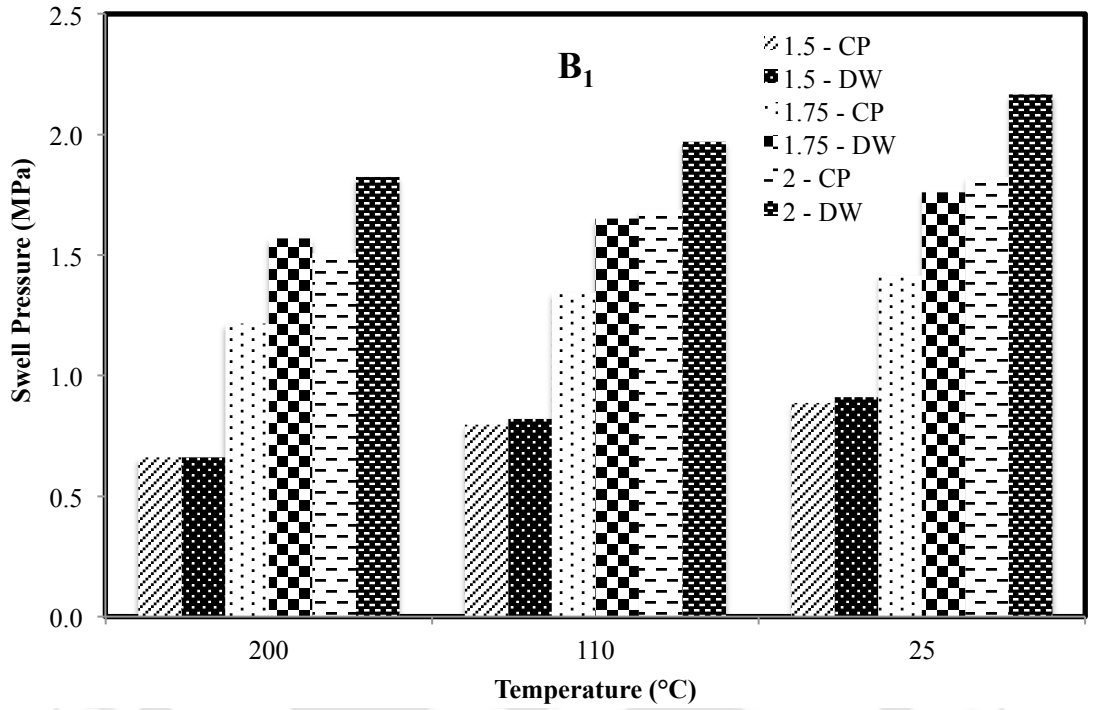

Fig. 6.11 Comparison of swell pressure of B_1 subjected to thermal history and the presence of corrosion product and without corrosion product

Whereas it was reported as 1.688 MPa and 1.969 MPa, respectively when heated at 110°C and 1.825 MPa and 2.166 MPa respectively for samples without heating. A similar trend was observed in the case of bentonite B_2. Fig. 6.12 represents a 3D plot of the variation of swell pressures of bentonite B_2 with and without corrosion products respectively and compacted at different densities of 1.5 Mg/m^3, 1.75 Mg/m^3, 2 Mg/m^3 subjected to thermal history. It was observed that the swell pressure in the case of bentonite B_1 was recorded to be more than that of B_2 in both cases. Also, the swell pressure in the presence of corrosion products was recorded less than that of samples without corrosion products.

When the bentonite has to survive under an alkaline environment, the structural lattice of the smectite gets disturbed. Also, the iron (Fe) from the waste canister diffused to compacted bentonite leads to the precipitation of magnetite (Hill, 2016). Other minerals, such as siderite, have less possibility of precipitation due to the limited availability of carbonate. As there are formation magnetite and other minerals inside the interlamellar gaps,

$$3Fe(OH)_2 \Rightarrow Fe_3O_4 + 2H_2O + H_2$$

Fe_3O_4 is magnetite, and it precipitated and clogged the pores of the bentonite as well. Due to the smectite dissolution, the swell pressure values are lesser as the temperature increased. This could be very well explained through XRD and EDX results.

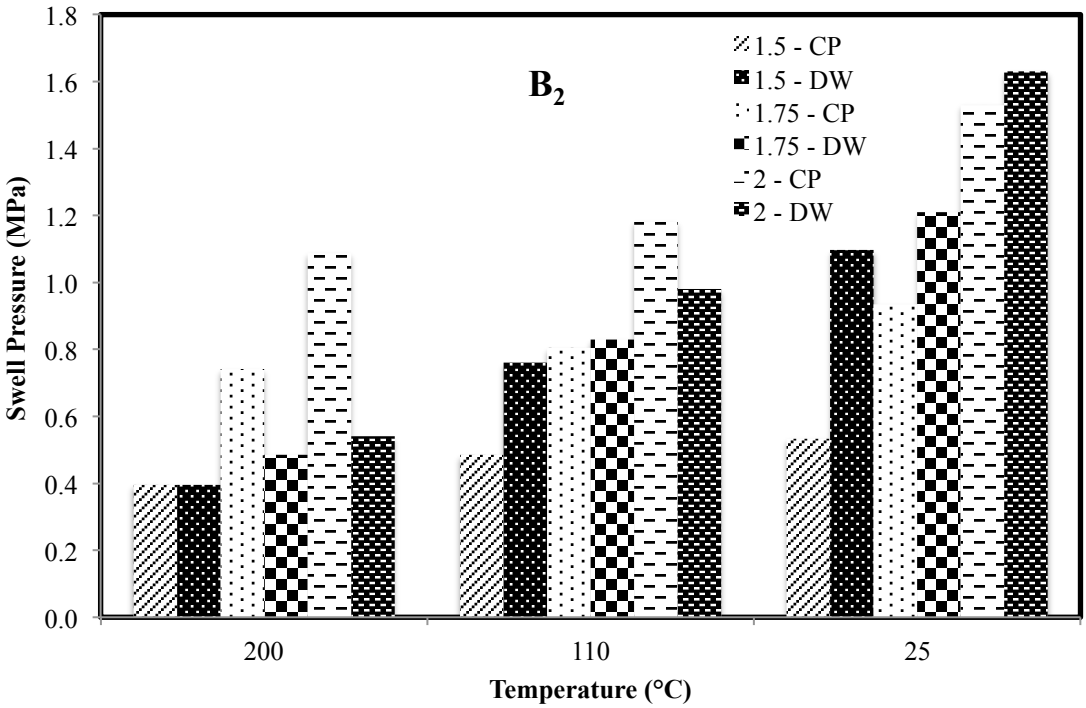

Fig. 6.12 Comparison of swell pressure of B_2 subjected to thermal history and the presence of corrosion product and without corrosion product

6.2.5 Comparison of time of saturation in case of distilled and corrosion products

Table 6.1 depicts the comparison of the total time of saturation of samples with corrosion products and without corrosion products. It could be clearly seen that though the swell pressure values are more in the absence of corrosion products (WCP), and the time taken for the saturation was more in the presence of corrosion products (CP).

After inducing the thermal history over the compacted bentonite samples, the gap might have created between the bentonite mass and the iron particles due to shrinkage by heating (Fig. 6.13). As soon as the compacted bentonite came in contact with the saturating fluid, it took time for the sample for the saturation to fill the gap. Also, the precipitation of secondary minerals might have clogged the pores of the bentonites, which increased its time of saturation.

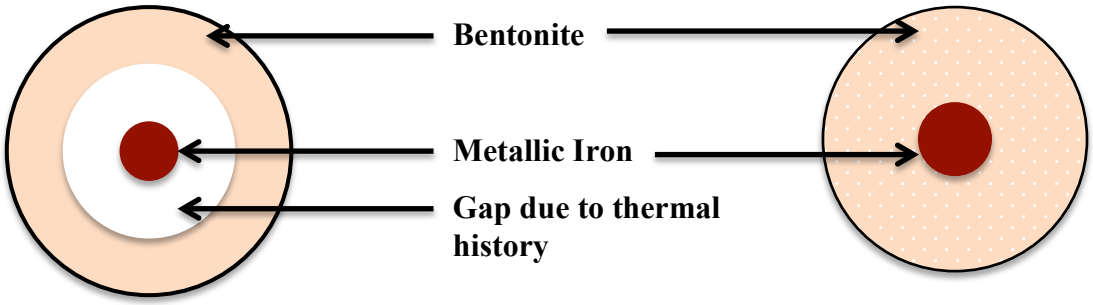

Fig. 6.13 Schematic representation of gap present between metallic iron particle and compacted bentonite after subjecting to thermal history

Table 6.1 Comparison of the total time of saturation of samples with corrosion product and without corrosion product

S.N.	Bentonite	Dry Density (Mg/m^3)	Temperature (°C)	Time (min) for WCP*	Time (min) for CP**
1	B_1	1.5	200	12960	18000
			110	15120	31680
			WH	17280	35280
		1.75	200	16560	33120
			110	18720	36720
			WH	20880	42480
		2	200	17288	44640
			110	19440	46080
			WH	22320	48960
2	B_2	1.5	200	12960	23040
			110	16560	25920
			WH	19440	29520
		1.75	200	15120	22320
			110	18000	26640
			WH	20888	30240
		2	200	16560	24480
			110	18720	30240
			WH	21600	40320

*- without corrosion products

**-with the corrosion products

6.2.6 X-ray diffraction (XRD) and energy-dispersive X-ray spectroscopy (EDX)

The various samples were observed under X-ray diffraction (XRD) analysis and energy-dispersive X-ray spectroscopy (EDX), and the presence of some secondary minerals was found, which could be clearly seen from Fig. 6.14. The plot shows the XRD pattern of Bentonite B_1 and B_2, the metallic iron powder (Fe), bentonite, and iron mix (B_1 + Fe and B_2 + Fe) saturated with distilled water under constant volume conditions. A peak of magnetite (Fe_3O_4) was observed in the bentonite B_1 + Fe and with a small intensity even in B_2 + Fe too. Whereas, a peak of siderite ($FeCO_3$) was observed in sample B_2 + Fe and not in B_1 + Fe. The percentage of carbon and oxygen after saturation in the case of B_1 + Fe was 15.2% and 29.3%, whereas it was 20% and 32.1%, respectively, in the case of B_2 + Fe. The possible reason for not finding a peak of siderite in the case of B_1 + Fe was may be due to the limited availability of carbonate in the sample, which could be observed in EDX (Fig. 6.15 and Fig. 6.16) analyses of bentonite samples mixed with corrosion product.

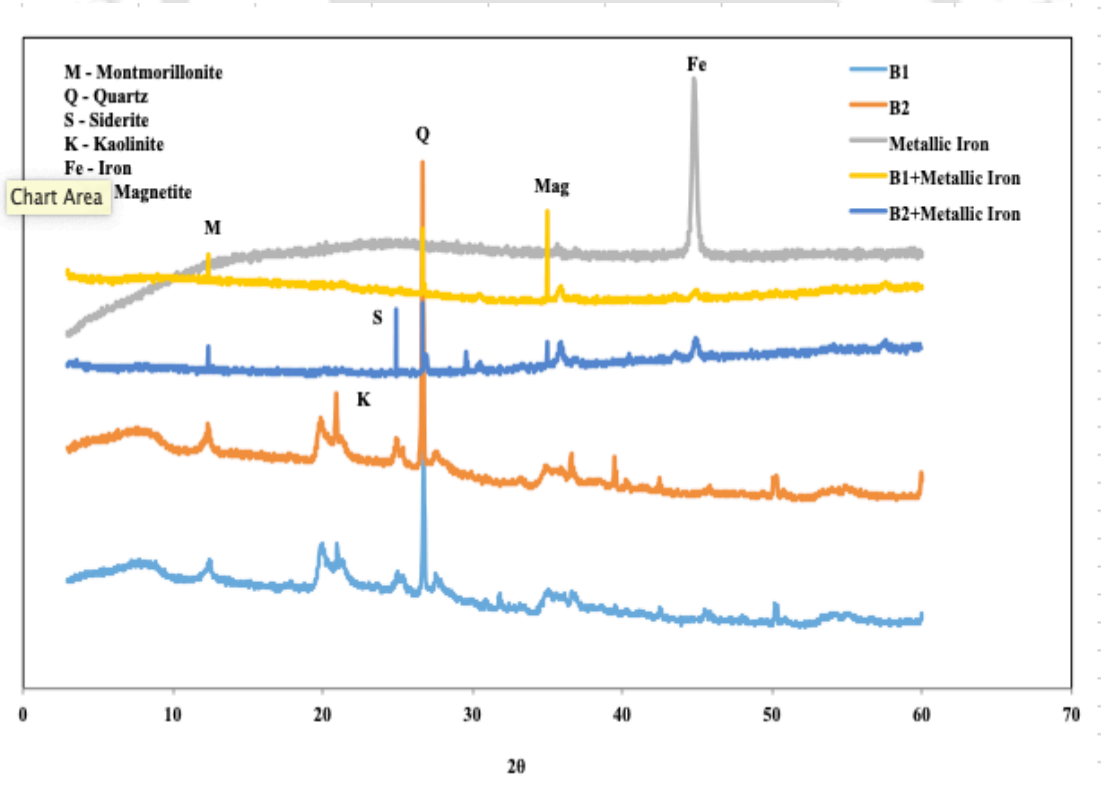

Fig. 6.14 X-Ray Diffraction patterns of bentonites, metallic iron and the combination of bentonites and metallic iron

The microstructural observations revealed that due to the formation of non-swelling minerals, the swell pressure of both the bentonites reduced. However, the behavior of

both bentonites was different due to the difference in their basic characterization.

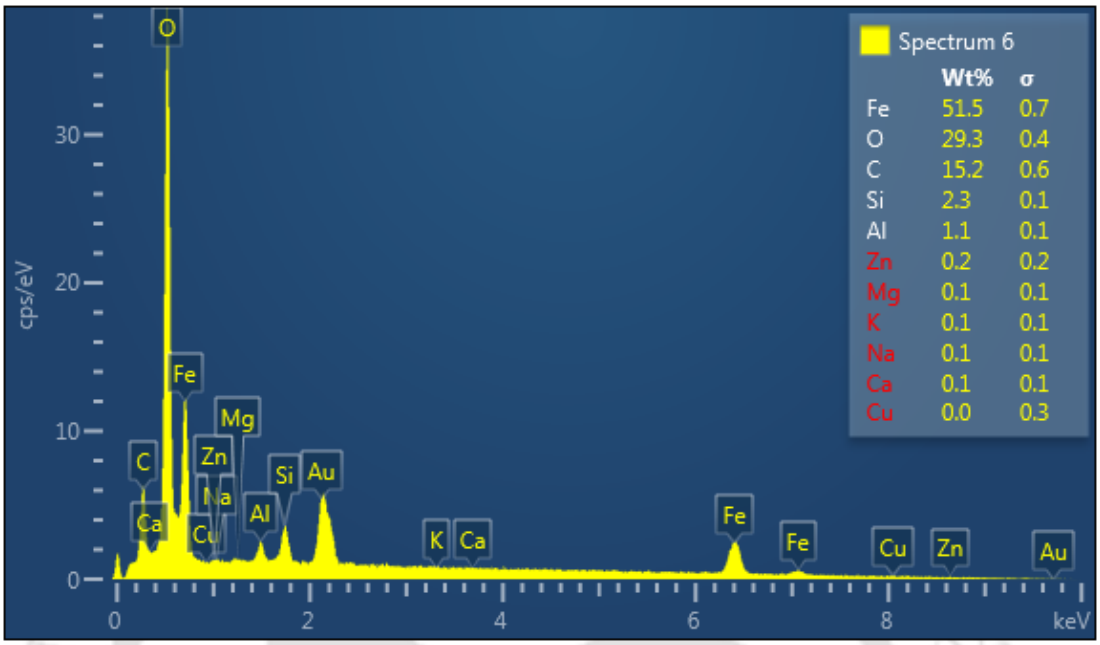

Fig. 6.15 Energy Dispersive X-Ray (EDX) pattern of Bentonite B_1

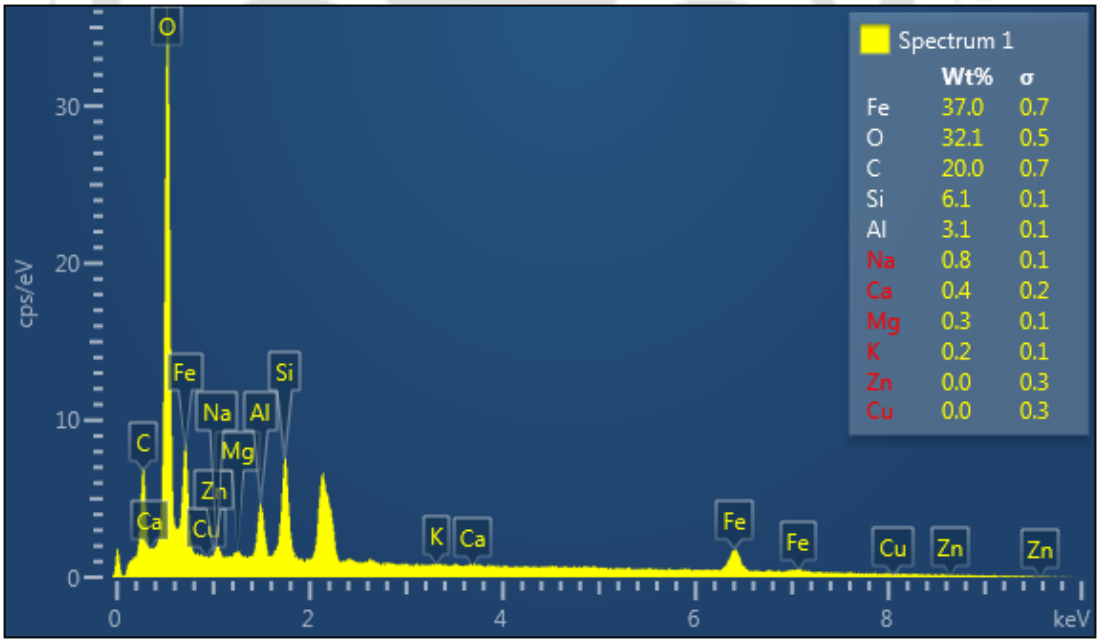

Fig. 6.16 Energy Dispersive X-Ray (EDX) pattern of Bentonite B_2

Phase II - Swell pressure of compacted bentonite saturated with hyperalkaline cement water at different thermal histories

6.2.7 Time swelling of compacted bentonites saturated with hyperalkaline cement water and subjected to thermal history

Fig. 6.17 depicts the plot of the variation of swell pressure with time for bentonite B_1 for the combination of thermal histories and compaction densities in addition to corrosion products saturated with hyperalkaline cement water. The time of saturation for the sample compacted at 1.5 Mg/m^3 was noted as 31680 min, 28080 min, and 18000 min for samples without heating, 110°C, and 200°C, respectively. Similarly, the time of saturation for the sample compacted at 1.75 Mg/m^3 was noted as 42480 min, 39600 min, and 33840 min for samples without heating, 110°C, and 200°C, respectively. Furthermore, the time of saturation for the sample compacted at 2 Mg/m^3 was noted as 49680 min, 46800 min, and 45360 min for samples without heating, 110°C, and 200°C, respectively.

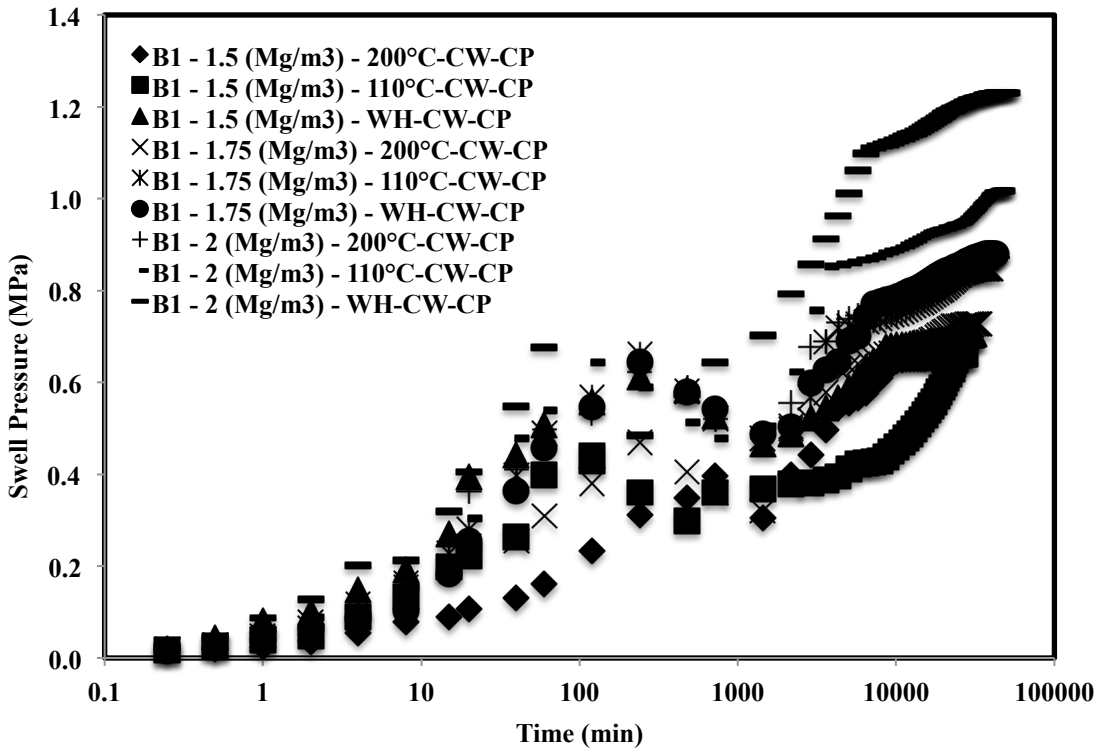

Fig. 6.17 Variation of swell pressure with the time of B_1 bentonite added with corrosion product, saturated with hyperalkaline cement water and subjected to thermal histories

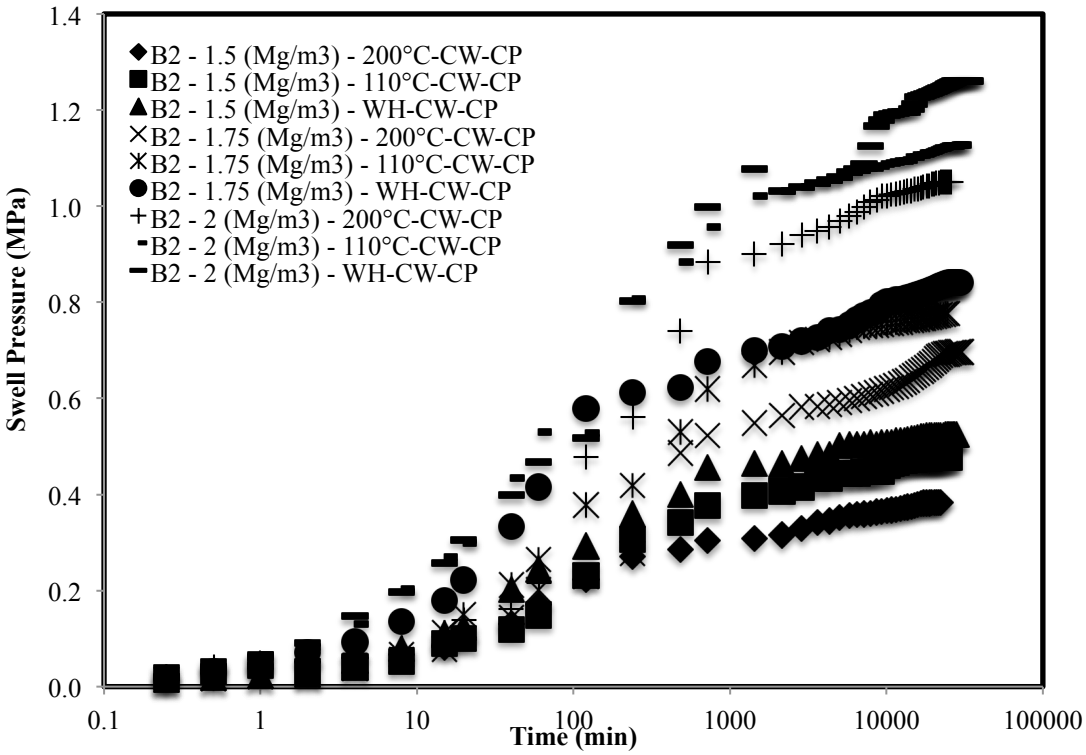

Fig. 6.18 Variation of swell pressure with the time of B_2 bentonite added with corrosion product, saturated with hyperalkaline cement water and subjected to thermal histories

Similarly, Fig. 6.18 represents the plot of swell pressure vs. time of bentonite B_2 for the combination of all compaction densities and thermal histories in addition to corrosion products and saturated with hyperalkaline cement water. It was observed that the time of saturation for the sample compacted at 1.5 Mg/m^3 was noted as 30240 min, 26640 min, and 23760 min without heating, 110°C, and 200°C, respectively. Similarly, the time of saturation for the sample compacted at 1.75 Mg/m^3 was noted as 34560 min, 33120 min, and 31680 min without heating, 110°C, and 200°C, respectively. Furthermore, the time of saturation for the sample compacted at 2 Mg/m^3 was noted as 41040 min, 36000 min, and 33840 min without heating, 110°C, and 200°C, respectively.

6.2.8 Swell pressure of compacted bentonites saturated with hyperalkaline cement water subjected to thermal history

The variation of swell pressure with a temperature of the bentonite B_1 and B_2 in addition to corrosion product and compacted at three different compaction densities 1.5 Mg/m^3, 1.75 Mg/m^3, and 2 Mg/m^3 and saturated with hyperalkaline cement water is presented in Fig. 6.19 and Fig. 6.20 respectively.

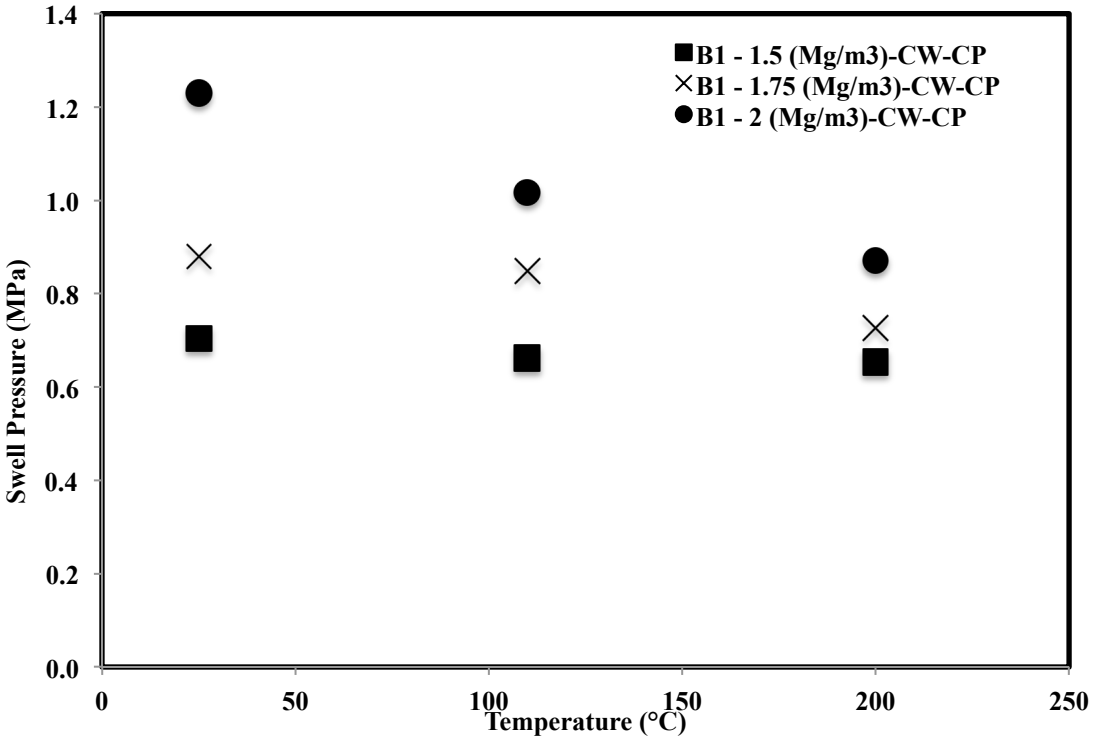

Fig. 6.19 Variation in swell pressures of bentonite B_1 with temperature and density, added with corrosion product (CP), and saturated with hyperalkaline cement water.

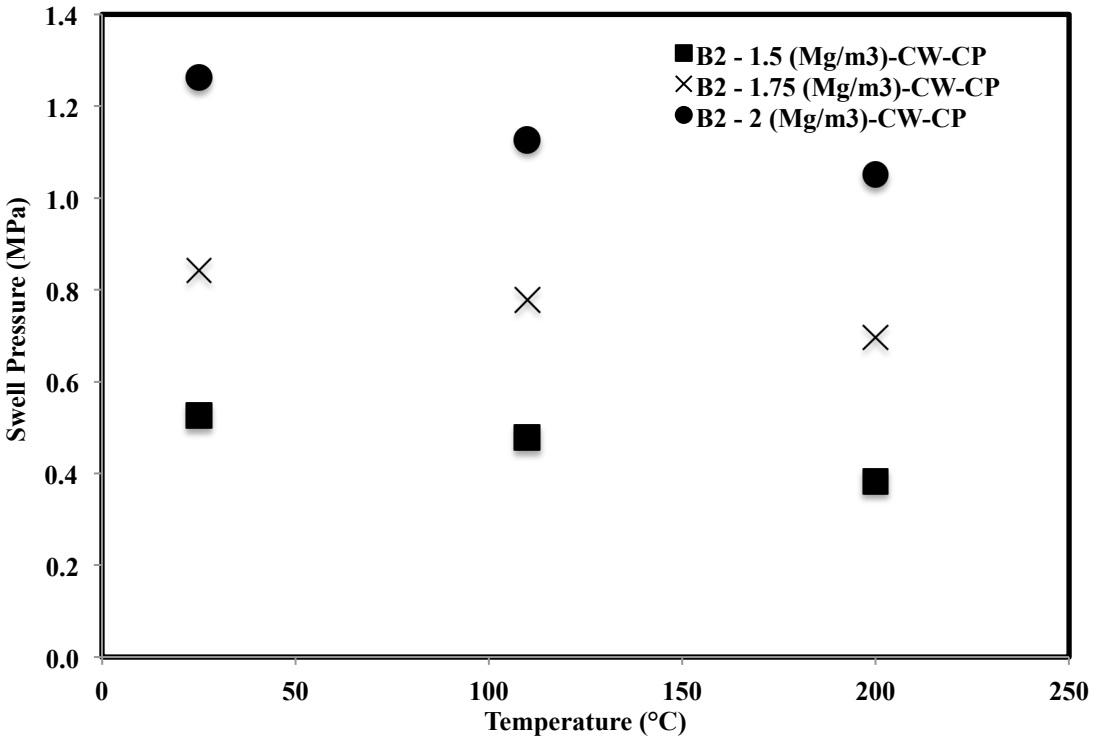

Fig. 6.20 Variation in swell pressures of bentonite B_2 with temperature and density, added with corrosion product (CP), and saturated with hyperalkaline cement water.

6.2.9 Comparison of time swelling of compacted bentonites with and without the addition of corrosion product when saturated with hyperalkaline cement water and subjected to thermal history

The variation of swell pressure of compacted bentonites specimens due to thermal history compacted at targeted densities of 1.5 Mg/m^3, 1.75 Mg/m^3, 2 Mg/m^3, and corrosion product and saturated with hyperalkaline cement water is shown in Fig. 6.21, 6.22, and 6.23. Fig. 6.21 represents the variation in swell pressure of bentonite B_1 at a density of 1.5 Mg/m^3.

It could be seen from the curves that the swell pressure of bentonite added with corrosion product and saturated with cement water without heating was 0.75 MPa, whereas the swell pressure when heated at 110°C was 0.694 MPa, and at 200°C, it was observed as 0.661 MPa.

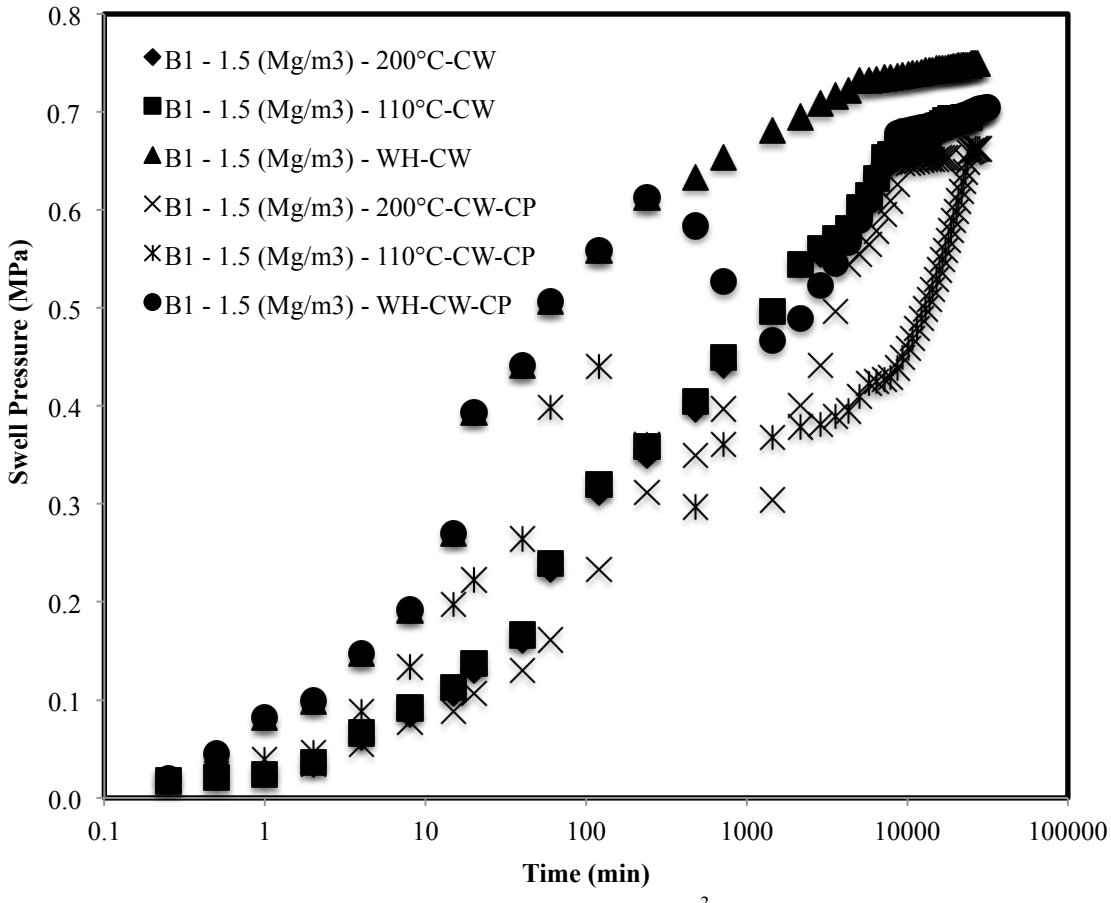

Fig. 6.21 Time swelling curve of B_1 bentonite (1.5 Mg/m^3) subjected to various thermal histories saturated with hyperalkaline cement water, with and without the addition of corrosion product.

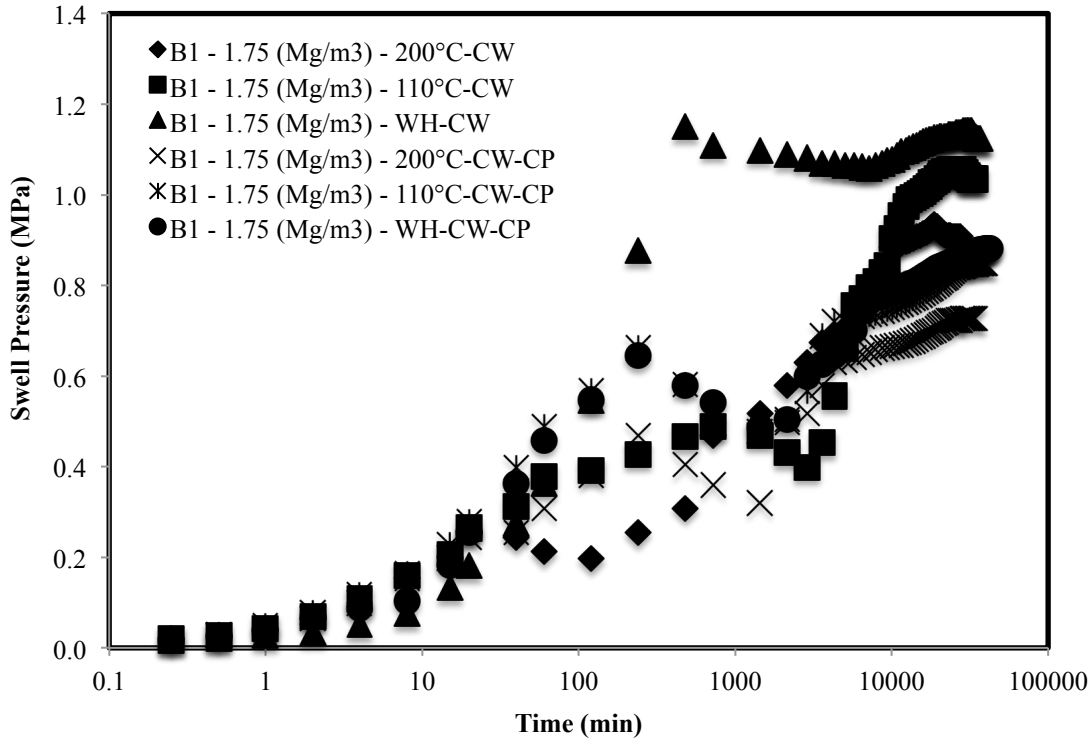

Fig. 6.22 Time swelling curve of B_1 bentonite (1.75 Mg/m^3) subjected to various thermal histories saturated with hyperalkaline cement water, with and without the addition of corrosion product.

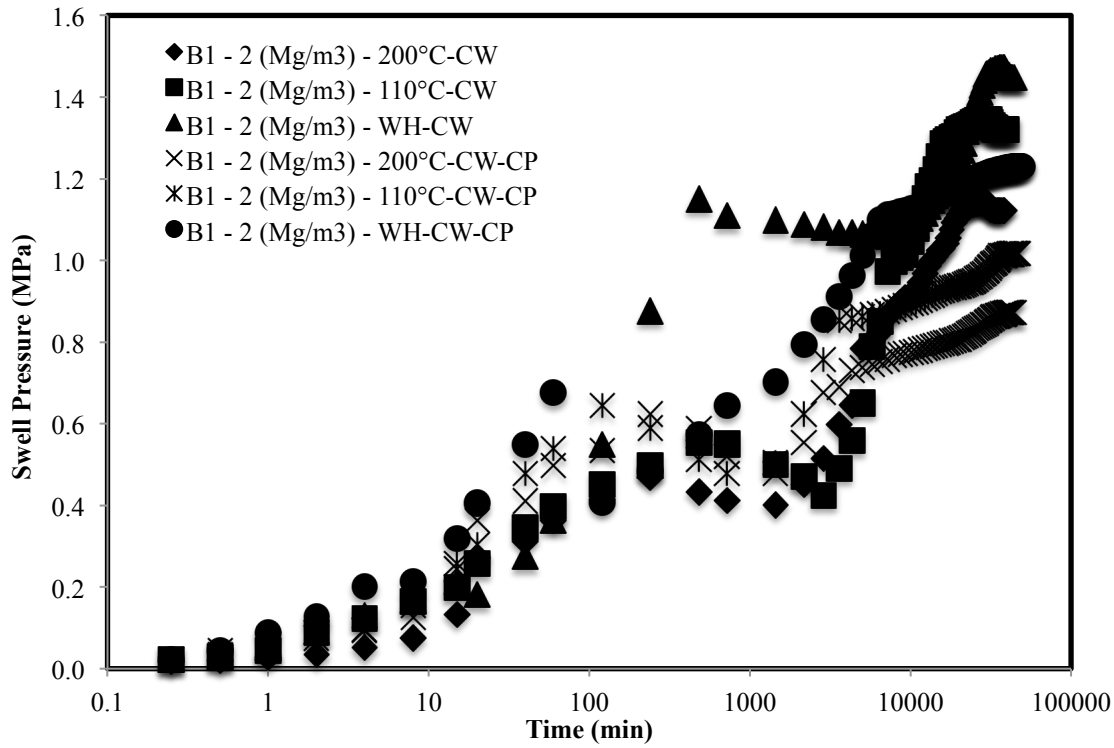

Fig. 6.23 Time swelling curve of B_1 bentonite (2 Mg/m^3) subjected to various thermal histories saturated with hyperalkaline cement water, with and without the addition of corrosion product.

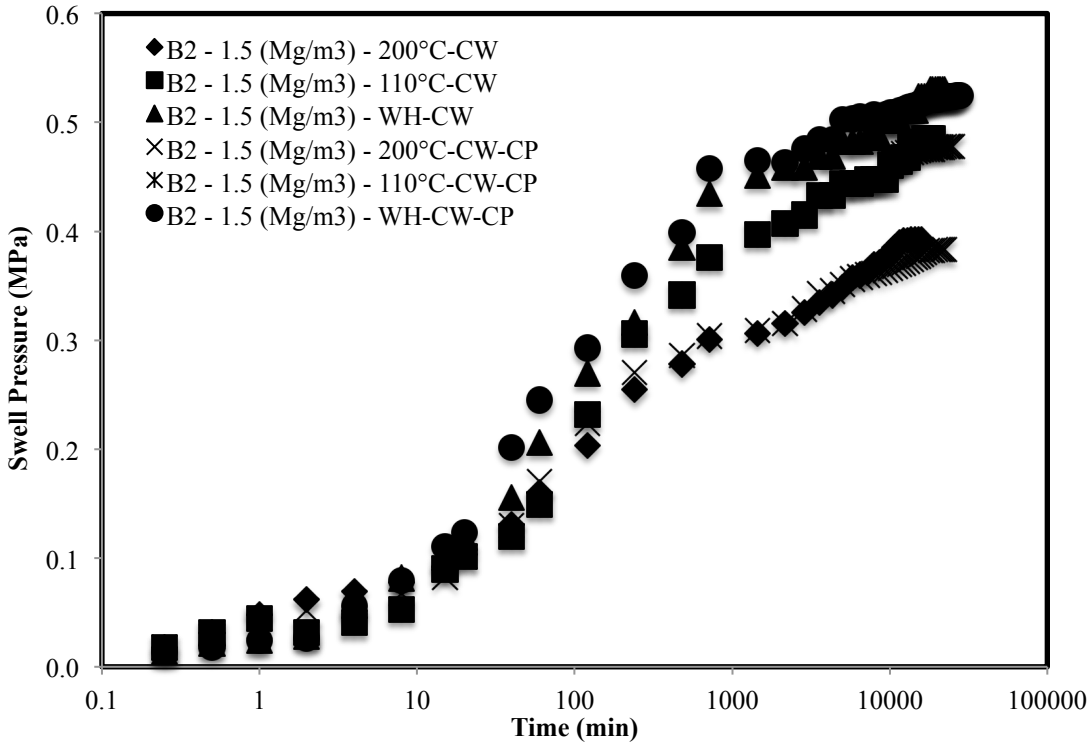

Fig. 6.24 Time swelling curve of B_2 bentonite (1.5 Mg/m^3) subjected to various thermal histories saturated with hyperalkaline cement water, with and without the addition of corrosion product.

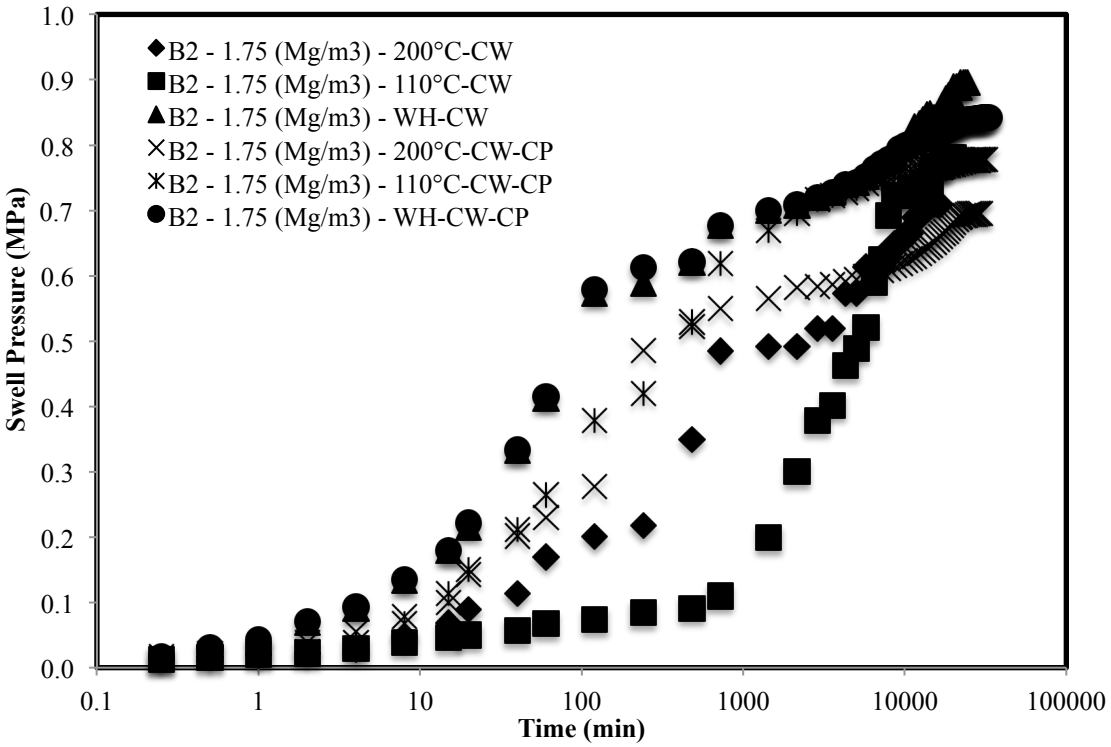

Fig. 6.25 Time swelling curve of B_2 bentonite (1.75 Mg/m^3) subjected to various thermal histories saturated with hyperalkaline cement water, with and without the addition of corrosion product.

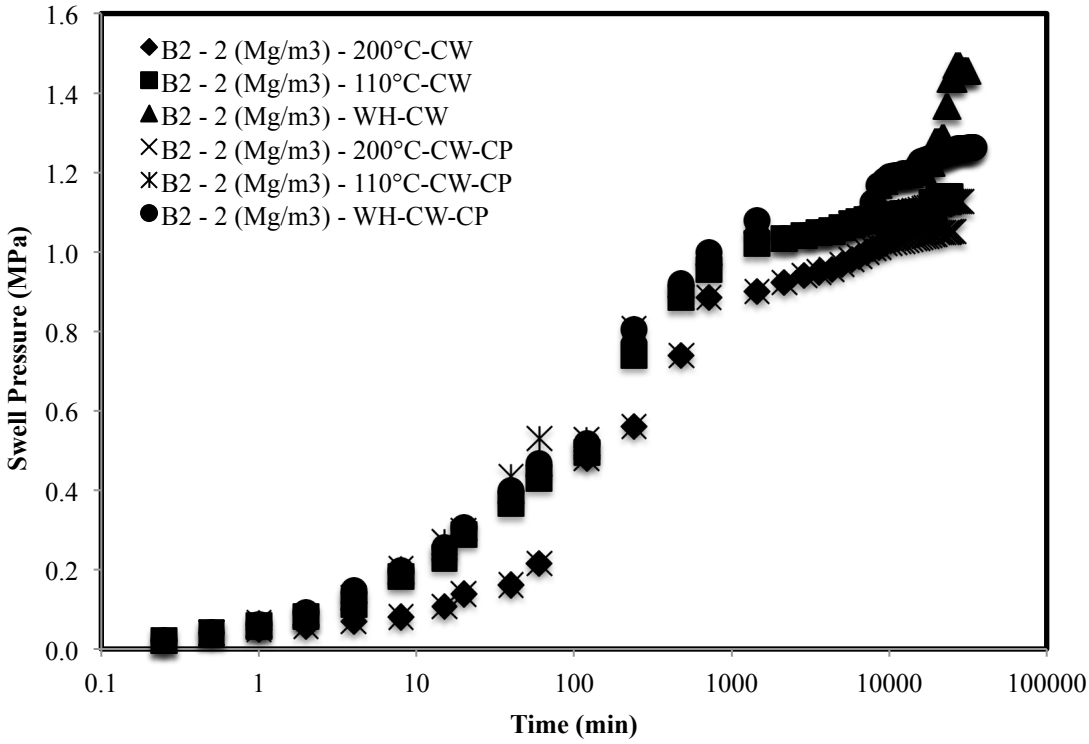

Fig. 6.26 Time swelling curve of B_2 bentonite (2 Mg/m^3) subjected to various thermal histories saturated with hyperalkaline cement water, with and without the addition of corrosion product.

Similarly, swell pressure of the same bentonite was observed as 0.705 MPa, whereas the swell pressure when heated at 110°C was 0.662 MPa, and at 200°C, it was observed as 0.653 MPa when saturated with cement solution and without the addition of corrosion product. A similar trend of results was reported for the higher densities of 1.75 Mg/m^3, 2 Mg/m^3 when saturated with both the solutions (Fig. 6.22 and 6.23). The results reported for bentonite B_2 showed a similar trend as B_1. It is represented in Fig. 6.24, 6.25, and 6.26.

6.2.10 Comparison of swell pressure of compacted bentonites with and without the addition of corrosion product saturated with hyperalkaline cement water when subjected to thermal history

Fig. 6.27 represents the variation of swell pressure of compacted bentonite B_1 saturated with hyperalkaline cement water, with and without corrosion product respectively, compacted at different densities of 1.5 Mg/m^3, 1.75 Mg/m^3, 2 Mg/m^3 and subjected to thermal history. It was observed that the swell pressure of bentonite (B_1) compacted at 1.5 Mg/m^3 with and without corrosion product was 0.653 MPa and 0.661

MPa, respectively, when heated at 200^{0}C. Whereas it was 0.662 MPa and 0.694 MPa, respectively, when heated at 110^{0}C and 0.705 MPa and 0.75 MPa, respectively, for samples without heating.

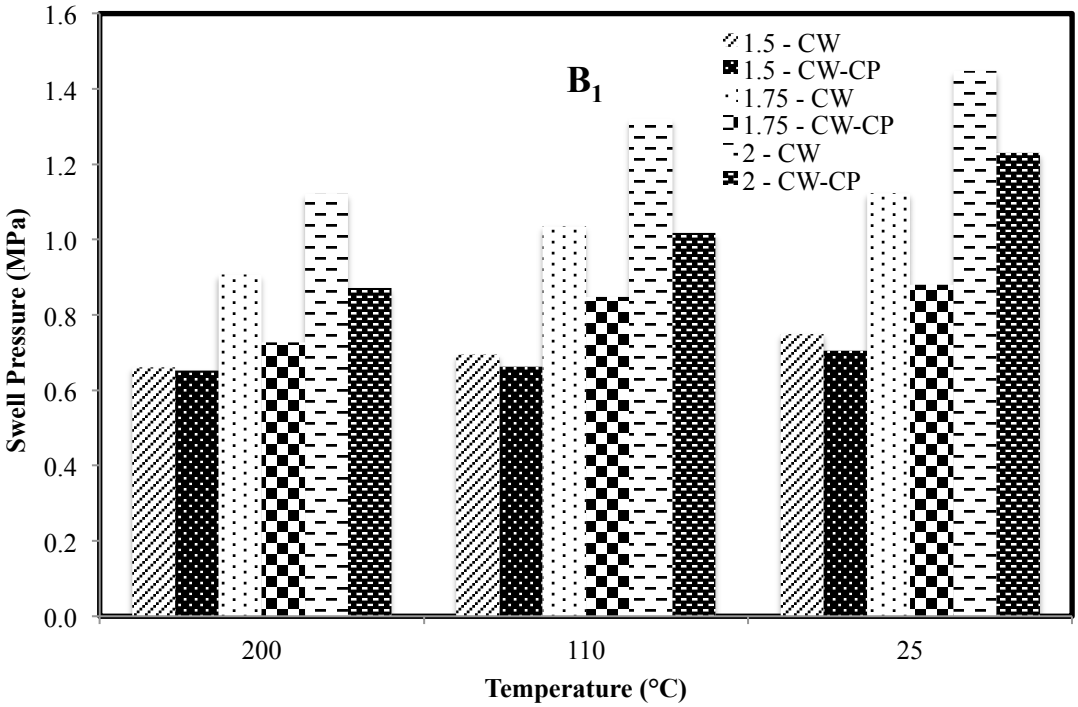

Fig. 6.27 Comparison of swell pressure of B_1 subjected to thermal history and saturated with hyperalkaline cement water in the presence of corrosion product and without corrosion product

Fig. 6.28 represents the variation of swell pressure of compacted bentonite B_2 saturated with hyperalkaline cement water, with and without corrosion product respectively, compacted at different densities of 1.5 Mg/m^3, 1.75 Mg/m^3, 2 Mg/m^3 and subjected to thermal history. It was observed that the swell pressure of bentonite (B_2) compacted at 1.5 Mg/m^3 with and without corrosion product was 0.383 MPa and 0.392 MPa, respectively, when heated at 200^{0}C. Whereas it was 0.478 MPa and 0.485 MPa, respectively, when heated at 110^{0}C and 0.525 MPa and 0.530 MPa, respectively, for samples without heating.

One more interesting observation was noted here that even in the case of hyperalkaline cement water as a saturating fluid, the swell pressure values were lesser in the case of the addition of corrosion products. Although together, they form an alkaline environment inside (hyperalkaline cement water, pH>12 and corrosion leachate, pH>8). The hyperalkaline cement water already reduced the value of swell pressure, but the

presence of corrosion product reduced it more than earlier. The presence of iron particles might have restricted the space of swelling for the bentonite particles.

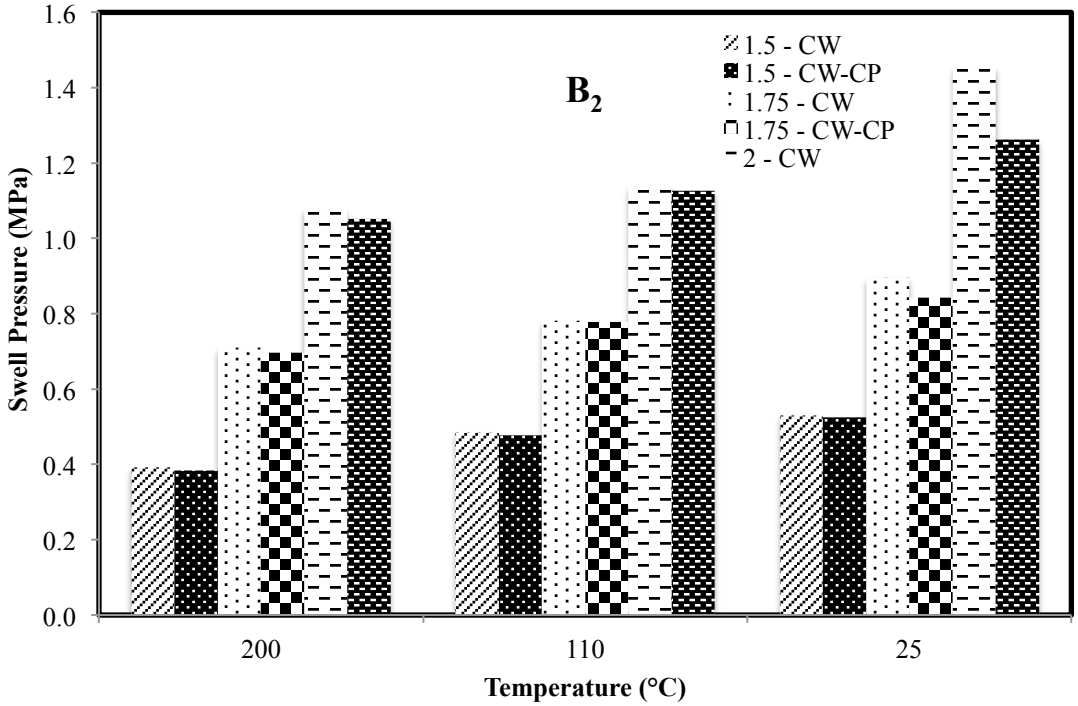

Fig. 6.28 Comparison of swell pressure of B_2 subjected to thermal history and saturated with hyperalkaline cement water in the presence of corrosion product and without corrosion product.

6.2.11 Comparison of Swell Pressure

Table 6.2 depicts the comparison of the final swell pressure values subjected to thermal history when saturated with distilled and hyperalkaline cement water also with and without the addition of corrosion products. It could be clearly seen that the swell pressure values were higher in the case of specimens without the addition of corrosion products. However, the specimens containing corrosion products and saturated with the hyperalkaline cement water exhibited the least values of swell pressure.

The dissolution of montmorillonite and clogging of pores could be a leading reason for the decrease in swell pressure along with the temperature at which the sample was subjected to particular thermal history. The formation of secondary minerals such as magnetite, siderite, etc., in case of corrosion products might be the reason for additional reduction in the swell pressure than earlier two cases.

Table 6.2 Comparison of total swell pressure of specimens with corrosion product (CP) and without corrosion product (WCP) for both the bentonites.

Density	Temperature	B_1				B_2			
		Distilled Water		Cement Water		Distilled Water		Cement Water	
		1.5 - CP	1.5 - WCP	1.5 - CP	1.5 - WCP	1.5 - CP	1.5 - WCP	1.5 - CP	1.5 - WCP
1.5	200	**0.661**	0.662	**0.653**	0.661	**0.396**	0.396	**0.383**	0.392
	110	**0.796**	0.821	**0.662**	0.694	**0.485**	0.761	**0.478**	0.485
	25	**0.886**	0.909	**0.705**	0.75	**0.534**	1.097	**0.525**	0.530
		1.75 - CP	1.75 - WCP	1.75 - CP	1.75 - WCP	1.75 - CP	1.75 - WCP	1.75 - CP	1.75 - WCP
1.75	200	**1.216**	1.57	**0.727**	0.907	**0.431**	0.486	**0.696**	0.710
	110	**1.343**	1.650	**0.848**	1.035	**0.804**	0.830	**0.778**	0.781
	25	**1.415**	1.760	**0.880**	1.123	**0.934**	1.210	**0.842**	0.896
		2 - CP	2 - WCP	2 - CP	2 - WCP	2 - CP	2 - WCP	2 - CP	2 - WCP
2	200	**1.507**	1.823	**0.872**	1.122	**0.540**	1.088	**1.051**	1.080
	110	**1.688**	1.969	**1.017**	1.320	**0.980**	1.182	**1.127**	1.139
	25	**1.825**	2.166	**1.130**	1.448	**1.530**	1.630	**1.262**	1.456

The reduction in swell pressure values for B_2 bentonite compacted at 2 Mg/m^3 was 34%, which might be due to the comparatively lesser cation exchange capacity, specific surface area, and liquid limit of the bentonite B_2.

6.3 CONCLUSION

In this chapter, swelling pressure tests were conducted on densely compacted (1.5 Mg/m^3, 1.75 Mg/m^3, and 2.0 Mg/m^3) Barmer bentonite specimens mixed with metallic iron powder, subjected to various thermal histories. The influence of corrosion leachates on the swell pressure of compacted bentonite under the created thermal history was analyzed by saturating specimens with distilled water and hyper alkaline cement water. The swell pressure was recorded to be decreased for the samples containing corrosion products for both the bentonites. However, the values were comparatively lower again in the case of samples with corrosion products and saturated with hyperalkaline cement water. So the sequence of swell pressure values could be written as –

Distilled water (WCP)> Distilled water (CP)> Cement water (WCP)> Cement water (WCP).

Anaerobic conditions expected inside the deep geological repository would corrode the high-level nuclear waste canister. The non-swelling minerals such as magnetite and siderite will form due to the reaction of corrosion products and react with the interlayers of montmorillonite. The corrosion of the canister could create an alkaline environment

inside the repository due to corrosion leachate that percolated through the compacted bentonite buffer. The hot canister induced the thermal history on the compacted bentonite buffer over a long period of time. As the corrosion started, it tried to alter the overall performance of the thermal history influenced compacted bentonite. The final swell pressure value of samples containing corrosion products and saturated with distilled water was found to be approximately 15% less than that of samples without corrosion products. At the same time, it was approximately 22% in the case of hyperalkaline cement water (At 2.0 Mg/m^3). The decrease was more significant, with an increase in temperature. The time of saturation in the presence of corrosion products was approximately two times more than that of samples without corrosion products in both cases; however, the time taken in case of samples with corrosion products and saturated with hyperalkaline cement water was slightly more than that in case of distilled water. The mineral dissolution could also be the reason for the decrease in swell pressure values as there is the formation of secondary minerals such as magnetite, siderite, etc. The reduction in swell pressure values for B_2 bentonite compacted at 2 Mg/m^3 was 34%, which might be due to the comparatively lesser cation exchange capacity, specific surface area, and liquid limit of the bentonite B_2. As the study observed that the corrosion product and hyperalkinity, as well as the thermal history, could influence the behavior of both the bentonites, it recommended considering these factors while designing the deep geological repository for the disposal of high-level nuclear waste.

Chapter 7

INFLUENCE OF THERMAL GRADIENT ON REACTIVE TRANSPORT THROUGH COMPACTED BENTONITE

7.1 INTRODUCTION

The engineering behavior of compacted swelling clays has been shown to be closely coupled with the hydro-geochemical processes that can occur in the clay-water-chemical system (Zheng and Samper, 2008; Pusch and Yong, 2006). Geochemical interactions between the ions, clay, and minerals can cause considerable changes in the physical, chemical, and mechanical behavior of the clay buffer under variable thermal, hydraulic, and chemical gradients in the geological repository. Therefore, an in-depth understanding of the thermal and chemical gradient on the compacted bentonite buffer is essential for the long-term performance assessment. An evolutionary step in the operating life of the bentonite buffer under HLW repository conditions begins after the compacted buffer is in the depositional holes and can be exposed to an elevated temperature at the boundary adjacent to the HLW canister (heating) and resaturation at the host rock interface (hydration). Over the last three decades or so, significant attempts were made in experimental trials at various scales and in quantitative simulation experiments, which were checked against findings in laboratory, mock-up, and in-situ heating and hydration testing, to investigate the thermal, chemical, and mechanical properties of compacted bentonite buffers. The long-term action of compacted bentonite in the sense of EBS also has computational modeling studies. (Steefel et al. 2010; Samper et al. 2008; Villar et al. 2008b; Yang et al. 2008;). Guimarães et al. 2007; Cuevas et al. 2002; ENRESA 2000)

The heating at one end (hot canister) and hydration from the other end (from host rock) create a thermal gradient on the compacted bentonite buffer (Estabragh et al., 2016). At the same, the anaerobic corrosion of steel could also interact with bentonite along with a hyperalkaline cement solution from the other end and under the influence of both thermal and hydraulic gradients. However, the long-term success of compacted bentonite as the buffer material relies on the smectite resilience against thermal and hydraulic adjustments, from which all the significant changes inside the repository may be maintained. Hence, the aim of this study is to investigate the alteration of

physicochemical and mechanical properties of bentonite through reactive transport by anaerobic corrosion of steel canister from one side along with the infiltration of hyperalkaline solution from another side under the influence of thermal gradient. The fabricated lab-scale set up was used in this experiment. The bentonite samples were compacted at 1.5 Mg/m^3, 1.75 Mg/m^3, and 2 Mg/m^3 densities and subjected to hydration from the top (distilled water and hyperalkaline cement water) and variable temperatures from the bottom (WH (without heating), 60°C, 110°C, 150°C, and 200°C) through a layer of metallic iron powder.

7.2 RESULTS AND DISCUSSIONS

Phase I - Influence of thermal and hydraulic gradient and canister corrosion on the saturation of compacted Barmer bentonite

7.2.1 Thermal analyses

The variation of the degree of saturation (S_r) from the hydration end towards the heating end for three different densities (1.5 Mg/m^3, 1.75 Mg/m^3, and 2 Mg/m^3) and five temperatures (WH (without heating), 60°C, 110°C, 150°C, and 200°C) for bentonite B_1 are represented in Fig. 7.1, Fig. 7.2, Fig. 7.3 respectively. The value of S_r for the samples without heating was observed as 0.94 at the outer part and 0.98 at the inner part for density 1.5 Mg/m^3 at the hydration side. However, towards the heater, it was observed as 0.77 at the outer part and 0.79 at the inner part in the middle portion and as 0.38 at the outer part and 0.39 at the inner part at the lower portion. Similarly, it was 0.70 at the outer part and 0.72 at the inner part in the upper portion, 0.51 at the outer part and 0.53 at the inner part in the middle portion, and was 0.32 at the outer part and 0.32 at the inner part at the lower portion at temperature 200°C. For the samples compacted at 1.75 Mg/m^3 and without heating, it was 0.87 at the outer part and 0.89 at the inner part, 0.66 at the outer part and 0.70 at the inner part in the middle portion and 0.28 at the outer part and 0.31 at the inner part at the lower portion. Also, it was 0.65 at the outer part and 0.68 at the inner portion, 0.50 at the outer part, and 0.52 at the inner part in the middle portion and as 0.18 at the outer part and 0.19 at the inner part at the lower portion at temperature 200°C. Similarly, For the samples compacted at 2 Mg/m^3 and without heating, it was 0.80 at the outer part and 0.83 at the inner part, 0.67 at the outer part and 0.70 at the inner part in the middle portion, and 0.15 at the outer part and 0.16 at the inner part at the

lower portion. Also, it was 0.60 at the outer part and 0.64 at the inner part, 0.46 at the outer part, and 0.44 at the inner part in the middle portion, and 0.09 at the outer part and 0.08 at the inner portion at the lower part at temperature 200°C.

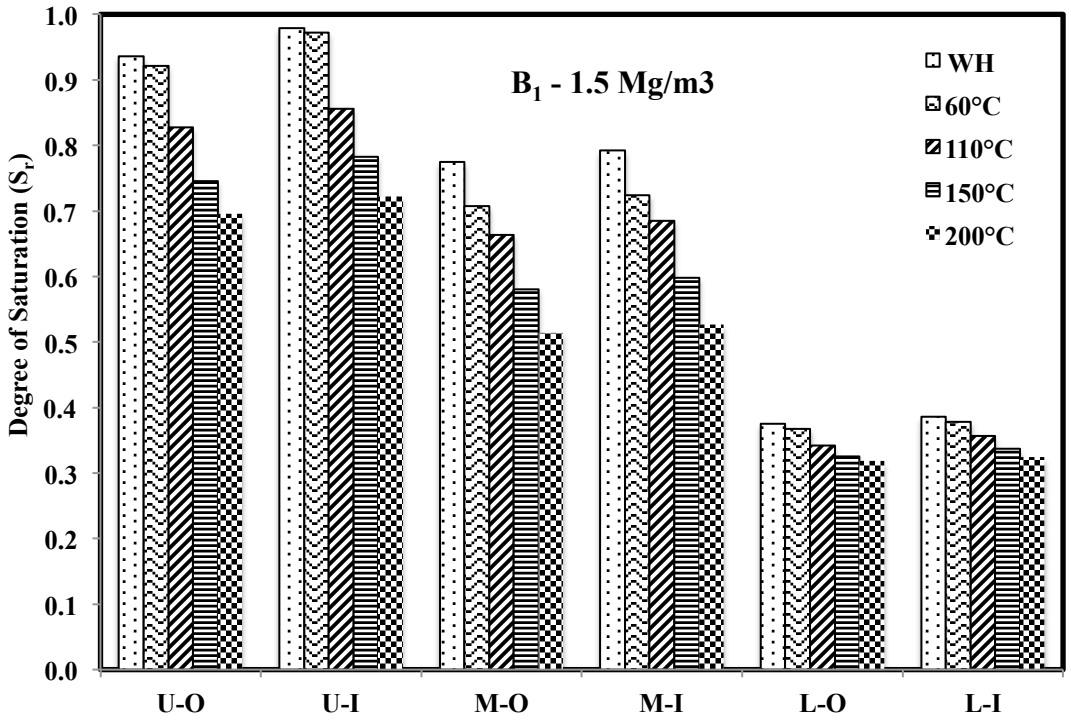

Fig. 7.1 Variation of the degree of saturation under a thermal gradient of bentonite B_1 for specimens compacted at 1.5 Mg/m^3

However, for bentonite B_2, the results obtained showed differences from bentonite B_1 in terms of the degree of saturation (Fig. 7.4, Fig. 7.5, Fig. 7.6). The value of S_r for the samples without heating was observed as 0.97 at the outer part and 0.99 at the inner part for density 1.5 Mg/m^3 at the hydration side. Towards the heater, it was observed as 0.86 at the outer part and 0.91 at the inner part in the middle part and as 0.52 at the outer part and 0.57 at the inner part at the lower portion. Similarly, it was 0.80 at the outer part and 0.85 at the inner part in the upper part, 0.69 at the outer part and 0.77 at the inner part in the middle part, and 0.40 at the outer part and 0.42 at the inner part at the lower portion at temperature 200°C. For the samples compacted at 1.75 Mg/m^3 and without heating, it was 0.90 at the outer part and 0.93 at the inner part, 0.68 at the outer part and 0.73 at the inner part in the middle part and 0.41 at the outer part and 0.45 at the inner part at the lower portion. Also, it was 0.70 at the outer part and 0.74 at the inner part, 0.52 at the

outer portion, and 0.54 at the inner part in the middle part and as 0.30 at the outer part and 0.33 at the inner part at the lower part at temperature 200°C. Similarly, For the samples compacted at 2 Mg/m^3 and without heating, it was 0.87 at the outer part and 0.90 at the inner part, 0.70 at the outer part and 0.74 at the inner part in the middle portion, and 0.30 at the outer part and 0.31 at the inner part at the lower portion. Also, it was 0.76 at the outer part and 0.78 at the inner part, 0.48 at the outer part, and 0.46 at the inner part in the middle portion, and 0.18 at the outer part and 0.22 at the inner part at the lower portion at temperature 200°C. Bentonite B_2 showed more percentage of saturation than B_1 in the same time span. The lesser clay content in B_2 made it saturated faster than B_1. For both bentonites, the outer part has a lesser value of saturation than the inner that might be because the outer part is in touch with the heating edge of the mould.

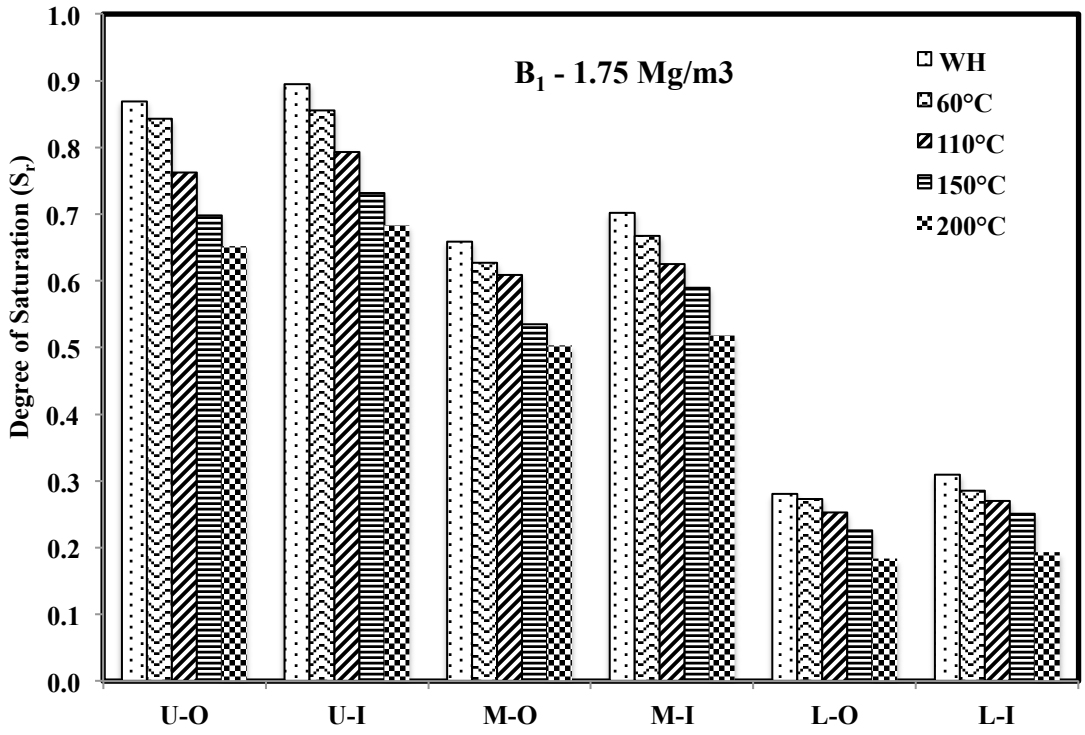

Fig. 7.2 Variation of degree of saturation under a thermal gradient of bentonite B_1 for specimens compacted at 1.75 Mg/m^3

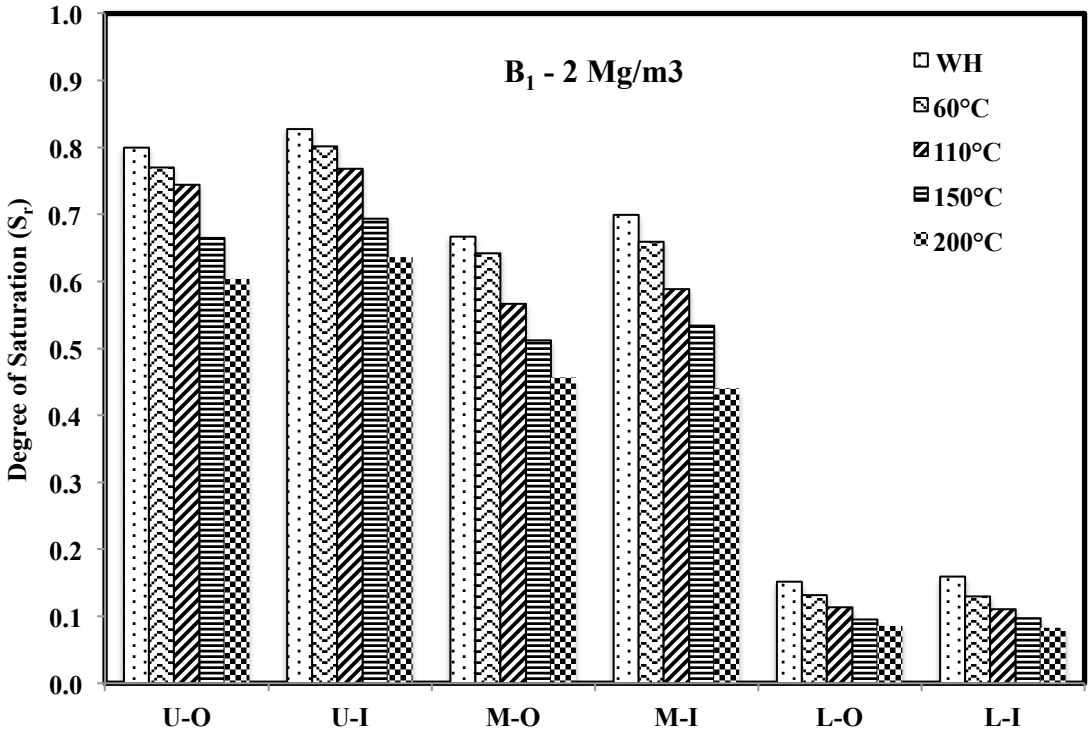

Fig. 7.3 Variation of degree of saturation under a thermal gradient of bentonite B_1 for specimens compacted at 2 Mg/m^3

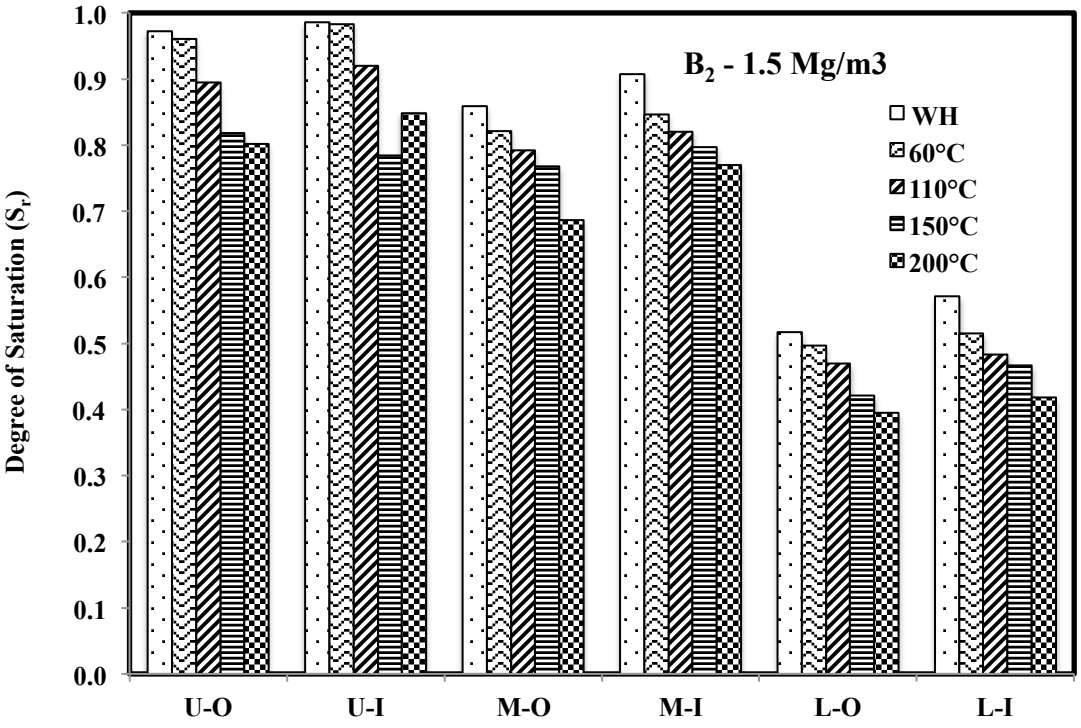

Fig. 7.4 Variation of degree of saturation under a thermal gradient of bentonite B_2 for specimens compacted at 1.5 Mg/m^3

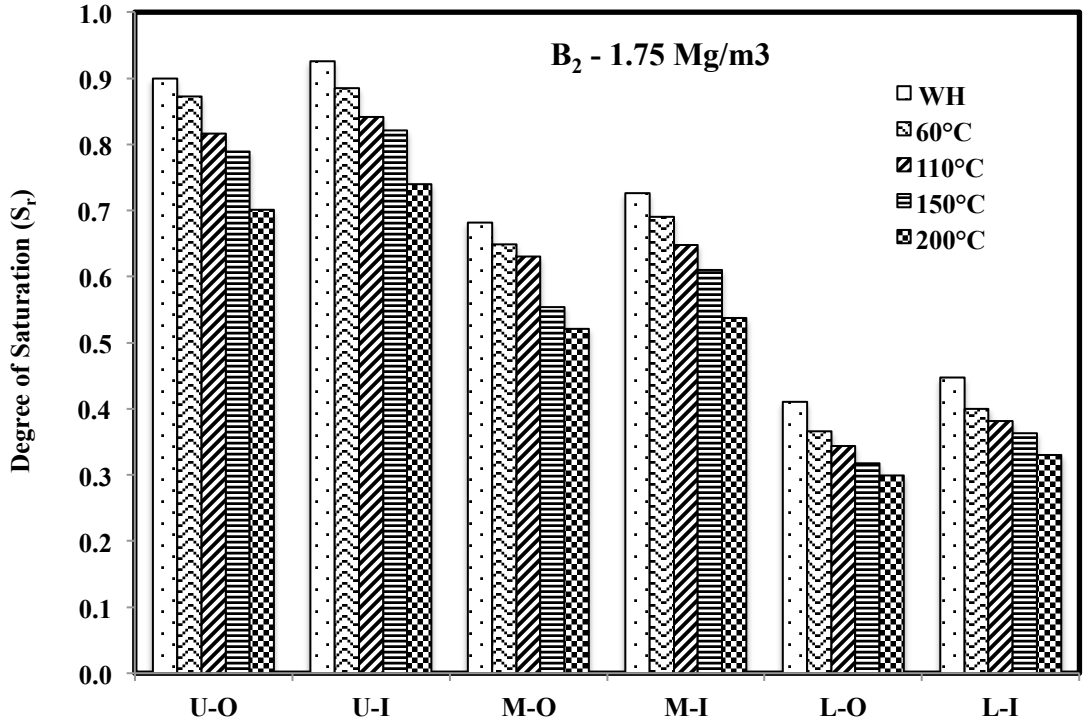

Fig. 7.5 Variation of degree of saturation under a thermal gradient of bentonite B_2 for specimens compacted at 1.75 Mg/m^3

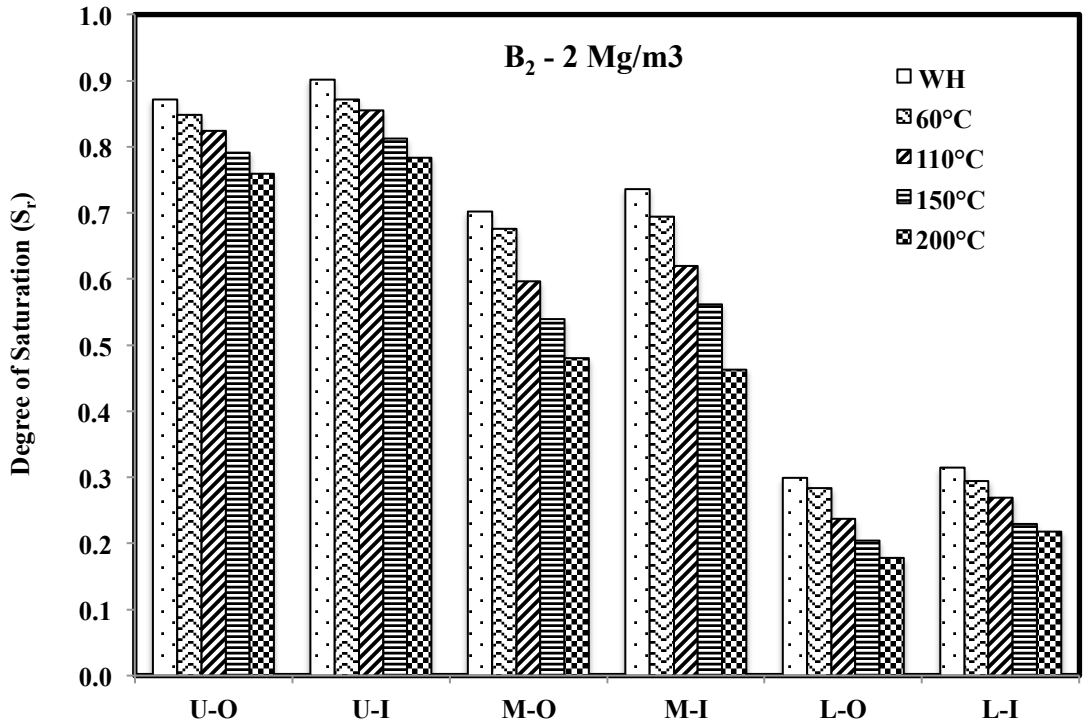

Fig. 7.6 Variation of degree of saturation under a thermal gradient of bentonite B_2 for specimens compacted at 2 Mg/m^3

The value of S_r was observed more at the hydration end and less at the heating end, but it also decreased with the increase in the temperature as well as density. Hence it could be said that the degree of saturation was the function of temperature as well as density. As this study is related particularly to the effect of thermal gradient on reactive transport, the plots of the degree of saturation vs. distance from the heater are presented for various temperatures. The specimen mould was kept heating at one end, and the other end was kept at room temperature, which created a difference in the temperature at both ends and accelerated the process of thermal diffusion. Due to the process of hydration and dehydration at the same time, the expansion or shrinkage of the clay microstructure was expected, which actually controlled the flow in the compacted bentonites. Also, in the process of drying, i.e., at high temperatures, the montmorillonite structure may collapsed, and it then required more quantity of moisture for saturation. The reactive transport could be explained with the help of two types of porosities that were present in the sample. Microporosity was present between the layer of smectite sheets, and macroporosity was present between the interparticle pores (Ravi and Rao, 2017). In these compacted bentonite samples, it was obvious to expect both types of porosities were present. Initially, when the sample started saturating, it tried to cover the macroporosity, and once that part was saturated, it was focused on microporosity. As the temperature went on increasing, the viscosity of both these pore moistures was lost. The moisture molecules from micropores tried to combine with the macropores, forming a network for the transport (Pusch et al. 1990). Also, with the increase in the compaction density, the macroporosity was reduced (Likos and Lu, 2006). Hence, the overall porosity of the sample was reduced, and the maximum burden went on the microporosity. Therefore, it could not get the contribution from the macropores, and hence the transport process had been slower at the higher density.

7.2.2 Chemical analyses

The outer part of the upper and middle portions showed a comparatively lesser value of cation exchange capacity than the original. However, the differences in the values were not significant, and the inner portions showed approximately the same values. An interesting observation was obsereved, that the lower portion had a reduced cation exchange capacity (Na^+, Ca^+, K^+, Mg^+). Fig. 7.7 and Fig. 7.8 show the temperature vs. cation exchange capacity of B_1 and B_2 bentonites for three densities, respectively.

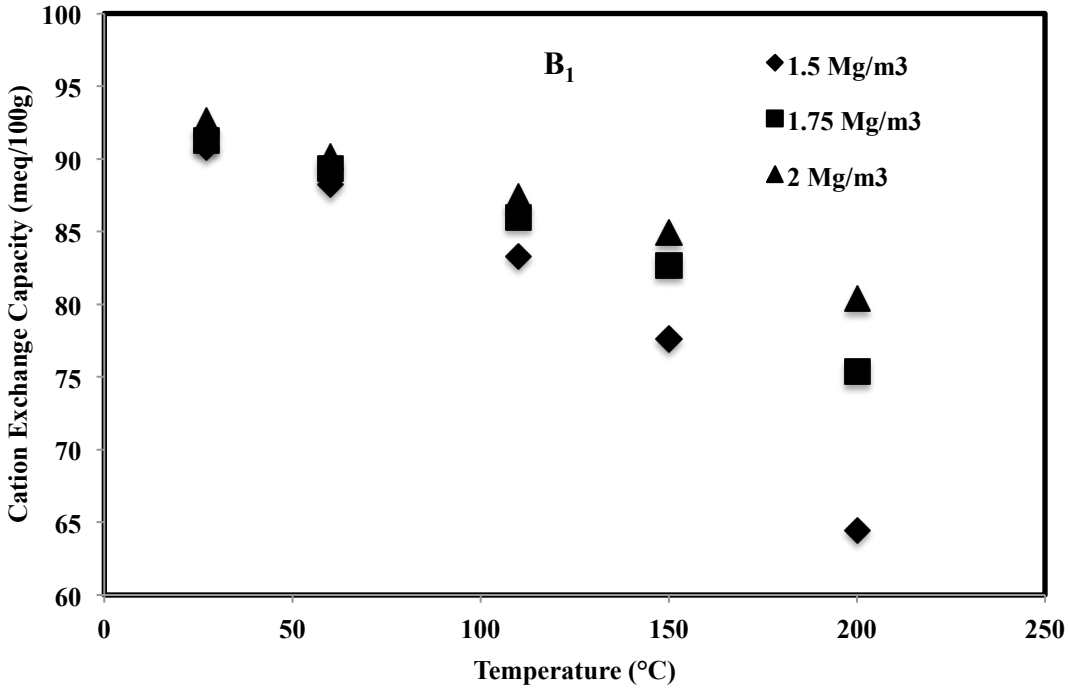

Fig. 7.7 Variation of cation exchange capacity at various thermal gradients of the lower portion of B_1 specimens.

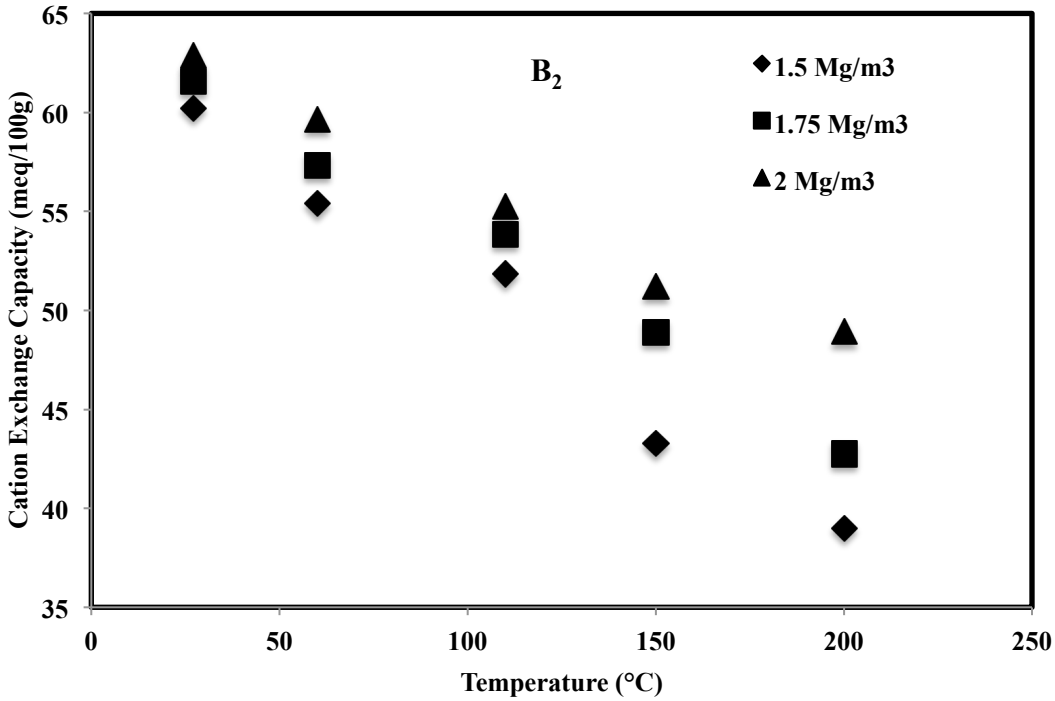

Fig. 7.8 Variation of cation exchange capacity at various thermal gradient of the lower portion of B_2 specimens.

It was observed that the lower portion of both the bentonites showed a reduced cation exchange capacity as the lower portion was in contact with the layer of metallic iron powder.

The reduction in the cation exchange capacity was found to be lesser for 2 Mg/m^3 than 1.75 Mg/m^3 than 1.5 Mg/m^3, which may be due to the availability of macropores at a lower density. Also, as the heat went on, increasing the reduction in the cation exchange capacity was also enhanced. The movement of moisture molecules from macropores to micropores was accelerated at high temperatures, and by combining these two moistures, it made it easy to exchange cations, hence reducing the cation exchange capacity of the bentonites (Pusch et al. 1990).

7.2.3 Microstructural investigation

The microstructural investigation of the lower portion of all densities and temperature was done by X-ray diffraction (XRD), energy dispersive X-ray (EDX), and field emission scanning electron microscope (FESEM). Fig. 7.9 represents the XRD of B_1 and B_2 bentonites (2 Mg/m^3 at 200°C). The peak of hematite was observed in both the samples with higher intensity in B_1 than B_2. To support this data, the same samples were undergone to EDX analyses where the percentage of Fe and O was maximum to form hematite (Fe_2O_3) and could be seen from Fig. 7.10 and 7.11 and Fig. 7.12 and 7.13 for B_1 and B_2 respectively.

The reduction in exchangeable Na^+, Ca^{2+} showed that due to the lesser charge, they might be replaced by Fe^{2+} or Fe^{3+} of metallic iron powder. Hence, in the EDX analyses, a tremendous increase in the percentage weight of Fe was observed. Fig. 7.14 and 7.15 represents the FESEM images of the same sample in which the impurity and different structural arrangement could be observed between the lamellar of bentonites. From XRD and EDX, it might be a structure of hematite.

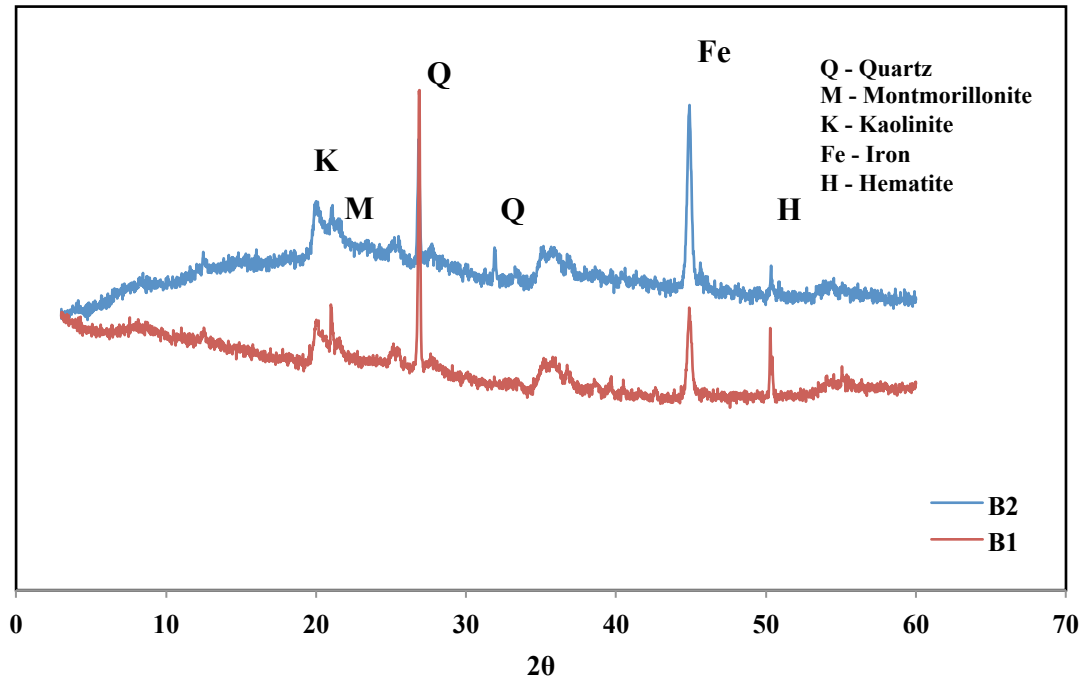

Fig. 7.9 XRD patterns of the lower portion of both bentonites compacted at 2 Mg/m^3.

Fig. 7.10 EDX spectrum image of bentonite B_1

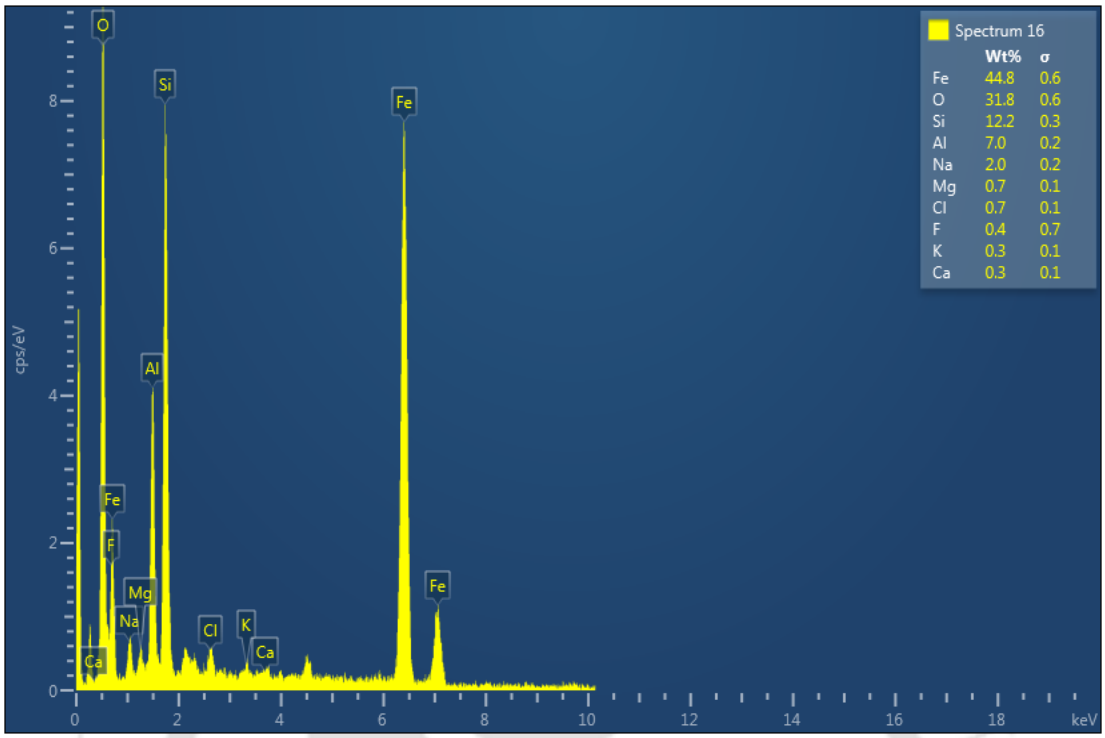

Fig. 7.11 EDX pattern of bentonite B_1

Fig. 7.12 EDX spectrum image of bentonite B_2

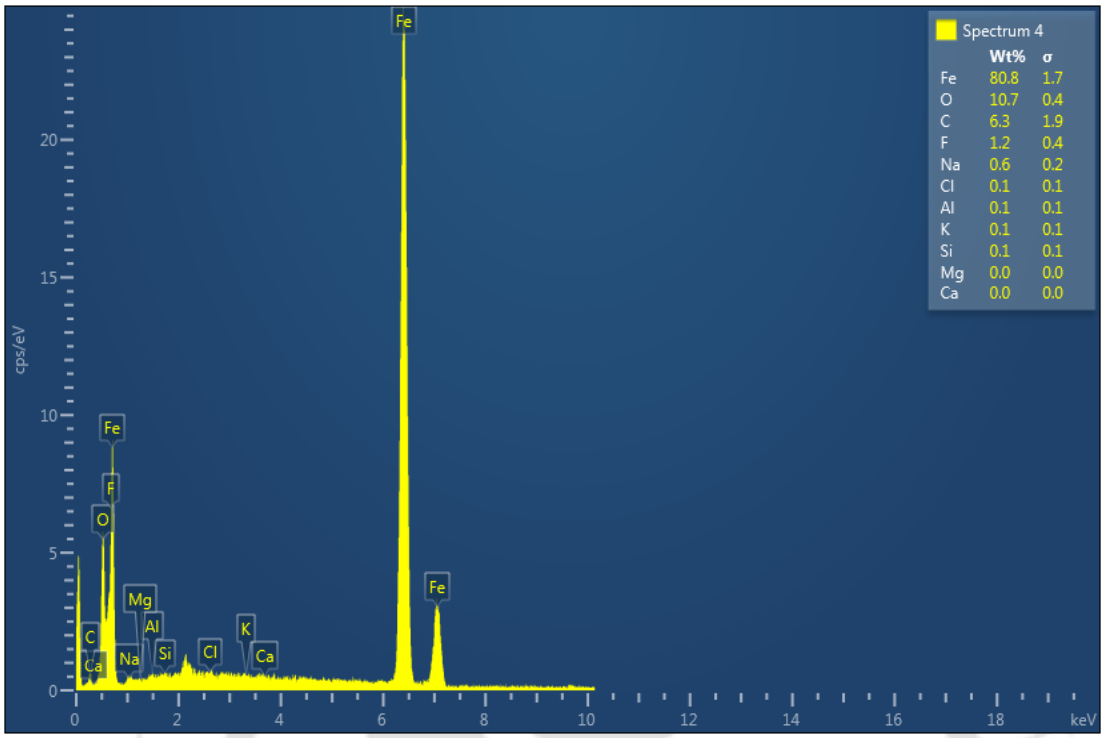

Fig. 7.13 EDX pattern of bentonite B_2

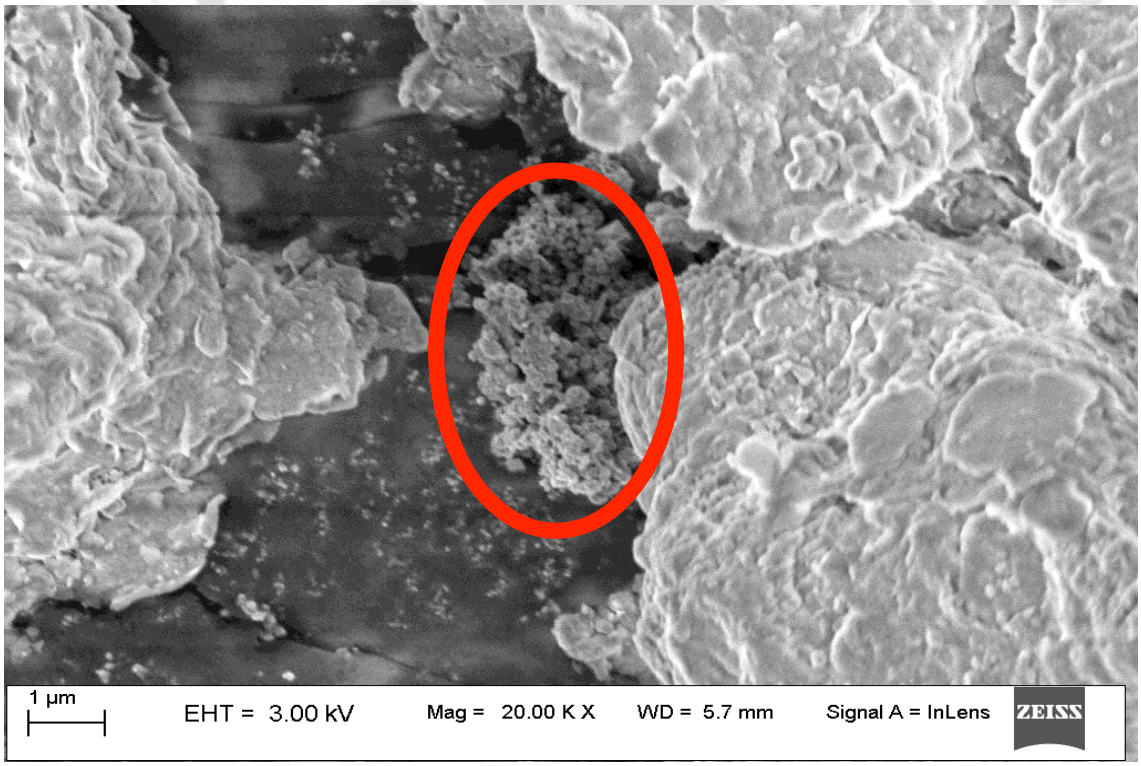

Fig. 7.14 FESEM image of bentonite B_1

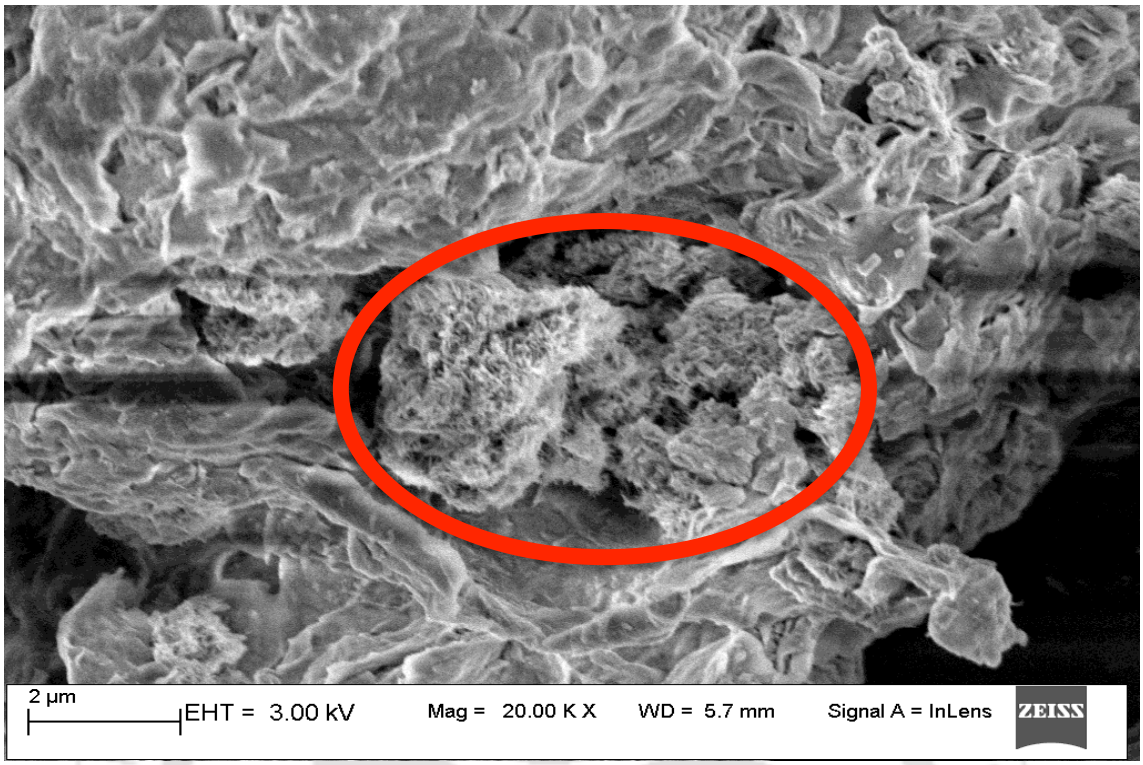

Fig. 7.15 FESEM image of bentonite B_2

Phase II - Reactive transport through compacted Barmer bentonite under the influence of thermal and chemical gradient

7.2.4 Thermal analyses

The variation of the degree of saturation (S_r) with five temperatures (i.e., WH (without heating), 60°C, 110°C, 150°C, and 200°C) for bentonite B_1 is represented in Fig. 7.16, Fig. 7.17, Fig. 7.18 respectively from the hydration end towards heating for three different densities (1.5 Mg/m^3, 1.75 Mg/m^3 and 2 Mg/m^3). The value of S_r for the samples heated from one end at 200°C and compacted at 1.5 Mg/m^3 was observed as 0.73 at the outer ring and 0.75 at the inner ring for the upper part, 0.60 at the outer ring and 0.63 at the inner ring for the middle part and 0.37 at the outer ring and 0.39 at the inner ring for the heating side, i.e., lower portion. Similarly, for samples compacted at 1.75 Mg/m^3 and heated at 200°C, the values S_r of was observed as 0.70 at the outer ring and 0.73 at the inner ring for the upper part, 0.55 at the outer ring and 0.57 at the inner ring for the middle part and 0.28 at the outer ring and 0.30 at the inner ring for the lower portion. And it was 0.71 at the outer ring and 0.74 at the inner ring for the upper part, 0.50 at the outer ring and 0.52 at the inner ring for the middle part and 0.17 at the outer ring and 0.18 at the inner ring for the lower portion at 2 Mg/m^3. If these results were

compared with the samples without heating, it was observed that the value of S_r compacted at 1.5 Mg/m^3 as 0.97 at the outer ring and 0.98 at the inner ring for the upper part, 0.87 at the outer ring and 0.90 at the inner ring for the middle part and 0.51 at the outer ring and 0.53 at the inner ring for the heating side, i.e., lower portion. Whereas, for samples compacted at 1.75 Mg/m^3, it was 0.92 at the outer ring and 0.94 at the inner ring for the upper part, 0.78 at the outer ring and 0.81 at the inner ring for the middle part, and 0.39 at the outer ring and 0.42 at the inner ring for the lower portion. And it was 0.87 at the outer ring and 0.90 at the inner ring for the upper part, 0.72 at the outer ring and 0.75 at the inner ring for the middle part and 0.24 at the outer ring and 0.27 at the inner ring for the lower portion at 2 Mg/m^3.

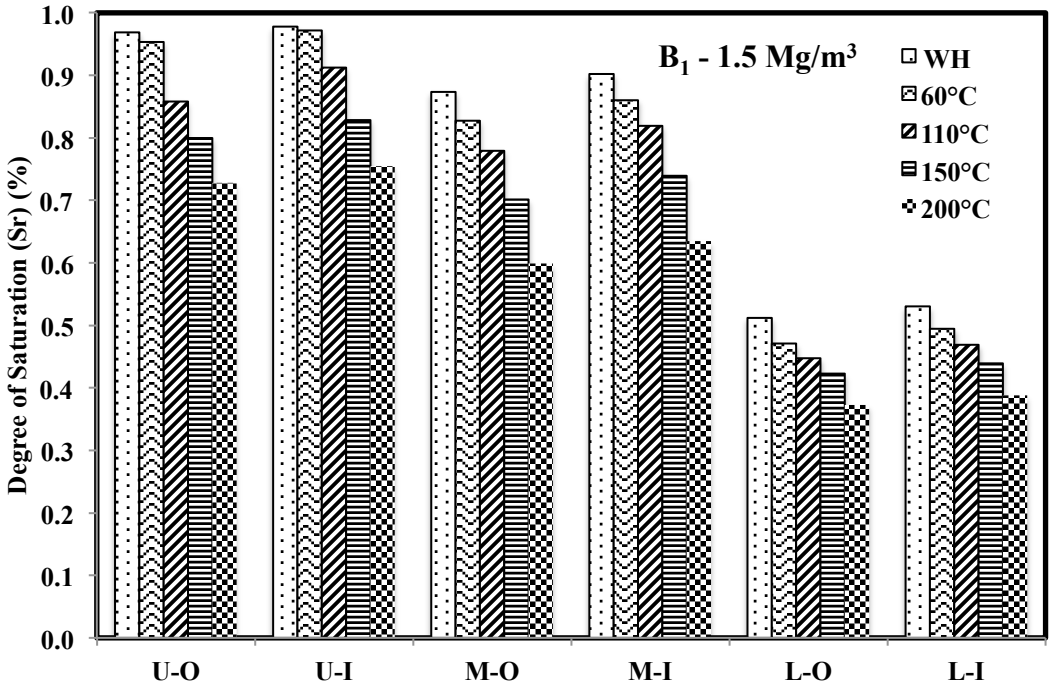

Fig. 7.16 Variation of degree of saturation under a thermal gradient of bentonite B_1 for specimens compacted at 1.5 Mg/m^3 saturated by cement water

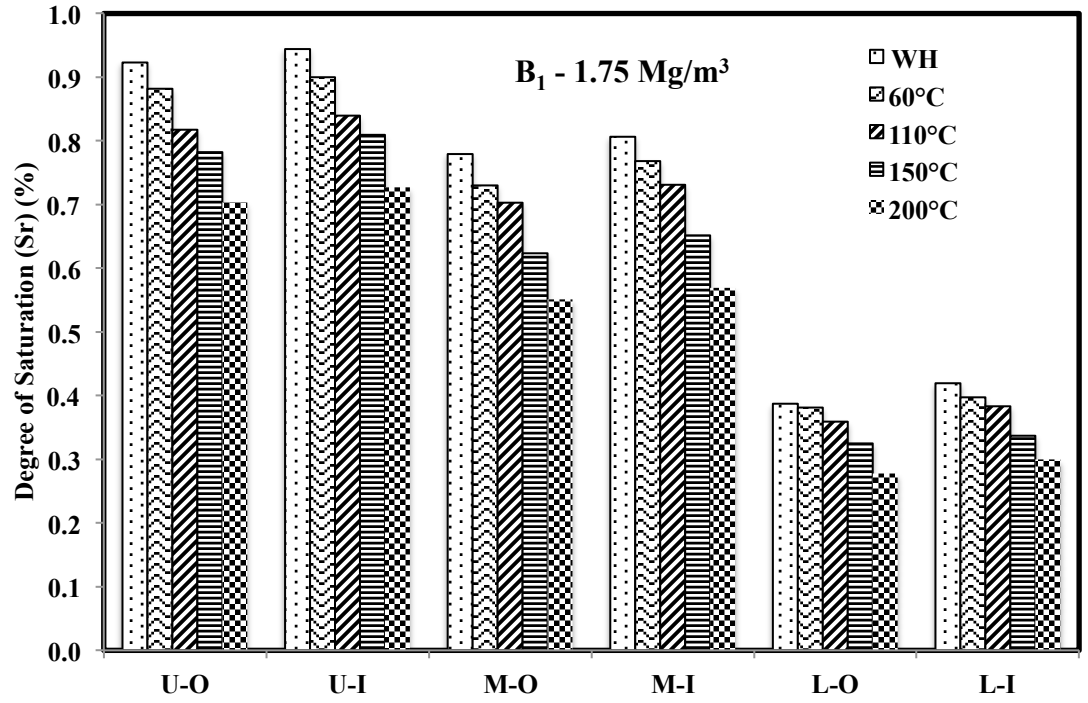

Fig. 7.17 Variation of degree of saturation under a thermal gradient of bentonite B_1 for specimens compacted at 1.75 Mg/m^3 saturated by cement water

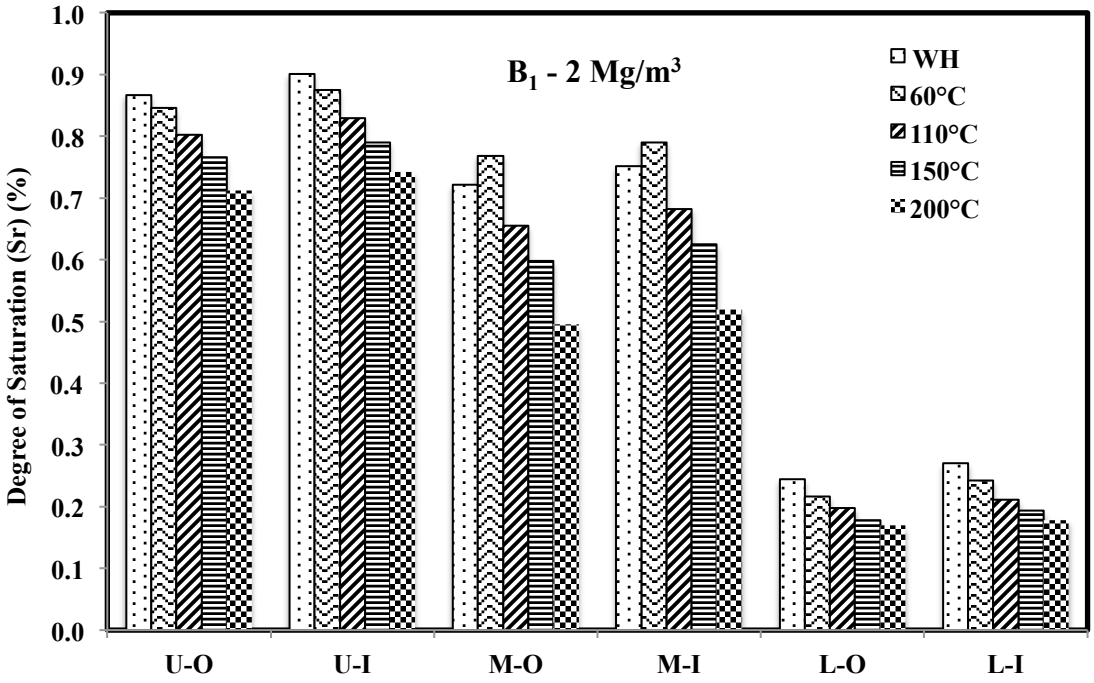

Fig. 7.18 Variation of degree of saturation under a thermal gradient of bentonite B_1 for specimens compacted at 2 Mg/m^3 saturated by cement water

Bentonite B_2, when tested for the same purpose, showed a similar trend of the result, but the value of S_r is more than that of bentonite B_1 (Fig. 7.19, Fig. 7.20, Fig. 7.21). That is maybe because, during the basic characterization of B_1 and B_2 bentonites, the bentonite B_2 showed lesser cation exchange capacity, specific surface area, liquid limit, etc., than B_1. In this case, it was observed as the value of S_r for the samples heated from one end at 200°C and compacted at 1.5 Mg/m^3, was observed as 0.75 at the outer ring and 0.78 at the inner ring for the upper part, 0.62 at the outer ring and 0.66 at the inner ring for the middle part and 0.39 at the outer ring and 0.41 at the inner ring for the heating side, i.e., lower portion. Similarly, for samples compacted at 1.75 Mg/m^3 and heated at 200°C, the values S_r of was observed as 0.70 at the outer ring and 0.74 at the inner ring for the upper part, 0.57 at the outer ring and 0.59 at the inner ring for the middle part and 0.31 at the outer ring and 0.32 at the inner ring for the lower portion. And it was 0.75 at the outer ring and 0.78 at the inner ring for the upper part, 0.52 at the outer ring and 0.55 at the inner ring for the middle part and 0.18 at the outer ring and 0.19 at the inner ring for the lower portion at 2 Mg/m^3. If these results were compared with the samples without heating, it was observed that the value of S_r compacted at 1.5 Mg/m^3 as 0.98 at the outer ring and 0.99 at the inner ring for the upper part, 0.92 at the outer ring and 0.94 at the inner ring for the middle part and 0.57 at the outer ring and 0.60 at the inner ring for the heating side, i.e., lower portion. Whereas, for samples compacted at 1.75 Mg/m^3, it was 0.92 at the outer ring and 0.95 at the inner ring for the upper part, 0.85 at the outer ring and 0.87 at the inner ring for the middle part, and 0.48 at the outer ring and 0.50 at the inner ring for the lower portion. It was 0.91 at the outer ring and 0.95 at the inner ring for the upper part, 0.76 at the outer ring and 0.79 at the inner ring for the middle part and 0.26 at the outer ring and 0.28 at the inner ring for the lower portion at 2 Mg/m^3.

The S_r value was noted more at the hydration end, and less at the heating end but also reduced as both temperature and density were increased. Therefore, it may be assumed that the degree of saturation depends on temperature and density. As one end of the mould was kept at high temperature and the other end was at room temperature, the thermal gradient was created between both ends, which could step up the process of forming the network. The high temperature would have caused the process of vaporization of macropore fluids at temperature 110°C and maybe from macro and micropores both at temperature 150°C and 200°C.

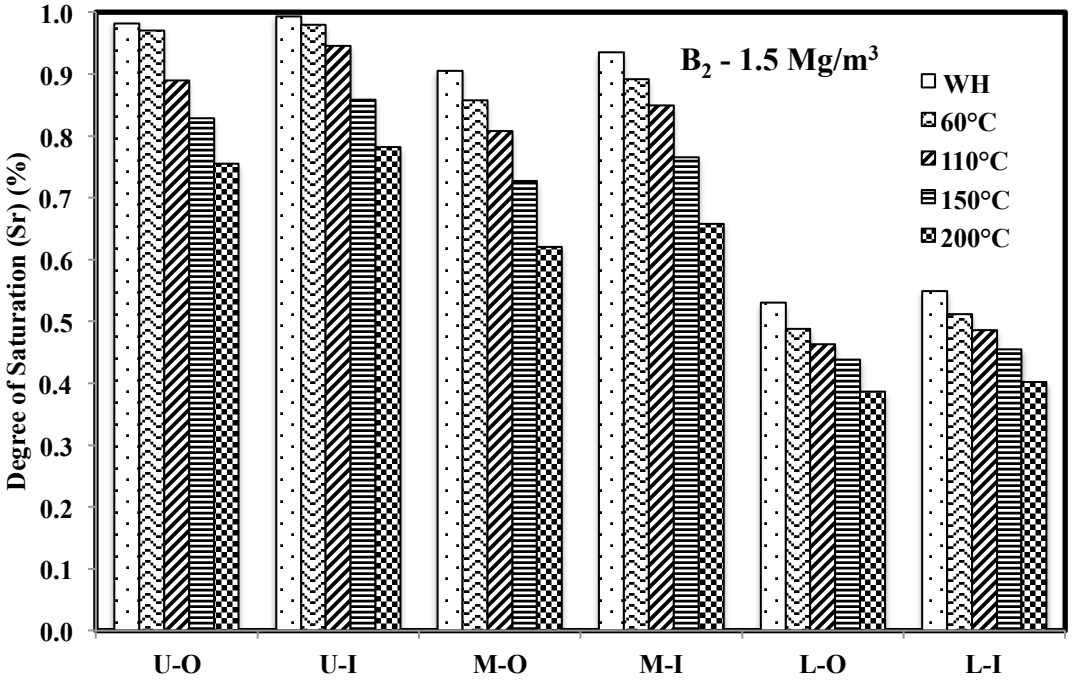

Fig. 7.19 Variation of degree of saturation under a thermal gradient of bentonite B_2 for specimens compacted at 1.5 Mg/m^3 saturated by cement water

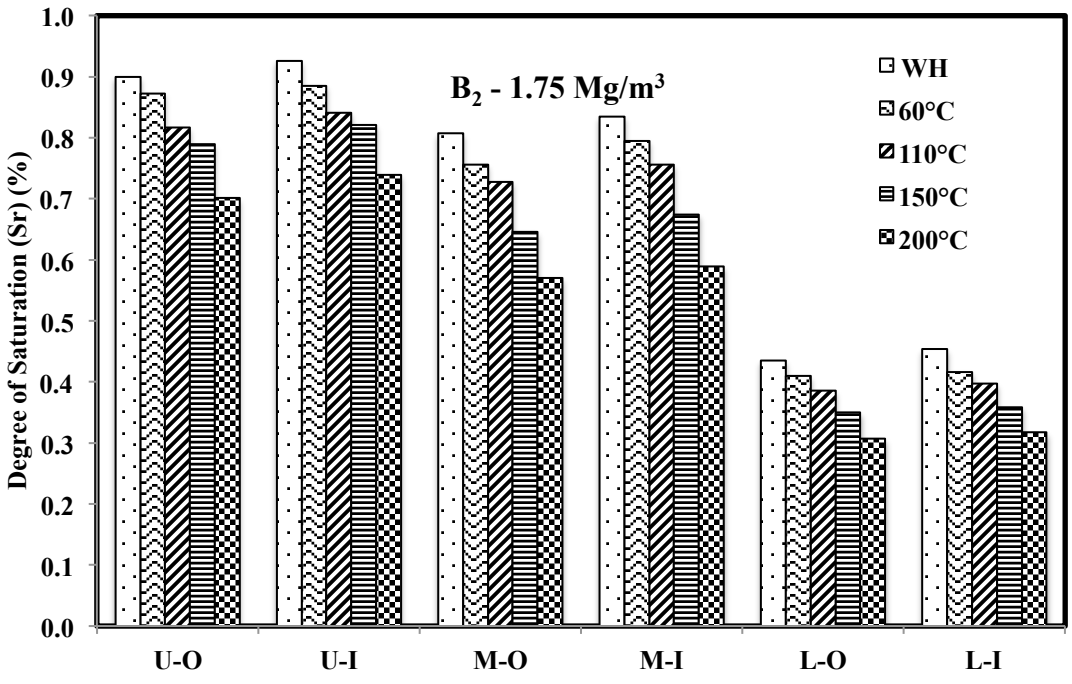

Fig. 7.20 Variation of degree of saturation under a thermal gradient of bentonite B_2 for specimens compacted at 1.75 Mg/m^3 saturated by cement water

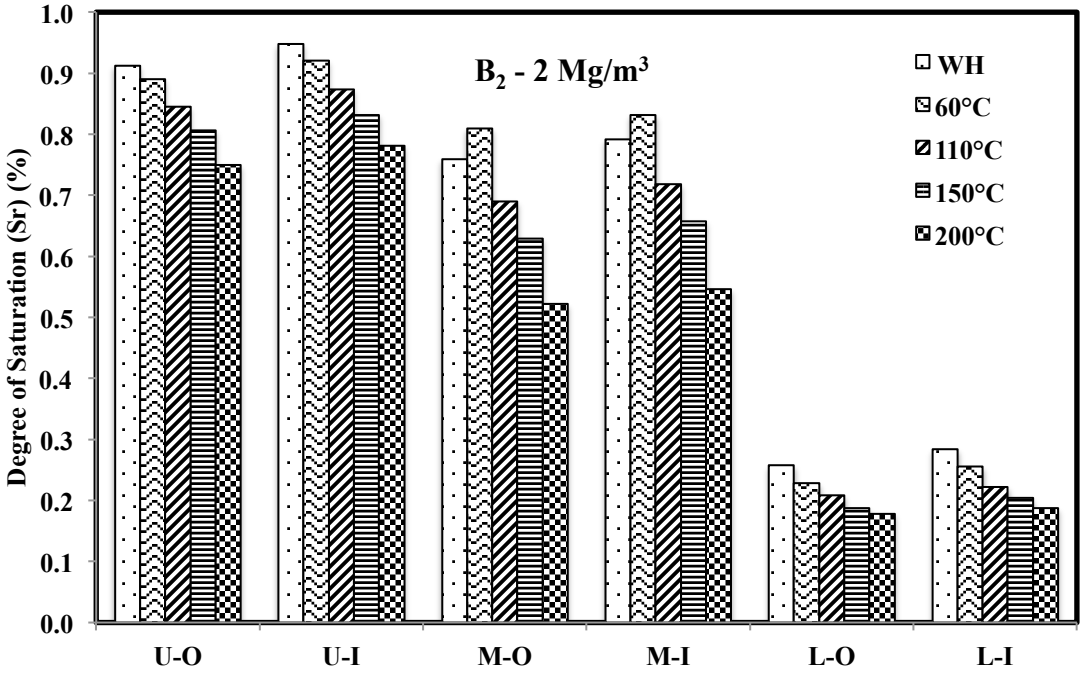

Fig. 7.21 Variation of degree of saturation under a thermal gradient of bentonite B_2 for specimens compacted at 2 Mg/m^3 saturated by cement water

At the same time, the process of condensation would also have caused higher densities, particularly at 2 Mg/m^3. At the same time, the process of drying and wetting was making the soil expand and shrink, and the combined effect had allowed the fluid to form a network and hence the upper and the middle portion was more saturated than the lower one for all densities at all temperatures. The above process also enhanced the combining of macropore fluids to micropores forming a network. However, at the higher densities, the macropores are lesser than micropores, and thus the transport network was slow at higher densities than lower.

7.2.5 Chemical analyses

The samples were cut in three sections (upper, middle, lower) and taken for cation exchange capacity measurement. It was observed that the upper part of all samples showed the difference in the meq/100 g concentration of Na^+, Ca^+, K^+, Mg^+, but the change was not significant (at 200°C) (Fig. 7.22, Fig. 7.23). However, a decreasing trend was observed for the concentration of Na from the upper part to the lower, and the concentration of Mg increased towards the heating end. The concentration of Ca

increased in the upper part, but more than that in the middle part but again was lower than the initial values in the lower part. The possible reason for an increase in the concentration of Ca is from the migration of cement to clay causing ion exchange and accumulating in the form of portlandite in the middle portion and clogging it. Therefore it was observed as the middle portion showed the values near to the upper portion when saturated with cement water. It means when subjected to an alkaline environment, the permeability of compacted Barmer bentonite was increased, which could be due to the dissolution of montmorillonite. The thermal and chemical gradient induced the movement of ions and pore fluids. However, the values of the degree of saturation were lower in the middle portion than the upper that might be because the portlandite clogged the maximum pores. The concentration of Ca was found to be lesser in the lower portion than the middle portion, maybe because of the cation exchange with the higher charge cation, i.e., Fe. The cation exchange capacity measurement of the lower portion showed lesser values of all the cations than the upper, middle, and initial values except Mg. According to Lantenois et al. (2005), dioctahedral smectites were destabilized due to the presence of iron.

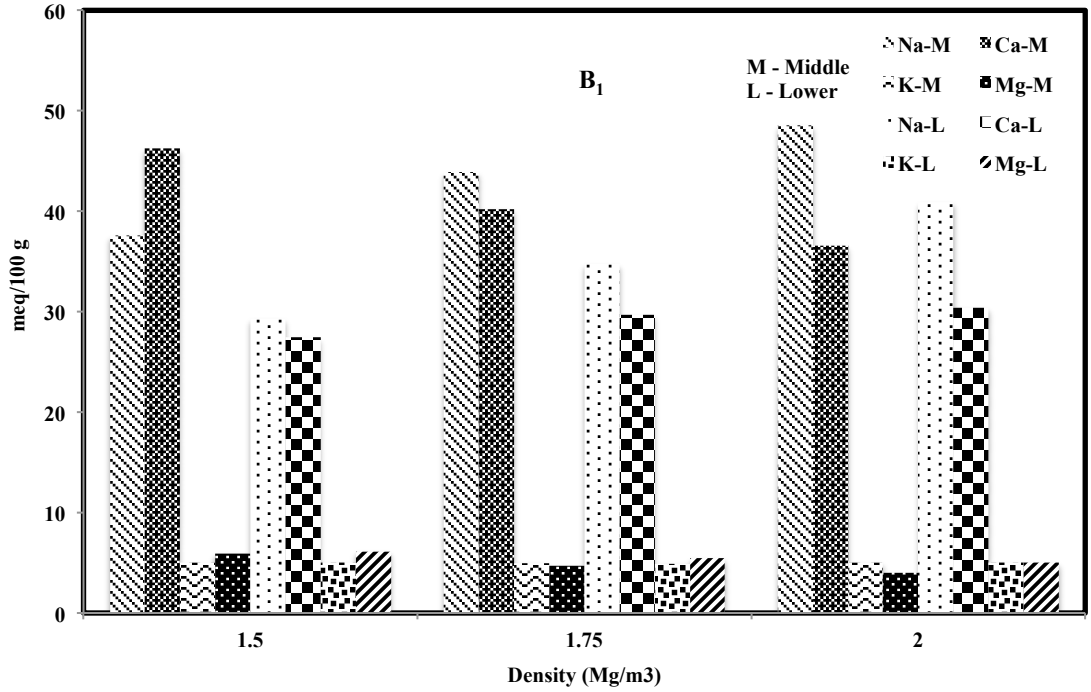

Fig. 7.22 Variation of cation concentration with a dry density of bentonite B_1

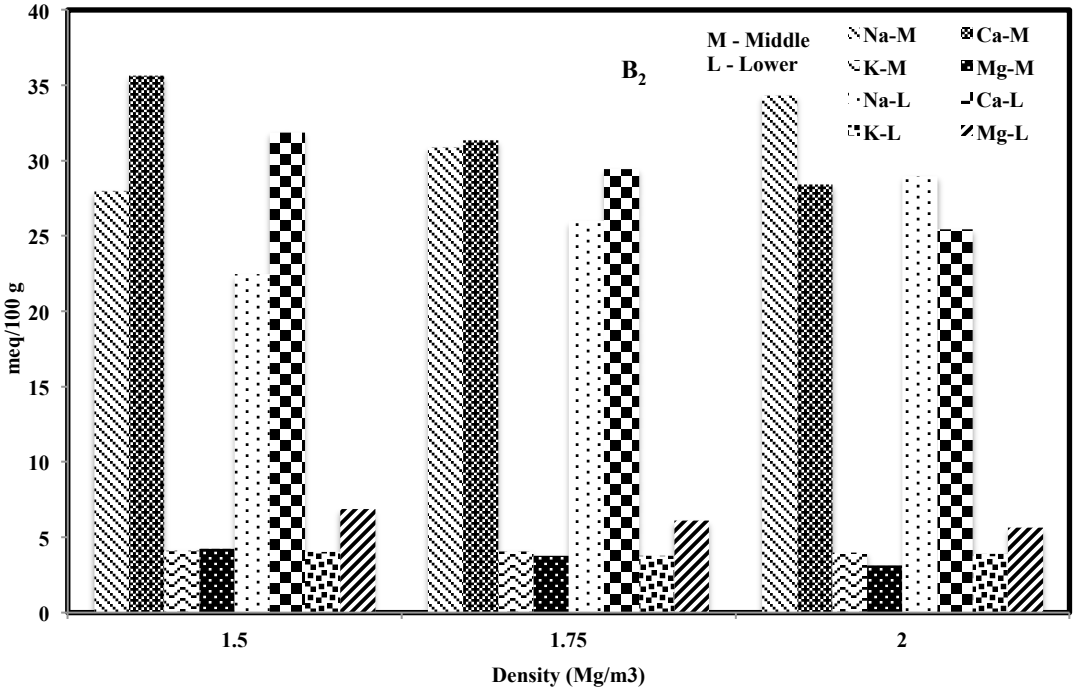

Fig. 7.23 Variation of cation concentration with a dry density of bentonite B_2

7.2.6 Comparison of results saturated with cement waster and distilled water

Similar sets of tests were conducted using distilled water as a saturation solution. The important outcome was observed when the results of these two tests were compared. It was observed that the overall values of degree of saturation for cement water were more than that of distilled water in the case of both the bentonites. This showed that the network forming ability was more in the case of the hyperalkaline environment, which created the conditions to cause reactive transport through the compacted bentonite buffer.

Table 7.1 Comparison of the degree of saturation between distilled water and cement water

Portion	B_1				B_2			
	Cement water		Distilled water		Cement water		Distilled water	
	WH	200°C	WH	200°C	WH	200°C	WH	200°C
U-O	0.87	0.71	0.80	0.60	0.91	0.78	0.87	0.76
U-I	0.90	0.74	0.83	0.64	0.95	0.80	0.90	0.78
M-O	0.72	0.50	0.67	0.46	0.76	0.52	0.70	0.48
M-I	0.75	0.52	0.70	0.44	0.79	0.55	0.74	0.46
L-O	0.24	0.17	0.15	0.09	0.30	0.20	0.26	0.18
L-I	0.27	0.18	0.16	0.08	0.31	0.22	0.31	0.20

The hyperalkaline environment, i.e., high pH was responsible for the dissolution of montmorillonite, and the montmorillonite is a key mineral which is responsible for swelling of bentonite and allows it to form a dense packing to act as buffer material; it lost the swelling ability, and automatically both advective and reactive transport became easy. For distilled water, the percentage change of degree of saturation for the upper portion and the middle portion was more than in the case of cement water (details are discussed in section 3.4). The detailed values are tabulated in Table 7.1. However, the sintering of the metallic iron was observed at the end of the experiment.

7.2.7 Mineralogical changes

The FESEM analyses of the upper, middle and lower parts are shown in Fig. 7.24, Fig. 7.25, Fig. 7.26, Fig. 7.27, and Fig. 7.28. Fig 7.24 and Fig. 7.25, is a FESEM image of the upper part, where some different structural arrangement was observed. According to the reported literature, it could be ettringite and sulphate, respectively. The middle portion of the compacted bentonite specimens showed the accumulation of portlandite ($Ca(OH)_2$), which could be clearly seen from the image (Fig. 7.26). The lower portion obviously showed the different structural arrangement between the lamellar of bentonite. It could be hematite that could be concluded from the XRD curve.

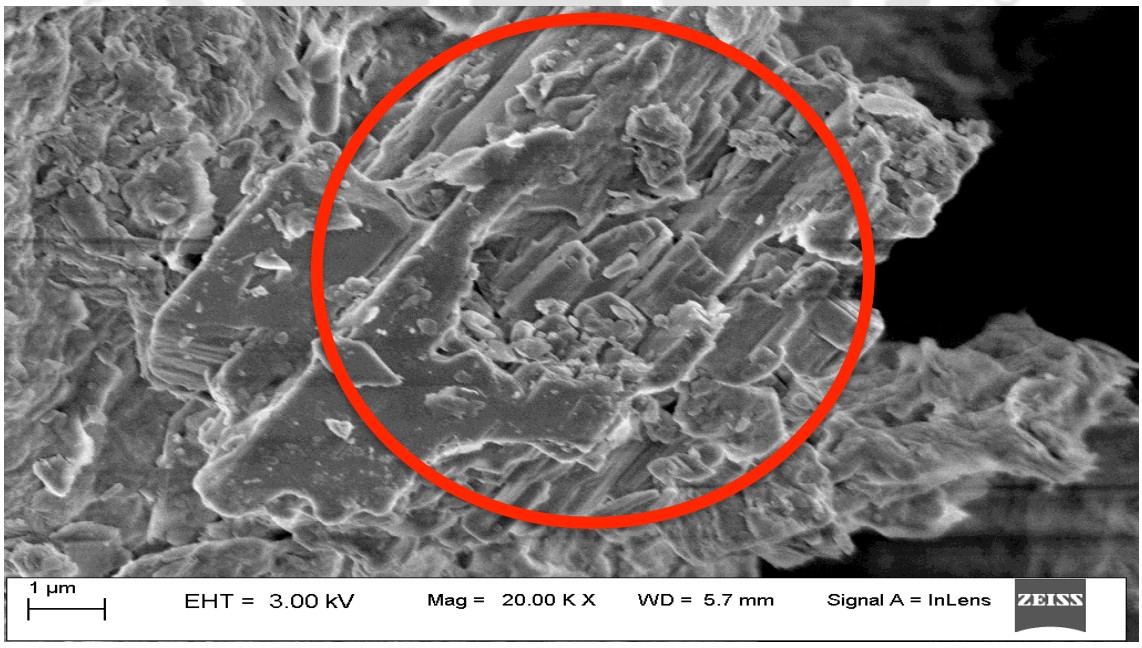

Fig. 7.24 FESEM image of the upper part (1) of the specimen

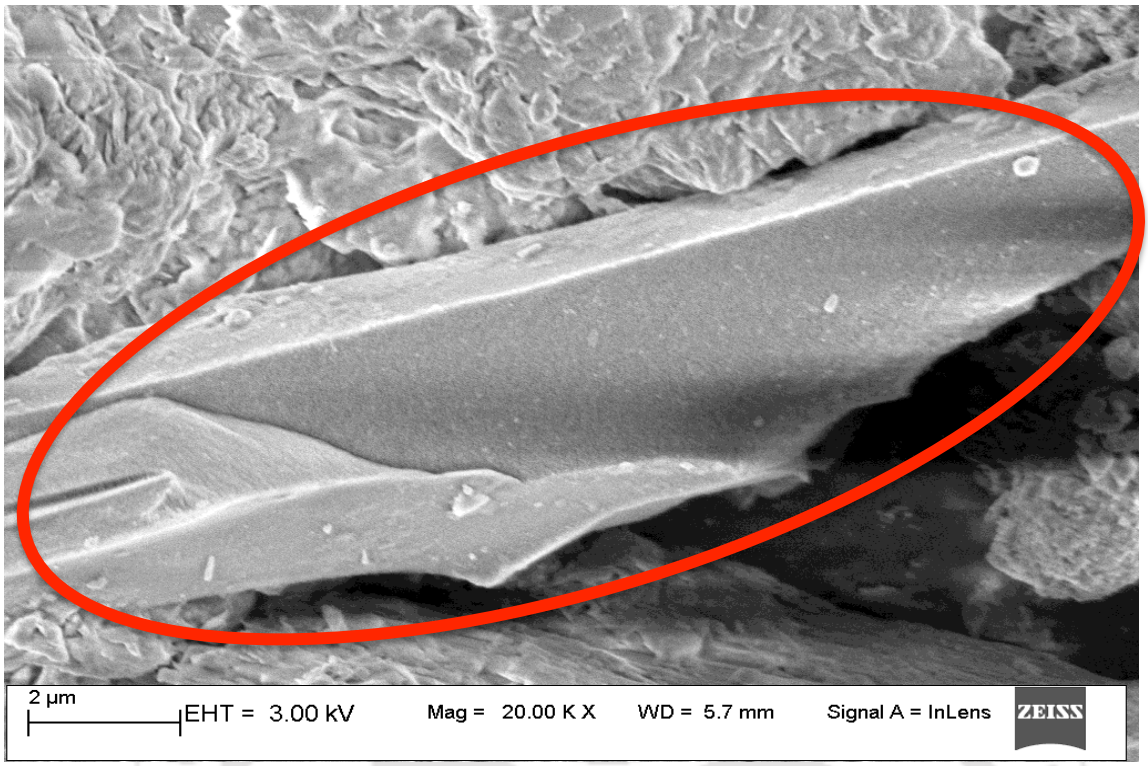

Fig. 7.25 FESEM image of the upper part (2) of the specimen

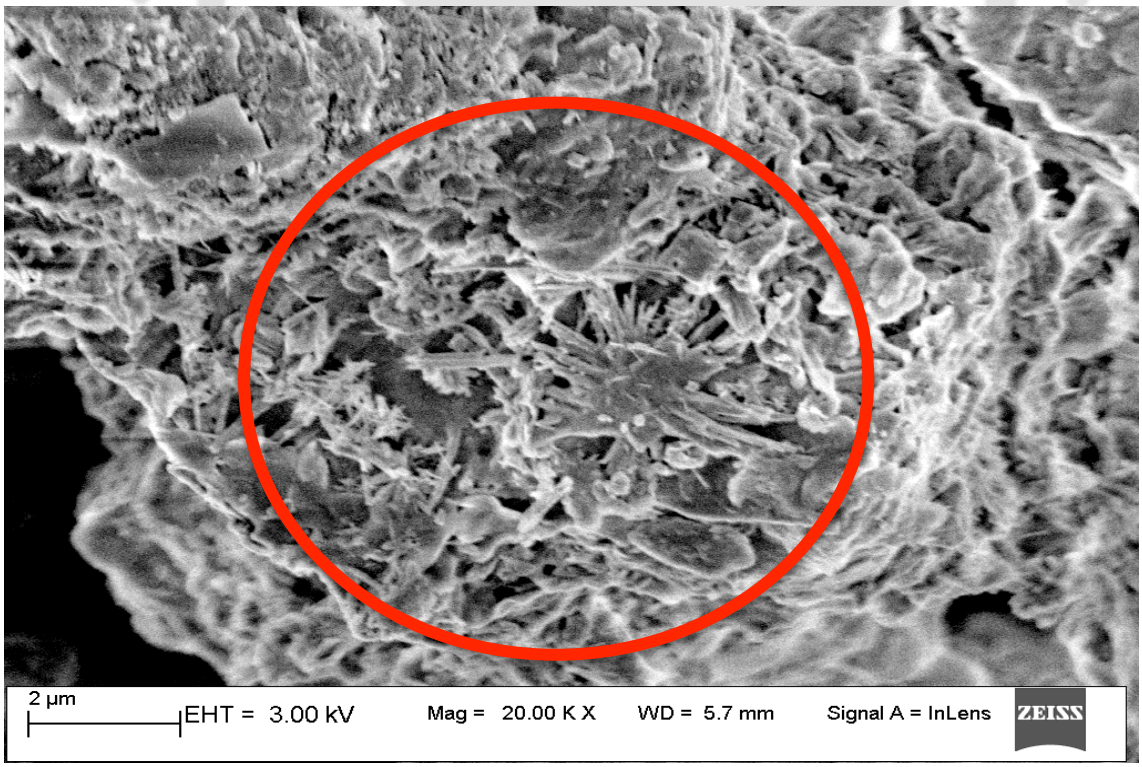

Fig. 7.26 FESEM image of the middle part (1) of the specimen

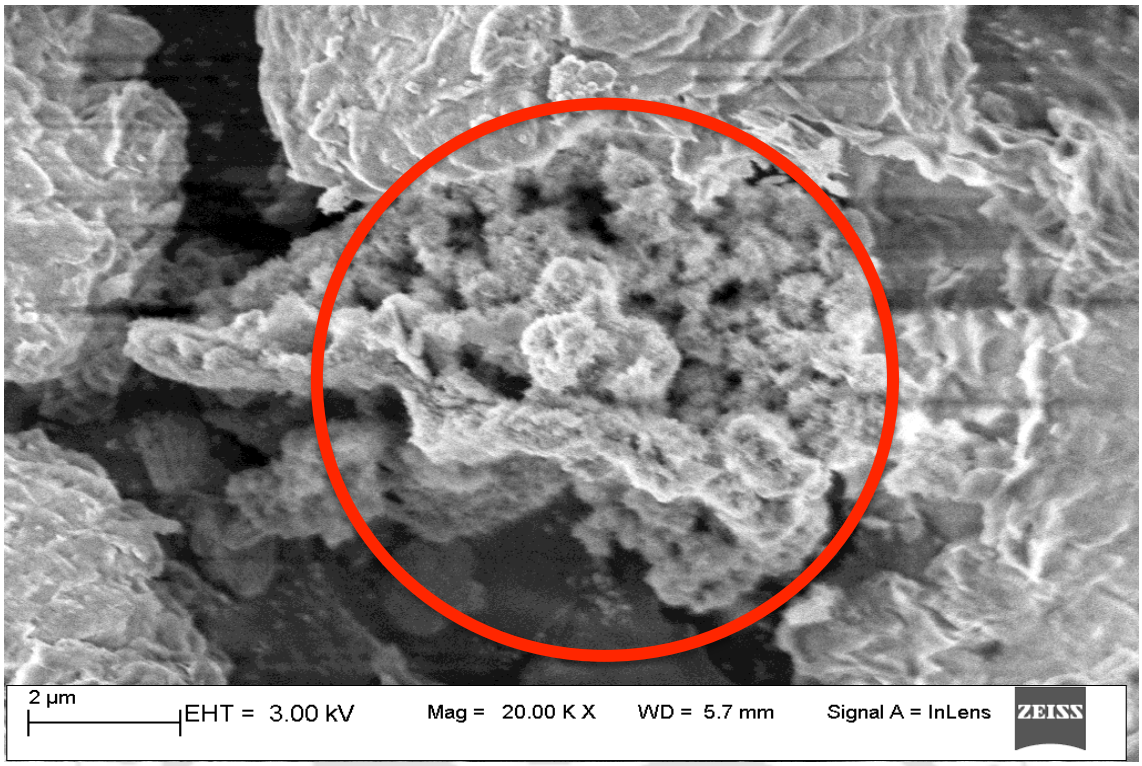

Fig. 7.27 FESEM image of the lower part of the specimen

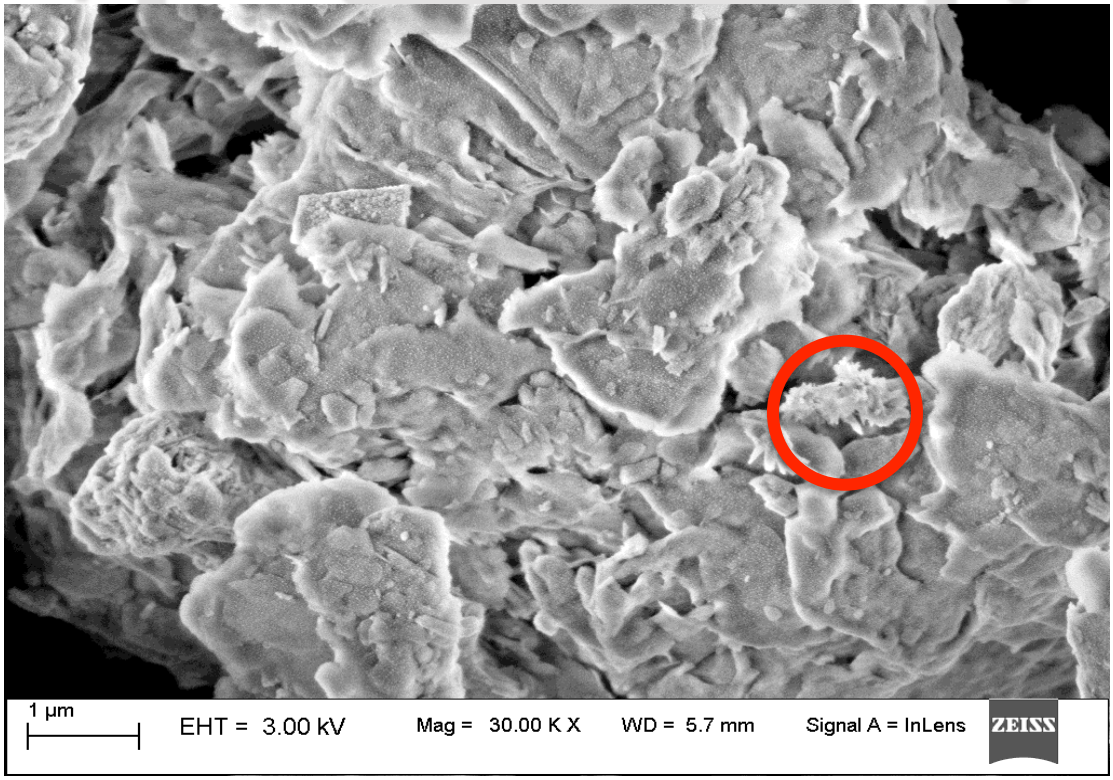

Fig. 7.28 FESEM image of the middle part (2) of the specimen

The XRD patterns of the upper, middle and lower portions are presented in Fig. 7.29, Fig. 7.30, and Fig. 7.31**,** respectively. When the upper part was analyzed, it could show the peak of illite, and ettringite and the structure of ettringite were also caught in the FESEM image. However, there is no evidence of sulphate in the XRD data. The Ca-rich layers observed through SEM were fairly homogeneous Fig. 7.28. They can be carbonates or portlandite that precipitate on the bentonite surface, which can have a significant effect on the decrease in compacted bentonite permeability. The XRD curve of the middle portion showed the peak of portlandite, i.e., the accumulation of $Ca(OH)_2$ in the middle portion, which might have clogged the pores and therefore, the degree of saturation of the lower portion is comparatively less than the upper and the middle one. The degree of saturation was more in the upper portion, but the middle portion was also nearly saturated in the case of cement water but not in the case of distilled water. This is because the hyperalkaline solution created the dissolution of montmorillonite. Also, the temperature increase allowed the mineral smectite to become brittle and turn into more stable phases of silicate, defined as illitization (Wang et al., 1990; Wersin et al., 2007).

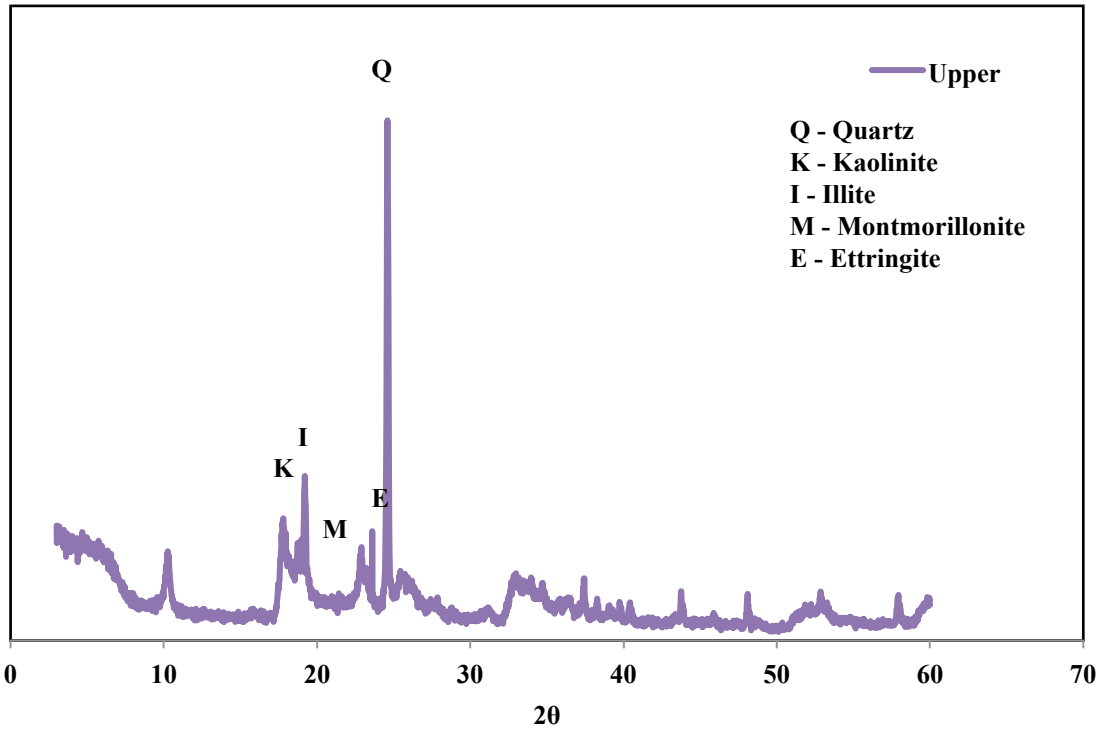

Fig. 7.29 XRD pattern of the upper portion

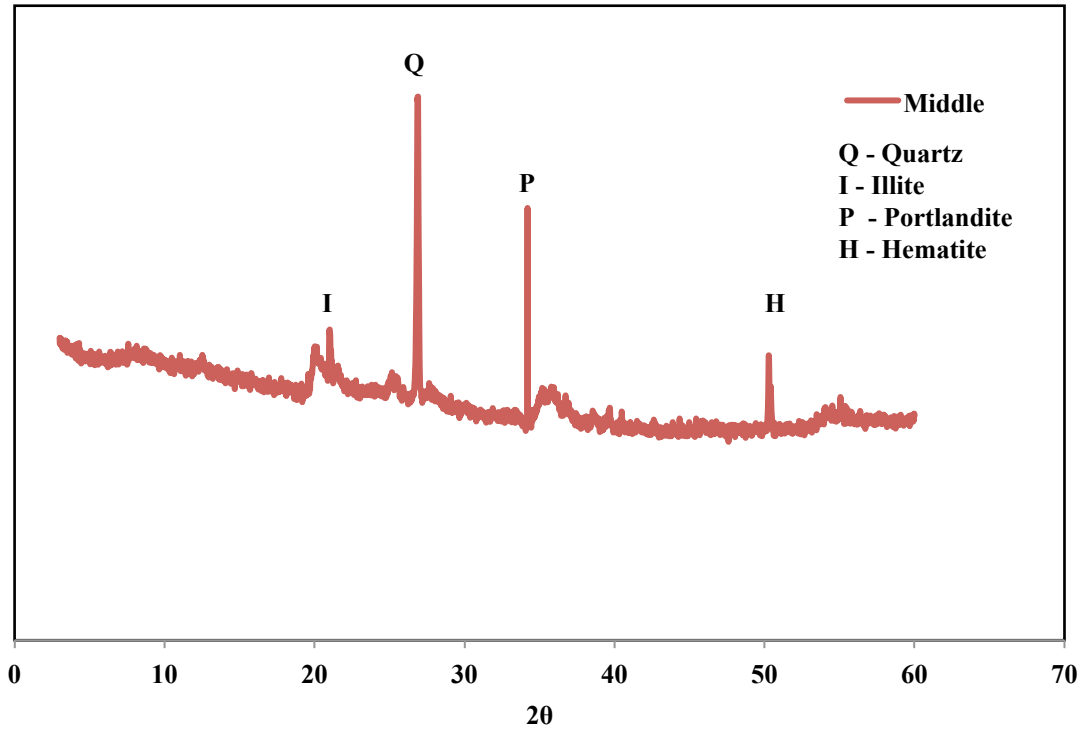

Fig. 7.30 XRD pattern of the middle portion

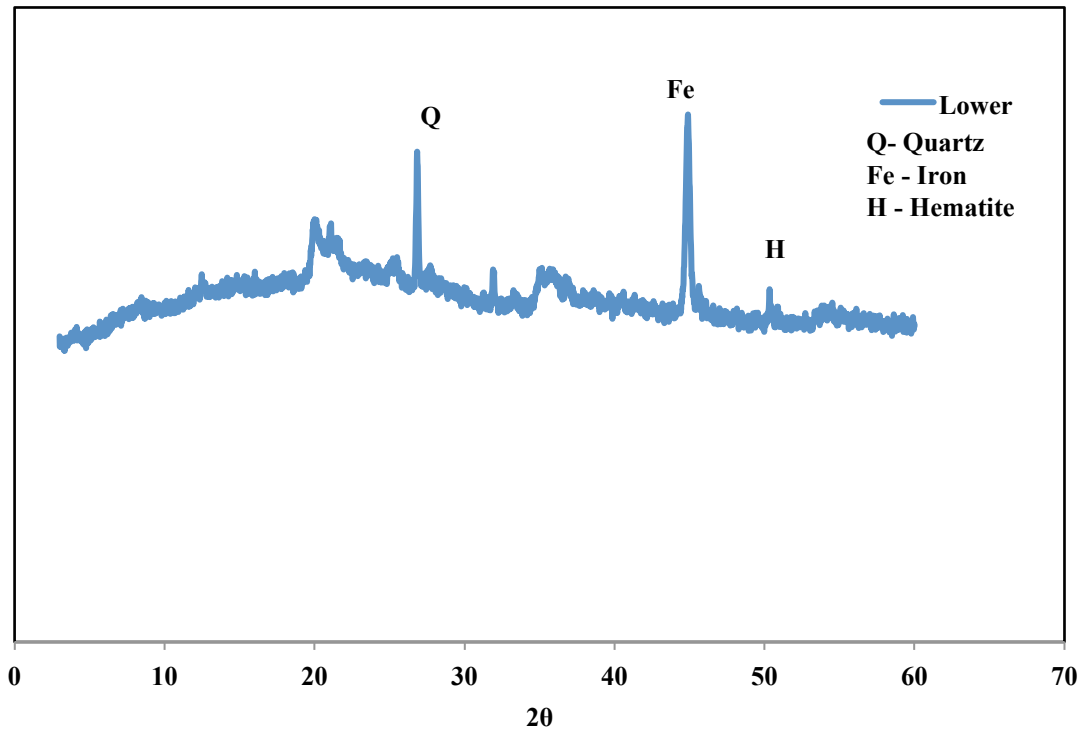

Fig. 7.31 XRD pattern of the lower portion

Leaching of the most soluble elements, such as hydroxide alkalis or portlandite

calcium ($Ca(OH)_2$), leads to a pH increase. The lower portion showed the peak of Fe, which was expected. There is a small peak in both the portions, which could be matched with the hematite. The lower portion has a high peak of Fe but a small peak of hematite, but surprisingly, the peak of hematite was also observed in the middle portion, which was the part of the concern. The XRD and FESEM results of the same samples clearly reveal the reactive transport from both sides, possibly due to the combined effect of thermal and chemical gradients.

7.3 CONCLUSION

The bentonite buffer is used as a sealant inside the deep geological repository. However, its performance might be hampered due to the thermochemical gradient. The combination of alkaline water from the host rock side and corrosion products from the canister side, along with the thermal gradient created by the hot canister at one end and comparatively lower temperature at the other end, could interfere in its execution as a sealant. The alteration in the properties of bentonite could lead to reactive transport through it. Theoretically, due to the degree of complexity between different processes occurring and its link is difficult to study. A small attempt has been made to set field conditions in the lab on a small-scale setup and to study the coupled thermomechanical effect on the reactive transport through compacted Barmer bentonite. Bentonite samples were compacted at 1.5 Mg/m^3, 1.75 Mg/m^3, and 2.0 Mg/m^3 densities kept at 60°C, 110°C, 150°C, and 200°C temperatures for 28 days. Thermal, chemical, and microstructural analyses were made, and the results were compared with the specimens saturated by distilled water. Some of the concluding remarks are –

1. The degree of saturation has been reduced by 18% at 200°C than the Sr in the case of distilled water, but for bentonite B_1 the degree of saturation is greater than B_2. Due to the high temperature, the moisture from the micropores to the macropores was reduced. The predicted macroporosity of B_2 was more pronounced, with B_2 having less clay content than B_1, which was why it was able to exhibit a lower degree of saturation.
2. The cation exchange capacity of the samples near the heater became lesser with increase in temperature. However, the higher density had fewer changes in cation exchange capacities than the lower density. As the density increased, the contribution of macropores reduced to form a network by combining with the

moisture from micropores and thus showed the lesser value of cation exchange capacity at a lower density.

3. The concentration of Mg^{+} increased towards the heater; however, the concentration of Na^{+} decreased. The concentration of Ca^{+} ions was increased in the upper and again rose in the middle portion, but the lower portion showed comparatively lower values of Ca^{+} concentration.
4. The hyperalkaline environment has induced montmorillonite dissolution. As montmorillonite is the main mineral that swells the bentonite and allows it to shape tightly packed material as a shield, it loses the ability to swell, and reactive transportation is immediately made easy. The dissolution of montmorillonite was observed from the elevated peak of "illite" in the XRD curve. It could be said that the hyper alkaline conditions could initiate the process of illitization.
5. The presence of Ca-rich layers through FESEM and the peak of portlandite could reveal the clogging of pores in the compacted bentonite.
6. The presence of hematite in the lower as well as the middle portion could indicate reactive transport through the compacted bentonite.

Chapter 8

CONCLUSION AND RECOMMENDATIONS

8.1 CONCLUSION

Deep geological disposal of high-level nuclear waste is based on a multi-barrier system concept to isolate the waste from the biosphere. Bentonite clay is identified as a potential buffer in deep geological repositories (DGR) for sealing high-level radioactive wastes (HLW) owing to its favorable physicochemical and hydromechanical properties. The impact of factors such as dry density, thermal history, temperature gradient, the chemical gradient on the long-term stability of bentonite was essential to study. With the view of the above-mentioned issues, the response of Barmer bentonites (B_1 and B_2) to thermal history, temperature, and chemical gradient under hyperalkaline and the corrosive environment has been examined.

It has been shown that there is an influence of thermal history on the physicochemical and hydromechanical properties of bentonite. The continuous heating of powdered bentonite for 28 days resulted in changes in mineralogical composition, which is the key factor of it to be used as a buffer material. The dissolution of montmorillonite and starting of illitization phase is observed, in increasing amounts with an increase of temperature and time. Hence, compacted bentonites were tasted for the impact thermal history for their hydromechanical properties. It could be concluded that due to thermal history, the swell pressure of bentonite was reduced. However, the effect is more significant in the case of hyperalkaline environment.

In an eventual repository, compacted bentonite would be subjected to leachate due to canister corrosion along with a hyperalkaline environment and thermal history. The swell pressure of Barmer bentonite was found to reduce with the addition of corrosion products; a further reduction in the swell pressure than the previous two cases was noted. The clogging of pores due to the accumulation of portlandite in the case of hyperalkaline solution and the presence of hematite in case of corrosion leachates are the reasons for the reduction in swell pressure.

Compacted bentonite also exposed to a thermal gradient and a chemical gradient due to hyperalkaline environment at one end and corrosion at the other end (between the hot canister and the host rock). Further analyses of compacted bentonite column heated from

one end and hydrated from another showed evidence of reactive transport of hyperalkaline cement solution from one side and the corrosion leachate from the other side through the compacted bentonite column under thermal gradient. If two bentonites are compared, bentonite B_1 could show better performance than bentonite B_2. This is due to the physicochemical properties of B_1 than B_2, i.e., cation exchange capacity, liquid limit, and specific surface area. If the densities are compared both bentonites performed better when compacted at 2 Mg/m^3 than other densities.

The major contributions from work can be summarized as follows-

1. The thermal history has an influence on both the powdered bentonites. The percentage reduction in the index and physicochemical properties of both the bentonites showed that the influence of thermal history should be considered while designing the deep geological repository. The fluctuation in results was significant from 60°C to 150°C, and a slight decrease in the trend was observed towards 200°C.
2. The swell pressure values were reduced when the compacted specimens were subjected to thermal histories and saturated with distilled water. A further reduction in the values of swell pressure was observed when the samples were subjected to thermal histories and saturated with hyperalkaline cement water. The sequence of swell pressure values are –

$$(SP)_{DW}>(SP)_{TH}>(SP)_{CW}>(SP)_{CWTH}$$

3. The swell pressure values were reduced when the compacted specimens with corrosion products were subjected to thermal histories and saturated with distilled water. A further reduction in the values of swell pressure was observed when the samples were subjected to thermal histories and saturated with hyperalkaline cement water. The sequence of swell pressure values are –

$$(SP)_{DW(WCP)}>(SP)_{DW(CP)}>(SP)_{CW(WCP)}>(SP)_{CW(CP)}$$

4. From these above points, it could be concluded that thermal history is an important phenomenon that showed that the influence of thermal history should be considered while designing the deep geological repository.
5. The combined influence of thermal and chemical gradient is equally important to consider as in the actual field condition; the compacted bentonite suffers the same. It was concluded that both the bentonites had an influence of thermal and chemical gradient. The degree of saturation was reduced when the temperature

increased; it further decreased when hyperalkaline cement water was continued to pass.

6. The cation exchange capacity of the samples near the heater became lesser with the increase in temperature. However, the higher density samples had fewer changes in cation exchange capacities than the lower density. As the density increased, the contribution of macropores reduced to form a network by combining with the moisture from micropores and thus showed the lesser value of cation exchange capacity at a lower density.
7. Dissolution of montmorillonite mineral and formation of secondary minerals and clogging is the additional reason for the reduction of swell pressure.

8.2. RECOMMENDATIONS FOR FUTURE WORK

- **Modeling through the experimental data for a longer duration**
  - The experimental data is for a limited time span, so the modeling of thermomechanical properties of compacted bentonite for thermal and chemical gradient could be modeled for 1000's year, which is the actual time span of working of the repository.
- **Two-dimensional flow study**
  - The flow arrangements from the lateral direction along with longitudinal direction along with temperature monitoring system at various points throughout the length could be altered in the assembly
  - The combined 2D effect of thermal and chemical gradient on compacted bentonite could be studied.
- **Concrete bentonite column study**
  - The concrete bentonite column study could be performed to have a detailed idea about concrete bentonite interface reactions and flow conditions.
- **Study on biochar amended bentonite**
  - Addition of biochar in various percentage in the bentonite
  - Addition of various percentage of sand in the bentonite
  - Comparative parametric study on the optimum percentage of sand or biochar or sand biochar mix in the bentonite

REFERENCES

Abu-Zreig, M. M., Al-Akhras, N. M., & Attom, M. F. (2001). Influence of heat treatment on the behavior of clayey soils. *Applied Clay Science*, *20*(3), 129-135.

Abuel-Naga, H. M., Bergado, D. T., Soralump, S., & Rujivipat, P. (2005). Thermal consolidation of soft Bangkok clay. *Lowland Technology International*, *7*(1, June), 13-21.

Ahmed, A. A., Saaid, I. M., Akhir, N. A. M., & Rashedi, M. (2016, October). Influence of various cation valence, salinity, pH and temperature on bentonite swelling behaviour. In *AIP Conference Proceedings* (Vol. 1774, No. 1, p. 040005). AIP Publishing LLC.

Alonso, E. E., Gens, A., & Josa, A. (1990). A constitutive model for partially saturated soils. *Géotechnique*, *40*(3), 405-430.

Alonso, E. E., Romero, E., Hoffmann, C., & García-Escudero, E. (2005). Expansive bentonite–sand mixtures in cyclic controlled-suction drying and wetting. *Engineering geology*, *81*(3), 213-226.

Alonso, E. E., Vaunat, J., & Gens, A. (1999). Modelling the mechanical behaviour of expansive clays. *Engineering geology*, *54*(1-2), 173-183.

Andersson, K., Allard, B., Bengtsson, M., & Magnusson, B. (1989). Chemical composition of cement pore solutions. *Cement and Concrete Research*, *19*(3), 327-332.

Bag, R., & Rabbani, A. (2017). Effect of temperature on swelling pressure and compressibility characteristics of soil. *Applied Clay Science*, *136*, 1-7.

Baille, W., Tripathy, S., & Schanz, T. (2010). Swelling pressures and one-dimensional compressibility behaviour of bentonite at large pressures. *Applied Clay Science*, *48*(3), 324-333.

Bao, C., Jiaxing, G., & Huixin, Z. (2016). Alteration of compacted GMZ bentonite by infiltration of alkaline solution. *Clay Minerals*, *51*(2), 237-247.

Bauer, A., & Velde, B. (1999). Smectite transformation in high molar KOH solutions. *Clay Minerals*, *34*(2), 259-273.

Bayram, H., Önal, M., Yılmaz, H., & Sarıkaya, Y. (2010). Thermal analysis of a white calcium bentonite. *Journal of thermal analysis and calorimetry*, *101*(3), 873-879.

Beles, A. A., & Stanculescu, I. I. (1954). Thermal treatment as a method of improving the stability of earth masses. *Geotechnique*, *8*(4).

Bildstein, O., Trotignon, L., Perronnet, M., & Jullien, M. (2006). Modelling iron–clay interactions in deep geological disposal conditions. *Physics and Chemistry of the Earth, Parts A/B/C*, *31*(10-14), 618-625.

Birgersson, M., & Karnland, O. (2009). Ion equilibrium between montmorillonite interlayer space and an external solution—consequences for diffusional transport. *Geochimica et Cosmochimica Acta*, *73*(7), 1908-1923.

Bolt, G. H. (1956). Physico-chemical analysis of the compressibility of pure clays. *Geotechnique*, *6*(2), 86-93.

Börgesson, L. (1985). Water flow and swelling pressure in non-saturated bentonite-based clay barriers. *Engineering geology*, *21*(3-4), 229-237.

Bruce, R. R., & Klute, A. (1956). The measurement of sol-water diffusivity. In *Soil Sci Soc Am Proc* (Vol. 20, p. 458562).

Bucher, F., & Müller-Vonmoos, M. (1989). Bentonite as a containment barrier for the disposal of highly radioactive wastes. *Applied Clay Science*, *4*(2), 157-177.

Caporuscio, F. A., Palaich, S. E., Cheshire, M. C., & Colón, C. J. (2017). Corrosion of copper and authigenic sulfide mineral growth in hydrothermal bentonite experiments. *Journal of Nuclear Materials*, *485*, 137-146.

Castellanos, E., Villar, M. V., Romero, E., Lloret, A., & Gens, A. (2008). Chemical impact on the hydro-mechanical behaviour of high-density FEBEX bentonite. *Physics and Chemistry of the Earth, Parts A/B/C*, *33*, S516-S526.

Chandrasekharan, E. C., Boominathan, S., Sadayan, E., & Narayanaswamy, S. K. (1969). INFLUENCE OF HEAT TREATMENT ON THE PULVERIZATION AND STABILIZATION· CHARACTERISTICS OF TYPICAL TROPICAL SOILS. *Highw. Res. Board Spec. Rep*, *103*, 161-172.

Chapman, H. D. (1965). Cation-exchange capacity. *Methods of Soil Analysis: Part 2 Chemical and Microbiological Properties*, *9*, 891-901.

Chapman, N., & Hooper, A. (2012). The disposal of radioactive wastes underground. *Proceedings of the Geologists' Association*, *123*(1), 46-63.

Chegbeleh, L.P., Nishigaki, M., Akudago, J.A., Alim, M.A., Komatsu, M. (2008). Concepts of Repository and the functions of bentonite in repository environments: A state of the art review. Journal of the Faculty of Environmental Science and Technology,Okayama University. 13(1), 1-5.

Chen, F. H. 1988. Foundations on expansive soils. Elsevier, New York.

Cho, W. J., Lee, J. O., & Kang, C. H. (2000). Influence of temperature elevation on the sealing performance of a potential buffer material for a high-level radioactive waste repository. *Annals of Nuclear Energy*, *27*(14), 1271-1284.

Cho, W. J., Lee, J. O., & Kang, C. H. (2002). Influence of salinity on the hydraulic conductivity of compacted bentonite. *MRS Online Proceedings Library Archive*, *713*.

Choi, J., Kang, C. H., & Whang, J. (2001). Experimental assessment of non-treated bentonite as the buffer material of a radioactive waste repository. *Journal of Environmental Science and Health, Part A*, *36*(5), 689-714.

Cuevas, J., De La Villa, R. V., Ramírez, S., Sánchez, L., Fernández, R., & Leguey, S. (2006). The alkaline reaction of FEBEX bentonite: a contribution to the study of the performance of bentonite/concrete engineered barrier systems. *Journal of Iberian Geology*, *32*(2), 151-174.

Cuisinier, O., Masrouri, F., Pelletier, M., Villieras, F., & Mosser-Ruck, R. (2008). Microstructure of a compacted soil submitted to an alkaline plume. *Applied Clay Science*, *40*(1-4), 159-170.

Dauzeres, A., Le Bescop, P., Sardini, P., & Coumes, C. C. D. (2010). Physico-chemical investigation of clayey/cement-based materials interaction in the context of geological waste disposal: Experimental approach and results. *Cement and Concrete Research*, *40*(8), 1327-1340.

De Combarieu, G., Schlegel, M. L., Neff, D., Foy, E., Vantelon, D., Barboux, P., & Gin, S. (2011). Glass–iron–clay interactions in a radioactive waste

geological disposal: an integrated laboratory-scale experiment. *Applied Geochemistry*, *26*(1), 65-79.

Debruyn, W., Dresselaers, J., Vermeiren, P., Kelchtermans, J., & Tas, H. (1991). *Corrosion of container and infrastructure materials under clay repository conditions* (No. EUR--13667). Commission of the European Communities.

Delage, P., Cui, Y. J., & Tang, A. M. (2010). Clays in radioactive waste disposal. *Journal of Rock Mechanics and Geotechnical Engineering*, *2*(2), 111-123.

Delage, P., Howat, M. D., & Cui, Y. J. (1998). The relationship between suction and swelling properties in a heavily compacted unsaturated clay. *Engineering geology*, *50*(1-2), 31-48.

Delage, P., Sultan, N., & Cui, Y. J. (2000). On the thermal consolidation of Boom clay. *Canadian Geotechnical Journal*, *37*(2), 343-354.

Deneele, D., Cuisinier, O., Hallaire, V., & Masrouri, F. (2010). Microstructural evolution and physico-chemical behavior of compacted clayey soil submitted to an alkaline plume. *Journal of Rock Mechanics and Geotechnical Engineering*, *2*(2), 169-177.

Di Maio, C., (1996). Exposure of bentonite to salt solution: osmotic and mechanical effects. Géotechnique 46 (4), 695–707.

Dixon, D. A., Gray, M. N., & Thomas, A. W. (1985). A study of the compaction properties of potential clay—sand buffer mixtures for use in nuclear fuel waste disposal. *Engineering geology*, *21*(3-4), 247-255.

Dixon, D.A., Gray, M.N., Graham, J., (1996). Swelling and hydraulic properties of bentonites from Japan, Canada and the USA. In: Kamon, M. (Ed.), Environmental Geotechnics. Balkema, Rotterdam, pp. 43–48.

Dolinar, B., & Škrabl, S. (2013). Atterberg limits in relation to other properties of fine-grained soils. *Acta Geotechnica Slovenica*, *10*(2), 4-13.

Dueck, A., Johannesson, L. E., Olsson, O. K. S., & Sjöland, A. (2011). Hydro-mechanical and chemical-mineralogical analyses of the bentonite buffer from a full-scale field experiment simulating a high-level waste repository. *Clays and Clay Minerals*, *59*(6), 595-607.

Eberl, D., Whitney, G., & Khoury, H. (1978). Hydrothermal reactivity of smectite. *American Mineralogist*, *63*(3-4), 401-409.

ENRESA, (2000). FEBEX Project — full scale engineered barriers experiments for a deep geological respiratory for high level radioactive waste in crystalline host rock. Final Report, Publicación Téechnica 1/2000. Empresa Nacional de Residuos Radiactivos SA.ENRESA, Madrid, Spain.

Estabragh, A. R., Khosravi, F., & Javadi, A. A. (2016). Effect of thermal history on the properties of bentonite. *Environmental Earth Sciences*, *75*(8), 657.

Ferguson, H., & Gardner, W. H. (1963). Diffusion theory applied to water flow data obtained using gamma ray absorption. *Soil Science Society of America Journal*, *27*(3), 243-246.

Fernández, R., Mäder, U. K., Rodríguez, M., De La Villa, R. V., & Cuevas, J. (2009). Alteration of compacted bentonite by diffusion of highly alkaline solutions. *European Journal of Mineralogy*, *21*(4), 725-735.

Féron, D., Crusset, D., & Gras, J. M. (2008). Corrosion issues in nuclear waste disposal. *Journal of nuclear materials*, *379*(1-3), 16-23.

Garcia Garcia, S. (2007). *The impact of groundwater chemistry on the stability of bentonite colloids* (Doctoral dissertation, KTH).

García-García, S., Jonsson, M., & Wold, S. (2006). Temperature effect on the stability of bentonite colloids in water. *Journal of Colloid and Interface Science*, *298*(2), 694-705.

Gardner, W. R., & Mayhugh, M. S. (1958). Solutions and tests of the diffusion equation for the movement of water in soil. *Soil Science Society of America Journal*, *22*(3), 197-201.

Gates, W.P., Bouazza, A., and Churchman, G.J. (2009) Bentonite clay keeps pollutants at bay. Elements, 5, 105–110.

Gaucher, E. C., & Blanc, P. (2006). Cement/clay interactions–a review: experiments, natural analogues, and modeling. *Waste Management*, *26*(7), 776-788.

Gens, A., & Alonso, E. E. (1992). A framework for the behaviour of unsaturated expansive clays. *Canadian Geotechnical Journal*, *29*(6), 1013-1032.

Gibb, F. G. (1999). High-temperature, very deep, geological disposal: a safer alternative for high-level radioactive waste?. *Waste Management*, *19*(3), 207-211.

Grim, R. E., & Kulbicki, G. (1957). Etude aux rayons X des reactions des mineraux argileux a haute temperature. *Bull. soc. franc. ceram*, 21-27.

Gu, B. X., Wang, L. M., Minc, L. D., & Ewing, R. C. (2001). Temperature effects on the radiation stability and ion exchange capacity of smectites. *Journal of Nuclear Materials*, *297*(3), 345-354.

Guimarães, A. D. M. F., Ciminelli, V. S. T., & Vasconcelos, W. L. (2009). Smectite organofunctionalized with thiol groups for adsorption of heavy metal ions. *Applied Clay Science*, *42*(3-4), 410-414.

Gupta, G. C., & Dutta, A. K. (1967). Water stability of aggregates in a heated black cotton soil. *Soil Science*, *104*(3), 210-216.

Güven, N. (1990). Longevity of bentonite as buffer material in a nuclear-waste repository. *Engineering Geology*, *28*(3-4), 233-247.

Habert, B., Jullien, M., Kohler, E., & Bonnin, D. (2006). Redox of iron in smectites. *Clay Science*, *12*(Supplement2), 149-153.

He, Y., Ye, W. M., Chen, Y. G., & Cui, Y. J. (2019). Effects of K+ solutions on swelling behavior of compacted GMZ bentonite. *Engineering Geology*, *249*, 241-248.

Herbert, H. J., Kasbohm, J., Moog, H. C., & Henning, K. H. (2004). Long-term behaviour of the Wyoming bentonite MX-80 in high saline solutions. *Applied Clay Science*, *26*(1-4), 275-291.

Herbert, H. J., Kasbohm, J., Sprenger, H., Fernández, A. M., & Reichelt, C. (2008). Swelling pressures of MX-80 bentonite in solutions of different ionic strength. *Physics and Chemistry of the Earth, Parts A/B/C*, *33*, S327-S342.

Hill, S. L. (2016). The Corrosion of Carbon Steel under Deep Geologic Nuclear Waste Disposal Conditions

Holtz, W. G. (1948, January). The determination of limits for the control of placement moisture in high rolled-earth dams. In *PROCEEDINGS-AMERICAN SOCIETY FOR TESTING AND MATERIALS* (Vol. 48, pp. 1240-1248). 100 BARR HARBOR DR, W CONSHOHOCKEN, PA 19428-2959: AMER SOC TESTING MATERIALS.

Holtz, W. G. (1954). Engineering properties of expansive clays. *Transactions of the American Society of Civil Engineers*, *121*, 641-677.

http://aneyefortexas.wordpress.com/2012/03/22/colors-of-bentonite/: Structure of montmorillonite.

Huang, W. L., Longo, J. M., & Pevear, D. R. (1993). An experimentally derived kinetic model for smectite-to-illite conversion and its use as a geothermometer. *Clays and Clay Minerals*, *41*(2), 162-177.

Hummel, W., & Schneider, J. W. (2005). Safety of nuclear waste repositories. *CHIMIA International Journal for Chemistry*, *59*(12), 909-915.

IAEA. (2018). *Regulations for the safe transport of radioactive material*. IAEA.

IS 2720, Part 2, 1973. Methods for Test for Soils: Determination of Moisture content. Bureau of Indian Standards, New Delhi.

IS 2720, Part 3, 1980. Methods of Test for Soils: Determination of Specific Gravity. Bureau of Indian Standards, New Delhi.

IS 2720, Part 4, 1985a. Methods of Test for Soils: Grain Size Analysis. Bureau of Indian Standards, New Delhi.

IS 2720, Part 40, 1970. Methods of Test for Soils: Free swell index. Bureau of Indian Standards, New Delhi.

IS 2720, Part 5, 1985. Methods of Test for Soils: Atterberg's limits. Bureau of Indian Standards, New Delhi.

IS 2720, Part 8, 1983. Methods of Test for Soils: Standard proctor test and modified proctor test. Bureau of Indian Standards, New Delhi.

IS 4031, Part 1, 1996. Methods of Physical Tests for Hydraulic Cement. Bureau of Indian Standards, New Delhi.

Jefferson, I., & Rogers, C. D. F. (1998). Liquid limit and the temperature sensitivity of clays. *Engineering geology*, *49*(2), 95-109.

Jenni, A., Gimmi, T., Alt-Epping, P., Mäder, U., & Cloet, V. (2017). Interaction of ordinary Portland cement and Opalinus Clay: Dual porosity modelling compared to experimental data. *Physics and Chemistry of the Earth, Parts A/B/C*, *99*, 22-37.

Karnland, O. (1997). *Bentonite swelling pressure in strong NaCl solutions. Correlation between model calculations and experimentally determined data* (No. SKB-TR--97-31). Swedish Nuclear Fuel and Waste Management Co..

Karnland, O., Olsson, S., Nilsson, U., & Sellin, P. (2007). Experimentally determined swelling pressures and geochemical interactions of compacted Wyoming bentonite with highly alkaline solutions. *Physics and Chemistry of the Earth, Parts A/B/C*, *32*(1-7), 275-286.

Kaufhold, S., & Dohrmann, R. (2009). Stability of bentonites in salt solutions| sodium chloride. *Applied clay science*, *45*(3), 171-177.

Kaufhold, S., & Dohrmann, R. (2010). Effect of extensive drying on the cation exchange capacity of bentonites. *Clay Minerals*, *45*(4), 441-448.

Kaufhold, S., Hassel, A. W., Sanders, D., & Dohrmann, R. (2015). Corrosion of high-level radioactive waste iron-canisters in contact with bentonite. *Journal of Hazardous Materials*, *285*, 464-473.

Kaufhold, S., Klimke, S., Schloemer, S., Alpermann, T., Renz, F., & Dohrmann, R. (2020). About the corrosion mechanism of metal iron in contact with bentonite. *ACS Earth and Space Chemistry*, *4*(5), 711-721.

Kim, G. (2000). Influence of physicochemical properties of soil on pH of pore water. *KSCE Journal of Civil Engineering*, *4*(4), 233-237.

Kim, J. S., Kwon, S. K., Sanchez, M., & Cho, G. C. (2011). Geological storage of high level nuclear waste. *KSCE Journal of Civil Engineering*, *15*(4), 721-737.

Komine, H. (2004). Simplified evaluation for swelling characteristics of bentonites. *Engineering geology*, *71*(3-4), 265-279.

Komine, H., & Ogata, N. (1994). Experimental study on swelling characteristics of compacted bentonite. *Canadian geotechnical journal*, *31*(4), 478-490.

Komine, H., & Ogata, N. (1996). Prediction for swelling characteristics of compacted bentonite. *Canadian Geotechnical Journal*, *33*(1), 11-22.

Komine, H., Yasuhara, K., & Murakami, S. (2009). Swelling characteristics of bentonites in artificial seawater. *Canadian Geotechnical Journal*, *46*(2), 177-189.

Komornik, A., & David, D. (1969). Prediction of swelling pressure of clays. *J. Soil Mech. Found. Div., Am. Soc. Civ. Eng.;(United States)*, *95*.

Lagaly, G. (1982). Layer charge heterogeneity in vermiculites. *Clays and Clay Minerals*, *30*(3), 215-222.

Laguros, J. G. (1969). Effect of temperature on some engineering properties of clay soils. *Highway Research Board Special Report*, (103).

Lambe, T.W. and Whitman, R.V. (1969). Soil Mechanics. New York: John Wiley.

Lantenois, S., Lanson, B., Muller, F., Bauer, A., Jullien, M., and Plancon, A. (2005) Experimental study of smectite interaction with metal Fe at low temperature: 1. Smectite destabilization. Clays and Clay Minerals, 53, 597–612.

Lee JO, Lim JG, Kang IM, Kwon S (2012). Swelling pressures of compacted Ca-bentonite. Eng Geo 129-130:20-26.

Lee, J. O., Choi, H., & Lee, J. Y. (2016). Thermal conductivity of compacted bentonite as a buffer material for a high-level radioactive waste repository. *Annals of Nuclear Energy*, *94*, 848-855.

Lee, J.O., Cho, W.J., Kang, C.H., Chun, K.S. (1999). Swelling and hydraulic properties of Ca- bentonite for the buffer of a waste repository, in: proceedings of symposium on technologies for the management of radioactive waste from nuclear power plants and back end nuclear fuel cycle activities, Taejon, Republic of Korea.

Legrand, L., Savoye, S., Chausse, A., & Messina, R. (2000). Study of oxidation products formed on iron in solutions containing bicarbonate/carbonate. *Electrochimica Acta*, *46*(1), 111-117.

Lloret, A., Villar, M. V., Sanchez, M., Gens, A., Pintado, X., & Alonso, E. E. (2003). Mechanical behaviour of heavily compacted bentonite under high suction changes. *Géotechnique*, *53*(1), 27-40.

Lu, N., Likos, W.J. (2004). Unsaturated soil mechanics. John Wiley and Sons, Inc., New Jersey.

Majed M. Abu-Zreig, Nabil M. Al-Akhras, Mousa F. Attom (2001). Influence of heat treatment on the behavior of clayey soils. Applied Clay Science 20:129–135

Marsh, G. P., & Taylor, K. J. (1988). An assessment of carbon steel containers for radioactive waste disposal. *Corrosion science*, *28*(3), 289-320.

Mata, C., Guimarães, L. D. N., Ledesma, A., Gens, A., & Olivella, S. (2005). A hydro-geochemical analysis of the saturation process with salt water of a bentonite crushed granite rock mixture in an engineered nuclear barrier. *Engineering geology*, *81*(3), 227-245.

Maugis, P., & Imbert, C. (2007). Confined wetting of FoCa clay powder/pellet mixtures: Experimentation and numerical modeling. *Physics and Chemistry of the Earth, Parts A/B/C*, *32*(8-14), 795-808.

Means, R.E. (1959). Buildings on expansive clays. Quarterly of the Colorado School of Mines. 54(4), 1-31.

Meunier, A., Velde, B., & Griffault, L. (1998). The reactivity of bentonites: a review. An application to clay barrier stability for nuclear waste storage. *Clay Minerals*, *33*(2), 187-196.

Mitchell J.K., (1993). Fundamentals of soil behavior. Secound Edition, Published by John Wiley and Sons, Inc.

Musso, G., Morales, E. R., Gens, A., & Castellanos, E. (2003). The role of structure in the chemically induced deformations of FEBEX bentonite. *Applied Clay Science*, *23*(1-4), 229-237.

Nakayama, S., Sakamoto, Y., Yamaguchi, T., Akai, M., Tanaka, T., Sato, T., & Iida, Y. (2004). Dissolution of montmorillonite in compacted bentonite by highly alkaline aqueous solutions and diffusivity of hydroxide ions. *Applied Clay Science*, *27*(1-2), 53-65.

Navarro, V., Yustres, Á., Asensio, L., De la Morena, G., González-Arteaga, J., Laurila, T., & Pintado, X. (2017). Modelling of compacted bentonite swelling accounting for salinity effects. *Engineering Geology*, *223*, 48-58.

Nayak, N. V., & Christensen, R. W. (1971). Swelling characteristics of compacted, expansive soils. *Clays and clay minerals*, *19*(4), 251-261.

NEA, (2010a). Geoscientific Information in the Radioactive Waste Management Safety Case. Main Messages from the AMIGO Project. OECD Nuclear Energy Agency, Paris, Publication 6395, 53pp.

NEA, (2010b). Reversibility and Retrievability (R&R) for the Deep Disposal of High- Level Radioactive Waste and Spent Fuel: Intermediate Findings and Discussion Document of the NEA R&R Project. OECD Nuclear Energy Agency, Paris, Publi- cation NEA/RWM(2010)10, 55pp.

Neaman, A., Pelletier, M., & Villieras, F. (2003). The effects of exchanged cation, compression, heating and hydration on textural properties of bulk bentonite and its corresponding purified montmorillonite. *Applied Clay Science*, *22*(4), 153-168.

Nielsen, D. R., Biggar, J. W., & Davidson, J. M. (1962). Experimental consideration of diffusion analysis in unsaturated flow problems. *Soil Science Society of America Journal*, *26*(2), 107-111.

Nirex, (2002). Research on the Alkaline Disturbed Zone Resulting from Cement- Water-Rock Reactions around a Cementitious Repository, Nirex Report N/054. United Kingdom Nirex Limited, Harwell.

OECD Nuclear Energy Agency. European Commission. (2003). *Engineered Barrier Systems and the Safety of Deep Geological Repositories: State-of-the-art Report*. Nuclear Energy Agency, Organisation for Economic Co-operation and Development.

Parolo, M. E., Pettinari, G. R., Musso, T. B., Sánchez-Izquierdo, M. P., & Fernández, L. G. (2014). Characterization of organo-modified bentonite sorbents: The effect of modification conditions on adsorption performance. *Applied surface science*, *320*, 356-363.

Patel, R., Punshon, C., Nicholas, J., Bastid, P., Zhou, R., Schneider, C., Bagshaw, N., Howse, D., Hutchinson, E., Asano, R., & King, F. (2012). Canister Design Concepts for Disposal of Spent Fuel and High Level Waste. Nagra Technical Report, NTB 12-06. Nagra, Wettingen, Switzerland.

Philip, J.R. (1955). The concept of diffusion applied to soil water. Proceedings of national academy of science (India). 24A, 93-104.

Pusch, R. (1982). *Chemical interaction of clay buffer materials and concrete* (No. SKBF-KBS-SFR--82-01). Swedish Nuclear Fuel Supply Co.

Pusch, R. (2002). *The buffer and backfill handbook. Part 1: definitions, basic relationships and laboratory methods* (No. SKB-TR--02-20). Swedish Nuclear Fuel and Waste Management Co.

Pusch, R., & Yong, R. N. (2006). *Microstructure of smectite clays and engineering performance*. CRC Press.

Pusch, R., O. Karnland, and H. Hokmark. (1990). GMM: A general micro-structural model for qualitative and quantitative studies of smectite clays, SKB. Technical Rep. No. SKB-90-43. Stockholm, Sweden: Swedish Nuclear Fuel and Waste Management Company.

Pusch, R., Zwahr, H., Gerber, R., & Schomburg, J. (2003). Interaction of cement and smectitic clay—theory and practice. *Applied Clay Science*, *23*(1-4), 203-210.

Ramana, M. V., Thomas, D. G., & Varughese, S. (2001). Estimating nuclear waste production in India. *Current Science*, 1458-1462.

Ramírez, S., Cuevas, J., Vigil, R., & Leguey, S. (2002). Hydrothermal alteration of "La Serrata" bentonite (Almeria, Spain) by alkaline solutions. *Applied Clay Science*, *21*(5-6), 257-269.

Rao, A. S., Phanikumar, B. R., & Sharma, R. S. (2004). Prediction of swelling characteristics of remoulded and compacted expansive soils using free swell index. *Quarterly Journal of Engineering Geology and Hydrogeology*, *37*(3), 217-226.

Rao, S. M., & Ravi, K. (2013). Hydro-mechanical characterization of Barmer 1 bentonite from Rajasthan, India. *Nuclear Engineering and Design*, *265*, 330-340.

Rao, S. M., & Ravi, K. (2014). Permeability of bentonite buffer: density and salinity effect. *Environmental Geotechnics*, *1*(1), 40-47.

Rao, S. M., & Ravi, K. (2015). Influence of initial degree of saturation on swell pressures of compacted Barmer bentonite specimens. *Annals of Nuclear Energy*, *80*, 303-311.

Rao, S. M., & Ravi, K. (2015). Influence of initial degree of saturation on swell pressures of compacted Barmer bentonite specimens. *Annals of Nuclear Energy*, *80*, 303-311.

Rao, S. M., & Revanasiddappa, K. (2005). Role of microfabric in matrix suction of residual soils. *Engineering Geology*, *80*(1-2), 60-70.

Rao, S. M., & Shivananda, P. (2005). Role of osmotic suction in swelling of salt-amended clays. *Canadian Geotechnical Journal*, *42*(1), 307-315.

Rao, S. M., & Thyagaraj, T. (2007). Swell–compression behaviour of compacted clays under chemical gradients. *Canadian Geotechnical Journal*, *44*(5), 520-532.

Rao, S. M., Kachroo, T. A., Allam, M. M., Joshi, M. R., & Acharya, A. (2008, October). Geotechnical characterization of some Indian bentonites for their use as buffer material in geological repository. In *Proceedings of*

12th international conference of international association for computer methods and advances in geomechanics (IACMAG) (pp. 1-6).

Ravi, K., & Rao, S. M. (2017). Estimation of Solute Concentrations in Micro-pore and Macro-pore Solutions of Compacted Bentonite–Sand Mixtures. *Geotechnical and Geological Engineering*, *35*(1), 517-525.

Romero, E., Villar, M. V., & Lloret, A. (2005). Thermo-hydro-mechanical behaviour of two heavily overconsolidated clays. *Engineering Geology*, *81*(3), 255-268.

Samper, J., Lu, C., & Montenegro, L. (2008). Reactive transport model of interactions of corrosion products and bentonite. *Physics and Chemistry of the Earth, Parts A/B/C*, *33*, S306-S316.

Sato T, Kuroda M, Yokoyama S, et al. Effect of pH on smectite dissolution rates under alkaline conditions (2002). In: Proceeding of the International Conference on Clays in Natural and Engineered Barriers for Radioactive Waste Confinement. Tours: [s.n.], 11–12.

Savage D., Walker C. & Arthur R. (2007) Alteration of bentonite by hyperalkaline fluids: A review of the role of secondary minerals. Physics and Chemistry of the Earth, 32, 287–297.

Savage, D., Noy, D., & Mihara, M. (2002). Modelling the interaction of bentonite with hyperalkaline fluids. *Applied Geochemistry*, *17*(3), 207-223.

Savage, D., Watson, C., Benbow, S., and Wilson, J. (2010). Modelling iron-bentonite interactions. Applied Clay Science, 47, 91–98.

Sawhney, B. L., & Zelitch, I. (1969). Direct determination of potassium ion accumulation in guard cells in relation to stomatal opening in light. *Plant physiology*, *44*(9), 1350.

Schanz, T., & Tripathy, S. (2009). Swelling pressure of a divalent-rich bentonite: Diffuse double-layer theory revisited. *Water Resources Research*, *45*(5).

Schofield, R. K. (1946). Ionic forces in thick films of liquid between charged surfaces. *Transactions of the Faraday Society*, *42*, B219-B225.

Seed, H. B., & Chan, C. K. (1959). Structure and strength characteristics of compacted clays. *Journal of the Soil Mechanics and Foundations Division*, *85*(5), 87-128.

Shirazi, S. M., Kazama, H., Kuwano, J., & Rashid, M. M. (2010). The influence of temperature on swelling characteristics of compacted bentonite for waste disposal. *Environmentasia*, *3*, 284-286.

Siddiqua, S., Blatz, J., & Siemens, G. (2011). Evaluation of the impact of pore fluid chemistry on the hydromechanical behaviour of clay-based sealing materials. *Canadian Geotechnical Journal*, *48*(2), 199-213.

Siddiqua, S., Siemens, G., Blatz, J., Man, A., & Lim, B. F. (2014). Influence of pore fluid chemistry on the mechanical properties of clay-based materials. *Geotechnical and Geological Engineering*, *32*(4), 1029-1042.

SKB (2011) Long-Term Safety for the Final Repository for Spent Nuclear Fuel at Forsmark: Main Report of the SR-Site Project. SKB Technical Report TR-11- 01. Available online. Swedish Nuclear Fuel and Waste Management Co., Stockholm, Sweden.

Sridharan, A. (1991). Engineering behaviour of clays-A fundamental approach. *Indian Geotech J*, *21*, 1-136.

Sridharan, A. (2014). Fourth IGS-Ferroco Terzaghi Oration: 2014: soil clay mineralogy and physico-chemical mechanisms governing the fine-grained soil behaviour. *Indian Geotechnical Journal*, *44*(4), 371-399.

Sridharan, A. S. U. R. I., Rao, A. S., & Sivapullaiah, P. V. (1986). Swelling pressure of clays. *Geotechnical Testing Journal*, *9*(1), 24-33.

Sridharan, A., & Prakash, K. (1999). Mechanisms controlling the undrained shear strength behaviour of clays. *Canadian Geotechnical Journal*, *36*(6), 1030-1038.

Steefel, C., Rutqvist, J., Tsang, C-F., Liu, H-H., Sonnenthal, E., Houseworth, J. and Birkholzer, J. (2010) Reactive Transport and Coupled THM Processes in Engineering Barrier Systems. Lawrence Berkeley National Laboratory Report. Lawrence Berkeley National Laboratory, Berkeley, California, USA.

Sun, Z., Chen, Y. G., Cui, Y. J., Xu, H. D., Ye, W. M., & Wu, D. B. (2018). Effect of synthetic water and cement solutions on the swelling pressure of compacted Gaomiaozi (GMZ) bentonite: The Beishan site case, Gansu, China. *Engineering Geology*, *244*, 66-74.

Suzuki, S., Sazarashi, M., Akimoto, T., Haginuma, M., & Suzuki, K. (2008). A study of the mineralogical alteration of bentonite in saline water. *Applied Clay Science*, *41*(3-4), 190-198.

Tan, Ö., Yılmaz, L., & Zaimoğlu, A. S. (2004). Variation of some engineering properties of clays with heat treatment. *Materials Letters*, *58*(7-8), 1176-1179.

Tang, A. M., Cui, Y. J., & Le, T. T. (2008). A study on the thermal conductivity of compacted bentonites. *Applied Clay Science*, *41*(3-4), 181-189.

Taubald, H., Bauer, A., Schäfer, T., Geckeis, H., Satir, M., & Kim, J. I. (2000). Experimental investigation of the effect of high-pH solutions on the Opalinus Shale and the Hammerschmiede Smectite. *Clay minerals*, *35*(3), 515-524.

Thakur, V. K., & Singh, D. N. (2005). Rapid determination of swelling pressure of clay minerals. *Journal of Testing and Evaluation*, *33*(4), 239-245.

Torres, E., Turrero, M. J., Escribano, A., & Martín, P. L. (2013). Geochemical Interactions at the Concrete-bentonite Interface of Column Experiments. *PEBS, FP7-249681*, 73.

Towhata, I., Kuntiwattanaku, P., Seko, I., & Ohishi, K. (1993). Volume change of clays induced by heating as observed in consolidation tests. *Soils and Foundations*, *33*(4), 170-183.

Tripathy S, Sridharan A, Schanz T (2004) Swelling pressures of compacted bentonites from diffuse double layer theory. Canadian Geotech J 41:437-450.

Van Geet, M., Bastiaens, W., Volckaert, G., Weetjens, E., Sillen, X., Maes, N., ... & Plas, F. (2009). RESEAL II: A large-scale in situ demonstration test for repository sealing in an argillaceous host rock–Phase II. *Nuclear Science and Technology (Commission, E. ed.) ftp://ftp. cordis. europa. eu/pub/fp6-euratom/docs/reseal-2-final-report-july-2009_en. pdf*.

van Olphen, H. (1977). Clay colloid chemistry. John Wiley and sons, New York.

Vasconcelos, R. G., Beaudoin, N., Hamilton, A., Hyatt, N. C., Provis, J. L., & Corkhill, C. L. (2018). Characterisation of a high pH cement backfill for the geological disposal of nuclear waste: The Nirex Reference Vault Backfill. *Applied geochemistry*, *89*, 180-189.

Villa De La, R. V., Cuevas, J., RAMÍREZ, S., & LEGUEY, S. (2001). Zeolite formation during the alkaline reaction of bentonite. *European Journal of Mineralogy*, *13*(3), 635-644.

Villar, M. V., & Lloret, A. (2004). Influence of temperature on the hydro-mechanical behaviour of a compacted bentonite. *Applied Clay Science*, *26*(1-4), 337-350.

Villar, M. V., & Lloret, A. (2008). Influence of dry density and water content on the swelling of a compacted bentonite. *Applied Clay Science*, *39*(1-2), 38-49.

Villar, M. V., Gómez-Espina, R., & Lloret, A. (2010). Experimental investigation into temperature effect on hydro-mechanical behaviours of bentonite. *Journal of Rock Mechanics and Geotechnical Engineering*, *2*(1), 71-78.

Villar, M. V., Martin, P. L., & Barcala, J. M. (2005). Modification of physical, mechanical and hydraulic properties of bentonite by thermo-hydraulic gradients. *Engineering Geology*, *81*(3), 284-297.

Villar, M. V., Martín, P. L., Romero, F. J., Iglesias, R. J., & Gutiérrez-Rodrigo, V. (2016). Saturation of barrier materials under thermal gradient. *Geomechanics for Energy and the Environment*, *8*, 38-51.

Volckaert G., Bernier F., Alonso E., Gens A., Samper J., Villar M., Martin-Martin P.L., Cuevas J., Campos R., Thomas H., Imbert C., Zingarelli V., (1993). Model development and validation of the thermal-hydraulic-mechanical and geomechanical behavior of the clay barrier. Annual progress report on CEC Contract No. F12W-CT90-0033 and F12W-CT91-0102.

Wang, M. C., Benway, J. M., & Arayssi, A. M. (1990). The effect of heating on engineering properties of clays. In *Physico-chemical aspects of soil and related materials*. ASTM International.

Wang, M. C., Jao, M., & Ghazal, M. S. (2008). Heating effect on swelling behaviour of expansive soils. *Geomechanics and Geoengineering: An International Journal*, *3*(2), 121-127.

Wang, Q., Tang, A. M., Cui, Y. J., Delage, P., & Gatmiri, B. (2012). Experimental study on the swelling behaviour of bentonite/claystone mixture. *Engineering Geology*, *124*, 59-66.

Watson, C., Savage, D., Wilson, J., Benbow, S., Walker, C., & Norris, S. (2013). The Tournemire industrial analogue: reactive-transport modelling of a cement–clay interface. *Clay Minerals*, *48*(2), 167-184.

Weimin, M. Y., Zhang, F., Chen, B., Chen, Y. G., Wang, Q., & Cui, Y. J. (2014). Effects of salt solutions on the hydro-mechanical behavior of compacted GMZ01 Bentonite. *Environmental earth sciences*, *72*(7), 2621-2630.

Wersin, Paul, L. H. Johnson, and I. G. McKinley. "Performance of the bentonite barrier at temperatures beyond 100 C: A critical review." Physics and Chemistry of the Earth, Parts A/B/C 32, no. 8-14 (2007): 780-788.

White R., (2006). Principles and practice of soil science. Blackwell Publishing.

Wohlbier, H., and Henning, D. (1969). Effect of preliminary heat treatment on the shear strength of kaolinite clay. Effect of Temperature and Heat on Engineering Behavior of Soils, Highway Research Board, Special Report 103, 287--300.

Xiaodong, L., Prikryl, R., & Pusch, R. (2011). THMC-testing of three expandable clays of potential use in HLW repositories. *Applied Clay Science*, *52*(4), 419-427.

Ye, W. M., He, Y., Chen, Y. G., Chen, B., & Cui, Y. J. (2016). Thermochemical effects on the smectite alteration of GMZ bentonite for deep geological repository. *Environmental Earth Sciences*, *75*(10), 906.

Ye, W. M., Wan, M., Chen, B., Chen, Y. G., Cui, Y. J., & Wang, J. (2012). Temperature effects on the unsaturated permeability of the densely compacted GMZ01 bentonite under confined conditions. *Engineering Geology*, *126*, 1-7.

Ye, W. M., Wan, M., Chen, B., Chen, Y. G., Cui, Y. J., & Wang, J. (2009). Effect of temperature on soil-water characteristics and hysteresis of compacted Gaomiaozi bentonite. *Journal of Central South University of Technology*, *16*(5), 821.

Ye, W. M., Zhang, Y. W., Chen, B., Zheng, Z. J., Chen, Y. G., & Cui, Y. J. (2012). Investigation on compression behaviour of highly compacted GMZ01 bentonite with suction and temperature control. *Nuclear engineering and design*, *252*, 11-18.

Ye, W. M., Zheng, Z. J., Chen, B., Chen, Y. G., Cui, Y. J., & Wang, J. (2014). Effects of pH and temperature on the swelling pressure and hydraulic conductivity of compacted GMZ01 bentonite. *Applied clay science*, *101*, 192-198.

Yevnin, A., & Zaslavsky, D. (1970). Some factors affecting compacted clay swelling. *Canadian Geotechnical Journal*, *7*(1), 79-91.

Yilmaz, G. (1999). The Effect of Heating on Engineering Properties of Kaolinite and Bentonite, 9. In *National Clay Symposium* (pp. 15-18).

Yilmaz, G. (2011). The effects of temperature on the characteristics of kaolinite and bentonite. *Scientific research and essays*, *6*(9), 1928-1939.

Yong, R. N. (1999). Overview of modeling of clay microstructure and interactions for prediction of waste isolation barrier performance. *Engineering Geology*, *54*(1-2), 83-91.

Yong, R. N., Boonsinsuk, P., & Wong, G. (1986). Formulation of backfill material for a nuclear fuel waste disposal vault. *Canadian Geotechnical Journal*, *23*(2), 216-228.

Youssef M S, SabryA, Ramli AHE (1961) Temperature Changes and their effects on some physical properties of soils, Proceedings of 5th International Conference on Soil Mechanics and Foundations, pp 419–421

Zhang, G., Germaine, J. T., Whittle, A. J., & Ladd, C. C. (2004). Index properties of a highly weathered old alluvium. *Geotechnique*, *54*(7), 441-451.

Zheng, L., Rutqvist, J., Birkholzer, J. T., & Liu, H. H. (2015). On the impact of temperatures up to 200 C in clay repositories with bentonite engineer barrier systems: A study with coupled thermal, hydrological, chemical, and mechanical modeling. *Engineering Geology*, *197*, 278-295.

Zheng, L., Samper, J., & Montenegro, L. (2008). Inverse hydrochemical models of aqueous extracts tests. *Physics and Chemistry of the Earth, Parts A/B/C*, *33*(14-16), 1009-1018.

Zhu, C. M., Ye, W. M., Chen, Y. G., Chen, B., & Cui, Y. J. (2013). Influence of salt solutions on the swelling pressure and hydraulic conductivity of compacted GMZ01 bentonite. *Engineering Geology*, *166*, 74-80.

Zhu, C.M., Zhu, C.M., Ye, W.M., Chen, Y.G., Chen, B., Cui, Y.J., (2015). Influence of cyclically infiltration of $CaCl_2$ solution and de-ionized water on volume change behavior of compacted GMZ01 bentonite. Eng. Geol. 184, 104–110.

PUBLICATIONS

A. INTERNATIONAL JOURNALS

- ***Published***

1. **Kale, R. C.**, Ravi, K. Influence of thermal history on swell pressures of compacted bentonite. **Process Safety and Environmental Protection**, 123, 199-205 (2019). (Elsevier)
2. **Kale, R. C.**, Ravi, K. Influence of thermal loading on the index and physicochemical properties of Barmer bentonite. **Applied Clay Science**, 165, 22–39 (2018). (Elsevier)

- ***Under Review***

1. **Kale, R. C.**, Bhanwariwal K., Ravi, K. (2020). Influence of thermal history and hyperalkaline cement water on the swell pressure of compacted bentonite. **(Nuclear Engineering and Design)** (Elsevier)
2. **Kale, R. C.**, Ravi, K. Thermo mechanical behavior of compacted buffer material used in nuclear waste disposal system: A critical review. **(Under Review) (Environmental Technology and Innovations)** (Elsevier)
3. **Kale, R. C.**, Ravi, K. Effect of iron corrosion on swell pressure of compacted bentonite subjected to thermal loading in nuclear waste repository. **(Under Review) (Materials in Civil Engineeing)** (ASCE)
4. **Kale, R. C.**, Ravi, K. Influence of canister corrosion on the behavior of compacted Barmer bentonite buffer under thermal gradient. **(Under Review) (Annals of Nuclear Energy)** (Elsevier)
5. **Kale, R. C.**, Ravi, K. Reactive transport through compacted Barmer bentonite under the influence of thermal gradient. **(Geomechanics and Geophysics for Geo-energy and Geo-resources)** (Springer)
6. **Kale, R. C.**, Ravi, K. Coupled iron corrosion and hyperalkaline environment on swell pressure of compacted bentonite subjected to thermal history. **(To be communicated)**

B. CONFERENCE PROCEEDINGS/BOOK CHAPTERS

1. **Kale R. C.**, Bhanwariwal K., K. Ravi, *Effect of Alkaline Environment on the Swell Pressures of Compacted Bentonite under Thermal History*, IGC, Surat, 2019, **Proceedings of Indian Geotechnical Conference**, Volume 134, Chapter 4. (Springer Nature)

2. **Kale R. C.**, K. Ravi, 2020, *Laboratory liquid limit determination comparison of expansive clays by Casagrande and cone penetration method*, 7 International Conference on Recent Advances in Geotechnical Earthquake Engineering and Soil Dynamics, Bangalore 2020, **Ground Improvement Techniques**, Volume 118, Chapter 27. (Springer Nature)

CONFERENCES

A. International

1. K. Ravi, **Kale R. C.**, 2016, *Critical review of swelling behavior of different types of bentonite and bentonite-sand mixtures*, **International conference on soil and environment, ICSE, Bangalore.**

B. National

2. **Kale R. C.**, K. Ravi, 2017, *Behaviour of compacted bentonite at high temperature*, **Indian Geotechnical Conference, IGC, Guwahati.**